
PRODERNA

Programa de Pós-Graduação em Engenharia de Recursos Naturais da Amazônia

# "ESTUDO DO PROCESSO DE UPGRADING CATALÍTICO DE VAPORES DA PIRÓLISE DE RESÍDUOS PLÁSTICOS DE EQUIPAMENTOS DE INFORMÁTICA EM REATOR CATALÍTICO COM CARVÃO ATIVADO IMPREGNADO COM NaOH"

**Augusto Fernando de Freitas Costa**

Belém, PA – Brasil

Abril de 2023

# “ESTUDO DO PROCESSO DE UPGRADING CATALÍTICO DE VAPORES DA PIRÓLISE DE RESÍDUOS PLÁSTICOS DE EQUIPAMENTOS DE INFORMÁTICA EM REATOR CATALÍTICO COM CARVÃO ATIVADO IMPREGNADO COM NaOH”

**Augusto Fernando de Freitas Costa**

Tese de Doutorado apresentada ao Corpo Docente do Programa de Pós-Graduação em Engenharia de Recursos Naturais da Amazônia, da Universidade Federal do Pará, como parte dos requisitos necessários para a obtenção do título de Doutor em Engenharia de Recursos Naturais.

Orientador: Prof. Dr. -Ing. Nélio Teixeira Machado

Belém, PA - Brasil

Abril de 2023

Universidade Federal do Pará

PRODERNA
Programa de Pós-Graduação em Engenharia de Recursos Naturais da Amazônia

ITEC INSTITUTO DE TECNOLOGIA UFPA

# "ESTUDO DO PROCESSO DE UPGRADING CATALÍTICO DE VAPORES DA PIRÓLISE DE RESÍDUOS PLÁSTICOS DE EQUIPAMENTOS DE INFORMÁTICA EM REATOR CATALÍTICO COM CARVÃO ATIVADO IMPREGNADO COM NAOH"

**Augusto Fernando de Freitas Costa**

TESE SUBMETIDA AO CORPO DOCENTE DO PROGRAMA DE PÓS-GRADUAÇÃO EM ENGENHARIA DE RECURSOS NATURAIS DA AMAZÔNIA - PRODERNA/ITEC/UFPA, COMO PARTE DOS REQUISITOS NECESSÁRIOS PARA OBTENÇÃO DO GRAU DE DOUTOR EM ENGENHARIA DE RECURSOS NATURAIS.

Aprovada por:

Prof. Dr. -Ing. Nélio Teixeira Machado
(Orientador – FAESA/ITEC/UFPA)

Dr. Lucas Pinto Bernar
(Membro Interno à Instituição - Bolsista DTI-A/CNPq/UFPA)

Prof. Dr. Douglas Alberto Rocha de Castro
(Membro Externo à Instituição – CEULM/AM)

Prof. Dr. Marcelo Costa Santos
(Membro Interno à Instituição – PPGEQ/UFPA)

Prof. Dr. Luiz Eduardo Pizarro Borges
(Membro Externo à Instituição – IME-RJ)

Profª. Drª. Carmen Gilda Barroso Tavares Dias
(Membro Interno ao Programa – PRODERNA/UFPA)

Belém, PA - Brasil

Abril de 2023

## AGRADECIMENTOS

Agradecimento inicial a Deus Todo-Poderoso, que me concede até hoje o fôlego de vida e que permitiu eu chegar até este momento da minha vida acadêmico-profissional.

Agradeço em memória de meu amado pai, Raymundo Armindo de Freitas Costa, que me criou e me incentivou a alcançar meus objetivos profissionais, mas que infelizmente não pôde testemunhar essa presente conquista. E não menos importante, agradeço também à minha amada mãe, Rosália Pinheiro Freitas Costa, que com seu amor e orações ajuda até o presente momento na minha caminhada pessoal e profissional. Sem ambos, não seria possível chegar a este momento.

Agradeço aos meus irmãos Rúbia Costa Lourenço, Rúbio Fernando de Freitas Costa, Tomaz Fernando de Freitas Costa, Fernando de Freitas Costa Neto e Rosália Costa Monteiro (Rosinha) pelas orações e incentivos nessa conquista. Agradeço também aos meus familiares paternos e maternos (tios, tias, primos, primas, sobrinhos e sobrinhas), cunhados e cunhadas, por caminharem junto comigo nesta jornada.

Agradeço à vida da minha amada filha Giovanna Figueiredo Maués Freitas, o presente que Deus entregou a mim.

Agradecimento especial ao Prof. Dr. -Ing. Nélio Teixeira Machado, que aceitou me orientar neste trabalho. Meu reconhecimento pessoal a ele por tudo que já produziu e ainda produz na Universidade Federal do Pará.

Agradecimento especial à minha amiga-irmã Syglea Rejane dos Santos Vieira, secretária do PRODERNA, por me ajudar incansavelmente na conclusão dessa jornada.

Aos meus amigos técnicos e docentes do LEQ/FEQ, pelo incentivo nessa conquista, os quais são: Drª. Lianne Maria Magalhães Dias, Dr. Dilson Nazareno Pereira Cardoso, M.Sc. Samara de Paula Pinheiro Menezes Marques, Drª. Wanessa Almeida da Costa, Laura Rafaela da Silva Costa, Jamilly Rocha de Araújo, Adria Evellin Godinho de Vilhena, M.Sc. Rafaela Oliveira Pinheiro, Dr. Matheus Braga Furtado (in memoriam), M.Sc. Maria Vitória Roma da Silva, Victor Hugo da Silva Coelho (secretário), Profª. Drª. Marlice Cruz Martelli e Prof. Dr. Célio Augusto Gomes de Souza (in memoriam).

Aos colegas que integram/integraram o GEMA-UFPA, pela participação direta e indireta na elaboração deste trabalho, a saber: Dr. Eng. Lucas Pinto Bernar, Prof. Dr. Marcelo Costa Santos, Prof. Dr. Douglas Alberto Rocha de Castro, Caio Campos Ferreira, Luiz Gabriel Santos Moreira, Nathália Lobato Moraes e Prof. Dr. Hélio da Silva Almeida (in memoriam).

Ao Instituto Militar de Engenharia (IME), do Exército Brasileiro, na pessoa do Prof. Dr. Luiz Eduardo Pizarro Borges, pela utilização da unidade semi-piloto.

Muito obrigado a todos!

**Resumo**

Este estudo investigou o craqueamento térmico e o upgrading (melhoramento) catalítico de vapores da pirólise de resíduos plásticos de equipamentos de informática em um reator em semi-batelada acoplado a um leito fixo catalítico aquecido (craqueamento a vapor em 2 estágios)**.** O catalisador utilizado foi cinza de Si-Al obtida a partir da ativação de pastilhas comerciais de carbono por meio de solução concentrada de NaOH e calcinação**.** O objetivo do estudo foi caracterizar o fluxo de resíduos por meio de termogravimetria (TG) e produtos de pirólise, estudar o efeito da temperatura (350 °C - 500 °C) e da quantidade de catalisador (0,0 % m/m – 7,5 % m/m) nos rendimentos de produtos de reação, propriedades físico-químicas e composição química do produto líquido orgânico, a fim de compreender e avaliar a produção de combustíveis e o upgrading catalítico a partir de resíduos plásticos usados como matérias-primas químicas. Amostras fracionadas foram coletadas em determinados tempos de reação (15 min, 30 min, 45 min e 60 min) para estudar a evolução das reações de craqueamento nos experimentos através da composição química dos produtos na análise do GC-MS. Trabalhos anteriores também foram comparados para mostrar semelhanças entre matérias-primas diferentes em unidades térmicas iguais à utilizada**.** Os resultados indicaram composição de acrilonitrila-butadieno-estireno bromado (ABS-Br), policarbonato (PC) e poliestireno de alto impacto (HIPS) para o resíduo plástico dos equipamentos de informática. À temperatura de 350 °C os resultados foram melhores quando se considera o índice de acidez, mas os rendimentos da fase líquida foram os menores (38 %) e os rendimentos da fase gasosa elevados (42 %). Os experimentos de upgrading catalítico revelaram o aumento da presença de hidrocarbonetos aromáticos policíclicos (PAH) com o aumento da viscosidade cinemática do produto líquido orgânico, o aumento do rendimento de carvão (de 11 % para 24 %) e a diminuição do rendimento de gases (de 15 % para 5 %). A composição química mostrou presença de hidrocarbonetos aromáticos como estireno, metil-estireno e difenil-propano, e de compostos nitrogenados como benzeno butano-nitrila, de compostos fenólicos, de hidrocarbonetos policíclicos aromáticos e de compostos bromados. A pirólise de resíduos plásticos de equipamentos de informática é desafiadora, devido à composição variável de contaminantes presentes e à avaliação da composição química de acordo com o tempo de reação, que fornece informações interessantes a respeito da evolução de experimentos de pirólise em semi-batelada/upgrading catalítico. A padronização e a reprodutibilidade do método devem ser conduzidas para continuar a avaliação da pirólise e o upgrading catalítico de uma ampla gama de matérias-primas.

**Palavras-chave:** craqueamento térmico; tempo de reação; termogravimetria; pirólise de ABS retardante de chama; propriedades físico-químicas

**Abstract**

This study investigated thermal cracking and catalytic upgrading of plastic waste from computer equipment on a semi-batch reactor coupled to a heated catalyst fixed bed (2-stage vapor cracking). The catalyst used was a Si–Al ash obtained from commercial activated carbon pellets treated with concentrated NaOH solution and calcination. The purpose of the study was to characterize the waste stream through its thermogravimetry (TG) analysis and pyrolysis products, study the effect of temperature (350 - 500 °C) and catalyst quantity (0.0 - 7.5 wt%) on yields of reaction products, physical chemical properties, and chemical composition of organic liquid product in order to understand and evaluate production of fuels and chemical feedstock by recycling of plastic waste from computer equipment through catalytic upgrading. Time-fractioned samples were taken in determined reaction times (15 min, 30 min, 45 min, and 60 min) to study the evolution of cracking reactions during experiment runs through changes to chemical composition (GC-MS). A comparison with other previous work was also presented to show similarities between different feedstocks using the same thermal unit. The results indicate composition of brominated acrylonitrile-butadiene-styrene (Br-ABS), polycarbonate (PC), and high impact polystyrene (HIPS) for the plastic waste from computer equipment. The temperature of 350 °C produced better results when considering acid value but presented lower liquid phase yields (38 %) and high gas phase yields (42 %). Catalytic upgrading experiments revealed the increased presence of polycyclic aromatic hydrocarbons (PAH) with an increase in kinematic viscosity of organic liquid product, increase in char yield (from 11 % to 24 %), and decrease in gas yields (15 % to 5 %). Chemical composition showed presence of aromatic hydrocarbons such as styrene, methyl-styrene, and diphenyl-propane and nitrogenated compounds such as benzene butane-nitrile, phenolic compounds, polycyclic aromatic hydrocarbons, and brominated compounds. Plastic waste from computer equipment pyrolysis is a challenging subject due to contaminant presence and varying composition, and chemical composition evaluation according to reaction time provides interesting insights into the evolution of semi-batch pyrolysis/catalytic upgrading experiments. Standardization and reproducibility of the tool should be conducted to continue the evaluation of pyrolysis and catalytic upgrading of a wide range of feedstocks.

**Keywords:** thermal cracking; reaction time; thermogravimetry; flame-retardant ABS pyrolysis; physical-chemical properties

## SUMÁRIO

## LISTA DE FIGURAS

# LISTA DE TABELAS

# LISTA DE NOMENCLATURA

| | |
|---|---|
| ABS | Copolímero Acrilonitrila-Butadieno-Estireno |
| ABS-Br | ABS Bromado |
| C/A | Razão Catalisador/Alimentação |
| DRX | Difração de Raios-X |
| EDX | Espectroscopia de Energia Dispersiva de Raios-X |
| FRX | Fluorescência de Raios-X |
| GC-MS | Cromatografia Gasosa/Espectrometria de Massa |
| HDPE | Polietileno de Alta Densidade |
| HIPS | Poliestireno de Alto Impacto |
| LDPE | Polietileno de Baixa Densidade |
| MEV | Microscopia Eletrônica de Varredura |
| PAH | Hidrocarboneto Aromático Policíclico |
| PC | Policarbonato |
| PET | Tereftalato de Polietileno |
| PLO | Produto Líquido Orgânico |
| PMMA | Polimetilmetacrilato |
| PP | Polipropileno |
| PPE | Éter de Polifenileno |
| PS | Poliestireno |
| PVC | Cloreto de Polivinila |
| RSU | Resíduos Sólidos Urbanos |
| SPI | Sociedade da Indústria dos Plásticos |
| TG | Termogravimetria |

# CAPÍTULO 1 – INTRODUÇÃO

Os plásticos desempenham papel importante no dia a dia do ser humano há mais de 50 anos. Características dos plásticos, como durabilidade, leveza e eficiência energética, tornaram esse tipo de material essenciais na vida cotidiana [**2**]. Na sociedade moderna, os plásticos estão presentes em vários setores, tais como o da construção civil, assistência médica, eletroeletrônicos, automotiva, embalagem, utensílios domésticos e outros [**1**]. Embora os plásticos sejam materiais extremamente úteis para o ser humano, tanto a sua produção quanto a geração de seus resíduos continuam a aumentar com o agravamento dos impactos ambientais [**3**]. Os resíduos plásticos representam um sério problema ambiental, pois levam muitos anos para se decomporem, poluindo assim tanto o ambiente terrestre quanto o aquático [**1**].

Em 2019, o consumo mundial médio de plásticos/indivíduo foi de 60 kg/ano, e essa quantidade só faz crescer há mais de duas décadas. Embora 63% dos resíduos plásticos em todo o globo sejam descartados corretamente em aterros sanitários (46%) ou incinerados (17%), 22% são mal armazenados ou jogados diretamente no lixo, e apenas 15% são coletados para reciclagem [**3**]. O descarte de resíduos plásticos em aterros sanitários pode ser um problema em regiões pequenas e superpovoadas devido à constante utilização desses locais, encarecendo ainda mais o processo de incineração que vier a ser usado. O processo de incineração consiste na queima dos resíduos a fim de reduzir o tamanho e o volume deles. O controle intensivo da poluição do ar é obrigatório, e apenas cerca de 20% a 25% da energia produzida pela reação são convertidos na forma de energia elétrica [**4**]. A conversão de resíduos plásticos em combustíveis líquidos é um processo alternativo de reciclagem, em que possivelmente mais energia pode ser recuperada, com a mesma eficácia, na redução do volume desses resíduos [**5**].

Sob o ponto de vista da sustentabilidade, a conversão de resíduos plásticos em combustíveis (ou melhor ainda, em monômeros individuais) conduz a uma gestão de resíduos bem mais ecológica, se comparada ao descarte em aterros sanitários [**6**]. A conversão de resíduos plásticos em PLO por meio de craqueamento térmico proporciona o máximo de economia e benefícios ambientais [**7**].

Como a maioria dos polímeros é composta de unidades simples de hidrocarbonetos (monômero), é possível converter resíduos plásticos em combustíveis líquidos por meio de processo de pirólise [**10** – **31**], em que o material inicial é aquecido a altas temperaturas (acima de 400 ° C) em atmosfera com ausência de oxigênio, quebrando as ligações químicas da estrutura polimérica e produzindo moléculas menores de hidrocarbonetos, indicadas na utilização como combustíveis líquidos [**12**, **16**, **19** e **20**]. Em algumas situações é possível obter frações líquidas com rendimento superior a 70% [**10 - 12**, **14 - 16**, **20**, **23** – **25**].

Resíduos plásticos são porções significantes dos resíduos sólidos urbanos (RSU), correspondendo de 10% a 15% da quantidade do lixo produzido [**33**]. Em geral, os resíduos sólidos se originam nos setores residencial, comercial e industrial, além dos resíduos hospitalares, sendo estes os que mais recebem atenção em relação ao seu descarte final, devido a sua alta toxicidade. Uma pesquisa sobre geração e destino final de resíduos sólidos urbanos no Brasil, mostrou que 60,8 milhões de toneladas de RSU foram geradas em 2010 e que 54,1 milhões de toneladas de RSU foram coletadas e destinadas, sendo que 57,6% dessa quantidade representaram a destinação adequada [**34**].

Passou a ser um ponto de interesse a gestão conjunta da geração de resíduos urbanos e geração de energia por meio de processos de conversão termoquímica, como pirólise e gaseificação, sendo mais eficiências do que a queima direta de combustível sólido, gerando assim menos $CO_2$/kWh de energia produzida. Além disso, a gaseificação de resíduos pode ser usada para produzir gás de síntese (mistura de CO, $H_2$, $CO_2$, $H_2O$ e $CH_4$), e que através dessa transformação, produz-se ampla gama de produtos químicos e combustíveis [**35**].

Para entender melhor como funciona a transformação de resíduos plásticos em produtos indispensáveis do cotidiano, devemos conhecer as quatro classificações de reciclagem: reciclagem primária, reciclagem secundária, reciclagem terciária e recuperação de energia [**1**]. Também conhecida como reciclagem de ciclo fechado, a reciclagem primária é o processo de coletar descartados não contaminados e transformá-lo diretamente no mesmo produto “novo”, sem perda as de suas propriedades [**102**]. A reciclagem secundária diz respeito à reciclagem mecânica, em que a identidade química do polímero é mantida inalterada, mas esse polímero é de alguma forma fisicamente reprocessado e, normalmente, utilizado para alguma finalidade diferente do seu uso original [**103**]. A reciclagem terciária, algumas vezes chamada de reciclagem química, usa processos químicos para transformar o polímero em commodities de valor agregado. Os processos típicos incluem hidrólise e pirólise de resíduos plásticos. O produto obtido é, portanto, utilizado como matéria-prima para a produção de combustíveis e novos polímeros. [**104** e **105**].

A última forma de reciclagem de resíduos plásticos é a incineração para recuperação de energia. Trata-se de um processo em que o polímero é incinerado e uma determinada quantidade de energia é recuperada na forma de calor [**102**].

A Figura 1 ilustra esquematicamente a distribuição desses 4 tipos de reciclagem de resíduos plásticos.

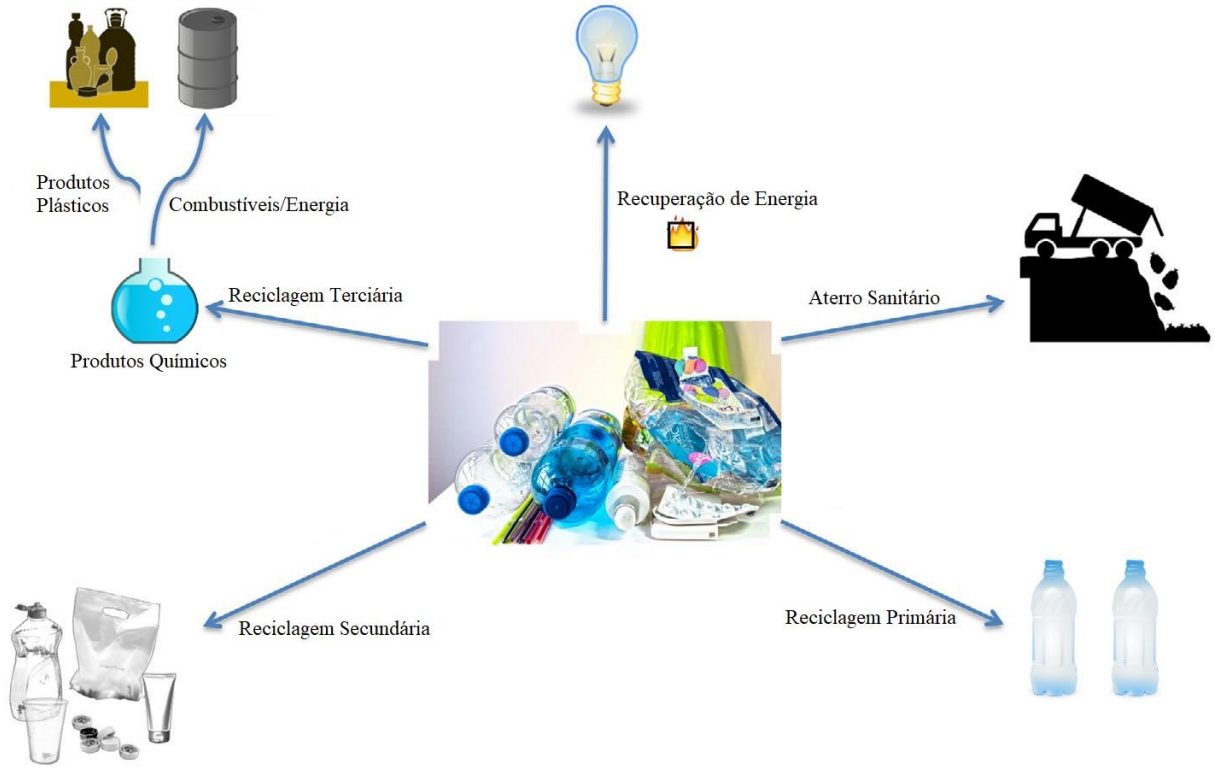


Figura 1: Destinos mais Comuns para os Resíduos Plásticos na Atualidade.
Fonte: Adaptado de [**1**].

A pirólise é o mecanismo de degradação térmica de moléculas de cadeia longa em moléculas menores usando aquecimento num ambiente livre de oxigênio, produzindo hidrocarbonetos líquidos (óleo), gases e carvão [**9**]. No processo de craqueamento térmico ocorre a quebra das cadeias poliméricas, resultando em compostos de peso molecular mais baixo. Os produtos do processo da pirólise de resíduos plásticos podem ser utilizados como combustíveis ou produtos químicos [**8**].

A gaseificação é um processo complexo que envolve a oxidação parcial de matérias-primas em gases simples, como CO e $H_2$, usando menos quantidade de vapor e/ou ar estequiométrico, e é composto de várias reações distintas. As reações de pirólise em gaseificadores ocorrem até certo ponto, e as frações líquidas pesadas produzidas (hidrocarbonetos de alto peso molecular e oxigenados) são sérios contaminantes no processo de gaseificação, causando entupimento da tubulação, quedas de pressão, corrosão e envenenamento do catalisador no processo de contra-corrente dos produtos de reação [**35**].

Pequenas quantidades de compostos inorgânicos, como metais e óxidos, também podem estar presentes nos resíduos plásticos, e seus acúmulos no interior das tubulações e equipamentos podem levar à corrosão e problemas operacionais ou de manutenção em plantas de gaseificação [**36**].

## 1.1 – Motivação

O que diferencia o resíduo sólido urbano comum do resíduo plástico de equipamentos de informática é que este último agrega alto valor de mercado, além do poder calorífico que possui. Trata-se de um tipo de resíduo largamente reaproveitável e viável do ponto de vista econômico.

Neste trabalho é proposto o estudo do processo de upgrading catalítico de vapores da pirólise de resíduos plásticos de equipamentos de informática em reator catalítico, como forma de utilizar esses materiais, outrora considerados inservíveis, como matéria-prima em experimentos de craqueamentos térmico e termocatalítico.

## 1.2 – Objetivos

### 1.2.1 – Objetivo Geral

Investigar a variação da composição química e propriedades físico-químicas, em função do tempo, do PLO proveniente da pirólise de resíduos plásticos de equipamentos de informática usando reator em semi-batelada acoplado a um leito fixo catalítico aquecido.

### 1.2.2 – Objetivos Específicos

- Pré-tratar e caracterizar o resíduo plástico por meio de análise termogravimétrica (ATG).
- Estudar o processo de craqueamento térmico.
- Estudar o upgrading catalítico através de amostragem do PLO fracionado com o tempo.
- Caracterizar os PLOs obtidos através de cromatografia gasosa acoplada à espectrometria de massas (GC-MS), densidade, viscosidade cinemática e índice de acidez.
- Sintetizar e caracterizar o catalisador utilizado na pirólise através de microscopia eletrônica de varredura (MEV), espectroscopia de energia dispersiva de raios-X (EDX), difração de raios-X (DRX) e fluorescência de raios-X (FRX).

# CAPÍTULO 2 – REVISÃO BIBLIOGRÁFICA

## 2.1 – Resíduos Plásticos de Equipamentos Eletroeletrônicos

Resíduos plásticos de equipamentos eletroeletrônicos são tipos de resíduo cujo fluxo é um dos que mais cresce no mundo, sendo que uma quantidade considerável desse material é descartada incorretamente em áreas urbanas e aterros sanitários. Diretrizes em todo o mundo incentivam a reutilização, reciclagem e recuperação desse tipo de material [**14**].

Os plásticos que geram esse tipo de resíduo estão presentes em uma ampla variedade de aparelhos, tais como eletrodomésticos (geladeiras, máquinas de lavar, liquidificadores, etc.), computadores, teclados, videogames, equipamentos médicos, entre outros. Estima-se que 32% em peso desses resíduos plásticos de equipamentos eletroeletrônicos sejam constituídos por polímeros plásticos, principalmente acrilonitrila-butadieno-estireno (ABS), polipropileno (PP), poliestireno (PS), policarbonato (PC), tereftalato de polietileno (PET) e outros [**37**]. A Figura 2 mostra um local de descarte de resíduos plásticos de equipamentos eletroeletrônicos.

Figura 2: Resíduos Plásticos de Equipamentos Eletroeletrônicos.

Fonte: [**112**]

Os polímeros predominantes no setor de equipamentos eletroeletrônicos são o ABS, o HIPS e blendas de PC/ABS, de HIPS/PPE e de ABS/PMMA. Além desses, compostos bromados têm bastante aplicabilidade neste setor, devido atuarem como retardantes de chama dos equipamentos [**109**]. O copolímero ABS é classificado como terpolímero justamente por ser formado por 3 monômeros diferentes (acrilonitrila, butadieno e estireno), decorrente da grafitização da acrilonitrila e do estireno sobre o polibutadieno [**108**].

A Figura 3 mostra as estruturas moleculares dos monômeros constituintes do ABS.

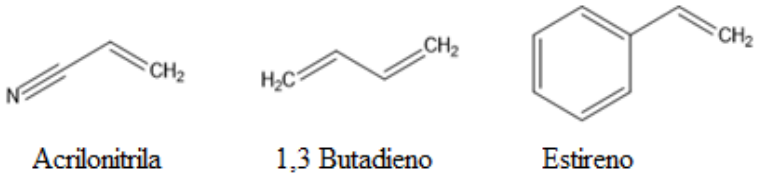


Figura 3: Estruturas Moleculares dos Monômeros do ABS.

Fonte: Adaptado de [**108**].

E a Figura 4 representa a estrutura molecular do copolímero ABS.

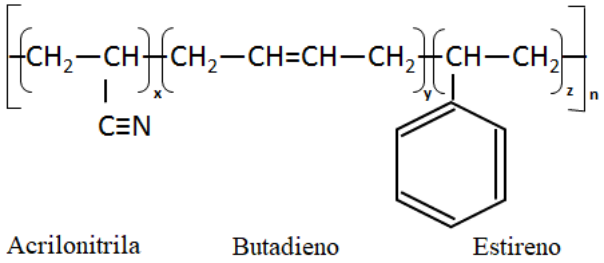


Figura 4: Estrutura Molecular do ABS.

Fonte: Adaptado de [**110**].

De acordo com o trabalho de Miranda [**108**], o copolímero ABS (acrilonitrila-butadieno-estireno) possui como característica importante a boa resistência ao impacto, sendo isso atribuído ao butadieno. As quantidades de acrilonitrila e butadieno têm influência direta na dureza do ABS, pois por causa da boa resistência que também possui, pode ser utilizado até a temperatura de 80 °C, mas que por outro lado, apresenta menor resistência às intempéries e maior resistência química que o PS e o HIPS (devido à acrilonitrila). A principal utilização do copolímero plástico ABS é na produção de eletroeletrônicos, eletrodomésticos e autopeças.

A principal propriedade do HIPS, que é a resistência ao impacto, é devido à quantidade de borracha de polibutadieno presente em estrutura. Quanto maior for essa quantidade, maior é resistência ao impacto. A borracha de polibutadieno que é adicionada ao HIPS é responsável pela absorção de impacto do material ao ser submetido a esforço mecânico. As principais aplicabilidades do HIPS são na produção de itens industriais que exigem satisfatória resistência ao impacto, a saber: peças de máquinas e veículos, caixas para rádio, televisores e microcomputadores, grades para aparelho de ar condicionado, peças internas e externas de aparelhos eletrônicos e de telecomunicações, e outros [**111**]. A Figura 5 mostra a estrutura molecular do HIPS.

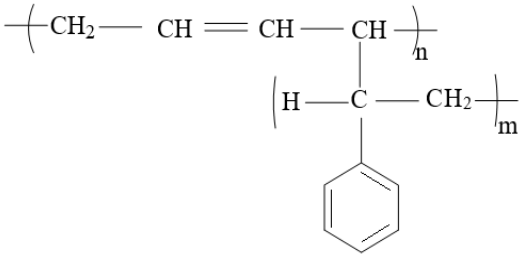

Figura 5: Estrutura Molecular do HIPS.
Fonte: Adaptado de [**111**].

Ainda de acordo com Peeters et al. [**109**], os polímeros PC (policarbonato), PPE (éter de polifenileno) e PMMA (polimetilmetacrilato), na forma de blenda, são muito utilizados na produção de televisores de tela plana, monitores de tela plana, televisores de tubo de raios catódicos e monitores de tubo de raios catódicos. A Figura 6, a Figura 7 e a Figura 8 mostram, respectivamente, as estruturas moleculares do PC, do PPE e do PMMA.

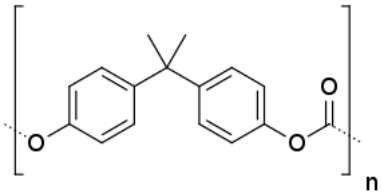

Figura 6: Estrutura Molecular do PC.
Fonte: Adaptado de [**109**]

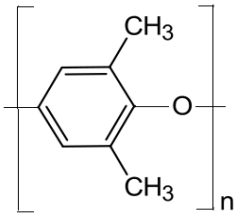

Figura 7: Estrutura Molecular do PPE.
Fonte: Adaptado de [**109**].

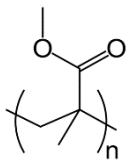

Figura 8: Estrutura Molecular do PMMA.
Fonte: Adaptado de [**109**].

A Tabela 1 apresenta alguns dos polímeros plásticos mais comuns, com suas respectivas estruturas moleculares e aplicações, de acordo com a Sociedade da Indústria dos Plásticos (SPI).

Tabela 1: Código SPI, Estrutura Molecular e Aplicações de Polímeros Plásticos.

| Código SPI | Polímero | Estrutura | Aplicações |
|---|---|---|---|
| 1 | Tereftalato de Polietileno (PET) | 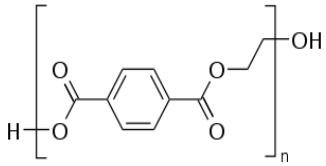 | Frascos de remédios, garrafas de molho de salada, garrafas de água e garrafas de refrigerantes. |
| 2 | Polietileno de Alta Densidade (HDPE) | 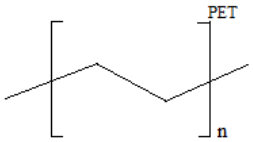 | Saboneteira, sacos de lixo, frascos de alvejantes e frascos de detergentes. |
| 3 | Cloreto de Polivinila (PVC) | 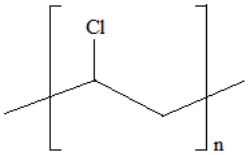 | Tubos, gradeamento e cabos. |
| 4 | Polietileno de Baixa Densidade (LDPE) | 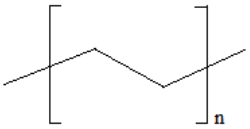 | Embalagens de sanduíches, filmes plásticos e sacolas de supermercado |
| 5 | Polipropileno (PP) | 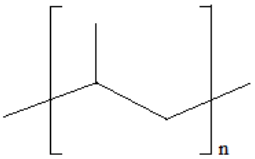 | Recipiente reutilizável de alimentos, frascos de prescrição e tampinhas de refrigerantes. |
| 6 | Poliestireno (PS) | 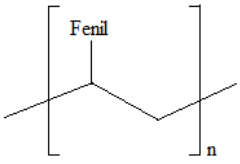 | Utensílios plásticos, isopor e embalagem de amendoim. |
| 7 | Outros | | |

Fonte: Adaptado de [**1**].

A pirólise de resíduos plásticos provenientes de equipamentos eletroeletrônicos pode ser uma maneira de transformar parte deles em produtos úteis, como combustíveis gasosos, líquidos e sólidos, todavia são frequentemente contaminados por derivados de bromo provenientes dos retardantes de chama adicionados ao plástico [**38**, **39** e **40**]. Isso pode representar um problema quando se leva em consideração esse resíduo plástico na transformação por meio de gaseificação [**36**].

**2.2 – Craqueamento Térmico**

O processo no qual um determinado tipo de material é submetido à ação do calor com o objetivo de romper as ligações químicas existentes em sua estrutura, para obtenção de novos produtos, é conhecido como craqueamento térmico ou pirólise [**89**].

É muito comum utilizar o craqueamento térmico (ou pirólise) para produzir combustíveis líquidos, sólidos e gasosos, convertendo moléculas de cadeias carbônicas longas e complexas em moléculas curtas e simples. O objetivo da utilização desse método é aumentar a proporção das quantidades dos produtos mais voláteis presentes no petróleo, por exemplo [**90]**.

Classicamente, existem 3 tipos de pirólise: lenta, rápida e flash. A pirólise lenta é normalmente realizada sob temperaturas entre 350 °C e 550 °C, com taxas de aquecimento de 1 °C/min a 10 °C/min e os tempos de residência do vapor sendo prolongados. O produto formado em maior quantidade na pirólise lenta é um resíduo sólido, chamado carvão ou coque, pois a uma taxa de aquecimento lenta é facilitada a formação desse material durante as reações paralelas que ocorrem durante o processo. A pirólise rápida frequentemente ocorre sob temperaturas entre 500 °C e 700 °C, com taxas de aquecimento estando acima de 1.000 °C/min e os tempos de residência do vapor normalmente na faixa de poucos segundos. Na pirólise rápida a produção de líquidos é favorecida e, dependendo do tipo de matéria-prima utilizada, o rendimento do líquido pode chegar até 90% em peso. Na pirólise flash a temperatura normalmente é acima de 700 °C, com taxas de aquecimento extremamente rápidas e os tempos de residência do vapor são de milissegundos. Quando a matéria-prima é biomassa, a pirólise flash pode produzir rendimentos mais altos de líquidos, porém produz maior quantidade de gases quando são usados diferentes tipos de resíduos plásticos [**6]**.

A pirólise apresenta como vantagem adicional a capacidade de ser um processo que lida também com mistura de resíduos plásticos contaminados, no entanto, no caso de decomposição térmica, os produtos resultantes apresentam baixo peso molecular. A pirólise também pode ser realizada sob diferentes tempos de reação, temperaturas e pressões, na presença de gases reativos com ou sem uso de catalisadores [**2]**.

O craqueamento térmico (ou pirólise) de plásticos é conduzida a altas temperaturas, dentro da faixa de 500 °C a 800 °C, para permitir o rompimento das estruturas macromoleculares em moléculas menores, resultando em um produto com ampla quantidade de hidrocarbonetos no processo, sem emissão de nenhum gás tóxico ou nocivo, pois não envolve incineração. O processo de pirólise apresenta algumas vantagens, pois ajuda a reduzir a poluição causada por resíduos plásticos, ao mesmo tempo que se torna fonte alternativa de produtos valiosos de hidrocarbonetos líquidos e gasosos [**2**].

Em geral, as vantagens do craqueamento térmico são que o produto obtido pode ser usado como combustível alternativo, enquanto as desvantagens estão associadas à alta temperatura de operação (300 °C – 700 °C) e ao longo tempo de residência, por exemplo [**106**].

A Tabela 2 mostra um resumo das pesquisas anteriores mais importantes relacionadas ao craqueamento térmico de resíduos plásticos.

Tabela 2: Condições Operacionais de Craqueamento Térmico de Trabalhos Anteriores.

| Autor | Tipo de Reator | Tipo de Plástico | Temperatura (°C) | Pressão (atmosfera) | Rendimento Máximo do PLO (% m/m) |
|---|---|---|---|---|---|
| F. J. Mastral | Leito Fluidizado | HDPE | 640 | $N_2$ | 68,5 |
| S. S. Kim | Batelada com Agitação | PS e PP | 300 - 500 | $N_2$ | 92,30 – 94,21 |
| S. J. Miller | Batelada | HDPE e PET | 450 | $N_2$ | 60 – 70 |
| W. Kaminsky | Batelada | PP | 400 | $N_2$ | 12,1 |
| S. Kumar | Semi-Batelada | HDPE | 450 | Atmosférica | 23,96 |
| M. Sarker | Aço Inoxidável | PS | 250 – 430 | Atmosférica | 87 |
| M. Stelmachowski | Semi-Batelada | PP | 359 – 358 | Atmosférica | 86,7 |
| S. M. Fakhrhoseini | Leito Fixo | PP | 500 | $N_2$ | 82,12 |
| B. K. Sharma | Batelada | HDPE | 420 – 440 | Atmosférica | 74 |
| R. Miandad | Escala Piloto Pequena | PP | 450 | Atmosférica | 42 |
| J. Lee | Quartzo | PET | 380 – 760 | $CO_2$ | 59,3 |
| R. Thahir | Leito Fixo | PP | 500 - 600 | $0,3x10^3$ (vácuo) | 88 |
| S. M. Al-Salem | Leito Fixo (Batelada) | HDPE | 550 | $N_2$ | 70 |
| Y. Zhang | Forno Rotativo em Semi-Batelada | PP | 500 | $N_2$ | 62 - 77 |
| S. Colantonio | Semi-Batelada | Mistura de PE, PP, PS e PET | 650 | $N_2$ | 84 |

Fonte: Adaptado de [**96**].

## 2.3 – Craqueamento Térmico de Plásticos de Equipamentos de Informática

De acordo com Brennan et al. [**113**], tipos de termoplásticos como o ABS, o HIPS, o PVC e o PC representam a maior quantidade da fração polimérica oriunda de resíduos eletroeletrônicos, destacando-se entre eles o ABS e o HIPS, que somados, representam em torno de 55% em peso de todo o conteúdo dos resíduos plásticos de equipamentos eletroeletrônicos. Em seu trabalho, realizaram pirólise a partir de ABS não reciclado na forma de carcaças de monitor de computador e HIPS não reciclados na forma de carcaças de teclado, como forma de reciclagem desses materiais.

O estudo de Muhammad et al. [**114**] foi de avaliar as reações de pirólise e pirólise catalítica, em reator de leito fixo, de resíduos plásticos provenientes de equipamentos de refrigeração (geladeiras e freezers) e de televisores e monitores de computador de tubos de raios catódicos (CRTs) descartados, a fim de comparar os resultados com os obtidos da pirólise catalítica dos polímeros ABS e HIPS puros. Foram utilizadas como catalisadores as zeólitas Y e ZMS-5.

Miranda [**95**] investigou a degradação térmica e catalítica dos polímeros poli(acrilonitrila-butadieno-estireno) (ABS) e poliestireno de alto impacto (HIPS) provenientes de resíduos eletroeletrônicos. O estudo foi realizado a partir de experimentos de pirólise e co-pirólise térmicas e catalíticas em reator equipado com leito catalítico, a partir de carcaças marfim e preta de computador (teclados), utilizando as zeólitas H-USY e H-ZSM5 como catalisadores.

## 2.4 – Upgrading Catalítico

O upgrading (melhoramento) catalítico de vapores de pirólise através da utilização de um segundo estágio de craqueamento de fase vapor é uma técnica promissora para superar problemas associados com frações líquidas formadas durante a conversão termoquímica de resíduos plásticos em combustíveis e matéria-prima química [**14**, **25**, **38**, **41** – **54**].

Basicamente, é um método que consiste em favorecer o contato dos vapores liberados no processo de pirólise com os poros do catalisador do leito fixo aquecido. Os sítios ativos da superfície do catalisador favorecem ainda mais a quebra das moléculas e/ou reações específicas, como a desoxigenação, a dessulfurização, a desnitrificação, a desalogenação, além de outras, como isomerização, aromatização e condensação. As reações específicas necessárias dependem da composição da alimentação e das características esperadas do produto. Portanto, uma escolha diversificada de catalisador pode ser decisiva para atingir os objetivos do processo [**44**, **49** e **52**]. O catalisador desempenha um papel importante no processo de pirólise de plásticos para recuperação de hidrocarbonetos dos resíduos plásticos que seguem um processo semelhante [**2**].

O papel crucial que os catalisadores realizam no processo termoquímico de resíduos plásticos se refere em promover reações direcionadas, redução da temperatura de reação e melhoria da eficiência do processo [**26**].

Regulamentos rígidos de controle de emissões em todo o mundo têm demonstrado a necessidade de se realizar processos eficientes e conservadores com alto rendimento, tornando-se uma das principais razões para o crescimento no mercado mundial. Como resultado, essa preocupação ambiental tem provocado o aumento da demanda de catalisadores de refinaria que melhorarão a eficiência do processo, sugerindo uma clara importância do catalisador em refinarias e pirólise. Conforme o tipo de catalisador que é utilizado, o resultado do processo pode sofrer modificações, pois catalisadores com alta área superficial possuem a capacidade de alterar a natureza da pirólise, afetando significativamente o resultado [**2**].

No trabalho de Panda e Singh [**91**], foram usados caulim e sílica-alumina ($SiO_2$-$Al_2O_3$) como catalisadores utilizando reator em semi-batelada na faixa de temperatura entre 400 °C e 500 °C, na realização do craqueamento termocatalítico de polipropileno para a produção de combustível líquido. Observou-se que entre esses 2 catalisadores utilizados, a $SiO_2$-$Al_2O_3$ foi considerada melhor do que o caulim em relação à diminuição do tempo de residência, rendendo 91% em peso de combustível líquido, sendo isso atribuído à maior acidez da $SiO_2$-$Al_2O_3$ em comparação ao caulim, concluindo que o óleo combustível resultante tem potencial para ser usado na produção de combustível de motor em processos mais longos.

O upgrading catalítico de vapores da pirólise de resíduos plásticos de equipamentos eletroeletrônicos foi estudado utilizando-se catalisadores de zeólitas, tais como zeólitas Y [**14** e **38**], zeólitas Beta (**53**) e ZSM-5 [**14**, **38**, **51** e **53**], catalisadores metálicos (Ni e Fe) impregnados em ZSM-5 [**44** e **52**], óxidos metálicos [**53**] e catalisadores metálicos impregnados em MCM-41 [**44** e **54**]. Os autores deram maior importância principalmente na distribuição do número de carbonos presentes nos produtos e na remoção de contaminantes, como Br ou Cl.

Até agora, nenhum catalisador de cinzas de Si-Al foi testado para o upgrading de vapores da pirólise de resíduos plásticos de equipamentos eletroeletrônicos, concentrando-se nos efeitos do catalisador na composição química e nas propriedades físico-químicas do PLO melhorado obtido, e mudando em relação ao tempo de reação.

Embora alguns autores tenham investigado os efeitos da razão catalisador/alimentação (C/A) na composição do produto [**25**, **42**, **43** e **47**] e os efeitos do tempo de reação [**48** e **49**], somente Nishino et al. [**47**] estudaram os efeitos do catalisador na composição química e nas propriedades físico-químicas do PLO melhorado em processos de grande escala, e cuja matéria-prima não era composta de resíduos plásticos de equipamentos eletroeletrônicos.

Além de trabalhos publicados que analisam os efeitos do tempo de reação, com ênfase no estudo da composição química e conversão [**48** e **49**], outros foram feitos sem a realização de análises físico-químicas para verificar os efeitos do tempo tanto na composição química quanto na conversão. A variação das propriedades físico-químicas e da composição química com o tempo de reação é uma forma interessante de analisar processos de pirólise usando reator em semi-batelada, indicando como as reações termocatalíticas alteram as composições da alimentação e dos produtos, permitindo comparar com outros projetos e escalas de melhoramento de pirólise catalítica. Em trabalhos anteriores, análises semelhantes foram utilizadas para estudar o upgrading catalítico de vapores da pirólise de gorduras residuais [**55** e **56**], sendo tais análises podendo ser comparadas à obtida neste trabalho.

Este trabalho investigou os efeitos da razão catalisador/alimentação e do tempo de reação na composição do produto e nas características físico-químicas do PLO produzido pelo upgrading (craqueamento a vapor em 2 estágios) dos vapores de pirólise obtido a partir de carcaças de computadores (gabinetes e monitores) e impressoras.

## 2.5 - Parâmetros que Influenciam no Craqueamento Térmico de Plásticos

Alguns parâmetros desempenham papel de grande relevância no craqueamento térmico de plásticos, e otimizá-los, possibilita o melhoramento do processo. Entre esses parâmetros podemos destacar a taxa de aquecimento, a temperatura de operação e as proporções do material misturado [**2**].

### 2.5.1 – Influência da Taxa de Aquecimento

A influência da taxa de aquecimento no rendimento do produto líquido a partir da pirólise de resíduos plásticos, sem o uso de catalisador, foi investigada e descobriu-se que aumentando-se essa taxa de 10 °C/min para 25 °C/min, o rendimento da fase líquida da pirólise diminui, levando ao entendimento que taxas de aquecimento baixas dão origem à reação secundária entre o sólido e o produto líquido, como resultado de tempos de residência mais longos e a taxa de aquecimento ótima sendo de 10 °C/min [**92**].

### 2.5.2 - Influência da Temperatura de Operação

A temperatura tem um papel importante no craqueamento térmico, e escolher a temperatura certa e otimizá-la é necessário para a manutenção da tecnologia do processo de pirólise. A co-pirólise (pirólise de resíduos plásticos com combustível fóssil, como carvão ou gasóleo leve) também é influenciada pela temperatura tanto quanto a pirólise de material individual. Na maioria dos estudos, descobriu-se que a temperatura de decomposição dos resíduos plásticos com outros óleos pesados de petróleo por meio do processo de co-pirólise era

mais baixa do que a da pirólise de material individual [**93**]. De fato, o processo de pirólise é muito sensível à temperatura e isso é um fator importante a ser observado ao realizar o craqueamento térmico de plásticos [**96**]. Uma vez que a quebra de polímeros depende dos níveis de temperatura, é possível considerar essa grandeza térmica como o fator mais importante que influencia a distribuição do produto [**97**]. A temperatura tem a capacidade de controlar o rompimento das cadeias poliméricas longas, uma vez que a interação de van der Waals entre as partículas entrará em colapso à medida que sua vibração aumenta [**98**].

### 2.5.3 - Influência das Proporções do Material Misturado

A mistura de 2 resíduos plásticos de produtos de valor relativamente baixo e resíduo de óleo de motor aumenta não apenas o rendimento do óleo líquido, mas também a qualidade dos produtos líquidos, com maior teor de parafína e nafta no óleo co-pirolítico do que o óleo obtido da pirólise das poliolefinas individuais [**94**].

### 2.5.4 – Influência da Pressão

Os produtos de pirólise são geralmente influenciados pela pressão de operação, que por sua vez é um fator relacionado ao tempo da reação [**99**]. Quanto maior a pressão, maior a quantidade de gases é formada durante a pirólise. Ressalta-se então que a maior parte das pesquisas sobre pirólise foi feita sob pressões atmosféricas. Por outro lado, operar sob pressão de vácuo, faz aumentar a formação de gases do produto [**97**].

### 2.5.5 – Influência do Tempo de Residência

Define-se tempo de residência como o tempo que uma alimentação permanece no reator e é considerado um dos elementos mais importantes nos processos de pirólise [**100**]. Quanto mais tempo o plástico permanecer no reator, mais produtos estáveis serão formados, como hidrocarbonetos de baixo peso molecular, provocando também maior taxa de formação de compostos aromáticos [**106** e **107**].

### 2.5.6 – Influência do Catalisador

Os catalisadores são materiais que ajudam a melhorar a qualidade dos produtos da reação de pirólise, ao mesmo tempo em que reduzem a temperatura da reação, reduzindo a energia de ativação necessária para a quebra da ligação, diminuindo também o tempo de retenção [**101**]. De acordo com o trabalho de Zahraa et al. [**96**], sílica-alumina, zeólitas (beta, USY, ZSM-5, REY, clinoptilolita, etc.) e MCM-41 são os catalisadores mais comumente usados na pirólise de resíduos plásticos.

# CAPÍTULO 3 – MATERIAIS E MÉTODOS

## 3.1 - Metodologia

A metodologia aplicada para desenvolver, analisar e discutir os resultados deste trabalho pode ser resumida em quatro etapas separadas, as quais são compostas por: pré-tratamento do material de alimentação, preparação do catalisador, coleta das amostras e experimentos de upgrading, e análise do catalisador e do produto líquido obtido. O fluxograma do processo ilustrado na Figura 9 resume as etapas e análises realizadas.

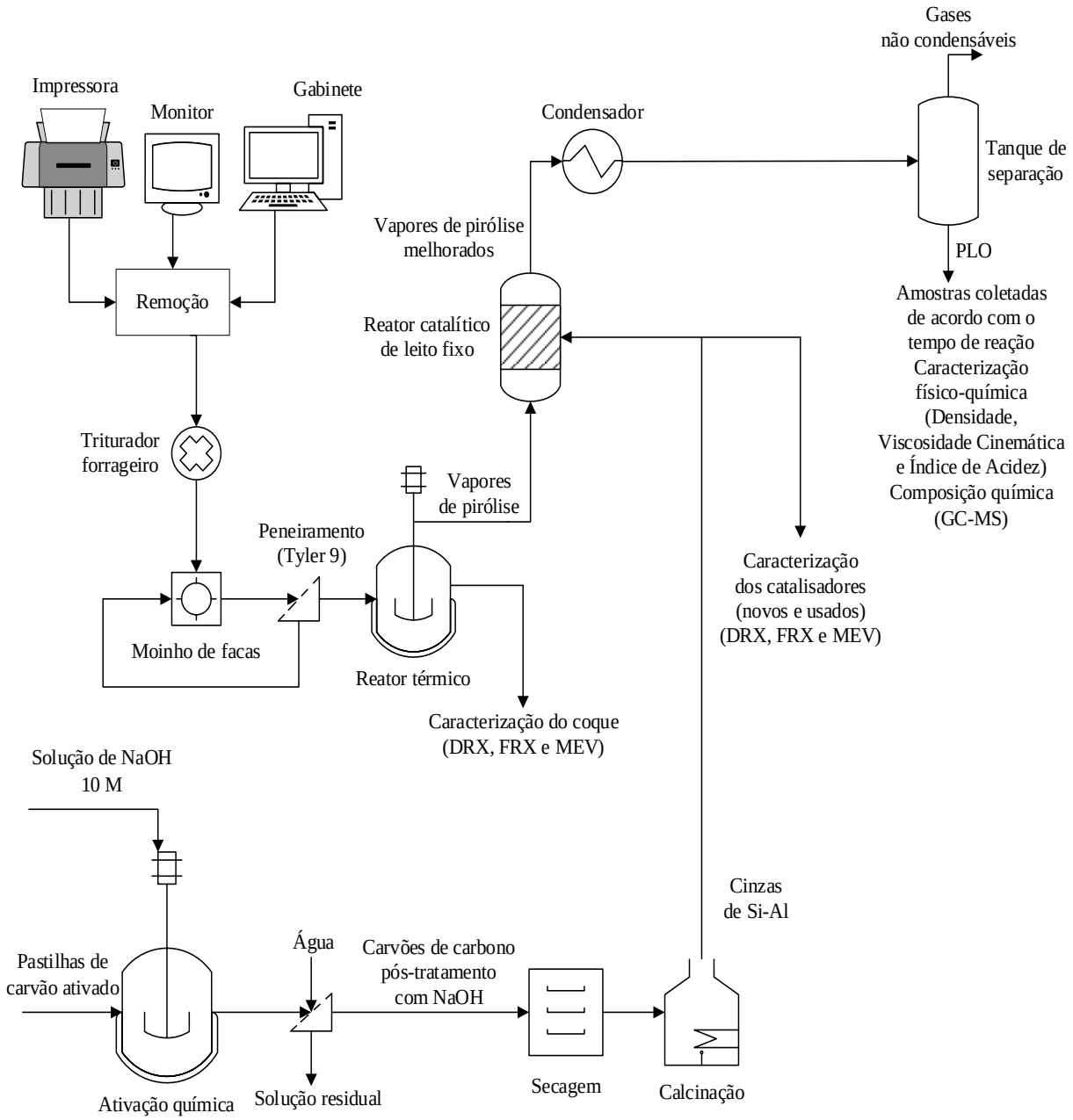


Figura 9: Fluxograma do Processo de Upgrading Catalítico de Vapores de Resíduos Plásticos de Equipamentos de Informática em Escala Semi-Piloto.

Fonte: Autor.

## 3.2 - Materiais

### 3.2.1 – Matéria-Prima

O ponto de partida para o início dos experimentos deste trabalho foi obter os resíduos plásticos que foram utilizados como matéria-prima. As carcaças de computadores, a partir de equipamentos de informática inservíveis, foram obtidas a partir de coleta realizada no prédio administrativo do Instituto de Tecnologia da Universidade Federal do Pará. Eram carcaças de material plástico retiradas de monitores, gabinetes e impressoras antigos.

Na Figura 10 temos alguns dos equipamentos de informática coletados.

Figura 10: Monitores, Gabinetes e Impressora.

Fonte: Autor.

Os tipos de componentes poliméricos foram removidos manualmente e quebrados em pedaços menores, exemplificado na Figura 11.

Figura 11: Carcaças Quebradas Manualmente.

Fonte: Autor.

O material despedaçado alimentou um triturador forrageiro (marca TRAPP, modelo TRF 600, motor elétrico trifásico de potência 7,5 CV) para reduzir o tamanho dos fragmentos, conforme ilustrado na Figura 12.

A alimentação no triturador forrageiro era individualizada para cada tipo de equipamento de informática (monitores, gabinetes e impressoras), sendo cada batelada na ordem de 2 kg durante 30 minutos.

Figura 12: Triturador Forrageiro.

Fonte: Autor.

O material triturado, conforme cada tipo de equipamento de informática, está ilustrado na Figura 13.

(a) (b) (c)

Figura 13: Resíduos Plásticos de Equipamentos de Informática Triturados. Monitores (a), Gabinetes (b), Impressoras (c).

Fonte: Autor.

Posteriormente, o material triturado alimentou um moinho de facas de bancada, com a finalidade de reduzir ainda mais o tamanho dos resíduos plásticos. O equipamento é mostrado na Figura 14.

Figura 14: Moinho de Facas de Bancada.

Fonte: Autor.

Em seguida, o resíduo plástico moído, de cada equipamento de informática, foi peneirado manualmente, utilizando-se peneira de malha Tyler 9. As partículas retidas no peneiramento foram novamente moídas no moinho de facas e peneiradas outra vez, até que mais de 95% da quantidade inicial de resíduos plásticos atingissem o tamanho da partícula desejado.

### 3.2.2 - O Catalisador

Neste trabalho foram utilizadas como catalisadores cinzas obtidas a partir de pastilhas comerciais de carvão ativado. As especificações dessas pastilhas de carvão ativado estão descritas na Tabela 2. Foi utilizado NaOH com 99% de pureza na preparação de solução de NaOH. Apenas de caráter informativo, toda a quantidade de água utilizada nos experimentos e na solução de NaOH era deionizada.

Tabela 3: Especificações das Pastilhas Comerciais de Carvão Ativado.

| **Especificações** | **Valor** |
|---|---|
| Tamanho da partícula (mm) | 3,9 – 4,1 |
| Diâmetro médio da partícula (mm) | 4,0 |
| Área superficial ($m^2/g$) | 900 |
| Teor de umidade (%) | 5,0 (máximo) |
| Densidade ($g/cm^3$) | 0,45 – 0,55 |
| pH | 9,0 – 11,0 |

Fonte: Autor

As pastilhas de carvão ativado foram tratadas com solução concentrada de NaOH para aumentar a estrutura do tamanho do mesoporo [**57**]. Um método detalhado para preparação de pastilhas catalisadoras é descrito no trabalho de Bernar et al. [**55**]. De forma resumida, as pastilhas ficaram em contato com a solução concentrada de NaOH, na proporção de 50 % m/m, durante o período de 8 horas. Em seguida, a mistura pastilhas + solução gasta foi separada por filtração simples e lavada com água deionizada para remover o excesso de álcali, até a faixa de pH entre 10,0 – 11,0. A solução residual filtrada foi então diluída com água e neutralizada com solução de $H_2SO_4$ diluída para enfim ser descartada corretamente. As pastilhas de carvão ativado foram secas em estufa de secagem com circulação de ar (marca DeLeo, modelo A3AFDI300) durante 24 horas a 105 °C e calcinadas em mufla (marca Linn Elektro Therm, modelo LM 312 SO 1729) a 600 °C pelo período de 3 horas. Ambos os equipamentos pertencem ao Laboratório de Engenharia Química – UFPA. Após esses processos, o catalisador obtido contendo menos carbono na composição, pôde ser chamado de cinza de Si-Al, pois análises posteriores revelaram que as pastilhas continham sílica e alumina. As Figuras 15 e 16 mostram os equipamentos usados na secagem e calcinação, respectivamente, das pastilhas de carvão ativado.

Figura 15: Estufa Usada na Secagem das Pastilhas.

Fonte: Autor.


Figura 16: Mufla Usada na Calcinação das Pastilhas.

Fonte: Autor.

A Figura 17 mostra os estados inicial e final do catalisador após as etapas de sua preparação serem descritas anteriormente.

(a) (b)

Figura 17: Catalisador. Pastilhas Comerciais de Carvão Ativado (a), Cinza de Si-Al (b).
Fonte: Autor.

Em processos de escala maior, seria necessária uma otimização no tratamento da concentração da solução de NaOH e da quantidade de solução residual gerada, alterando a eficiência de contato do catalisador com uma solução alcalina e possivelmente mudando o tempo de contato. Mesmo que as quantidades do catalisador usado para experimentos de upgrading catalítico sejam baixas (2,5 % m/m a 7,5 % m/m), soluções residuais geradas e sua alcalinidade seriam inaceitáveis em escala maior.

### 3.3 – Equipamento e Procedimentos Experimentais

#### 3.3.1 – Reator em Semi-Batelada

A unidade semi-piloto de craqueamento termocatalítico em 2 estágios, do Instituto Militar de Engenharia - RJ, foi bem descrita em trabalhos anteriores [**55** e **56**] e mostrada na Figura 18.


Figura 18: Unidade Semi-Piloto de Craqueamento Termocatalítico.

Fonte: Autor.

E a Figura 19 mostra uma representação esquemática dessa unidade semi-piloto.

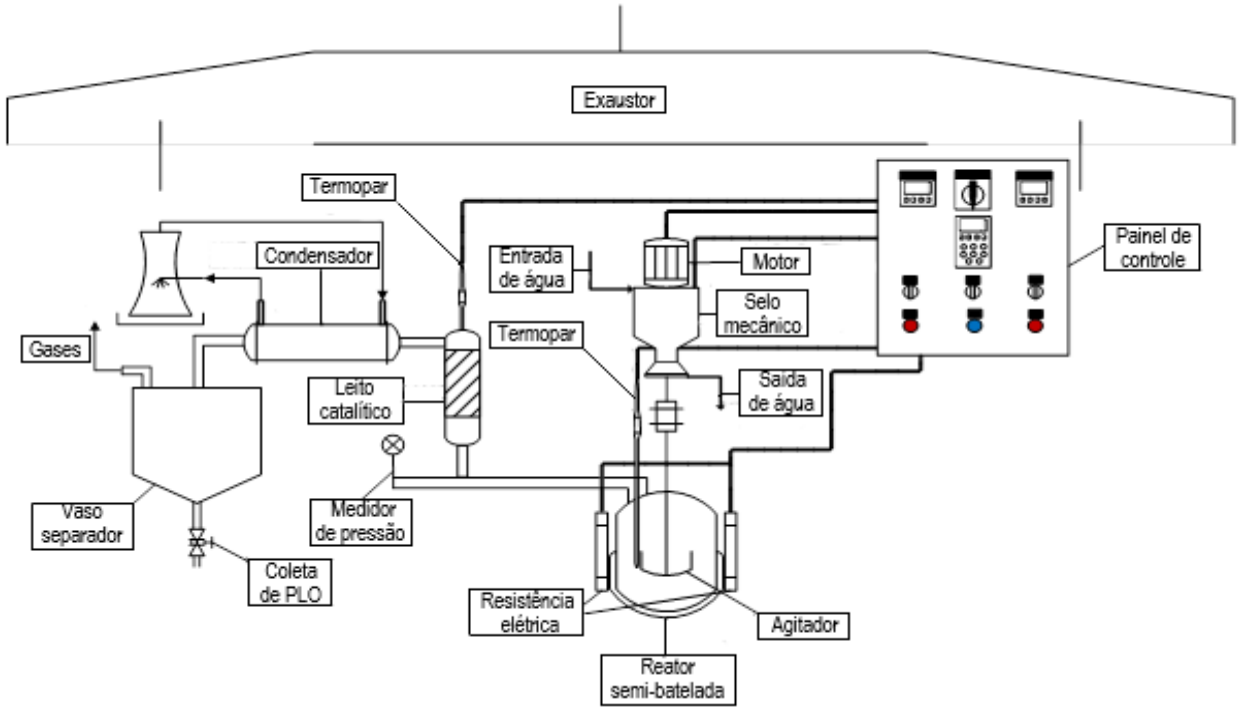


Figura 19: Representação Esquemática da Unidade Semi-Piloto.

Fonte: Adaptado de [**107**].

Os experimentos foram conduzidos na unidade semi-piloto usando-se duas linhas de investigação: craqueamento térmico e craqueamento termocalítico (upgrading catalítico).

### 3.3.2 – Craqueamentos Térmico e Termocatalítico

Primeiro, o craqueamento térmico dos resíduos plásticos de equipamentos de informática foi realizado em 4 diferentes temperaturas (350 °C, 400 °C, 450 °C e 500 °C) para avaliar o rendimento do produto. Para esses experimentos, a montagem da unidade foi feita utilizando-se apenas o reator em semi-batelada R-1 acoplado diretamente ao condensador. Não havia leito fixo catalítico nesse procedimento. Isso foi feito para avaliar melhor a dinâmica da temperatura do processo e escolher a temperatura que forneceu melhores rendimentos líquidos, para avaliação do efeito da quantidade de catalisador na composição e rendimentos do produto. Estudar a composição química da fração líquida do craqueamento térmico ajuda a entender o que acontece na superfície aquecida do catalisador em experimentos termocatalíticos, uma vez que a composição do vapor que alimenta o reator R-2 deve ser muito semelhante à fração líquida obtida na pirólise sem catalisador.

Em seguida, o leito fixo catalítico R-2, composto por um tubo de aço inoxidável (comprimento = 300 mm e diâmetro interno = 15 mm) e aquecimento por resistência elétrica (Potência = 1,5 kW), foi acoplado entre o reator térmico R-1 e o condensador, e os experimentos foram testados usando diferentes proporções em massa de catalisador (2,5 % m/m, 5,0 % m/m e 7,5 % m/m) em relação à alimentação de matéria-prima a fim de estimar mais tempo de residência de vapores em contato com o catalisador no reator R-2. Mesmo que a resistência elétrica possa fornecer calor a todo o comprimento do tubo, apenas o volume ocupado pelo catalisador aquecido é contado como leito fixo catalítico, ou seja, maior quantidade de catalisador corresponde a um maior leito fixo catalítico.

Os procedimentos em cada experimento de craqueamento foram bem similares entre si. Para os experimentos de craqueamento térmico, inicialmente a unidade semi-piloto foi preparada acionando o condensador, deixando-o atingir a temperatura de 15 °C para a água de resfriamento. Depois, foi iniciado e verificado o fornecimento de água para o selo mecânico do rotor. Em seguida, o interior do reator R-1 foi alimentado manualmente (600 g) com os resíduos plásticos de equipamentos de informática após ser desacoplado do sistema. Essa quantidade de matéria-prima era constituída da mistura dos 3 tipos de resíduos plásticos, sendo que a massa de cada um deles correspondia a 1/3 da massa total da alimentação. Então o reator R-1 foi reacoplado ao sistema, tomando-se o cuidado de inseri-lo e ajustá-lo corretamente para garantir que não houvesse folga entre o reator e sua tampa ou torque excessivo no rotor. Já que o estado físico da alimentação era sólido, é mais difícil montar o reator do que quando se trata de líquidos ou semi-líquidos, como visto em trabalhos anteriores [**55** e **56**]. O reator R-1 foi fechado e acoplado ao sistema por meio de 8 conjuntos de parafusos e porcas com diâmetro interno de 12 mm. Cada conjunto é composto por 1 parafuso e duas porcas. Os conjuntos de parafusos e porcas foram montados em pares diametralmente opostos entre si, após a fixação de cada par usando chave de boca 16 mm. O par subsequente foi montado de forma transversal ao conjunto anteriormente fixado, fechando assim adequadamente o reator R-1 para evitar vazamento de vapores. Foi usada também entre o reator R-1 e sua tampa uma vedação de grafite, para evitar ainda mais vazamentos de vapores. Após concluída a montagem do reator R-1, os parâmetros operacionais foram estabelecidos no painel de controle da unidade, isto é, a frequência do rotor (100 rpm), a temperatura final desejada e a taxa de aquecimento (10 °C/min). No auxílio ao monitoramento e controle do andamento do processo, os parâmetros operacionais foram registrados a cada 10 min. Para cada experimento, o tempo e a temperatura do fluxo inicial de vapores do reator R-1 foram registrados, e as amostras sendo coletadas após 15, 30, 45 e 60 min do tempo inicial de reação (fluxo de saída dos vapores), para avaliar a composição e as propriedades físico-químicas do produto conforme o aumento do tempo de reação.

Os gases não condensáveis foram queimados na linha de saída de gás. Considerava-se finalizada a reação quando não havia mais vapores visíveis na saída de gás.

Os experimentos de craqueamento termocatalítico foram feitos de maneira semelhante em relação à alimentação e montagem do reator R-1, com etapas adicionais na preparação do reator catalítico de leito fixo R-2. Após a montagem do reator R-1, as cinzas catalíticas foram inseridas ao reator R-2 desacoplado. O reator R-2 foi coberto com lã de vidro, que funcionou como isolante térmico, permitindo que os vapores fluíssem de maneira mais uniforme através do leito fixo catalítico. Inseriu-se então um termopar ao reator R-2, que por fim foi acoplado ao sistema. Vedações de borracha de alta capacidade térmica foram usadas entre cada flange para evitar vazamentos no sistema.

Após a montagem do reator R-2, os parâmetros operacionais de temperatura final desejada e taxa de aquecimento (10 °C/min), para este reator, foram estabelecidos no painel de controle da unidade. Foi importante pré-aquecer o reator para atingir adequadamente a temperatura desejada do catalisador, antes que os vapores saíssem do reator R-1, e evitar queda de temperatura, pois no início, os vapores mais frios entram em contato com os catalisadores aquecidos. Por causa disso, a temperatura do reator R-2 foi controlada inicialmente na faixa de 20 °C a 30 °C acima dos pontos de ajuste desejados.

É importante salientar que se optou por realizar experimentos de craqueamento termocatalítico a 450 °C porque, apesar dos experimentos de craqueamento térmico a 450 °C e 500 °C terem apresentado rendimentos da fase líquida aproximadamente iguais, economiza-se energia elétrica (convertida em térmica) a 450 °C do que a 500 °C. Além disso, o experimento de craqueamento térmico a 450 °C apresentou menor valor médio do índice de acidez em comparação ao realizado a 500 °C.

### 3.4 – Caracterização da Matéria-Prima

Os resíduos plásticos de equipamentos de informática foram caracterizados separadamente por Análise Termogravimétrica (ATG) para cada tipo de resíduo plástico coletado (monitores, gabinetes e impressoras) e também para a mistura dos 3 tipos desses resíduos. As análises foram realizadas em escala térmica de 20 °C a 800 °C, sendo a massa de cada amostra de 5 mg em cadinho de platina sob atmosfera de ar sintético (vazão de 5 mL/min) e taxa de aquecimento de 10 °C/min. Foi utilizado o analisador termogravimétrico (marca Shimadzu, modelo DTG-60H) pertencente ao Laboratório de Óleos da Amazônia, localizado no PCT-Guamá / UFPA, como está ilustrado na Figura 20.

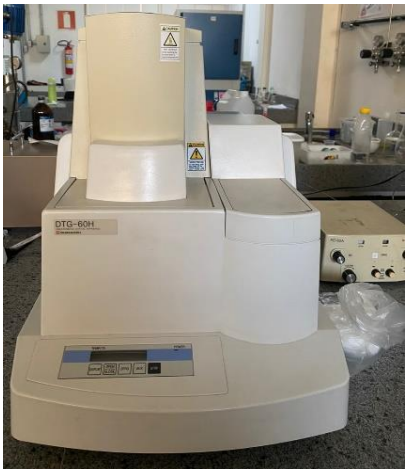


Figura 20: Analisador Termogravimétrico.

Fonte: Autor

### 3.5 – Caracterização do PLO

#### 3.5.1 – Composição Química do PLO

A composição química do PLO foi obtida através da análise de GC-MS, conforme detalhamento no trabalho de Castro et al. [**58**], em cromatógrafo a gás (marca Agilent Technologies, modelo CG-7890B) acoplado a um espectrômetro de massa (marca Agilent Technologies, modelo MS-5977A), ambos equipamentos pertencentes à Central de Análises Químicas/UEA. Foi usada uma coluna capilar de sílica fundida (marca SLB-5ms, dimensões: comprimento 30 m x diâmetro interno 0,25 mm x espessura do filme 0,25 µm).

O injetor de amostra foi programado para a temperatura de 250 °C, com taxa de aquecimento de 10 °C/min. Foi injetado 1,0 µL de amostra no modo de divisão (1:50). A vazão do gás de arraste utilizado foi de 6,0 mL/min. A temperatura da coluna foi aumentada de 60 °C para 280 °C. O detector foi programado para 230 °C e a temperatura do quadrupolo para 150 °C. As concentrações foram expressas em área, pois não foi utilizado padrão interno para comparar as áreas dos picos.

#### 3.5.2 – Propriedades Físico-Químicas do PLO

As propriedades físico-químicas do PLO foram obtidas medindo-se sua viscosidade cinemática, densidade e índice de acidez.

A viscosidade cinemática foi medida de acordo com a adaptação do método padrão ASTM D2515 em um banho termostático à temperatura controlada de 40 °C, realizando-se sucção manual. O tempo foi medido manualmente usando-se cronômetro, sendo realizadas medidas em triplicata para cada amostra. Viscosímetros Cannon-Fenske de números 50, 200 e 300 foram usados conforme a faixa de viscosidade estimada das amostras, sendo então a viscosidade cinemática determinada usando-se o bulbo inferior.

A densidade foi medida usando-se uma metodologia adaptada do método padrão AOCS CC 10c-95 em picnômetro de vidro de 5 mL aferido com água destilada.

O índice de acidez foi determinado através da titulação de 0,2 g de amostra dissolvido em 50 mL de solvente composto isopropanol-tolueno (50/50 % m/m) com solução padrão de KOH 0,1 N e fenolftaleína como indicador ácido-base. O método de titulação do índice de acidez foi adaptado da metodologia AOCS Cd3d-63 [**55** e **56**].

### 3.6 – Caracterização da Cinza de Si-Al e Carvões

#### 3.6.1 – Análises de MEV e EDX

A caracterização morfológica da superfície do catalisador (pastilha comercial e cinza de Si–Al antes e após os experimentos termocatalíticos) e dos carvões obtidos, foi realizada por microscopia eletrônica de varredura, utilizando-se um microscópio (marca TESCAN GmbH, modelo Vega 3) com as ampliações 338x, 838x, 1670x, 3330x, 5000x e 6670x. No preparo para a análise, as amostras foram cobertas com uma fina camada de ouro, sendo isso feito por um Sputter Coater (marca Leica Biosystems, modelo Balzers SCD 050). A análise elementar e o mapeamento foram realizados por espectroscopia de energia dispersiva de raios-X (marca Oxford Instruments, modelo Aztec 4.3). As duas análises foram realizadas no Laboratório de Caracterização Estrutural/UNIFESSPA.

#### 3.6.2 – Análise de DRX

A análise morfológica para identificar a presença de fases cristalinas no catalisador **(**cinza de Si-Al antes e após os experimentos termocatalíticos) e nos carvões obtidos, foi realizada por difração de raios-X, utilizando-se o difratômetro (marca PANalytical, modelo Empyrean) do Laboratório de Caracterização Mineral/UFPA, constituído das seguintes especificações: tubos de raios-X cerâmicos de anodo de Co ($K_{\alpha}$=1,789010 Å), foco fino longo, filtro $K_{\beta}$ de Fe, detector PIXEL3D Medpix3 1x1, no modo scanning, voltagem de 40 kV, corrente de 35 mA, varredura de 3 ° a 9 ° em 2θ, tamanho do passo 0,006 ° em 2θ, tempo/passo de 20 s, fenda divergente de 1/4 °, antiespalhamento de 1/2 ° e máscara de 10 mm. A Figura 21 mostra o difratômetro utilizado na análise.

Figura 21: Difratômetro de Raios-X.

Fonte: Autor.

### 3.6.3 – Análise de FRX

A espectrometria de fluorescência de raios-X foi realizada para confirmar a identificação da composição química do catalisador **(**cinza de Si-Al antes e após os experimentos termocatalíticos) e dos carvões obtidos. Na determinação da composição química das amostras foi utilizado o espectrômetro WDS sequencial (marca PANalytical, modelo Axios Minerals), com tubo de raios-X cerâmico, anodo de Rh e máximo nível de potência de 2,4 kW. A preparação das amostras foi feita por pastilha prensada, produzindo-se uma mistura de 0,5 g de amostra, 3,0 g de substrato (ácido bórico) e 0,15 g de aglomerante (cera de parafina). Em seguida a mistura foi prensada (marca SPEX Sample Prep., modelo 3635 X-Press) com carga de 25 ton. Ambos os equipamentos utilizados na análise pertencem ao Laboratório de Caracterização Mineral/UFPA e são mostrados nas Figuras 22 e 23. As aquisições e tratamento dos dados foram realizados através do software SuperQ Manager, versão 5.3 da PANalytical.

Figura 22: Espectrômetro de FRX.

Fonte: Autor


Figura 23: Prensa Hidráulica de Pastilha.

Fonte: Autor.

### 3.7 – Balanços de Massa e Cálculos dos Rendimentos dos Produtos de Reação

A massa da alimentação foi pesada antes de abastecer o reator R-1. A cada vez, uma fração do PLO coletado era pesada e somada para encontrar a massa total obtida de PLO. Após o resfriamento, o reator R-1 era desmontado e o carvão (coque) removido e pesado. A massa de gás foi calculada por um balanço de massa global integral, considerando toda a unidade semi-piloto como o volume de controle.

Balanços de massa integrais são melhores para analisar processos em batelada ou em semi-batelada. Esses tipos de balanços são obtidos pela integração de um balanço de massa diferencial feito no sistema.

A Equação (1) descreve o balanço de massa diferencial:

$$\frac{dM}{dt} = \dot{M}_E - \dot{M}_S + G - C \tag{1}$$

onde $\dot{M}_E$ e $\dot{M}_S$ são os fluxos de massa dentro e fora do volume de controle delimitado, respectivamente; G e C correspondem aos termos de geração e consumo de espécies químicas devido às reações químicas que ocorrem.

Embora o craqueamento térmico consista numa variedade de reações químicas, para balanços de massa globais não há geração ou consumo de massa. Esses termos são importantes apenas quando determinadas espécies químicas são consideradas dentro do volume de controle.

Para o balanço de massa global, G – C = 0, e a Equação (1) se torna:

$$\frac{dM}{dt} = \dot{M}_E - \dot{M}_S \tag{2}$$

Multiplicando a Equação (2) por dt e integrando, obtém-se a Equação (3):

$$\int_{t_i}^{t_f} \frac{dM}{dt} dt = \int_{t_i}^{t_f} \dot{M}_E dt - \int_{t_i}^{t_f} \dot{M}_S dt$$

$$M_{t_f} - M_{t_i} = \int_{t_i}^{t_f} \dot{M}_E dt - \int_{t_i}^{t_f} \dot{M}_S dt \quad (3)$$

onde:

$M_{t_f}$ corresponde ao material restante no reator R-1 no tempo final ($t_f$) da reação, neste caso o resíduo de carvão restante no reator ($M_{carvão}$);

$M_{t_i}$ é a massa inicial no reator R-1, correspondendo à massa de resíduos plásticos de equipamentos de informática inseridas no reator ($M_{alim.}$).

Se não há fluxo de massa adicionado ao volume de controle, então $\dot{M}_E = 0$.

$\dot{M}_S$ corresponde ao fluxo de massa que sai do volume de controle projetado e que representa os vapores de pirólise que saem do reator R-1 e chegam ao condensador, onde é separado em duas frações: $\dot{M}_{PLO}$ e $\dot{M}_{gases}$. Logo, $\dot{M}_S = \dot{M}_{PLO} + \dot{M}_{gases}$.

Substituindo esses parâmetros na Equação (3), obtém-se a Equação (4):

$$M_{carvão} - M_{alim.} = -\left[\int_{t_i}^{t_f} \dot{M}_{PLO} dt + \int_{t_i}^{t_f} \dot{M}_{gases} dt\right]$$

$$M_{alim.} - M_{carvão} = \int_{t_i}^{t_f} \dot{M}_{PLO} dt + \int_{t_i}^{t_f} \dot{M}_{gases} dt \quad (4)$$

Considerando que os fluxos de massa do PLO e dos gases são constantes, o rearranjo da Equação (4) resulta na forma final do balanço de massa global, para a unidade semi-piloto de upgrading catalítico, na Equação (5):

$$M_{alim.} - M_{carvão} - M_{PLO} = M_{gases} \quad (5)$$

Os valores das quantidades de alimentação, carvão e PLO obtidos permitem calcular a massa de gases não condensáveis que saem da unidade semi-piloto.

Sabendo-se que a quantidade de gases é calculada indiretamente, deve-se tomar cuidado para medir corretamente as massas de alimentação, carvão e PLO, pois qualquer oscilação nessas quantidades medidas irá refletir nos rendimentos da fase gasosa obtida.

O carvão corresponde apenas ao resíduo sólido restante do reator R-1, devido à dificuldade em pesar com precisão a cinza catalítica recuperada no final dos experimentos. Quase sempre após os experimentos a massa da cinza catalítica apresentava-se em quantidade menor, devido à fragmentação e a sua perda na corrente gasosa ou durante a desmontagem do leito fixo catalítico. Como a quantidade de catalisador é inferior a 10% da quantidade de alimentação, essa perda foi considerada desprezível.

Os rendimentos dos produtos da reação foram calculados em relação à massa de alimentação, da seguinte forma:

$$R_{PLO}(\%) = \frac{M_{PLO}}{M_{alim.}} \text{ x } 100 \quad (6)$$

$$R_{carvão}(\%) = \frac{M_{carvão}}{M_{alim.}} \text{ x } 100 \quad (7)$$

$$R_{gases}(\%) = \frac{M_{gases}}{M_{alim.}} \text{ x } 100 \quad (8)$$

# CAPÍTULO 4 – RESULTADOS E DISCUSSÃO

Neste Capítulo foi inserido o Artigo publicado "**Catalytic Upgrading of Plastic Waste of Electric and Electronic Equipment (WEEE) Pyrolysis Vapors over Si–Al Ash Pellets in a Two-Stage Reactor.**"

energies

MDPI

*Article*

# Catalytic Upgrading of Plastic Waste of Electric and Electronic Equipment (WEEE) Pyrolysis Vapors over Si–Al Ash Pellets in a Two-Stage Reactor

**Augusto Fernando de Freitas Costa [1], Caio Campos Ferreira [1], Simone Patrícia Aranha da Paz [1], Marcelo Costa Santos [1], Luiz Gabriel Santos Moreira [2], Neyson Martins Mendonça [2], Fernanda Paula da Costa Assunção [3], Ana Carolina Gomes de Albuquerque de Freitas [4], Roseane Maria Ribeiro Costa [4], Isaque Wilkson de Sousa Brandão [5], Carlos Emmerson Ferreira da Costa [5], Sílvio Alex Pereira da Mota [6], Douglas Alberto Rocha de Castro [7], Sergio Duvoisin, Jr. [8], Luiz Eduardo Pizarro Borges [9], Nélio Teixeira Machado [1,2,*] and Lucas Pinto Bernar [1]**

1 Graduate Program of Natural Resources Engineering of Amazon, Campus Profissional-UFPA, Universidade Federal do Pará, Rua Augusto Corrêa Nº 01, Belém 66075-110, Brazil
2 Faculty of Sanitary and Environmental Engineering, Campus Profissional-UFPA, Universidade Federal do Pará, Rua Corrêa Nº 01, Belém 66075-110, Brazil
3 Graduate Program of Civil Engineering, Campus Profissional-UFPA, Universidade Federal do Pará, Rua Augusto Corrêa Nº 01, Belém 66075-110, Brazil
4 Graduate Program of Pharmaceutical Sciences, Campus Profissional-UFPA, Universidade Federal do Pará, Rua Augusto Corrêa Nº 01, Belém 66075-110, Brazil
5 Graduate Program of Chemistry, Universidade Federal do Pará, Rua Augusto Corrêa Nº 01, Belém 66075-110, Brazil
6 Graduate Program of Chemistry, Universidade Federal do Sul e Sudeste do Pará, Folha 31, Quadra 7, Lote Especial—Nova Marabá, Marabá 68507-590, Brazil
7 Centro Universitário Luterano de Manaus—CEULM/ULBRA, Avenida Carlos Drummond de Andrade Nº 1460, Manaus 69077-730, Brazil
8 Faculty of Chemical Engineering, Universidade do Estado do Amazonas-UEA, Avenida Darcy Vargas Nº 1200, Manaus 69050-020, Brazil
9 Laboratory of Catalyst Preparation and Catalytic Cracking, Section of Chemical Engineering, Instituto Militar de Engenharia-IME, Praça General Tibúrcio Nº 80, Rio de Janeiro 22290-270, Brazil
* Correspondence: machado@ufpa.br; Tel.: +55-91-984-620-325

**Abstract:** This study investigated thermal cracking and catalytic upgrading of waste from electric and electronic equipment (WEEE) plastics on a semi-batch reactor coupled to a heated catalyst fixed bed (2-stage vapor cracking). The catalyst used is a Si–Al ash obtained from commercial activated carbon pellets treated with concentrated NaOH solution and calcination. The purpose of the study was to characterize the waste stream through its thermogravimetry (TG) analysis and pyrolysis products, study the effect of temperature (350–500 °C) and catalyst quantity (0.0–7.5 %.wt) on yields of reaction products, physical chemical properties, and chemical composition of OLP in order to understand and evaluate production of fuels and chemical feedstock by recycling of WEEE plastic through catalytic upgrading. Time-fractioned samples were taken in determined reaction times (15, 30, 45, and 60 min) to study the evolution of cracking reactions during experiment runs through changes to chemical composition (GC-MS). A comparison with other previous work is also presented to show similarities between different feedstocks using the same thermal unit. The results indicate composition of brominated acrylonitrile-butadiene-styrene (Br-ABS), polycarbonate (PC), and high impact polystyrene (HIPS) for the WEEE plastic. The temperature of 350 °C produced better results when considering acid value but presented lower liquid phase yields (38 %) and high gas phase yields (42 %). Catalytic upgrading experiments revealed the increased presence of polycyclic aromatic hydrocarbons (PAH) with an increase in kinematic viscosity of organic liquid product, increase in char yield (from 11 % to 24 %), and decrease in gas yields (15 % to 5 %). Chemical composition showed presence of aromatic hydrocarbons such as styrene, methyl-styrene, and diphenyl-propane and nitrogenated compounds such as benzene butane-nitrile, phenolic compounds, polycyclic aromatic hydrocarbons, and brominated compounds. WEEE plastic pyrolysis is a challenging subject due to contaminant presence and varying composition, and

check for updates

**Citation:** de Freitas Costa, A.F.; Ferreira, C.C.; da Paz, S.P.A.; Santos, M.C.; Moreira, L.G.S.; Mendonça, N.M.; da Costa Assunção, F.P.; de Freitas, A.C.G.d.A.; Costa, R.M.R.; de Sousa Brandão, I.W.; et al. Catalytic Upgrading of Plastic Waste of Electric and Electronic Equipment (WEEE) Pyrolysis Vapors over Si–Al Ash Pellets in a Two-Stage Reactor. *Energies* **2023**, *16*, 541. https://doi.org/10.3390/en16010541

Academic Editor: Diego Luna

Received: 29 November 2022
Revised: 27 December 2022
Accepted: 28 December 2022
Published: 3 January 2023

chemical composition evaluation according to reaction time provides interesting insights into the evolution of semi-batch pyrolysis/catalytic upgrading experiments. Standardization and reproducibility of the tool should be conducted to continue the evaluation of pyrolysis and catalytic upgrading of a wide rangeof feedstocks.

**Keywords:** thermal cracking; reaction time; thermogravimetry; WEEE; flame-retardant ABS pyrolysis; physical–chemical properties

## 1. Introduction

### *1.1. E-Waste*

Plastic waste poses a serious environmental problem, as it can take several years to decompose and pollutes terrestrial and aquatic environments [1–3]. In modern society, though, synthetic polymers are ubiquitous in the form of packaging, clothing, biomedical devices, electronic equipment, and household items, among others utilized by human society [1]. As of 2019, the average world consumption of plastics per capita was 60 kg/year, and the number has kept growing for over two decades. Even though 63% of world plastic waste is correctly disposed of in landfills (46%) or incinerated (17%), 22% is mismanaged or littered, and only 15% is collected for recycling [3]. Disposal in landfills can be a problem in some overpopulated and small areas due to extensive usage of space, and the more expensive process of incineration is used. The operation consists of burning the waste to reduce its size and volume. Intensive air pollution control is mandatory, and only about 20–25% of the energy produced by the reaction is recovered as electric energy [4]. Conversion of plastic waste into liquid fuels is an alternative recycling process where possibly more energy can be recovered with the same effectiveness in reducing waste volume [5–9].

Since most polymers are composed of hydrocarbon single units (monomer), it is possibleto recycle waste plastics into liquid biofuels through pyrolysis or cracking processes [10–31],where the starting material is heated in an oxygen-deficient atmosphere to high temperatures (above 400 °C), breaking chemical bonds in the polymeric structure and producing smaller hydrocarbon molecules suited for use as liquid fuels [12, 16, 19, 20]. In some cases, it is possible to obtain high yield of liquid fractions above 70 % [10–12, 14–16, 20, 23–25], and the hydrocarbon composition of initial feed reduces the need for catalyzed steps and/or further purification through separation processes and chemical reactions [12, 13, 17, 19, and 25]. Nevertheless, it is desirable to control the degree of cracking in the pyrolysis reaction to be able to produce fuel within the specification range. This can be hard to achieve due to distillation of initial vapor products of the reaction if done in atmospheric pressure [32], so heavy-like fractions form such as waxes and heavy oils ($C_{20}$–$C_{30+}$) [11, 12, 17, 19, 21, 24, and 25].Plastic waste is a significant portion of urban municipal waste (MHSW), comprising between 10–15 % in weight of generated waste [33 and 34]. Considerable interest is being generated in coupling management of urban waste and energy generation through thermochemical conversion processes such as pyrolysis and gasification, achieving higher efficiencies than directly burning solid fuel, thus generating less $CO_2$ per MJ of energy produced. Besides, waste gasification can be used to produce syngas (a mixture of CO, $H_2$, $CO_2$, $H_2O$, and $CH_4$) and, through its transformation, produce a wide array of chemicals and fuels [35]. Gasification is a complex process involving partial oxidation of starting materials into simple gases such as CO and $H_2$ using less than stoichiometric air and/or steam, and it is composed of several different reactions. Thermal pyrolysis reactions occur to a degree in gasifiers, and heavy liquid fractions produced (high molecular weight hydrocarbons and oxygenates) are serious contaminants in the gasification process, causing clogging, pressure drops, corrosion, and catalyst poisoning in upstream processing of reaction products [35]. Small quantities of inorganic compounds such as metals and oxides may also be present in plastic waste, and its accumulation inside vessels and equipment can lead to corrosion and operational/maintenance problems in gasification plants [36].

Waste electric and electronic equipment (WEEE) is one of the fastest growing waste streams in the world, and a considerable amount of it is disposed of incorrectly in urban areas and landfills. Directives around the world encourage its reuse, recycling, and recovery [14]. It consists of a wide range of devices such as refrigerators, washing machines, electric domestic equipment, computers, keyboards, videogames, medical equipment, and others. It is estimated that 32 %. wt of WEEE is composed of plastic polymers, mainly acrylonitrile-butadiene-styrene (ABS), polypropylene, polystyrene, polycarbonate, polyethylene terephthalate, and others [37]. Pyrolysis of plastic waste from WEEE can be one way to recycle part of it into useful products such as gaseous, liquid, and solid fuels, but they are often contaminated with bromine derived from flame retardants added to plastic [38–40]. This can be a problem when considering this plastic waste for transformation via gasification [36].

### *1.2. Catalytic Upgrading*

Catalytic upgrading of pyrolysis vapors through utilization of a second stage of vapor-phase cracking is a promising technique to overcome problems associated with liquid fractions formed during thermochemical conversion of plastic waste into fuels and chemical feedstock [14, 25, 38, 41–54]. Basically, it consists of contacting the vapors flowing out of a thermal pyrolysis process with a porous catalyst heated fixed bed. Active sites at the catalyst surface promote further cracking of molecules and/or specific reactions such as deoxygenation, desulfurization, denitrification, dehalogenation, and others like isomerization, aromatization, and condensation [44, 49, and 52]. The necessary specific reactions depend on the composition of feed and desired product characteristics. Therefore, a diverse catalyst choice can be made to achieve the process design goals.

Catalytic upgrading of pyrolysis vapors of WEEE plastic was studied using zeolite catalysts as Y-zeolites [14 and 38], Beta-zeolites [53], and ZSM-5 [14, 38, 51, and 53]; metal catalysts (Ni and Fe) impregnated into ZSM-5 [44 and 52]; metal oxides [53]; and metal catalysts impregnated into MCM-41 [44 and 54]. The authors focused mainly on carbon number distribution of products and removal of contaminants such as Br or Cl. Until now, no Si–Al ash catalyst was tested for the upgrading of WEEE plastic pyrolysis vapors focusing on the catalyst effects on the chemical composition and physical-chemical properties of obtained upgraded OLP changing with respect to reaction time. Even though some authors investigated catalyst-to-feed ratio (C/F) effects on product composition [25, 42, 43, and 47] and reaction time effects [48 and 49], only Nishino et al. studied those effects at a larger process scale [47], and the feedstock was not composed of WEEE. Aside from papers published analyzing effects of reaction time focused on studying chemical composition and conversion [48 and 49], no physical-chemical analyses were done to check the effects of time on those properties. This work studied C/F ratio and reaction time effects on product composition and physical-chemical characteristics of OLP produced by the upgrading (2-stage vapor cracking) of pyrolysis vapors obtained from casings of scrap computers (WEEE) on a semi-pilot scale.

Chemical composition and physical-chemical properties' variation with reaction time is an interesting way of analyzing semi-batch pyrolysis processes, indicating how thermo-catalytic reactions change the composition of feed and of products facilitating the comparison, design, and scaling of catalytic upgrading pyrolysis. In previous work, we used similar analyses to study catalytic upgrading of waste fats [55 and 56], and the analysis can be compared to the one obtained in this work.

## 2. Materials and Methods

### *2.1. Methodology*

The methodology applied to develop, analyze, and discuss the results of this work can be summarized by four separate tasks composed of: feed material pre-processing, catalyst preparation, upgrading experiments and sample collecting, and analysis of catalyst and liquid product obtained. The process flowchart illustrated in Figure 1 summarizes tasks and analysis conducted.

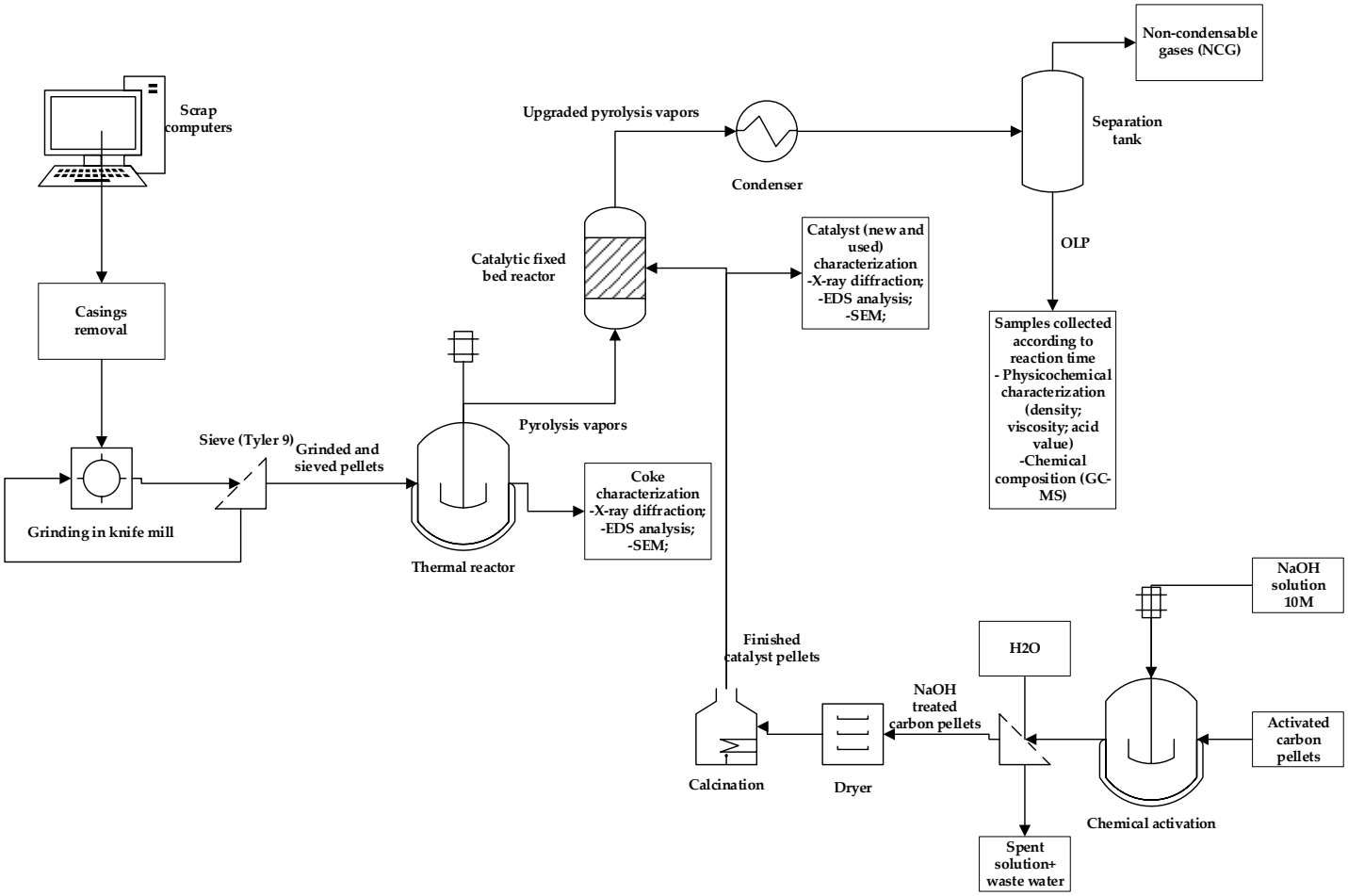


**Figure 1.** Process flowchart of catalytic upgrading of WEEE vapors using Si–Al ash catalyst pellets, in semi-pilot scale.

### 2.2. Materials

Scrap computers were obtained as the e-waste collected over the years in the building of the Institute of Technology (ITEC) located at Federal University of Pará (UFPA). They were composed of plastic material removed from old monitors, personal computers, and printers. The polymeric casings were manually removed and broken into smaller pieces to be fed into a knife mill, illustrated in Figure 2. The casings were ground in batches of 2 kg for 30 min. Afterwards, the ground WEEE plastic was sieved through a Tyler 9 mesh. The retained particles were subjected to grinding again and sieved until more than 95 % of the initial material was ground to the desired particle size. Figure 3 shows WEEE before and after the grinding process.

For catalyst preparation, the carbon pellets used were commercial grade with an activated filter for water, and their specification follows in Table 1. NaOH 99 % purity was utilized for preparation of the NaOH solution. Unless specified, all water utilized in these experiments and solution was deionized water.

The activated carbon was further treated with the concentrated NaOH solution to increase the mesopore size structure [57]. A detailed method for preparation of catalyst pellets was described in a previous work [55]. Briefly, the pellets were left in contact with two times their weight of concentrated (50 % wt/wt) NaOH solution for 8 h. Afterwards, the pellets + spent solution mixture was separated using paper filters and washed with deionized water to remove excessive alkali until a pH of 10.0–11.0 was reached in water. The pellets were dried and calcined in a muffle (Linn Elektro Therm, Germany, Model: LM 312 SO 1729) at 600 °C for 3 h at air atmosphere. After this process, the prepared catalyst contained even less carbon and can be called Si–Al ash, as further analysis revealed that the

pellets contained Si and alumina. The wastewater generated by the chemical treatment was neutralized with diluted sulfuric acid solution and discarded. For a scaled-up process, though, considerable optimization of NaOH solution concentration and quantity of wastewater generated would be needed, changing contact efficiency of the catalyst with an alkaline solution, and possibly changing contact time. Even though catalyst quantities used for catalytic upgrading experiments are low (2.5–7.5 %. wt), wastewater generated, and its alkalinity would be unacceptable on a large scale.

**Figure 2.** Knife mill utilized for grinding WEEE plastic to adequate particle size to be fed into the pyrolyzer.

(a) (b)

**Figure 3.** WEEE plastic before (**a**) and after grinding (**b**).

**Table 1.** Specifications of commercial grade carbon pellets for activation.

| Specifications | Units |
|---|---|
| Particle size [mm] | 3.9–4.1 |
| Mean particle diameter [mm] | 4.0 |
| Surface area [$m^2/g$] | 900 |
| Moisture [%] | 5.0 (maximum) |
| Density [$g/cm^3$] | 0.45–0.55 |
| pH | 9.0–11.0 |

### 2.3. Experimental Procedure

The 2-stage catalytic cracking semi-pilot unit was well described in previous work [55 and 56]. Figure 4 presents a schematic diagram of said unit. Experiments were conducted using two types of investigation. First, thermal pyrolysis of WEEE plastic was done over a temperature range (300, 350, 400, and 450 °C) to evaluate product yields. For those experiments, the unit assembly was done using only the batch reactor (R-1) coupled directly to the condensing unit. There was no catalytic fixed bed. This was done to better evaluate process temperature dynamics and choose the temperature that gave better liquid yields for evaluation of the effect of catalyst quantity on product yields and composition. Studying chemical composition of the liquid fraction from thermal pyrolysis helps to understand what happens at the heated catalyst surface in the catalytic experiments, since the vapor composition fed to reactor R-2 should be very similar to the liquid fraction obtained in thermal pyrolysis. Afterwards, the catalytic fixed bed (R-2), composed of an electrically heated (P = 1.5 kW) stainless steel tube (length = 300 mm, i.d. = 15 mm), was coupled between thermal reactor R-1 and the condensing unit, and experiments were tested using different amounts relating to feed weight (2.5, 5.0, 7.5 %. wt) of catalyst pellets so as to simulate longer residence times of vapors in contact with the catalyst at R-2. Even though the electrical heater can supply heat to the entire length of the tube, only the volume occupied by heated catalyst is counted as the catalyst fixed bed, so a higher amount of catalyst corresponds to a bigger catalyst fixed bed.

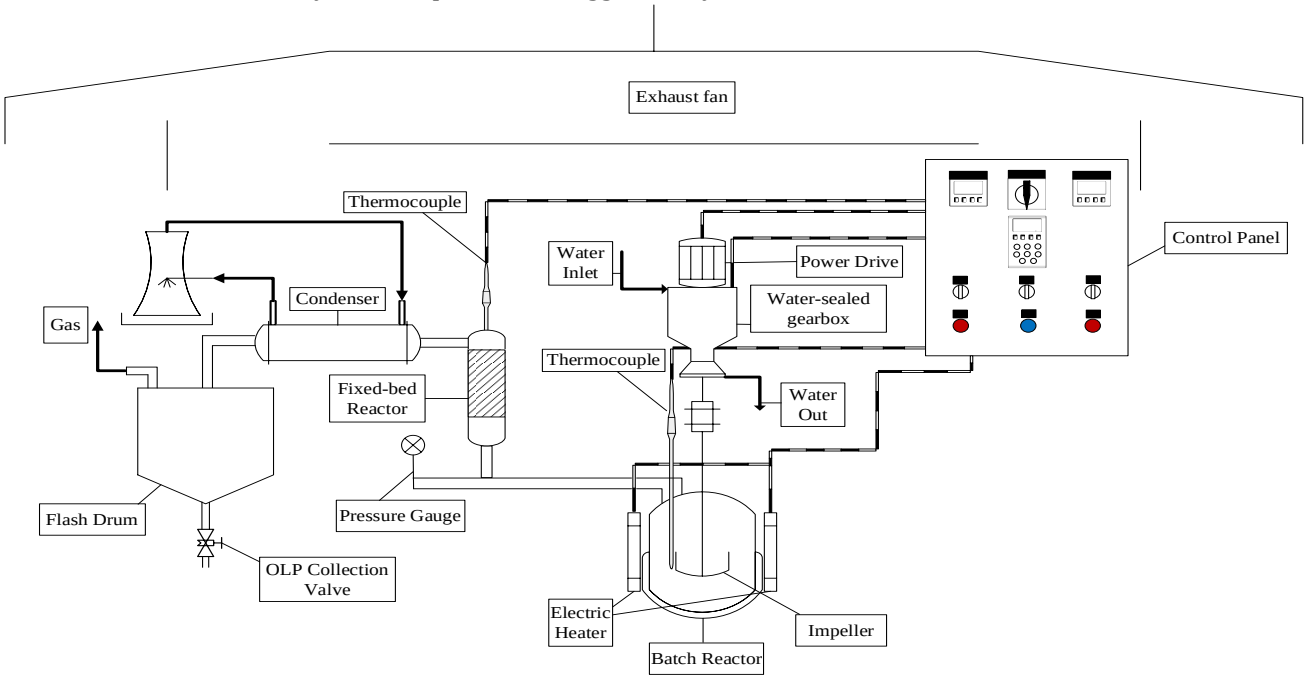


**Figure 4.** Schematic diagram of bench-scale stainless steel catalytic cracking reactor with a pyrolysis/batch reactor and a fixed bed reactor.

A typical run consisted of a few steps, very similar to both sets of experiments. For the thermal cracking experiments, first the unit was prepared by starting the condenser unit and allowing it to reach the desired temperature of 15 °C for the cooling water. Second, the water supply to the mechanical impeller seal was started and verified. Third, reactor R-1 was uncoupled from the system and the WEEE plastic (600 g) was fed manually to the inside of reactor R-1. Then, reactor R-1 was re-coupled to the system, taking care to correctly insert and adjust it to make sure that no gap was observed between the reactor and its cover or considerable torque would be observed in the impeller. As the feed is solid, it is harder to assemble the reactor when compared to feed liquids or semi-liquids as in our previous work [55 and 56]. The reactor was closed and coupled to the system using 8 sets of screws

and bolts having an internal diameter of 12 mm. Each set was composed of one screw and two bolts. The screw-and-bolts sets were assembled in pairs diametrically opposed to each other after securing one pair using a 16 mm tire iron. The subsequent pair was installed in a crosswise manner to the previously secured set-in order to adequately close the reactor and avoid leakage of vapors in the reactor R-1. A graphite seal was also used between the reactor and its cover to further avoid leaks. After reactor setup, operating parameters were set on the control panel as impeller speed (100 rpm), desired final temperature, and heating rate (10 °C/min). To assist in monitoring and control of the process, operating parameters were recorded every 10 min. For each experiment done, the time and temperature of the initial flowing of vapors from reactor R-1 were recorded and samples were withdrawn after 15, 30, 45, and 60 min from the initial time of reaction (vapors flowing out of the vent) to evaluate product composition and physical-chemical characteristics with increasing reaction time. The non-condensable gases were vented or burned at the gas exit line. The reaction was deemed finished when there were no visible vapors flowing out of the gas exit line.

The catalytic experiments were done in similar manner in respect to feed and assembly of reactor R-1, with added steps to set up the catalytic fixed bed reactor R-2. After assembly of reactor R-1, catalyst pellets were added to uncoupled reactor R-2. Glass wool was used before and after catalyst pellets to help secure them and make the vapors flow more evenly through the catalytic fixed bed. The R-2 thermocouple was then inserted, and the reactor was coupled to the system. High temperature rubber seals were used between each flange to avoid leaks in the system. After reactor R-2 setup, operating parameters were set on the control panel for the desired R-2 temperature and heating rate (10 °C/min). It is important to pre-heat the reactor to properly achieve desired pellet temperature before vapors flow out of reactor R-1 and to avoid temperature drop as, initially, cooler vapors meet heated pellets. Because of this, reactor R-2 temperature was controlled initially at 20–30 °C higher than the desired set points.

### *2.4. Feed Characterization*

WEEE plastic was characterized separately with thermogravimetry (TG) analysis for each plastic waste collected (personal computers, monitors, and printers) and for the final mix of the three types. The TG analysis was done on a thermal scale (DTG-60H, Shimadzu, Tokyo, Japan) from 20 to 800 °C using a mass of 5 mg in air atmosphere inside a platinum crucible, using a 10 °C/min heating rate and a gas flow of 5 mL/min.

### *2.5. Physical-Chemical and Chemical Characterization of OLP*

#### 2.5.1. Physical-Chemical Properties of OLP

The physical-chemical characterization of OLP was done by measuring its kinematic viscosity, density, and acid value. The kinematic viscosity was obtained according to adaptation of standard method ASTM D2515 on a temperature-controlled 40 °C thermostatic bath using manual suction. Time was measured manually using a chronometer, and three replicates were done for each sample. Cannon–Fenske viscosimeters of nº 50, 200, and 300 were used depending on estimated viscosity range of samples, and kinematic viscosity was determined using the lower bulb. The density was measured using a methodology adapted from standard method AOCS CC 10c-95 using a 5 mL glass pycnometer calibrated with distilled water. The acid value was determined by titration of 0.2 g of sample dissolved in 50 mL of combined isopropanol/toluene solvent (50/50 %. wt/wt) with 0.1 N KOH standard solution and phenolphthalein as the acid–base indicator. The acid value titration method was adapted from AOCS Cd3d-63 [55 and 56].

#### 2.5.2. Chemical Composition of OLP

The chemical composition of OLP was obtained through GC–MS analysis as detailed elsewhere [58] on a gas chromatographer (CG-7890B, Agilent Technologies, Santa Clara, CA, USA) coupled to a mass spectrometer (MS-5977A, Agilent Technologies). A fused silica SLBTM-5ms capillary column (30 m x 0.25 mm x 0.25 µm) was used. The sample

injector was set at a temperature of 250 °C with a heating rate of 10 ° C/min. 1.0 µL of sample was injected in split mode (1:50). The carrier gas flowrate used was 6.0 mL/min.The column temperature was increased from 60 to 280 °C. The detector was set to 230 °C and the quadrupole temperature was set to 150 °C. The concentrations were expressed in area, as no internal standard was used for comparison of the peak areas.

### *2.6. Characterization of Si–Al Ash Pellets and Chars*

#### 2.6.1. SEM and EDX Analysis

The morphological characterization of the Si–Al ash pellets' surface was performed by scanning electron microscopy using a microscope (Tescan GmbH, Brno, Czech Republic, Model: Vega 3) with 338x, 838x, 1.67kx, 3.33kx, 5.00kx, and 6.67kx magnifications. To prepare samples for analysis, coating with a thin layer of gold was done in the samples using a Sputter Coater (Leica Biosystems, Nußloch, Germany, Model: Balzers SCD 050). Elemental analysis and mapping were carried out by energy dispersive X-ray spectroscopy (Oxford Instruments, Abingdon, UK, Model: Aztec 4.3)

#### 2.6.2. XRD Analysis

The presence of crystalline phases in catalysts and chars was analyzed by X-ray diffraction (PANalytical, Model: Empyrean) at the Laboratory of Mineral Characterization (UFPA). Generator power was 600 W with Cu-tube voltage of 40 kV and current of 35 mA, scanning range of 3 to 90 ° (accuracy = 0.006 °), and PIXEL3D Medpix3 1x1 as the detector.

#### 2.6.3. XRF Analysis

X-ray fluorescence spectrometry was conducted to better identify the composition of catalyst pellets and chars obtained. A WDS spectrometer (PANanalytical, Model: Axios Minerals) at the Laboratory of Mineral Characterization (UFPA). The spectrometer is equipped with a ceramic X-ray tube and a rhodium (Rh) anode was used, and the maximum power level was 2.4 kW. The sample was prepared using 0.5 g of sample, 0.15 g of agglomerant (paraffin), and 3.0 g of substrate material pressed with a 25 ton charge. SuperQ Manager v5.3 software was used to acquire and treat data.

### *2.7. Mass Balances and Calculation of Yield of Reaction Products*

The feed weight was recorded before loading the reactor. Each time, a fraction of the OLPobtained was weighed and added up to find the total mass of OLP obtained. After cooling, reactor R-1 was unmounted, and the char was removed and weighed. The mass of gas was calculated by an integral global mass balance considering the whole semi-pilot unit as the control volume. Integral mass balances are better for analyzing batch or semi-batch processes. Integral mass balances are obtained by integrating a differential mass balance done on the system. Equation (1) describes differential mass balance:

$$\frac{dM}{dt} = \dot{M}_I - \dot{M}_O + G - C \quad (1)$$

where $\dot{M}_I$ and $\dot{M}_O$ are mass flow rates in and out of the delimited control volume, respectively. $G$ and $C$ are terms corresponding to generation and consumption of chemical species by existence of chemical reactions. Even though pyrolysis consists of a variety of chemical reactions, for global mass balances, there is no mass generation or consumption, those terms being important only when one considers a particular chemical species inside the control volume. For global mass balance, $G - C = 0$, and Equation (1) becomes:

$$\frac{dM}{dt} = \dot{M}_I - \dot{M}_O \quad (2)$$

Multiplying Equation (2) by dt and integrating, Equation (3) is obtained:

$$\int_{t_i}^{t_f} \frac{dM}{dt} dt = \int_{t_i}^{t_f} \dot{M}_I dt - \int_{t_i}^{t_f} \dot{M}_O dt$$

$$M_{t_f} - M_{t_i} = \int_{t_i}^{t_f} \dot{M}_I dt - \int_{t_i}^{t_f} \dot{M}_O dt \quad (3)$$

where $M_{t_f}$ corresponds to material remaining in the reactor R-1 at the final time of reaction, $t_f$ ; in this case, the char residue remaining in the reactor, $M_{char}$. $M_{t_i}$ is the initial mass in reactor R-1, corresponding to the mass of WEEE plastic loaded into reactor R-1, $M_{feed}$. There is no mass flow rate being added to the control volume, so $\dot{M}_I = 0$ . $\dot{M}_O$ corresponds to mass flow rates flowing out of the designed control volume, and it represents the pyrolysis vapors flowing out of reactor R-1 and going to the condenser, where it is separated into two fractions, $\dot{M}_{olp}$ and $\dot{M}_{gas}$, so $\dot{M}_O = \dot{M}_{olp} + \dot{M}_{gas}$. Substituting these parameters in Equation (3), Equation (4) is obtained.

$$M_{char} - M_{feed} = -\left[\int_{t_i}^{t_f} \dot{M}_{olp} dt + \int_{t_i}^{t_f} \dot{M}_{gas} dt\right]$$

$$M_{feed} - M_{char} = \int_{t_i}^{t_f} \dot{M}_{olp} dt + \int_{t_i}^{t_f} \dot{M}_{gas} dt \quad (4)$$

Assuming that mass flow rates of OLP and gases are constant, rearrangement of Equation (4) yields the final form of global mass balance for the semi-pilot unit of catalytic upgrading on Equation (5).

$$M_{feed} - M_{char} - M_{olp} = M_{gas} \quad (5)$$

Weighing the amount of feed, solid char, and OLP obtained allows for calculating the mass of non-condensable gases evolved from the semi-pilot unit. Since the amount of gas is indirectly calculated, care must be taken to correctly measure feed, OLP, and char weights, because any fluctuation in these measured quantities will reverberate in gas yields obtained. The solid char corresponds to just the remaining solid residue of reactor R-1, due to the difficulty in accurately weighing the recovered catalyst pellets at the end of experiment runs. Often, the weight of catalyst pellets was lower after runs, due to fragmentation and loss of pellets in the gas stream or during disassembling of the catalyst fixed bed. Since catalyst loading is lower than 10 % of the feed, this loss was assumed to be negligible. The yields of reaction products are calculated in relation to feed weight as follows:

$$Y_{olp}[\%] = \frac{M_{olp}}{M_{feed}} \text{x} 100 \quad (6)$$

$$Y_{char}[\%] = \frac{M_{char}}{M_{feed}} \text{x} 100 \quad (7)$$

$$Y_{gas}[\%] = \frac{M_{gas}}{M_{feed}} \text{x} 100 \quad (8)$$

## 3. Results

### *3.1. Characterization of the Catalyst*

#### 3.1.1. SEM Analysis

Figure 5a–c are different magnifications (838x, 3,300x, and 6,670x) of pellets before any chemical activation process was done. It can be seen that it exhibits a highly porous structure already as per specifications provided in Table 1 of 900 $m^2/g$. Higher magnification (6,670x) reveals the presence of flat-shaped flakes of irregular order. After chemical

activation, SEM images depicted in Figure 6a–c show presence of cavities with sizes between 4.0 and 10.0 μm. By comparing the SEM images depicted in Figures 5 and 6, the effects of treating pellets with a high concentration NaOH solution can be seen. The chemical activation treatment provided more depth to the porous structure and reduced flake sizes. Tseng et al. described how concentrated NaOH solution could be used to increase porosity and surface area of activated carbons and even control it to some degree [57]. The effects of the activated carbon used in this work were not quite as effective as the ones in Tseng et al.'s work [57], probably due to chemical activation being done on the whole pellets as opposed to being done with char powder. The SEM images of Si–Al ash pellets after upgrading of WEEE plastic pyrolysis vapors illustrate the carbon deposition that occurred on the porous surface of catalyst due to gas–solid reactions occurring as pyrolysis vapors flow through the catalyst fixed bed, as shown in Figure 7c and corroborated in Table 2 concerning EDX analysis, as coke deposits form on the surface of catalysts by polymerization of aromatics present in the pyrolysis vapors or during reaction at the gas–solid interface [59]. In fact, Si–Al ash pellets, which were brick red after calcination, became black after catalytic upgrading experiments due to the carbonization that takes place inside the pores of the Si–Al ash catalyst.

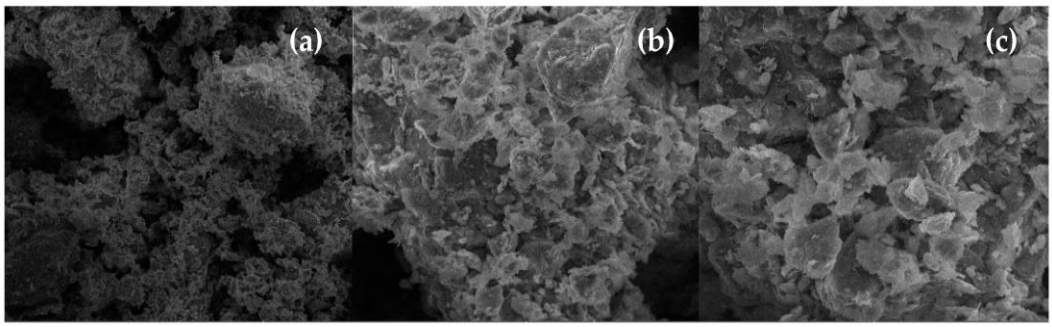


**Figure 5.** SEM of virgin pellets [MAG: 838x (**a**); MAG: 3.33kx (**b**); MAG: 6.67kx (**c**)].

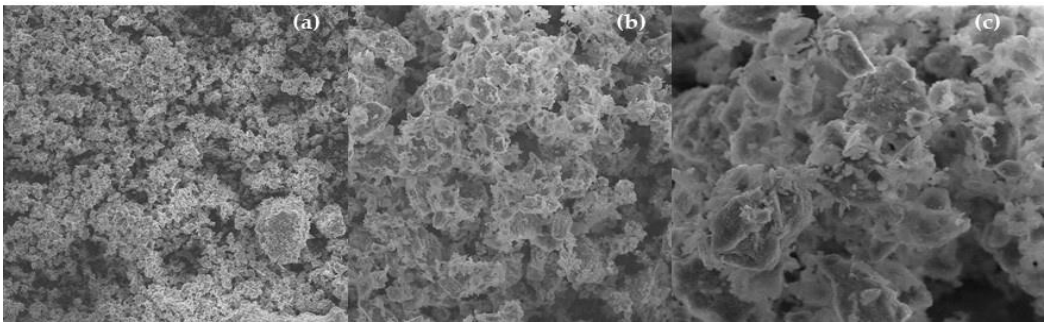


**Figure 6.** SEM of Si–Al ash pellets [MAG: 338x (**a**); MAG: 1.67kx (**b**); MAG: 5.00kx (**c**)].

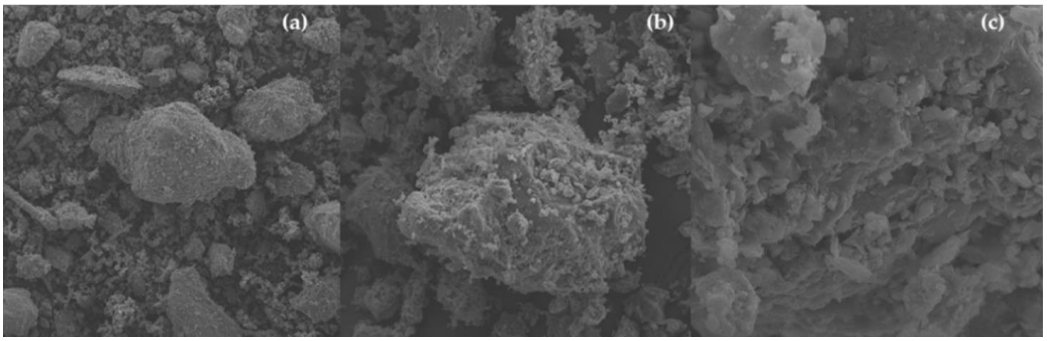


**Figure 7.** SEM of Si–Al ash pellets after catalytic upgrading of WEEE plastic pyrolysis vapors [MAG:838x (**a**); MAG: 3.33kx (**b**); MAG: 6.67kx (**c**)].

**Table 2.** Percentages in mass and atomic mass of virgin pellets, Si–Al ash pellets, and pellets after upgrading experiments.

| | Catalyst | | | | | | | | |
|---|---|---|---|---|---|---|---|---|---|
| | Virgin Pellets | | | Si–Al Ash Pellets | | | Used Si–Al Ash Pellets | | |
| Chemical Elements | Mass [%.wt] | Atomic Mass [%.wt] | SD | Mass [%.wt] | Atomic Mass [%.wt] | SD | Mass [%.wt] | Atomic Mass [%.wt] | SD |
| C | - | - | - | - | - | - | 43.28 | 56.58 | 0.37 |
| O | 58.21 | 72.00 | 0.11 | 61.67 | 74.58 | 0.08 | 31.67 | 31.08 | 0.30 |
| Mg | 0.94 | 0.77 | 0.02 | 1.01 | 0.80 | 0.02 | 0.30 | 0.19 | 0.02 |
| Al | 10.93 | 8.02 | 0.04 | 10.77 | 7.73 | 0.03 | 4.20 | 2.44 | 0.04 |
| Si | 22.49 | 15.85 | 0.07 | 17.88 | 12.32 | 0.04 | 8.67 | 4.85 | 0.07 |
| K | 2.05 | 1.04 | 0.02 | 1.93 | 0.96 | 0.01 | 1.18 | 0.47 | 0.02 |
| Ca | 1.40 | 0.69 | 0.01 | 1.72 | 0.83 | 0.01 | 4.84 | 1.90 | 0.04 |
| Fe | 3.07 | 1.09 | 0.02 | 2.20 | 0.76 | 0.01 | 3.50 | 0.98 | 0.04 |
| Ti | 0.45 | 0.19 | 0.01 | 0.49 | 0.20 | 0.01 | 0.23 | 0.08 | 0.01 |
| Na | 0.40 | 0.34 | 0.03 | 1.82 | 1.53 | 0.02 | 2.05 | 1.40 | 0.04 |
| Mn | 0.06 | 0.02 | 0.01 | 0.05 | 0.02 | 0.01 | 0.08 | 0.02 | 0.01 |

SD = Standard Deviation.

### 3.1.2. EDX Analysis

Table 2 show results from the elemental analysis conducted by dispersive X-ray energy for virgin, ready, and used pellets on the catalytic upgrading of WEEE plastic pyrolysis vapors. According to this analysis, pellets are composed of oxygen (58.21 %), Si (22.49 %), and Al (10.93 %), suggesting composition of silicates ($SiO_x$) and alumina ($Al_2O_3$). Chemical treatment with concentrated sodium hydroxide lowered levels of Si as expected. Silicates react with NaOH, producing a soluble compound and water as per the following chemical reaction [60]:

$$SiO_2 + 6(NaOH)_{H_2O(L)} \rightarrow (Si_4O_{11}Na_6)_{H_2O(L)} + 3H_2O$$

This reaction is responsible for the increase in surface area and catalyst porosity, facilitating access of pyrolysis vapors inside the pores and active sites of the catalyst. There was a slight increase in sodium levels, probably due to adsorption and impregnation of some active sites with sodium oxide hydrates, also shown in the XRD analysis of Figure 8. After upgrading experiments on WEEE plastic pyrolysis vapors, coke deposits formed, increasing carbon content to 43.28 %. The high carbon deposition suggests rapiddeactivation of the catalyst, a troubling indication for packed bed operations, since the catalyst would need costly regeneration routines and generate unsecure conditions due to the possibility of plugging of the catalyst fixed bed with a dangerous pressure increase in the vessels. Considering semi-batch operations, whole batches could suffer from bad quality due to a recently deactivated catalyst. The authors wrote about reasons for catalyst activity loss in OLP upgrading experiments. In general, there are two main methods ofcatalyst deactivation: one is reversible deactivation over time, and the other is irreversible deactivation over regeneration cycles [61–64]. Oxygenated compounds like acids cause generation of coke deposits on active sites of metal oxide, and the coating of active sites results in loss of activity by preventing vapors access to the inside surfaces of the catalyst, causing reversible deactivation. Regeneration of the catalyst through burning of carbon deposits is then possible, but subsequent regeneration cycles tend to cause irreversible deactivation through sintering and poisoning of the catalyst active site at high temperatures required for regeneration [61 and 62]. The appearance of carbon deposits also shows that vaporscould reach the insides of pores and active sites of catalysts, since coke-forming reactionstend to occur in later stages of cracking [59 and 65].

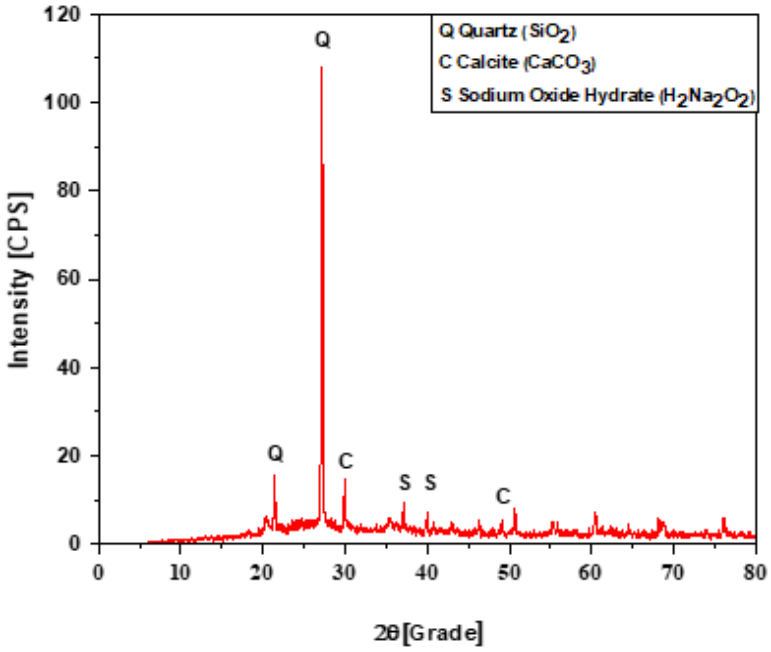


**Figure 8.** XRD of Si–Al Ash catalyst pellets.

### 3.1.3. XRD Analysis

The XRD diffractogram of the chemically treated pellets is shown in Figure 8. Three crystalline phases were observed, in accordance with the XRF analysis shown in Table 3, showing peaks for quartz ($SiO_2$) at positions 2θ: 26.6 and 2θ: 20.8; calcite ($CaCO_3$) peaks at position 2θ: 29.4 and another of low intensity at position 2θ: 48.6; and sodium oxide hydrate ($H_2Na_2O_2$) showed 2 peaks on positions 2θ: 37.1 and 2θ: 40.8. As was determined by EDX analysis (Table 3), pellets are composed of silica ($SiO_2$), and the NaOH treatment added some crystalline phases to the catalyst structure like calcite and sodium oxide, formed by residual NaOH present in catalyst pellets after calcination. Figure 9 shows the XRD diffractogram of carbon pellets after upgrading experiments of WEEE plastic OLP, suggesting that heating and contact with pyrolysis vapors had little effect on the present crystalline phases. Even though EDX and SEM analysis revealed presence of carbon deposits (coke), DRX analysis could not show crystalline phases for carbon. No leaching of the mineralogical part of the pellets was done, so it is hard to observe peaks for graphitic carbon in the catalyst sample.

**Table 3.** Composition of chemically Si–Al ash pellets used as the catalyst for catalytic upgrading experiments, obtained by way of XRF fluorescence.

| Component | %.wt/wt |
|---|---|
| $SiO_2$ | 44.01 |
| $Al_2O_3$ | 15.59 |
| $Fe_2O_3$ | 6.28 |
| CaO | 5.21 |
| MgO | 1.19 |
| $TiO_2$ | 0.95 |
| $P_2O_5$ | 0.12 |
| $Na_2O$ | 3.92 |
| $K_2O$ | 2.14 |
| Fire loss | 20.59 |

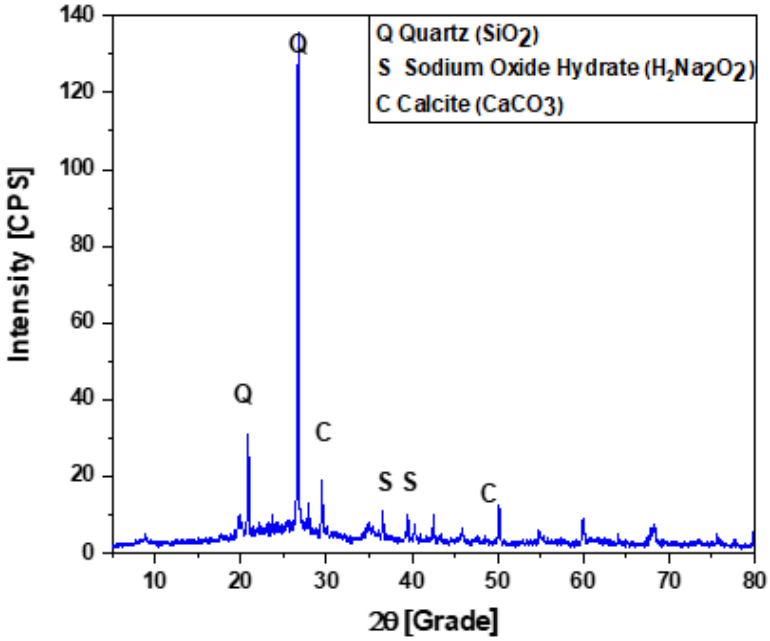


**Figure 9.** XRD of Si–Al ash pellets after upgrading experiments.

#### 3.1.4. XRF Analysis

The XRF analysis of the Si–Al ash pellets is presented in Table 3 and confirms the presence of $SiO_2$ with 44.0 %.wt, 15.6 %.wt $Al_2O_3$, 6.0 %.wt of $Fe_2O_3$, and CaO 5.2 %.wt. The sample showed 20.6 % weight loss in the fire loss experiment, revealing it to be composed of a largely inorganic matrix. As hinted at earlier by elemental analysis of Table 3, the prepared catalyst contains minimal amounts of carbon and, after calcination in air atmosphere at 600 °C, most carbon content was burned or decomposed; the remaining ash was composed of silica and aluminum oxides, effectively being the catalyst used.

### *3.2. Feed Characterization (TG Analysis)*

Due to the nature of the WEEE plastic used in the thermal and catalytic experiments, a TG analysis was conducted for each material comprising the plastic waste. Figure 10 corresponds to the TG analysis done for monitors, PCs, printers, and a mix of them. The TG analyses were compared to analysis of pure samples of polymers commonly used as casings for computer-related paraphernalia, such as high impact polystyrene (HIPS), acrylonitrile-butadiene-styrene copolymer (ABS), polycarbonate (PC), and polyvinylchloride (PVC) [40]. It can be observed that all three computer parts composing the mix have distinct weight loss patterns. The monitors' TG show one peak of weight loss at around 400 °C. Hall et al. analyzed samples of computer monitors through TG analysis and found a similar pattern of one peak decomposition for all three different samples analyzed. They concluded the material was composed of ABS copolymer [40]. The early decomposition of CPU cabinets could mean the presence of flame retardants as brominated compounds or PVC [66]. Polycarbonate exhibits decomposition at higher temperatures, around 450–500°C, and PC/ABS blends show similar decomposition patterns as the printers in this work [67]. The high temperature decomposition peaks observed for the materials could mean presence of polycarbonate. Roussi et al. commented about the fact that blends of polymers can degrade at lower temperatures due to radicals formed on thermal decomposition, initiating further degradation [68]. Indeed, thermal pyrolysis was initiated at low temperatures, and a high quantity of gases was obtained. Jung et al. conducted thermal pyrolysis of brominated ABS (Br–ABS) on a fluidized bed reactor and obtained similar results to those of this work, with respect to chemical composition of OLP, yields, and TG analysis, even though the system used was largely different [69]. The mix of the three different computer plastics showed a pattern of weight loss combining the three other materials

comprising thefeedstock, obviously. Degradation of combined samples initiated with lower temperatures and the pyrolysis experiments showed the same behavior, confirming the presence of flame retardants or PVC. The GC-MS analysis could not identify chlorinated compounds but showed the presence of brominated compounds in minor fraction as bromophenols.

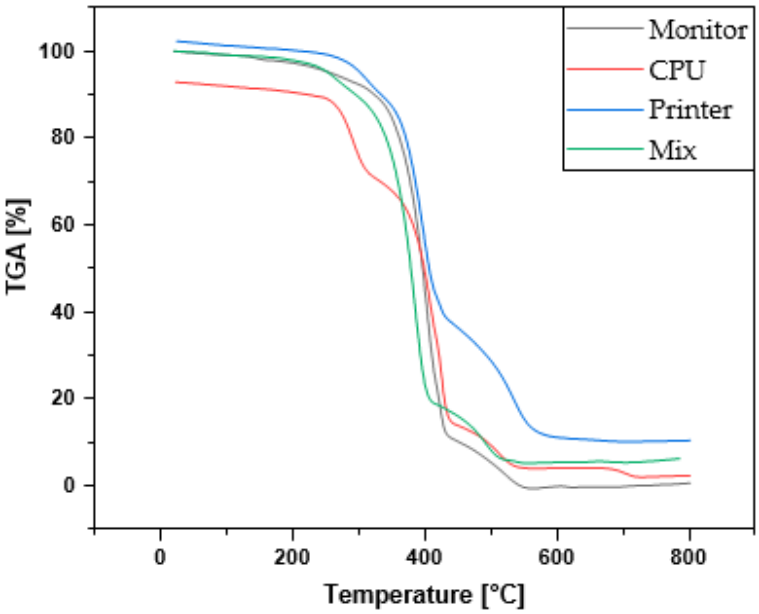


**Figure 10.** TG analysis of different computer parts comprising the mixed WEEE plastic feed used for thermal and catalytic cracking experiments.

### *3.3. Investigation of Thermal Cracking of WEEE Plastic*

#### 3.3.1. Mass Balance and Yield of Reaction Products

As it was stated previously in Section 2.3, first an investigation was done on thermal cracking of WEEE plastic, without a catalyst fixed bed, over a determined range of temperature (350–500 °C) to evaluate process conditions, yields, chemical composition of OLP, and time evolution of the process. Table 4 shows process parameters and yields obtained over the temperature range used on thermal cracking.

**Table 4.** Mass balance and yields of reaction products of thermal cracking of WEEE plastic over the temperature range of 350–500 °C.

| Process Parameters | Temperature [°C] | | | |
|---|---|---|---|---|
| | 350 | 400 | 450 | 500 |
| Mass of plastic waste [g] | 600.5 | 600.5 | 600.5 | 615.0 |
| Cracking time [min] | 120 | 120 | 120 | 120 |
| Mass of solids (coke) [g] | 115.1 | 128.8 | 149.8 | 112.5 |
| Mass of liquids (OLP) [g] | 232.9 | 357.0 | 382.5 | 393.1 |
| Mass of gas [g] | 252.5 | 114.7 | 68.2 | 109.4 |
| Yield of liquids [%] | 38.78 | 59.45 | 63.70 | 63.92 |
| Yield of solids [%] | 19.17 | 21.45 | 24.94 | 18.29 |
| Yield of gas [%] | 42.05 | 34.22 | 11.36 | 17.79 |

Table 4 shows yields of OLP and char increasing with temperature, while that of gaseous products reduces, as depicted graphically in Figure 11. OLP yields increased by 64.82 % at 500 °C in relation to the initial bio-oil yield of 38.78 % at a temperature of 350 °C. OLP yields are consistent with what is found in the academic literature [70 and

71]. Jung et al. [70] pyrolyzed high-impact polystyrene (HIPS) and acrylonitrile-butadiene-styrene (ABS copolymer) in a fluidized bed fast pyrolysis reactor and found yields ranging from 70–87 % for HIPS and 62–84 % for ABS over a temperature range of 410–550 °C. The higher yields of liquids are probably due to a more efficient heat transfer obtained by fluidized bed fast pyrolysis when compared to a fixed bed reactor (slow pyrolysis). Slow pyrolysis reactors, such as the electrically heated fixed bed reactor utilized in this work, show lower heat transfer rates (especially when pyrolyzing solid material) than fluidized bed fast pyrolysis reactors. Lower heat transfer rates are associated with lower OLP yields and higher solid fraction (char) yields for lignocellulosic biomass [72]. Even though there is large difference between polymeric material present in WEEE and lignocellulosic biomass, the same behavior is demonstrated here concerning heat rates and pyrolysis reactors. Studies showed that conventional fixed bed pyrolysis of ABS produces lower OLP yields when compared to fluidized bed fast pyrolysis of the same material [69 and 71], corroborating the same behavior for ABS containing polymers. Bhaskar et al. [71] pyrolyzed ABS copolymers in a laboratory scale fixed bed reactor and found liquid yields of 39%, consistent with the yields found in this work.

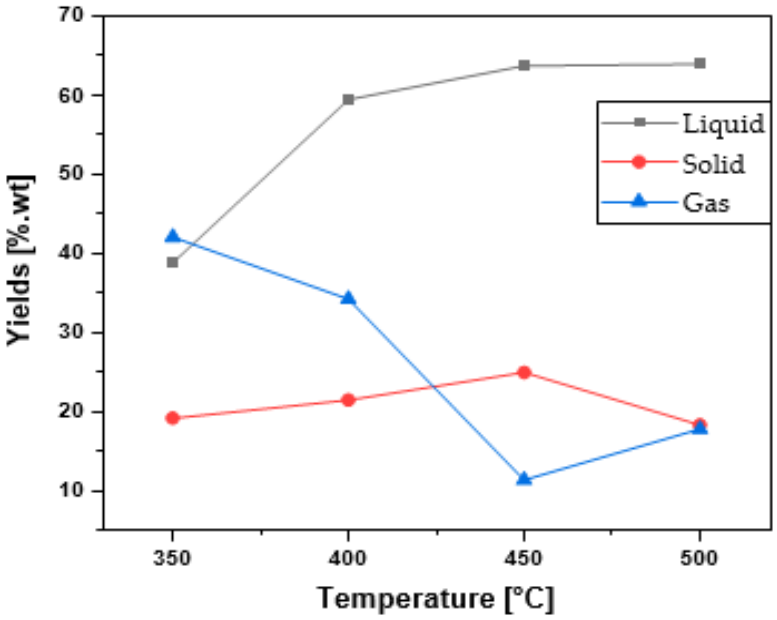


**Figure 11.** Effect of temperature on yields of products obtained through thermal cracking of WEEE plastics.

The plastic feed used in the semi-pilot unit showed a tendency to form gases and liquid products at low temperatures, as low as 200 °C, as evidenced by the TG analysis done in Figure 12, which shows small peaks of weight loss starting at 143 °C to 289 °C, with a combined weight loss of 9.7%. Some polymers containing flame retardants exhibit the tendency to depolymerize at low temperatures, including those found among WEEE plastics, such as ABS [69 and 71]. Normally, reactions occurring by thermal decomposition are endothermic and, because of this, reactor R-1 could only supply heat for occurring reactions, maintaining the reaction temperature until most products that had initially formed at the corresponding temperature had distillated to the condensing unit. Only then, would the reaction proceed and reach higher temperatures in reactor R-1. That said, the defined temperatures chosen to correspond to the final temperatures reached and maintained until no more vapors or liquid products could be collected. This is why we decided to investigate lower temperatures for the thermal cracking experiments, until the maximum designed temperature allowed for reactor R-1 of 500 °C.

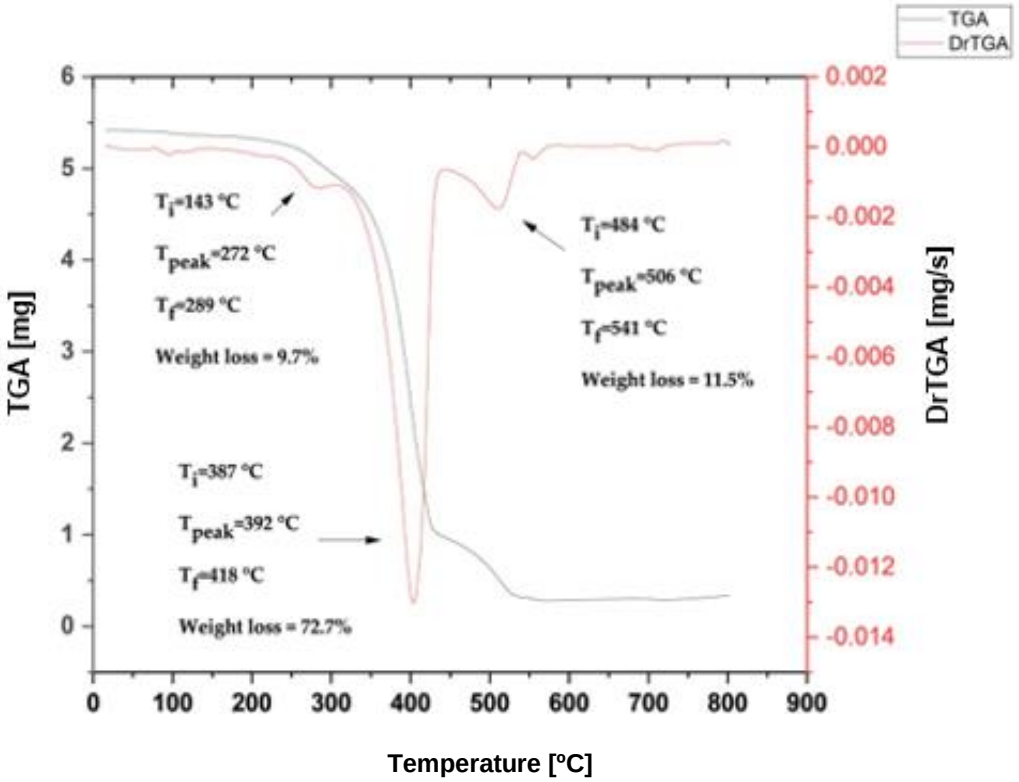


**Figure 12.** TG analysis of WEEE plastic feedstock.

At a first glance, temperature effects on OLP yields seem different from what is observed for most plastic feeds, where liquid fractions tend to decrease with increasing temperature [73–77]. Temperature is a key parameter affecting product yields [8], as higher temperatures are said to promote cracking reactions occurring along the polymeric chains of plastic feed. Additionally, temperature affects the initial products formed, producing smaller, more volatile substances, thus reducing yields of liquid and solid fractions, but increasing gas quantity [73–77]. As was stated earlier, though, cracking reactions are endothermic and proper temperature control of such processes is no easy task, especially when considering a semi-batch fixed bed reactor. In order to control process temperature, one needs to design reactors and process parameters capable of supplying enough heat to overcome the energy needs of occurring endothermic reactions. Research focused on study temperature effects on yields of pyrolysis products achieve desired temperatures in a variety of ways, including using small quantities of feed [75, 76, and 78], pressurized vessels [77], fluidized bed reactors with pre-heated inert beds [73], 2-stage vapor cracking [25], and high heating rates [75 and 76]. In our case, the reaction temperature indicates the extent at which the material was pyrolyzed, much like thermogravimetry analysis. The TGA of Figure 12 shows the highest peak of weight loss between 400 and 450 °C, so one could make the assumption that liquid and/or gas yields increase until after that temperature range. In fact, OLP yields shown in Figure 10 increased until reaching a plateau at around 450–500 °C. The temperature range investigated is located around the zones with higher weight loss demonstrated by the TG analysis, so liquid yields tend to increase with increasing temperature. Studies focusing on temperature effects on plastic pyrolysis yields investigated higher temperatures (usually over 500 °C), having some sort of control over the degradation temperature used [73, 74, and 76]. The studies investigating lower temperatures also found that liquid yields tend to increase until the 450–500 °C range [75, 77, and 78]. Miskolczi et al. [79] reported the same behavior for flame retardant ABS polymer: liquid yields increasing in a temperature range of 360–440 °C.

Observing the TG analysis of Figure 12, it is expected that high yields of solid fraction would be obtained for temperatures below 400 °C, since little weight loss was observed (9.7 %). Instead, solid yields remained in the range of 20 % for all experiments, and a

high yield of gases was achieved for 350 and 400 °C, of 42.05 % and 34.22 %, respectively. This happened because experiments were conducted until no more vapors flowed out of reactor R-1. Temperatures were maintained on setpoints even when higher temperatures could be achieved and the time required to thermally degrade samples was constant throughout all experiments, as shown in Table 4. From previous work with the same unit [55 and 56], one can observe that solid fraction yields are influenced by the extent of reaction, i.e., low reaction times mean a higher yield of solids. Maintaining reaction at temperatures below the highest peak observed in the TG had a marked influence on gas yields, producing a high quantity of gases. This differs considerably from other work, where low yields of gas were obtained for the pyrolysis of flame-retardant ABS using temperatures exceeding 400 °C [69–71, and 79]. Authors commented on the fact that flame-retardant ABS polymers can produce gases such as HCN and $NH_3$ for ABS at low temperature pyrolysis by cyclization of acrylonitrile units [79 and 80], and halogenated containing polymers like PVC produce HCl [76]. Brominated compounds are also thought to be produced at low temperatures for flame-retardant ABS [71]. Nitrogenated compounds accumulate in the liquid fraction of ABS pyrolysis [80], and low pyrolysis temperature programs can be one way of lowering these compounds' concentration in the OLP by producing N-containing gases. Brebu et al. conducted thermal degradation of ABS copolymers and found out that a programmed step of 300 °C for a set amount of time could reduce nitrogenated compounds in the OLP composition [80]. The pyrolysis process done in the semi-pilot unit differs considerably from the TG analysis with respect to temperature control when the desired setpoint temperature is lower than 450 °C. Due to the amount of WEEE plastic loaded into reactor R-1 and power supplied by the electrical heater (2.5 kW), the pyrolysis temperature could not reach values beyond 400 °C until most of the feed had cracked and vaporized. Therefore, only for the experiments done using setpoint temperatures of 350 °C and 400 °C could a desired temperature control around the reaction temperature be adequately maintained until no more vapors flowed out of the reactor. For experiments with a setpoint of 450 and 500 °C, the reaction temperature was increased using a heating rate of 10 °C/min until reaching cracking and flowing of vapors out of the reactor, and this was maintained until reaching 450 and 500 °C, respectively. The time of reaction was the same for all experiments, though, and seems to be related to feed weight loaded into reactor R-1. Maintaining reaction at lower temperature stages seems to influence product quality, and further physical–chemical analysis shows that lower acid values were obtained for experiments done using 350 °C as the setpoint. Further analysis of gas composition should be done to evaluate this effect, and since gas quantity generated was measured by difference, fluctuations in weight readings of other variables can profoundly affect the gas yields. Details of low temperature cracking of WEEE plastics could be the subject of upcoming papers.

A black solid fraction remained as a residue inside the fixed bed reactor. This product can be classified as a charcoal or char, composed of amorphous and crystalline carbon, including a fraction of high boiling point hydrocarbon compounds such as polycyclic aromatic hydrocarbons (PAH) and aliphatic compounds with long carbon chains ($C_{100}$–$C_{200}$) [59]. PAH and the asphalt-like compounds of high carbon numbers are the last products formed by polymerization, aromatization, and condensation reactions that occur in later stages of cracking before turning into elemental carbon [59 and 65]. Even though there is considerable difference among structures of different polymers, the char formed presents a relatively consistent chemical composition throughout all plastic feedstocks; the quantity and composition of PAH and long chain hydrocarbons in char are dependent on variables like feedstock type, temperature, heating rate, time of reaction, and process design [81]. For instance, it is possible to conduct pyrolysis of plastic until little to no char is produced due to primary depolymerization reactions dominating the reaction mechanism, reducing the extent of aromatization, condensation, and polymerization forming the char precursors (PAH) [59 and 81]. The XRF analysis revealed that 91.0% was composed of carbon and 2.76 % of bromine (Br), confirming that WEEE plastic is composed of flame-retardant Br–ABS. The XRD analysis of the obtained char in thermal experiments at 450 °C is presented in Figure 13.

No leaching of the mineralogical part was done to really look at the carbon structure present [82]; instead, the high peaks observed are due to inorganic components present, such as titanium dioxide, commonly used as a pigment for this type of plastic [83 and 84]. We also investigated presence of other types of inorganic flame-retardants, such as $Sb_2O_3$ [85]. Major peaks were found at positions 2θ of 25.6, 32.0, and 36.4 °.

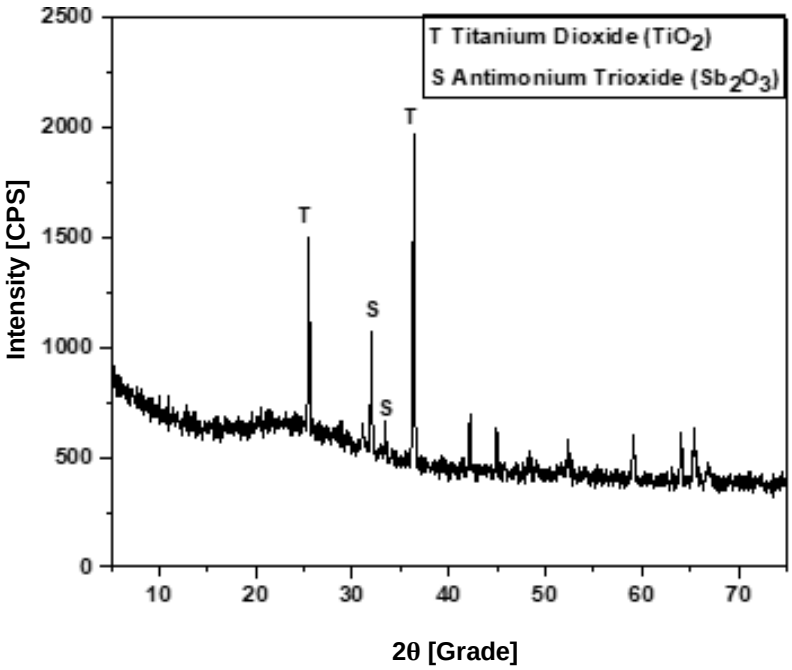


**Figure 13.** XRD analysis of char obtained through thermal cracking experiments at 450 °C of WEEE plastic.

Char yields showed a slight tendency to increase from 350 to 450 °C for our WEEE feed- stock, in accordance with the academic literature, where higher temperature and residence time of remaining feed inside the reactor allow the reaction to reach the later stages, where condensation and polymerization reactions occur between reaction products [59]. Between 450–500 °C, the last decomposition peak showed by TG analysis occurs, possibly due to polycarbonate cracking [67]. Indeed, the char yield reduced from 450 to 500 °C, while the gas yield increased with no increase in the liquid fraction. Further investigation of this temperature range and gas analysis of the system could be the subject of upcoming papers.

### 3.3.2. Physical–Chemical Properties and Chemical Composition of ThermalCracking OLP

The OLP obtained through thermal cracking had a standard aspect when considering plastic feedstock, being a dark liquid of acrid odor with some sort of green or red hue to it. As the OLP obtained was fractioned in samples given a predetermined reaction time, the weighted average of each physical-chemical property was calculated using the individual values of measured properties and their respective mass of collected OLP at a given reaction time. The measured properties and their respective mass fractions are shown in Table 5 along with the weighted averages of properties at their respective run temperatures. Mean density of OLP remained between 0.92–0.94 g/cm$^3$ and kinematic viscosity between 1.24–1.44 mm$^2$/s. These values can be compared to other work in which the thermal degradation of commonly used plastics for WEEE was conducted. Plastics considered are HIPS, ABS, PC, and PVC. Brebu et al. conducted thermal degradation experiments of ABS on a fixed bed glass reactor at 450 °C and obtained densities of 0.89 g/cm$^3$ for the OLP [80]. The viscosities of the WEEE OLP showed values similar to other plastic feedstock pyrolysis oils. The OLP from plastic feedstocks shows lower viscosities whencompared to other feeds, such as lignocellulosic material or lipid-based ones [55, 56, and 58].This is associated with the presence of aromatic compounds and volatiles, not commonlypresent for triglyceride material, in the case of thermal cracking.

Plastic feedstock OLP seems richer in compounds of higher volatility (gasoline range) while lipid-based ones present longer chain alkanes and alkenes (diesel range) [55 and 56]. The acid values shown in the samples are linked to the presence of acidic and oxygenated compounds. The chemical composition analysis showed the presence of phenolic compounds possibly related to the presence of polycarbonates in the composition of WEEE [67], probably responsible for a major fraction of acidity of the samples. The experiments done at 350 °C showed lower acidities and presented high gas yields, indicating the presence of decarboxylation reactions happening with those oxygenated compounds.

**Table 5.** Weighted average of determined physical–chemical properties and their respective measured properties of time fractions for thermal experiments.

| Temperature [°C] | Reaction Time [min] | OLP Quantity [g] | Density [g/cm$^3$] | Kinematic Viscosity [mm$^2$/s] | Acid Value [mg KOH/g] |
|---|---|---|---|---|---|
| 350 | 15 | 96.5 | 0.92 | 1.30 | 26.9 |
| | 30 | 82.5 | 0.92 | 1.33 | 27.7 |
| | 45 | 53.9 | 0.92 | 1.44 | 27.5 |
| | **Total** | **232.9** | **0.92** | **1.34** | **27.4** |
| 400 | 15 | 100.2 | 0.91 | 0.98 | 80.9 |
| | 30 | 101.3 | 0.93 | 1.35 | 26.2 |
| | 45 | 98.2 | 0.94 | 1.38 | 31.7 |
| | 60 | 57.3 | 0.95 | 1.26 | 48.8 |
| | **Total** | **357.0** | **0.93** | **1.24** | **46.7** |
| 450 | 15 | 103.2 | 0.91 | 1.46 | 33.0 |
| | 30 | 95.5 | 0.98 | 1.36 | 24.8 |
| | 45 | 94.7 | 0.96 | 1.36 | 77 |
| | 60 | 89.1 | 0.91 | 1.32 | 28.3 |
| | **Total** | **382.5** | **0.94** | **1.38** | **40.8** |
| 500 | 15 | 85.9 | 0.95 | 1.50 | 134.0 |
| | 30 | 97.8 | 0.91 | 1.56 | 23.1 |
| | 45 | 150.3 | 0.92 | 1.38 | 18.1 |
| | 60 | 59.1 | 0.96 | 1.31 | 84.7 |
| | **Total** | **393.1** | **0.93** | **1.44** | **54.7** |

The chemical compositions of each time fraction were also determined by GC-MS and are available as tables in the Supplementary Materials. Mostly, the OLP is comprised of aromatic hydrocarbons such as benzene derivatives (benzene, 1,1′-(1,3-propanediyl) bis- and benzene(1-methylethyl)-); styrene derivatives (styrene and methyl-styrene); nitrogenated compounds derived from nitriles such as benzene butane–nitrile and other nitrogenated aromatic compounds; and PAH such as ramified naphthalenes and phenolic compounds (phenol and cumenol). The thermal degradation of polymers is said to function on a random scission model [66], and the styrene and acrylonitrile derivatives are indicative of the feed matrix being composed of ABS, while the phenolic compounds formed indicate presence of polycarbonate material. No chlorinated compounds were detected in the GC-MS analysis, indicating that the feed material did not contain PVC. The high amount of nitrogenated compounds suggests that gas formed on the thermal experiments as nitrogen related gases HCN or $NH_3$ [79 and 80]. Those compounds detected were mainly formed by scission of bonds, but they could also be formed between highly reactive intermediary compounds formed during cracking. Benzene butane–nitrile seem to be formed in the reaction between a styrene unit and acrylonitrile [71]. The chemical functions of each OLP obtained at different temperatures (350–500 °C) are presented as a function of reaction time in Figure 14.

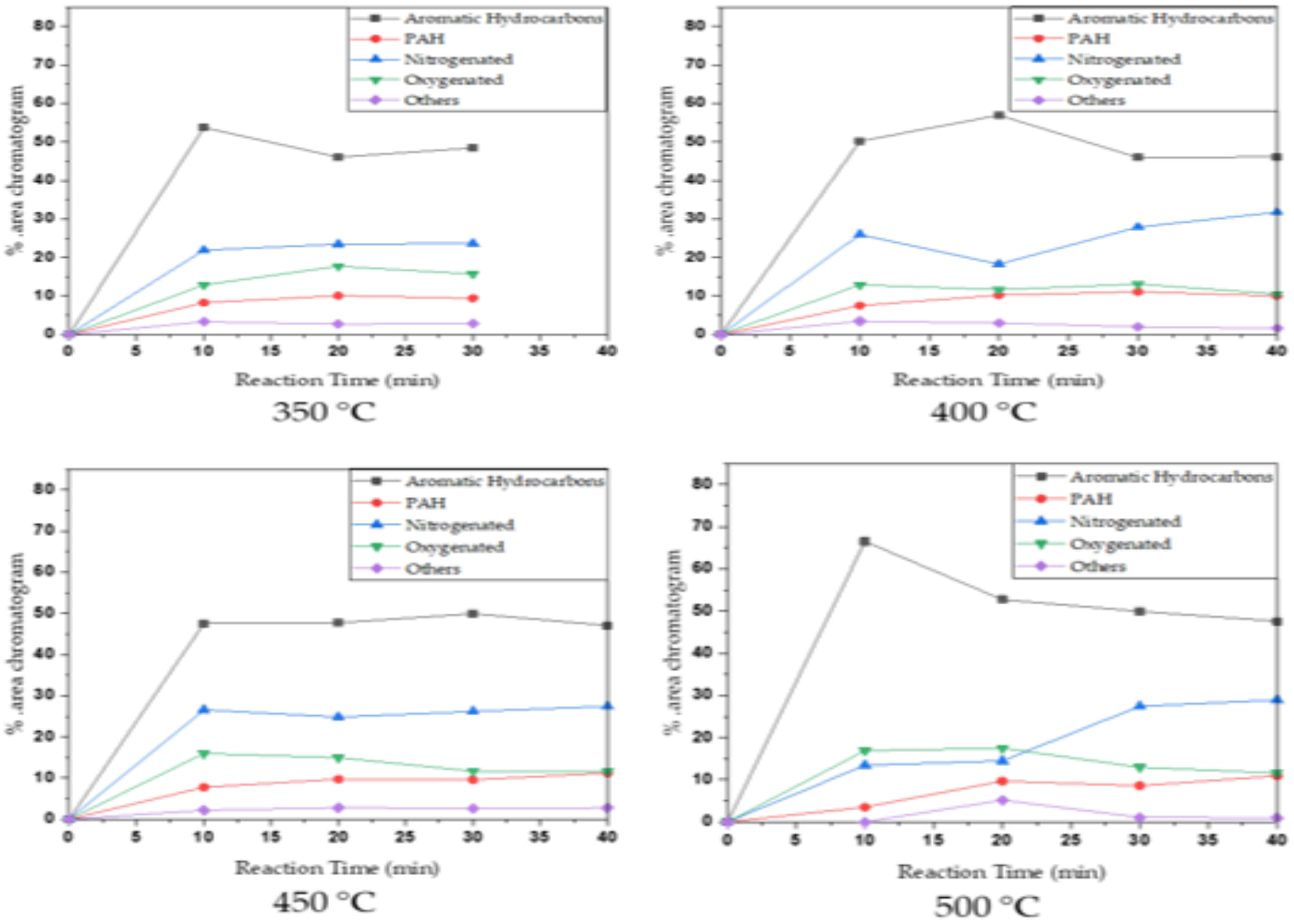


**Figure 14.** Time behavior of chemical functions present in thermal cracking of WEEE plastic at 350, 400, 450, and 500 °C.

The evaluation of chemical functions with reaction time revealed presence of aromatic hydrocarbons in the range of 45 to 70 %; nitrogenated compounds as aromatic nitriles and benzene butane–nitrile in the range of 20–30 %; and the presence of PAH increasing with reaction time, indicating the evolution of cracking reactions until polymerization of aromatic compounds and formation of char. The oxygenated compounds were phenols and ketones, while the other fraction corresponds to non-identified compounds. The fraction of nitrogenated compounds seems to be related to the reaction temperature, increasing to the range of 30 % for 400 °C and 500 °C. Lower fractions of nitrogenated compounds were obtained using 350 °C, and we already commented on the possibility of rejecting nitrogen in the gas stream as $NH_3$ or HCN. Overall, the evolution of chemical function fractions of the thermal cracking experiments presented constant compositions, despite being a semi-batch reactor where the feed composition changes as vapors are formed, suggesting that thermal decomposition of WEEE plastics occurs, forming the same chemical species throughout the entire reaction time, possibly due to uniform decomposition of the entire feed. Indeed, thermal decomposition of plastic polymers is said to function on a random radical scission model where the same smaller molecules are formed and vaporized continuously, consuming heat supplied by an electrical heater and maintaining the remainder of the feed almost unchanged [66]. This thermal decomposition behavior may explain why some polymers produce high yields of their respective monomers, such as decomposition of polystyrene generating high yields of styrene monomer [86].

A previous work using the same analysis in the same pyrolysis unit but using a different feedstock, waste animal fat [56], showed that chemical composition of OLP obtained through thermal pyrolysis suffers radical changes with reaction time, where initially the feed is largely composed of fatty acids and, in later stages of reaction, converts itself almost entirely to aliphatic hydrocarbons, indicating that the mechanism of thermal decomposition of lipid based materials follows a largely different route. Composition and physical–chemical analysis of fractioned samples of OLP considering reaction time is a powerful tool to analyze process evolution and even reaction mechanisms.

### *3.4. Upgrading of WEEE Plastic Pyrolysis Vapors Over Chemically Treated Carbon Pellets*

#### 3.4.1. Mass Balance and Yield of Reaction Products

After testing and acquiring some knowledge about thermal cracking of the WEEE plastic feedstock, the catalyst fixed bed was coupled and loaded with catalyst pellets to conduct experiments of catalytic upgrading using 2.5, 5.0, and 7.5 %.wt. of the catalyst related to the weight of the feed at 450 °C. The reasons behind using 450 °C for the catalytic experiments include the excellent yield of OLP obtained in thermal experiments and consistency of chemical functions present in the OLP. In the case of upgrading experiments, the catalyst fixed bed was always maintained at 450 °C, even when the reactor was producing vapors at a low temperature. Table 6 presents the results of mass balance and yield of reaction products.

**Table 6.** Mass balance and yields of reaction products of catalytic upgrading of WEEE plastic pyrolysis vapors over catalyst fixed bed of 0.0, 2.5, 5.0, and 7.5 %.wt at 450 °C.

| Process Parameters | Catalyst Quantity [%.wt] | | | |
|---|---|---|---|---|
| | 0.0 | 2.5 | 5.0 | 7.5 |
| Mass of plastic waste [g] | 600.5 | 600.5 | 600.5 | 600.5 |
| Cracking time [min] | 120 | 120 | 120 | 120 |
| Mass of solids (coke) [g] | 149.8 | 70.5 | 104.6 | 148.3 |
| Mass of liquids (OLP) [g] | 382.5 | 437.7 | 417.2 | 418.4 |
| Mass of gas [g] | 68.2 | 92.3 | 78.6 | 33.8 |
| Yield of liquids [%] | 63.70 | 72.88 | 69.47 | 69.67 |
| Yield of solids [%] | 24.94 | 11.74 | 17.42 | 24.70 |
| Yield of gas [%] | 11.36 | 15.37 | 13.09 | 5.63 |

It can be observed that the use of the catalyst slightly improved OLP yields, while reducing gas and solid yields, when compared to thermal experiments done using 450 °C as the setpoint temperature. With respect to catalyst quantity, solid yields increased, while gas yields decreased. OLP yields remained in the range of 70 %. Muhammad et al. conducted catalytic upgrading experiments using a 2-stage vapor cracking reactor at 500 °C and obtained similar results for the degradation of ABS copolymers [14]. They used zeolite Y and HZSM-5 as catalysts with a C/F (catalyst-to-feed ratio) of 1. Hall et al. pyrolyzed Br–ABS in a fixed bed reactor containing zeolite Y and HZSM-5 as catalysts and found low yields of liquid in the range of 24–35 % and a low quantity of gas. They used a C/F of 1 at 440 °C. A significant amount of coke was deposited on the surface of the catalysts [38]. Ma et al. conducted upgrading experiments with Br–ABS at 450 °C with different C/F ratios of 0.02, 0.2, and 0.4 using HZSM-5 and a Fe-loaded catalyst to determine influence on yields of products. They reported yields very similar to the ones obtained in this work, with over 80 % of OLP yield and 13 % for gas [52]. They commented on the fact that the high surface area provided by the catalyst and acidic sites contributed to plastic decomposition. The Fe catalyst with lower acidity than HZSM-5 promoted higher OLP yields since higher acidity contributes to gas formation. Indeed, gas yields tended to reduce with increasing catalyst content. The higher amount of char formed may be related to the increase in residence time of vapors inside the thermal reactor because of increased pressure due to the catalyst fixed bed being in place. A similar effect was observed in previous experiments made using the same unit [55 and 56].

It is possible that some reflux occurs due to the increased pressure drop of the catalyst fixed bed being in place, affecting products in reactor R-1, including char quality and yields. The extent of the reflux, if any, is affected by the specific configuration used in the semi-pilot unit, where reactor R-2 is vertically positioned, increasing pressuredrop through the catalyst fixed bed. This is also affected by the tube diameter of reactor R-2 and the shape of the packed bed particles, influencing how pyrolysis vapors flow through the catalyst bed. The surface area of catalyst pellets also increases residence time and contact with a hot surface. The increased residence time allows the reaction to reach the later stage, producing PAH and carbon, forming the residual char. Figure 15 presents the information in Table 6 in the form of chart for better insight into the effect of catalystquantity on the yield of reaction products.

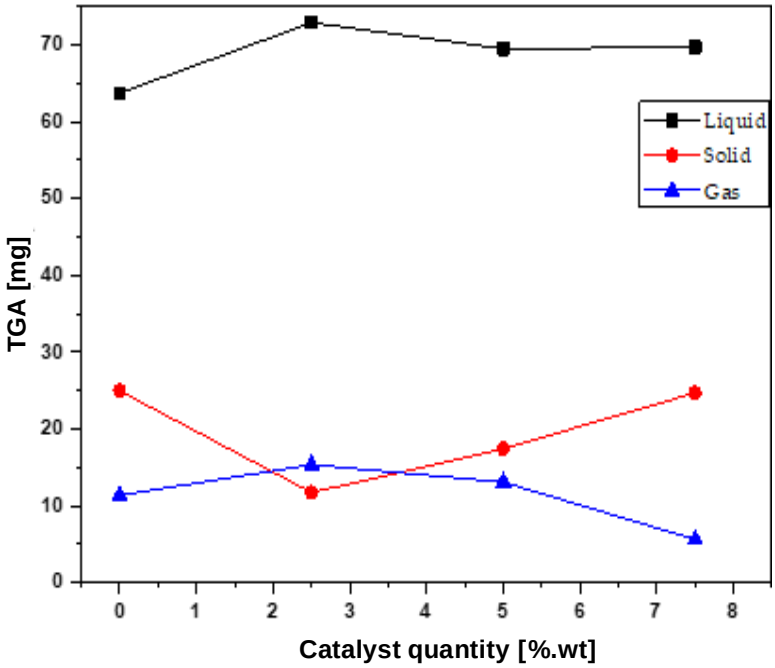


**Figure 15.** Effect of catalyst quantity on the catalytic upgrading of WEEE plastics.

Nunome et al. studied the generation behavior of tar (PAH) during pyrolysis of ABS and concluded that PAHs form due to incorporation of $C_2$ and $C_2H_2$ units and that they were formed mostly by nitrogen-containing hetero-PAHs, oxygen-containing hetero-PAHs, and PAHs. They did not use any catalysts but used temperatures greater than 700 °C [87]. The same behavior was found for the WEEE plastic OLP in this work, but the surface area provided by the catalyst was responsible for the increase in those types of reactions, explaining why there was a reduction of gas yields with increasing bed height. It was observed that there was an increase in char generated, suggesting that the increased bed height may allow some reflux to happen, effectively increasing the residence time of the process, including affecting the production of char in reactor R-1. Zhang et al.conducted 2-stage pyrolysis of LDPE using activated carbon as a catalyst, and they found that using a catalyst of high surface area and lower micropore structure increases formation of aromatic compounds and PAHs. They reported that chemical activation enlarged pore volume but reduced micropore structure. There were medium gas yields, though (30 %), suggesting that smaller products of reaction got through the porous structure of the catalyst, different from ABS. The chain radicals formed by LDPE are indeed much smaller than ABS pyrolysis products, and the gas composition revealed an increased presence of hydrogen. A similar behavior was observed for the higher temperature of the pyrolysis process of LDPE, producing mainly mono-aromatic and double-ring aromatics such as naphthalene [88].

### 3.4.2. Physical–Chemical Properties and Chemical Composition of OLP Obtained Through Catalytic Upgrading

The same procedure for calculation of mean values for the physical–chemical properties determined for thermal cracking was used for the catalytic experiments. Mass fractions, measured properties, and mean calculated values of density, kinematic viscosity, and acid value of the upgraded OLP are shown in Table 7.

**Table 7.** Weighted average of determined physical–chemical properties and their respective measured properties of time fractions for catalytic upgrading experiments.

| Catalyst Quantity [%] | Reaction Time [min] | OLP Quantity [g] | Density [g/cm$^3$] | Kinematic Viscosity [mm$^2$/s] | Acid Value [mg KOH/g] |
|---|---|---|---|---|---|
| 0.0 | 15 | 103.2 | 0.91 | 1.46 | 33.0 |
| | 30 | 95.5 | 0.98 | 1.36 | 24.8 |
| | 45 | 94.7 | 0.96 | 1.36 | 77 |
| | 60 | 89.1 | 0.91 | 1.32 | 28.3 |
| | **Total** | **382.5** | **0.94** | **1.38** | **40.8** |
| 2.5 | 30 | 169.8 | 0.90 | 0.93 | 16.8 |
| | 45 | 138.2 | 0.92 | 1.28 | 18.8 |
| | 60 | 129.7 | 0.92 | 1.52 | 23.0 |
| | **Total** | **437.7** | **0.91** | **1.21** | **19.3** |
| 5.0 | 15 | 90.4 | 0.91 | 1.06 | 10.4 |
| | 30 | 103.5 | 0.89 | 0.94 | 14.4 |
| | 45 | 104.2 | 0.92 | 1.34 | 21.6 |
| | 60 | 119.1 | 0.92 | 1.34 | 15.7 |
| | **Total** | **417.2** | **0.91** | **1.18** | **15.7** |
| 7.5 | 15 | 127.7 | 0.88 | 0.99 | 33.8 |
| | 30 | 106.6 | 0.90 | 1.19 | 20.8 |
| | 45 | 73.7 | 0.90 | 1.65 | 15.3 |
| | 60 | 110.4 | 0.90 | 1.61 | 1.15 |
| | **Total** | **418.4** | **0.89** | **1.38** | **16.6** |

Overall, density reduced slightly, while kinematic viscosity tended to increase when compared to the thermal cracking experiments at 450 °C due to formation of PAHs and double-ring nitrogenated aromatics. Acid values were remarkably lower, suffering a reduction of over 50 %. Contact with the thermally heated catalyst increased residence time of vapors, allowing it to reach later stages of cracking and, possibly, obtain better deoxygenation of phenolic compounds present. Acid value analysis is not that common in research into pyrolysis fuels, even though fuel acidity is a critical measurement for adequate functioning of a compression–ignition engine. This is mainly because acid value is an analysis tool for vegetable oil and the biodiesel industry and is more closely related to lipid-based feedstocks. When pyrolysis initiates, fatty acids are produced and later converted to hydrocarbons; the acid value gives insight into conversion of pyrolysis of oils and fats [55, 56, and 65]. For plastic feedstocks, only a few studies have published acid value measurements [45] because acid value is related to the presence of oxygenated compounds and most plastic feedstocks contain minimal amounts of oxygen. For WEEE plastic, though, polycarbonate material is present and can possibly generate phenolic compounds. Wang et al. conducted upgrading of a vinyl-based plastic and found acid values of 17.8 mg KOH/g for the plastic pyrolysis oil and acid values lower than 6 mg KOH/g for the upgraded OLP, indicating better deoxygenation.

In the case of polymers containing flame-retardants and PVC, there is a possibility of generating inorganic acids such as HCN, HCl, and even $NH_3$ that could contribute to the balance of acidity in OLP [79 and 80]. Supposedly, most of these compounds are gases and would be released in the pyrolysis process. They could accumulate in the water phase, but these experiments produced only an organic phase. They could instead react with organic compounds, forming brominated or chlorinated substances different

from the original substances. The chemical composition of both thermal cracking and upgrading experiments showed the presence of brominated compounds but not chlorinated ones. The organobromine compounds detected in the GC-MS were 5-Bromo-2-methoxy-1,3- dimethylbenzene and bromophenol. Commonly used brominated flame-retardants are polybrominated diphenyl ethers and tetrabromobisphenol A, which can also contribute to phenolic compound formation. Table 8 presents the mean composition of brominated compounds in the OLP with increasing catalyst quantity, and Figure 16 exemplifies the effect of reaction time on the concentration of brominated compounds for thermal and catalytic experiments. The presence of brominated compounds reduces with reaction time, probably due to initial volatiles of the brominated compounds being produced, and the TG analysis showed early decomposition of the WEEE plastic mix. The composition of brominated compounds increased for the OLP produced with the catalyst fixed bed in place, suggesting that the catalyst pore size and volume retained more of the brominated compounds in the OLP phase.

**Table 8.** Brominated compound composition of OLP obtained through thermal cracking and catalytic upgrading with Si–Al ash pellets at 450 °C.

| Catalyst Quantity [%.wt] | Brominated Composition [%.area] |
|---|---|
| 0.0 | 0.17 |
| 2.5 | 0.59 |
| 5.0 | 0.40 |
| 7.5 | 0.44 |

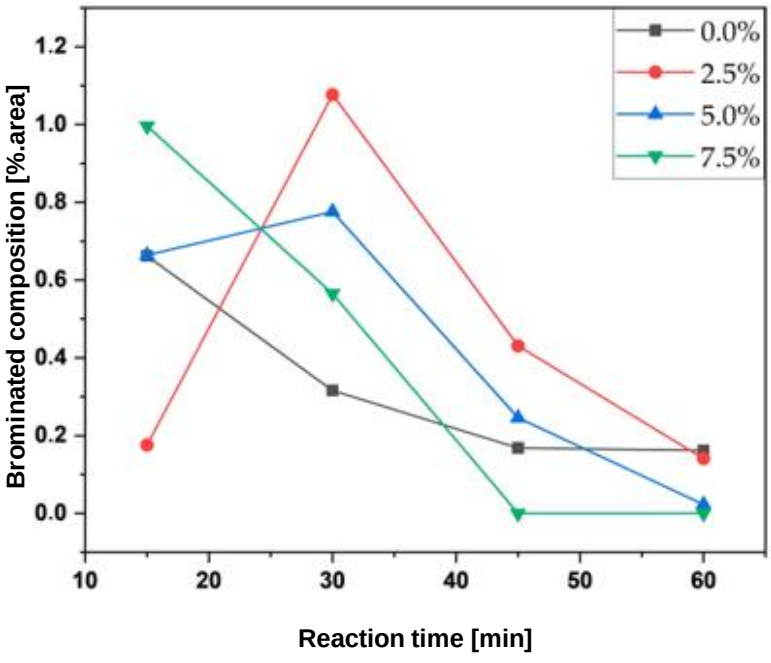


**Figure 16.** Effect of reaction time on brominated compound composition.

Chemical composition revealed an increased presence of PAH in the upgraded OLP, indicating the surface area provided by the solid catalyst increased residence time for cracking reactions to occur, allowing secondary product formation by condensation and polymerization reactions. It can be observed that, as the catalyst fixed bed increased in height, the quantity of char formed increased, while gas yields reduced, and the liquid phase remained constant. The density and kinematic viscosity of OLP shown in Table 7 reveal that density tended to decrease while viscosities increased with catalyst quantity for the OLP, suggesting that the catalyst with its porous structure allowed the formation of PAH

in the OLP and increased char content through aromatization, condensation, and polymerization reactions of the products of reaction [65]. Even though the catalyst is not in contact with the thermal reactor, perhaps some reflux happens between the reactor and catalyst fixed bed, affecting the yields of char obtained. The decreased gas yields indicate that the catalyst could fixate the gas formed into heavier products. A similar trend for the same catalyst was observed in one of our previous works, even though the feedstock was composed of triglyceride materials and high gas yields were obtained. The composition was largely different, though, with linear hydrocarbons comprising the finished product and fatty acids as the principal intermediaries and contaminants; few aromatic products were formed, but PAH was observed as naphthalene in the chemical composition [55]. The OLP obtained from WEEE plastic is largely composed of aromatic hydrocarbons such as diphenyl-propane and nitriles such as benzene butane–nitrile, and this may be why the effect of generating PAHs could be better observed. Additionally, the presence of nitrogenated compounds in the composition of OLP introduces the possibility of side reactions of condensation between products of reaction. Indeed, nitrogenated/oxygenated compounds such as quinolines and pyrroles were found in the composition of the nitrogenated fraction.

Figure 17 illustrates the chemical composition change produced with increasing reaction time for all four experiments considering the overall change in the chemical composition. Overall, the chemical composition remained constant throughout all experiments with increasing PAH content and lower oxygenated values. There was little change when comparing the catalytic experiments, though, perhaps because of the little C/F range investigated. Fan et al. investigated catalytic upgrading of LDPE using an ex-situ catalyst fixed bed and a C/F range of 0.6–2.71 to clearly assess the performance of the catalyst used [25]. Fan et al. studied C/F on the catalytic upgrading of LDPE using MgO as the catalyst, and they used a C/F range of 0.06–0.33. Even though there was an effect when comparing thermal and catalytic experiments, the change was remarkably lower for a C/F higher than 0.1 [42]. Nishino et al. also studied C/F and found a constant behavior of chemical composition with a decreasing C/F ratio, but the highest C/F ratio studied was 0.1. They pyrolyzed five different types of plastic on a semi-pilot unit [47].

The same behavior can be observed for all catalytic experiments with respect to changes in chemical composition with reaction time observed for thermal experiments, of almost constant composition. Since the feed is loaded into reactor R-1, pyrolysis vapors arriving at reactor R-2 have the same composition as the vapors comprising thermal cracking OLP and gases, so there is no reason to believe that chemical composition would change more effectively with reaction time even when catalytically upgrading the OLP. Overall, very little effect of the catalyst is observed when comparing the two set of experiments, and it can be theorized that this is because of rapid deactivation of the catalyst. After runs, the elemental composition of catalyst pellets showed presence of over 40 % of carbon as coke, possibly plugging catalyst pores and impeding access of vapors to the catalyst surface. High flowrate and presence of preferential pathways through the catalyst fixed bed could also be responsible for the small catalytic effect of the Si–Al ash pellets. Nevertheless, chemical composition analysis of time samples of OLP could be used to effectively check catalyst activity when comparing thermal cracking and catalytic upgrading of WEEE plastics.

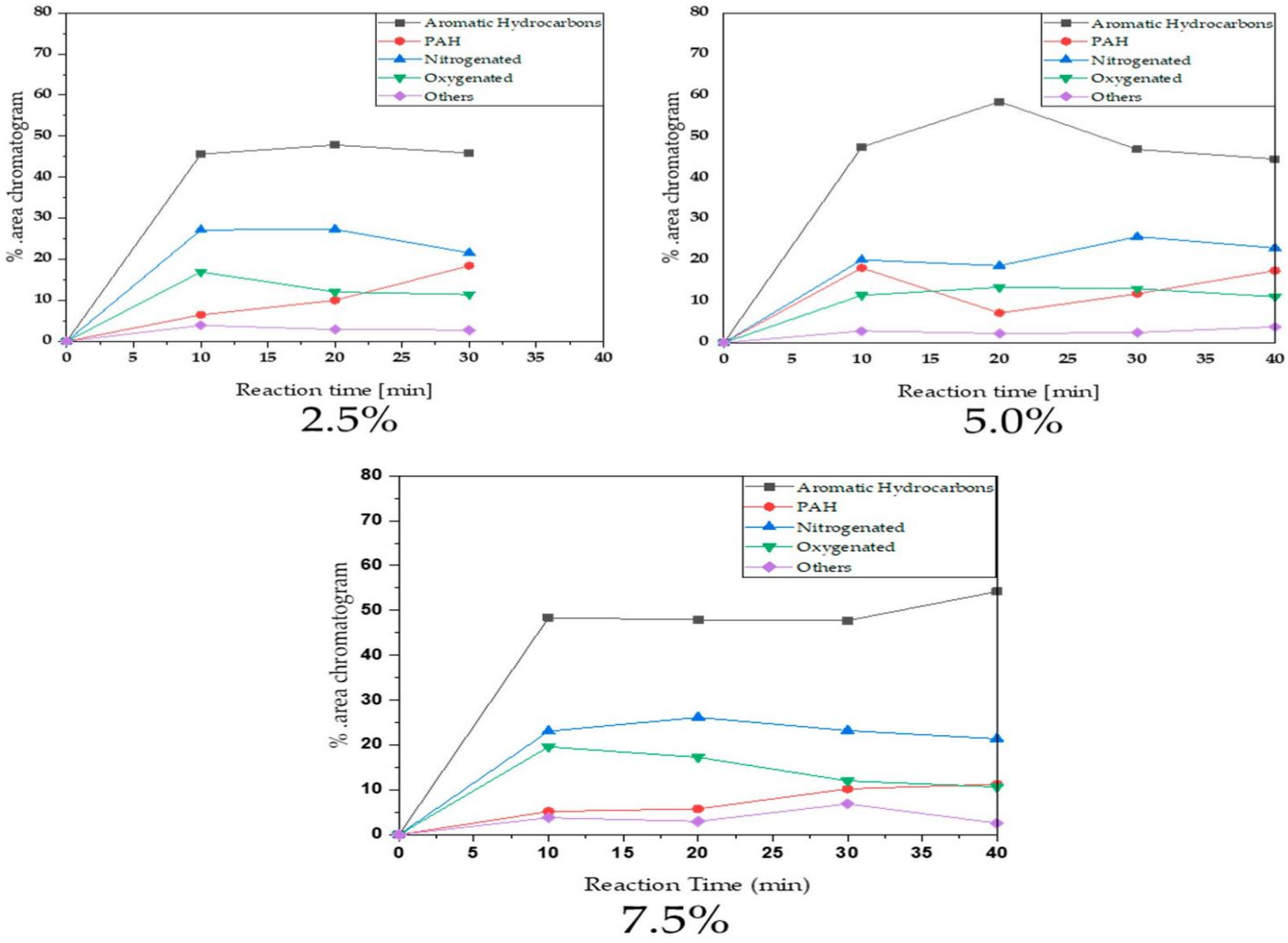


**Figure 17.** Reaction time effect on chemical composition of OLP obtained through catalytic upgrading of WEEE plastic at 450 °C, over 2.5, 5.0, and 7.5 % catalyst.

## 4. Conclusions

Computer scraps were pyrolyzed and catalytically upgraded with Si–Al ash pellets as the catalyst to study and investigate the effects of temperature, catalyst quantity, and reaction time on reaction yields, physical–chemical properties, and chemical composition of OLP obtained. Catalyst characterization by SEM, EDX, XRD, and XRF revealed a highly porous structure composed of silica and alumina. Feed characterization by TG analysis indicated presence of ABS and PC polymers, as well the possibility of containing brominated compounds such as tetrabromobisphenol A as flame-retardants. High amounts of gases were produced for low temperatures of cracking, decreasing with an increase in temperature. The opposite trend was observed for the liquid phase. The TG analysis showed a three-peak decomposition of the WEEE plastic mix, indicating that the early decomposition occasioned by the brominated flame-retardant compounds and maintenance of reaction temperature at the low temperature of 350 °C were responsible for the initial high gas yields. Liquid yields increased until 450 °C because of the biggest peak of decomposition at 418 °C. The third decomposition peak and increased char yields may indicate the presence of polycarbonate material for the feed. Acid value analysis showed increased values for higher temperatures, indicating that low temperatures favored deoxygenation reactions and elimination of gases such as HCN and $NH_3$. Mostly, the OLP is composed of aromatic hydrocarbons such as benzene derivatives (benzene, 1,1′-(1,3-propanediyl) bis- and benzene(1-methylethyl)-); styrene

derivatives (styrene and methyl-styrene); nitrogenated compounds derived from nitriles such as benzenebutanenitrile and other nitrogenated aromatic compounds; and PAH such as ramified naphthalenes and phenolic compounds (phenol and cumenol). Catalytic upgrading favored production of char and reduced production of gases, affecting density and kinematic viscosity of OLP produced due to increased presence of PAHs and heteroatom PAHs (nitrogenated and oxygenated) produced by incorporation of smaller hydrocarbon gases produced. Some reflux of products is suggested from reactor R-2 to R-1, explaining the increase in char content with increased bed height. The acid value reduced to values around 17 mg KOH/g, indicating better deoxygenation than in thermal experiments. Organobromine content tended to decrease with reaction time but showed higher values for the catalytic upgrading experiments. Overall, the chemical composition of OLP obtained (thermal cracking or catalytic upgrading) remained fairly constant with respect to reaction time, even though composition of the feed changes in a semi-batch reactor. This confirms that chemical composition and physical–chemical property analysis with respect to reaction time is a powerful tool of analysis of pyrolysis and catalytic upgrading processes, even when using different types of feedstocks.

**Supplementary Materials:** The following supporting information can be downloaded at: https://www.mdpi.com/article/10.3390/en16010541/s1, Table S1: Classes of compounds, summation of peak areas, CAS number, and retention times of chemical compounds identified by GC-MS in OLP by thermal cracking of WEEE plastic at 350 °C, 1.0 atm, reaction time = 30 min, in semi-pilot scale two-stage reactor of 2.0 L. Table S2: Classes of compounds, summation of peak areas, CAS number, and retention times of chemical compounds identified by GC-MS in OLP by thermal cracking of WEEE plastic at 350 °C, 1.0 atm, reaction time = 45 min, in semi-pilot scale two-stage reactor of 2.0 L. Table S3: Classes of compounds, summation of peak areas, CAS number, and retention times of chemical compounds identified by GC-MS in OLP by thermal cracking of WEEE plastic at 350 °C, 1.0 atm, reaction time = 60 min, in semi-pilot scale two-stage reactor of 2.0 L. Table S4: Classes of compounds, summation of peak areas, CAS number, and retention times of chemical compounds identified by GC-MS in OLP by thermal cracking of WEEE plastic at 400 °C, 1.0 atm, reaction time = 15 min, in semi-pilot scale two-stage reactor of 2.0 L. Table S5: Classes of compounds, summation of peak areas, CAS number, and retention times of chemical compounds identified by GC-MS in OLP by thermal cracking of WEEE plastic at 400 °C, 1.0 atm, reaction time = 30 min, in semi-pilot scale two-stage reactor of 2.0 L. Table S6: Classes of compounds, summation of peak areas, CAS number, and retention times of chemical compounds identified by GC-MS in OLP by thermal cracking of WEEE plastic at 400 °C, 1.0 atm, reaction time = 45 min, in semi-pilot scale two-stage reactor of 2.0 L. Table S7: Classes of compounds, summation of peak areas, CAS number, and retention times of chemical compounds identified by GC-MS in OLP by thermal cracking of WEEE plastic at 400 °C, 1.0 atm, reaction time = 60 min, in semi-pilot scale two-stage reactor of 2.0 L. Table S8: Classes of compounds, summation of peak areas, CAS number, and retention times of chemical compounds identified by GC-MS in OLP by thermal cracking of WEEE plastic at 450 °C, 1.0 atm, reaction time = 15 min, in semi-pilot scale two-stage reactor of 2.0 L. Table S9: Classes of compounds, summation of peak areas, CAS number, and retention times of chemical compounds identified by GC-MS in OLP by thermal cracking of WEEE plastic at 450 °C, 1.0 atm, reaction time = 30 min, in semi-pilot scale two-stage reactor of 2.0 L. Table S10: Classes of compounds, summation of peak areas, CAS number, and retention times of chemical compounds identified by GC-MS in OLP by thermal cracking of WEEE plastic at 450 °C, 1.0 atm, reaction time = 45 min, in semi-pilot scale two-stage reactor of 2.0 L. Table S11: Classes of compounds, summation of peak areas, CAS number, and retention times of chemical compounds identified by GC-MS in OLP by thermal cracking of WEEE plastic at 450 °C, 1.0 atm, reaction time = 60 min, in semi-pilot scale two-stage reactor of 2.0 L. Table S12: Classes of compounds, summation of peak areas, CAS number, and retention times of chemical compounds identified by GC-MS in OLP by thermal cracking of WEEE plastic at 500 °C, 1.0 atm, reaction time = 15 min, in semi-pilot scale two-stage reactor of 2.0 L. Table S13: Classes of compounds, summation of peak areas, CAS number, and retention times of chemical compounds identified by GC-MS in OLP by thermal cracking of WEEE plastic at 500 °C, 1.0 atm, reaction time = 30 min, in semi-pilot scale two-stage reactor of 2.0 L. Table S14: Classes of compounds, summation of peak areas, CAS number, and retention times of chemical compounds identified by GC-MS in OLP by thermal cracking of WEEE plastic at 500 °C, 1.0 atm, reaction time = 45 min, in semi-pilot scale two-stage reactor of 2.0 L. Table S15: Classes of compounds, summation of peak

areas, CAS number, and retention times of chemical compounds identified by GC-MS in OLP by thermal cracking of WEEE plastic at 500 °C, 1.0 atm, reaction time = 60 min, in semi-pilot scale two-stage reactor of 2.0 L. Table S16: Classes of compounds, summation of peak areas, CAS number, and retention times of chemical compounds identified by GC-MS in OLP by catalytic upgrading of WEEE plastic pyrolysis vapors at 450 °C, 1.0 atm, on a fixed catalyst bed loaded with 2.5 %.wt of Si–Al ash pellets, reaction time = 30 min, in semi-pilot scale two-stage reactor of 2.0 L. Table S17: Classes of compounds, summation of peak areas, CAS number, and retention times of chemical compounds identified by GC-MS in OLP by catalytic upgrading of WEEE plastic pyrolysis vapors at 450 °C, 1.0 atm, on a fixed catalyst bed loaded with 2.5 %.wt of Si–Al ash pellets, reaction time = 45 min, in semi-pilot scale two-stage reactor of 2.0 L. Table S18: Classes of compounds, summation of peak areas, CAS number, and retention times of chemical compounds identified by GC-MS in OLP by catalytic upgrading of WEEE plastic pyrolysis vapors at 450 °C, 1.0 atm, on a fixed catalyst bed loaded with 2.5 %.wt of Si–Al ash pellets, reaction time = 60 min, in semi-pilot scale two-stage reactor of 2.0 L. Table S19: Classes of compounds, summation of peak areas, CAS number, and retention times of chemical compounds identified by GC-MS in OLP by catalytic upgrading of WEEE plastic pyrolysis vapors at 450 °C, 1.0 atm, on a fixed catalyst bed loaded with 5.0 %.wt of Si–Al ash pellets, reaction time = 15 min, in semi-pilot scale two-stage reactor of 2.0 L. Table S20: Classes of compounds, summation of peak areas, CAS number, and retention times of chemical compounds identified by GC-MS in OLP by catalytic upgrading of WEEE plastic pyrolysis vapors at 450 °C, 1.0 atm, on a fixed catalyst bed loaded with 5.0 %.wt of Si–Al ash pellets, reaction time = 30 min, in semi-pilot scale two-stage reactor of 2.0 L. Table S21: Classes of compounds, summation of peak areas, CAS number, and retention times of chemical compounds identified by GC-MS in OLP by catalytic upgrading of WEEE plastic pyrolysis vapors at 450 °C, 1.0 atm, on a fixed catalyst bed loaded with 5.0 %.wt of Si–Al ash pellets, reaction time = 45 min, in semi-pilot scale two-stage reactor of 2.0 L. Table S22: Classes of compounds, summation of peak areas, CAS number, and retention times of chemical compounds identified by GC-MS in OLP by catalytic upgrading of WEEE plastic pyrolysis vapors at 450 °C, 1.0 atm, on a fixed catalyst bed loaded with 5.0 %.wt of Si–Al ash pellets, reaction time = 60 min, in semi-pilot scale two-stage reactor of 2.0 L. Table S23: Classes of compounds, summation of peak areas, CAS number, and retention times of chemical compounds identified by GC-MS in OLP by catalytic upgrading of WEEE plastic pyrolysis vapors at 450 °C, 1.0 atm, on a fixed catalyst bed loaded with 7.5 %.wt of Si–Al ash pellets, reaction time = 15 min, in semi-pilot scale two-stage reactor of 2.0 L. Table S24: Classes of compounds, summation of peak areas, CAS number, and retention times of chemical compounds identified by GC-MS in OLP by catalytic upgrading of WEEE plastic pyrolysis vapors at 450 °C, 1.0 atm, on a fixed catalyst bed loaded with 7.5 %.wt of Si–Al ash pellets, reaction time = 30 min, in semi-pilot scale two-stage reactor of 2.0 L. Table S25: Classes of compounds, summation of peak areas, CAS number, and retention times of chemical compounds identified by GC-MS in OLP by catalytic upgrading of WEEE plastic pyrolysis vapors at 450 °C, 1.0 atm, on a fixed catalyst bed loaded with 7.5 %.wt of Si–Al ash pellets, reaction time = 45 min, in semi-pilot scale two-stage reactor of 2.0 L. Table S26: Classes of compounds, summation of peak areas, CAS number, and retention times of chemical compounds identified by GC-MS in OLP by catalytic upgrading of WEEE plastic pyrolysis vapors at 450 °C, 1.0 atm, on a fixed catalyst bed loaded with 7.5 %.wt of Si–Al ash pellets, reaction time = 60 min, in semi-pilot scale two-stage reactor of 2.0 L.

**Author Contributions:** A.F.d.F.C. contributed with formal analysis and writing original draft preparation, investigation and methodology, C.C.F. contributed with investigation and methodology, S.P.A.d.P. contributed with XRF and XRD investigation and methodology, M.C.S. contributed with investigation and methodology, L.G.S.M. contributed with chemical analysis, A.C.G.d.A.d.F. con- tributed with chemical analysis, N.M.M. contributed with contributed with resources and chemical analysis, F.P.d.C.A. contributed with chemical analysis, R.M.R.C. and C.E.F.d.C. contributed with TG chemical and formal analysis, S.A.P.d.M. and I.W.d.S.B. contributed with investigation, methodology and chemical analysis, D.A.R.d.C. contributed with formal analysis, investigation and methodology, S.D.J. contributed with resources and chemical analysis, L.E.P.B. with co-supervision and resources, and N.T.M. and L.P.B. contributed with supervision, conceptualization, and data curation. All authors have read and agreed to the published version of the manuscript.

**Funding:** This research received no external funding.

**Acknowledgments:** N.T.M. would like to acknowledge and dedicate this research in memory to Hélio da Silva Almeida. He used to work at the Faculty of Sanitary and Environmental Engineering/UFPA and passed away on 13 March 2021. His contagious joy, dedication, intelligence, honesty, seriousness, and kindness will always be remembered in our hearts.

**Conflicts of Interest:** The authors declare no conflict of interest.

## Abbreviations

| | |
|---|---|
| ABS | Acrylonitrile–butadiene–styrene copolymer |
| Br–ABS | Brominated ABS |
| C/F | Catalyst-to-feed ratio |
| EDX | Dispersive energy spectrometry |
| GC-MS | Gas chromatography-mass spectrometry |
| HDPE | High-density polyethylene |
| HIPS | High-impact polystyrene |
| LDPE | Low-density polyethylene |
| MHSW | Municipal household solid waste |
| NCG | Non-condensable gas |
| OLP | Organic liquid product |
| PAH | Polycyclic aromatic hydrocarbon |
| PC | Polycarbonate |
| PE | Polyethylene |
| PET | Polyethylene terephthalate |
| PP | Polypropylene |
| PVC | Polyvinylchloride |
| SEM | Scanning electron microscopy |
| TG | Thermogravimetry |
| XRD | X-ray diffraction |
| XRF | X-ray fluorescence |
| WEEE | Waste electric and electronic equipment |

## References

1. Thiounn, T.; Smith, R.C. Advances and Approaches for Chemical Recycling of Plastic Waste. *J. Polym. Sci.* **2020**, *58*, 1347–1364.[CrossRef]
2. Kasar, P.; Sharma, D.K.; Ahmaruzzaman, M. Thermal and Catalytic Decomposition of Waste Plastics and Its Co-Processing withPetroleum Residue through Pyrolysis Process. *J. Clean. Prod.* **2020**, *265*, 121639. [CrossRef]
3. *Global Plastics Outlook*; OECD: Paris, France, 2022; ISBN 9789264654945.
4. Neuwahl, F.; Cusano, G.; Benavides, J.G.; Holbrook, S.; Roudier, S. *Best Available Techniques (BAT) Reference Document for Waste Incineration*; European Comission, Publications Office of the European Union: Luxembourg, 2019; ISSN 1831-9424. [CrossRef]
5. Wong, S.L.; Ngadi, N.; Abdullah, T.A.T.; Inuwa, I.M. Current State and Future Prospects of Plastic Waste as Source of Fuel: AReview. *Renew. Sustain. Energy Rev.* **2015**, *50*, 1167–1180. [CrossRef]
6. Papari, S.; Bamdad, H.; Berruti, F. Pyrolytic Conversion of Plastic Waste to Value-Added Products and Fuels: A Review. *Materials.* **2021**, *14*, 2586. [CrossRef]
7. Jha, K.K.; Kannan, T.T.M. Recycling of Plastic Waste into Fuel by Pyrolysis—A Review. *Mater. Today Proc.* **2021**, *37*, 3718–3720.[CrossRef]
8. Panda, A.K.; Singh, R.K.; Mishra, D.K. Thermolysis of Waste Plastics to Liquid Fuel: A Suitable Method for Plastic Waste Management and Manufacture of Value-Added Products—A World Prospective. *Renew. Sustain. Energy Rev.* **2010**, *14*, 233–248.[CrossRef]
9. Jahirul, M.I.; Rasul, M.G.; Schaller, D.; Khan, M.M.K.; Hasan, M.M.; Hazrat, M.A. Transport Fuel from Waste Plastics Pyrolysis—AReview on Technologies, Challenges and Opportunities. *Energy Convers. Manag.* **2022**, *258*, 115451. [CrossRef]
10. Williams, P.T.; Slaney, E. Analysis of Products from the Pyrolysis and Liquefaction of Single Plastics and Waste Plastic Mixtures. *Resour. Conserv. Recycl.* **2007**, *51*, 754–769. [CrossRef]
11. Mangesh, V.L.; Padmanabhan, S.; Tamizhdurai, P.; Ramesh, A. Experimental Investigation to Identify the Type of Waste PlasticPyrolysis Oil Suitable for Conversion to Diesel Engine Fuel. *J. Clean. Prod.* **2020**, *246*, 119066. [CrossRef]
12. Sharma, B.K.; Moser, B.R.; Vermillion, K.E.; Doll, K.M.; Rajagopalan, N. Production, Characterization and Fuel Properties ofAlternative Diesel Fuel from Pyrolysis of Waste Plastic Grocery Bags. *Fuel Process. Technol.* **2014**, *122*, 79–90. [CrossRef]
13. Li, D.; Lei, S.; Wang, P.; Zhong, L.; Ma, W.; Chen, G. Study on the Pyrolysis Behaviors of Mixed Waste Plastics. *Renew. Energy.* **2021**, *173*, 662–674. [CrossRef]

14. Muhammad, C.; Onwudili, J.A.; Williams, P.T. Catalytic Pyrolysis of Waste Plastic from Electrical and Electronic Equipment. *J.Anal. Appl. Pyrolysis* **2015**, *113*, 332–339. [CrossRef]
15. Sudhir, M.; Desai, B.; Chetan, M.; Galage, K. Production and Analysis of Pyrolysis Oil from Waste Plastic in Kolhapur City. *Int. J.Eng. Res. Gen. Sci.* **2015**, *3*, 590–595.
16. Lee, K.H.; Shin, D.H. Characteristics of Liquid Product from the Pyrolysis of Waste Plastic Mixture at Low and High Temperatures:Influence of Lapse Time of Reaction. *Waste Manag.* **2007**, *27*, 168–176. [CrossRef] [PubMed]
17. Kiran, N.; Ekinci, E.; Snape, C.E. Recyling of Plastic Wastes via Pyrolysis. *Resour. Conserv. Recycl.* **2000**, *29*, 273–283. [CrossRef]
18. Sogancioglu, M.; Ahmetli, G.; Yel, E. A Comparative Study on Waste Plastics Pyrolysis Liquid Products Quantity and EnergyRecovery Potential. *Energy Procedia* **2017**, *118*, 221–226. [CrossRef]
19. Kumar, S.; Prakash, R.; Murugan, S.; Singh, R.K. Performance and Emission Analysis of Blends of Waste Plastic Oil Obtained byCatalytic Pyrolysis of Waste HDPE with Diesel in a CI Engine. *Energy Convers. Manag.* **2013**, *74*, 323–331. [CrossRef]
20. Miskolczi, N.; Nagy, R. Hydrocarbons Obtained by Waste Plastic Pyrolysis: Comparative Analysis of Decomposition Describedby Different Kinetic Models. *Fuel Process. Technol.* **2012**, *104*, 96–104. [CrossRef]
21. Miskolczi, N.; Angyal, A.; Bartha, L.; Valkai, I. Fuels by Pyrolysis of Waste Plastics from Agricultural and Packaging Sectors in aPilot Scale Reactor. *Fuel Process. Technol.* **2009**, *90*, 1032–1040. [CrossRef]
22. Papuga, S.V.; Gvero, P.M.; Vukić, L.M. Temperature and Time Influence on the Waste Plastics Pyrolysis in the Fixed Bed Reactor. *Therm. Sci.* **2016**, *20*, 731–741. [CrossRef]
23. Khan, M.Z.H.; Sultana, M.; Al-Mamun, M.R.; Hasan, M.R. Pyrolytic Waste Plastic Oil and Its Diesel Blend: Fuel Characterization. *J. Env. Public Health* **2016**, *2016*, 1–6. [CrossRef] [PubMed]
24. Das, P.; Tiwari, P. The Effect of Slow Pyrolysis on the Conversion of Packaging Waste Plastics (PE and PP) into Fuel. *Waste Manag.* **018**, *79*, 615–624. [CrossRef] [PubMed]
25. Zhang, Y.; Duan, D.; Lei, H.; Villota, E.; Ruan, R. Jet Fuel Production from Waste Plastics via Catalytic Pyrolysis with ActivatedCarbons. *Appl. Energy* **2019**, *251*, 113337. [CrossRef]
26. Ratnasari, D.K.; Nahil, M.A.; Williams, P.T. Catalytic Pyrolysis of Waste Plastics Using Staged Catalysis for Production of GasolineRange Hydrocarbon Oils. *J. Anal. Appl. Pyrolysis* **2017**, *124*, 631–637. [CrossRef]
27. Xue, Y.; Johnston, P.; Bai, X. Effect of Catalyst Contact Mode and Gas Atmosphere during Catalytic Pyrolysis of Waste Plastics. *Energy Convers. Manag.* **2017**, *142*, 441–451. [CrossRef]
28. Singh, R.K.; Ruj, B.; Sadhukhan, A.K.; Gupta, P.; Tigga, V.P. Waste Plastic to Pyrolytic Oil and Its Utilization in CI Engine: Performance Analysis and Combustion Characteristics. *Fuel* **2020**, *262*, 116539. [CrossRef]
29. Kremer, I.; Tomić, T.; Katančić, Z.; Erceg, M.; Papuga, S.; Vuković, J.P.; Schneider, D.R. Catalytic Pyrolysis of Mechanically Non-Recyclable Waste Plastics Mixture: Kinetics and Pyrolysis in Laboratory-Scale Reactor. *J. Env. Manag.* **2021**, *296*, 113145.[CrossRef] [PubMed]
30. Barbarias, I.; Lopez, G.; Artetxe, M.; Arregi, A.; Bilbao, J.; Olazar, M. Valorisation of Different Waste Plastics by Pyrolysis and In-Line Catalytic Steam Reforming for Hydrogen Production. *Energy Convers. Manag.* **2018**, *156*, 575–584. [CrossRef]
31. Huo, E.; Lei, H.; Liu, C.; Zhang, Y.; Xin, L.; Zhao, Y.; Qian, M.; Zhang, Q.; Lin, X.; Wang, C.; et al. Jet Fuel and Hydrogen Produced from Waste Plastics Catalytic Pyrolysis with Activated Carbon and MgO. *Sci. Total Environ.* **2020**, *727*, 138411. [CrossRef] [PubMed]
32. Pratt, L.M.; Kim, J.; Lo, H.Y.; Xiao, D. Brown Grease Pyrolysis under Pressure: Extending the Range of Reaction Conditions and Hydrocarbon Product Distributions. *Fuel* **2021**, *289*, 119782. [CrossRef]
33. Balcazar, J.G.C.; Dias, R.A.; Balestieri, J.A.P. Analysis of Hybrid Waste-to-Energy for Medium-Sized Cities. *Energy* **2013**, *55*, 728–741. [CrossRef]
34. Hasan, M.M.; Rasul, M.G.; Khan, M.M.K.; Ashwath, N.; Jahirul, M.I. Energy Recovery from Municipal Solid Waste Using Pyrolysis Technology: A Review on Current Status and Developments. *Renew. Sustain. Energy Rev.* **2021**, *145*, 111073. [CrossRef]
35. Sikarwar, V.S.; Zhao, M.; Clough, P.; Yao, J.; Zhong, X.; Memon, M.Z.; Shah, N.; Anthony, E.J.; Fennell, P.S. An Overview ofAdvances in Biomass Gasification. *Energy Environ. Sci.* **2016**, *9*, 2939–2977. [CrossRef]
36. Sikarwar, V.S.; Zhao, M.; Fennell, P.S.; Shah, N.; Anthony, E.J. Progress in Biofuel Production from Gasification. *Prog. Energy Combust. Sci.* **2017**, *61*, 189–248. [CrossRef]
37. Buekens, A.; Yang, J. Recycling of WEEE Plastics: A Review. *J. Mater. Cycles Waste Manag.* **2014**, *16*, 415–434. [CrossRef]
38. Hall, W.J.; Williams, P.T. Removal of Organobromine Compounds from the Pyrolysis Oils of Flame Retarded Plastics UsingZeolite Catalysts. *J. Anal. Appl. Pyrolysis* **2008**, *81*, 139–147. [CrossRef]
39. Hall, W.J.; Williams, P.T. Analysis of Products from the Pyrolysis of Plastics Recovered from the Commercial Scale Recycling ofWaste Electrical and Electronic Equipment. *J. Anal. Appl. Pyrolysis* **2007**, *79*, 375–386. [CrossRef]
40. Hall, W.J.; Williams, P.T. Fast Pyrolysis of Halogenated Plastics Recovered from Waste Computers. *Energy Fuels* **2006**, *20*, 1536–1549. [CrossRef]
41. Nakaji, Y.; Tamura, M.; Miyaoka, S.; Kumagai, S.; Tanji, M.; Nakagawa, Y.; Yoshioka, T.; Tomishige, K. Low-Temperature Catalytic Upgrading of Waste Polyolefinic Plastics into Liquid Fuels and Waxes. *Appl. Catal. B* **2021**, *285*, 119805. [CrossRef]
42. Fan, L.; Zhang, Y.; Liu, S.; Zhou, N.; Chen, P.; Liu, Y.; Wang, Y.; Peng, P.; Cheng, Y.; Addy, M.; et al. Ex-Situ Catalytic Upgrading of Vapors from Microwave-Assisted Pyrolysis of Low-Density Polyethylene with MgO. *Energy Convers. Manag.* **2017**, *149*, 432–441. [CrossRef]

43. Fan, L.; Su, Z.; Wu, J.; Xiao, Z.; Huang, P.; Liu, L.; Jiang, H.; Zhou, W.; Liu, S.; Ruan, R. Integrating Continuous-Stirred Microwave Pyrolysis with Ex-Situ Catalytic Upgrading for Linear Low-Density Polyethylene Conversion: Effects of Parameter Conditions. *J.Anal. Appl. Pyrolysis* **2021**, *157*, 105213. [CrossRef]
44. Ma, C.; Yu, J.; Yan, Q.; Song, Z.; Wang, K.; Wang, B.; Sun, L. Pyrolysis-Catalytic Upgrading of Brominated High Impact Polystyreneover Fe and Ni Modified Catalysts: Influence of HZSM-5 and MCM-41 Catalysts. *Polym. Degrad. Stab.* **2017**, *146*, 1–12. [CrossRef]
45. Wang, S.; Kim, H.; Lee, D.; Lee, Y.R.; Won, Y.; Hwang, B.W.; Nam, H.; Ryu, H.J.; Lee, K.H. Drop-in Fuel Production with Plastic Waste Pyrolysis Oil over Catalytic Separation. *Fuel* **2021**, *305*, 121440. [CrossRef]
46. Bagri, R.; Williams, P.T. Catalytic Pyrolysis of Polyethylene. *J. Anal. Appl. Pyrolysis* **2002**, *63*, 29–41. [CrossRef]
47. Nishino, J.; Itoh, M.; Ishinomori, T.; Kubota, N.; Uemichi, Y. Development of a Catalytic Cracking Process for Converting Waste Plastics to Petrochemicals. *J. Mater. Cycles Waste Manag.* **2003**, *5*, 89–93. [CrossRef]
48. Dai, L.; Zhou, N.; Cobb, K.; Chen, P.; Wang, Y.; Liu, Y.; Zou, R.; Lei, H.; Mohamed, B.A.; Cheng, Y.; et al. Insights into Structure–Performance Relationship in the Catalytic Cracking of High Density Polyethylene. *Appl. Catal. B* **2022**, *318*, 121835. [CrossRef]
49. Zhou, N.; Dai, L.; Lyu, Y.; Wang, Y.; Li, H.; Cobb, K.; Chen, P.; Lei, H.; Ruan, R. A Structured Catalyst of ZSM-5/SiC Foam for Chemical Recycling of Waste Plastics via Catalytic Pyrolysis. *Chem. Eng. J.* **2022**, *440*, 135836. [CrossRef]
50. Hwang, K.R.; Choi, S.A.; Choi, I.H.; Lee, K.H. Catalytic Cracking of Chlorinated Heavy Wax from Pyrolysis of Plastic Wastes to Low Carbon-Range Fuels: Catalyst Effect on Properties of Liquid Products and Dechlorination. *J. Anal. Appl. Pyrolysis* **2021**,*155*, 105090. [CrossRef]
51. Marino, A.; Aloise, A.; Hernando, H.; Fermoso, J.; Cozza, D.; Giglio, E.; Migliori, M.; Pizarro, P.; Giordano, G.; Serrano, D.P. ZSM-5 Zeolites Performance Assessment in Catalytic Pyrolysis of PVC-Containing Real WEEE Plastic Wastes. *Catal. Today* **2022**, *390–391*, 210–220. [CrossRef]
52. Ma, C.; Yu, J.; Chen, T.; Yan, Q.; Song, Z.; Wang, B.; Sun, L. Influence of Fe Based ZSM-5 Catalysts on the Vapor Intermediates from the Pyrolysis of Brominated Acrylonitrile-Butadiene-Styrene Copolymer (Br-ABS). *Fuel* **2018**, *230*, 390–396. [CrossRef]
53. Shafaghat, H.; Gulshan, S.; Johansson, A.C.; Evangelopoulos, P.; Yang, W. Selective Recycling of BTX Hydrocarbons from Electronic Plastic Wastes Using Catalytic Fast Pyrolysis. *Appl. Surf. Sci.* **2022**, *605*, 125964. [CrossRef]
54. Chen, T.; Yu, J.; Ma, C.; Bikane, K.; Sun, L. Catalytic Performance and Debromination of Fe–Ni Bimetallic MCM-41 Catalyst forthe Two-Stage Pyrolysis of Waste Computer Casing Plastic. *Chemosphere* **2020**, *248*, 125964. [CrossRef] [PubMed]
55. Pinto Bernar, L.; Campos Ferreira, C.; Fernando de Freitas Costa, A.; Jorge da Silva Ribeiro, H.; Gomes dos Santos, W.; Martins Pereira, L.; Mathias Pereira, A.; Lobato Moraes, N.; Paula da Costa Assunção, F.; Alex Pereira da Mota, S.; et al. Catalytic Upgrading of Residual Fat Pyrolysis Vapors over Activated Carbon Pellets into Hydrocarbons-like Fuels in a Two-Stage Reactor: Analysis of Hydrocarbons Composition and Physical-Chemistry Properties. *Energies* **2022**, *15*, 4587. [CrossRef]
56. Ferreira, C.C.; Bernar, L.P.; de Freitas Costa, A.F.; da Silva Ribeiro, H.J.; Santos, M.C.; Moraes, N.L.; Costa, Y.S.; Baia, A.C.F.; Mendonça, N.M.; da Mota, S.A.P.; et al. Improving Fuel Properties and Hydrocarbon Content from Residual Fat Pyrolysis Vapors over Activated Red Mud Pellets in Two-Stage Reactor: Optimization of Reaction Time and Catalyst Content. *Energy* **2022**, *15*, 5595. [CrossRef]
57. Tseng, R.L. Mesopore Control of High Surface Area NaOH-Activated Carbon. *J. Colloid Interface Sci* **2006**, *303*, 494–502. [CrossRef]
58. Rocha de Castro, D.; da Silva Ribeiro, H.; Hamoy Guerreiro, L.; Pinto Bernar, L.; Jonatan Bremer, S.; Costa Santo, M.; da Silva Almeida, H.; Duvoisin, S.; Pizarro Borges, L.; Teixeira Machado, N. Production of Fuel-Like Fractions by Fractional Distillation ofBio-Oil from Açaí (Euterpe Oleracea Mart.) Seeds Pyrolysis. *Energy* **2021**, *14*, 3713. [CrossRef]
59. Appleby, W.G.; Gibson, J.W.; Good, G.M. Coke Formation in Catalytic Cracking. *Ind. Eng. Chem. Process Des. Dev.* **1962**, *1*, 102–110. [CrossRef]
60. Fertani-Gmati, M.; Brahim, K.; Khattech, I.; Jemal, M. Thermochemistry and Kinetics of Silica Dissolution in NaOH Solutions:Effect of the Alkali Concentration. *Acta* **2014**, *594*, 58–67. [CrossRef]
61. David Jackson, S. Processes Occurring during Deactivation and Regeneration of Metal and Metal Oxide Catalysts. *Chem. Eng. J.* **2006**, *120*, 119–125. [CrossRef]
62. Argyle, M.; Bartholomew, C. Heterogeneous Catalyst Deactivation and Regeneration: A Review. *Catalysts* **2015**, *5*, 145–269. [CrossRef]
63. Zhang, X.; Sun, L.; Chen, L.; Xie, X.; Zhao, B.; Si, H.; Meng, G. Comparison of Catalytic Upgrading of Biomass Fast Pyrolysis Vapors over CaO and Fe(III)/CaO Catalysts. *J. Anal. Appl. Pyrolysis* **2014**, *108*, 35–40. [CrossRef]
64. Sun, Z.; Xu, B.; Rony, A.H.; Toan, S.; Chen, S.; Gasem, K.A.M.; Adidharma, H.; Fan, M.; Xiang, W. Thermogravimetric and Kinetics Investigation of Pine Wood Pyrolysis Catalyzed with Alkali-Treated CaO/ZSM-5. *Energy Convers. Manag.* **2017**, *146*, 182–194. [CrossRef]
65. Chang, C.-C.; Wan, S.-W. China's Motor Fuels from Tung Oil. *Ind. Eng. Chem.* **1947**, *39*, 1543–1548. [CrossRef]
66. Vasile, C.; Brebu, M.A.; Karayildirim, T.; Yanik, J.; Darie, H. Feedstock Recycling from Plastic and Thermoset Fractions of Used Computers (I): Pyrolysis. *J. Mater. Cycles Waste Manag.* **2006**, *8*, 99–108. [CrossRef]
67. Saraji-Bozorgzad, M.; Geissler, R.; Streibel, T.; Mühlberger, F.; Sklorz, M.; Kaisersberger, E.; Denner, T.; Zimmermann, R. Thermogravimetry Coupled to Single Photon Ionization Quadrupole Mass Spectrometry: A Tool To Investigate the Chemical Signature of Thermal Decomposition of Polymeric Materials. *Anal. Chem.* **2008**, *80*, 3393–3403. [CrossRef]

68. Roussi, A.T.; Vouvoudi, E.C.; Achilias, D.S. Pyrolytic Degradation Kinetics of HIPS, ABS, PC and Their Blends with PP and PVC. *Acta* **2020**, *690*, 178705. [CrossRef]
69. Jung, S.-H.; Kim, S.-J.; Kim, J.-S. Thermal Degradation of Acrylonitrile–Butadiene–Styrene (ABS) Containing Flame Retardants Using a Fluidized Bed Reactor: The Effects of Ca-Based Additives on Halogen Removal. *Fuel Process. Technol.* **2012**, *96*, 265–270. [CrossRef]
70. Jung, S.-H.; Kim, S.-J.; Kim, J.-S. The Influence of Reaction Parameters on Characteristics of Pyrolysis Oils from Waste High Impact Polystyrene and Acrylonitrile–Butadiene–Styrene Using a Fluidized Bed Reactor. *Fuel Process. Technol.* **2013**, *116*, 123–129. [CrossRef]
71. Bhaskar, T.; Murai, K.; Matsui, T.; Brebu, M.A.; Uddin, M.A.; Muto, A.; Sakata, Y.; Murata, K. Studies on Thermal Degradation of Acrylonitrile–Butadiene–Styrene Copolymer (ABS-Br) Containing Brominated Flame Retardant. *J. Anal. Appl. Pyrolysis* **2003**, *70*, 369–381. [CrossRef]
72. Bridgwater, A.V. Renewable Fuels and Chemicals by Thermal Processing of Biomass. *Chem. Eng. J.* **2003**, *91*, 87–102. [CrossRef]
73. Mastral, F.J.; Esperanza, E.; García, P.; Juste, M. Pyrolysis of High-Density Polyethylene in a Fluidised Bed Reactor. Influence ofthe Temperature and Residence Time. *J. Anal. Appl. Pyrolysis* **2002**, *63*, 1–15. [CrossRef]
74. Al-Salem, S.M.; Lettieri, P. Kinetic Study of High Density Polyethylene (HDPE) Pyrolysis. *Chem. Eng. Res. Des.* **2010**, *88*, 1599–1606. [CrossRef]
75. Abbas-Abadi, M.S.; Haghighi, M.N.; Yeganeh, H.; McDonald, A.G. Evaluation of Pyrolysis Process Parameters on PolypropyleneDegradation Products. *J. Anal. Appl. Pyrolysis* **2014**, *109*, 272–277. [CrossRef]
76. López, A.; de Marco, I.; Caballero, B.M.; Laresgoiti, M.F.; Adrados, A. Influence of Time and Temperature on Pyrolysis of PlasticWastes in a Semi-Batch Reactor. *Chem. Eng. J.* **2011**, *173*, 62–71. [CrossRef]
77. Onwudili, J.A.; Insura, N.; Williams, P.T. Composition of Products from the Pyrolysis of Polyethylene and Polystyrene in a ClosedBatch Reactor: Effects of Temperature and Residence Time. *J. Anal. Appl. Pyrolysis* **2009**, *86*, 293–303. [CrossRef]
78. Maniscalco, M.; la Paglia, F.; Iannotta, P.; Caputo, G.; Scargiali, F.; Grisafi, F.; Brucato, A. Slow Pyrolysis of an LDPE/PP Mixture:Kinetics and Process Performance. *J. Energy Inst.* **2021**, *96*, 234–241. [CrossRef]
79. Miskolczi, N.; Hall, W.J.; Angyal, A.; Bartha, L.; Williams, P.T. Production of Oil with Low Organobromine Content from thePyrolysis of Flame Retarded HIPS and ABS Plastics. *J. Anal. Appl. Pyrolysis* **2008**, *83*, 115–123. [CrossRef]
80. Brebu, M.; Azhar Uddin, M.; Muto, A.; Sakata, Y.; Vasile, C. The Role of Temperature Program and Catalytic System on theQuality of Acrylonitrile-Butadiene-Styrene Degradation Oil. *J. Anal. Appl. Pyrolysis* **2002**, *63*, 43–57. [CrossRef]
81. Harussani, M.M.; Sapuan, S.M.; Rashid, U.; Khalina, A.; Ilyas, R.A. Pyrolysis of Polypropylene Plastic Waste into CarbonaceousChar: Priority of Plastic Waste Management amidst COVID-19 Pandemic. *Sci. Total Environ.* **2022**, *803*, 149911. [CrossRef]
82. Manoj, B.; Kunjomana, A.G. Study of Stacking Structure of Amorphous Carbon by X-ray Diffraction Technique. *Int. J. Electrochem.Sci.* **2012**, *7*, 3127–3134.
83. Iwanek (nee Wilczkowska), E.M.; Kirk, D.W. Application of Slow Pyrolysis to Convert Waste Plastics from a Compost-RejectStream into Py-Char. *Energy* **2022**, *15*, 3072. [CrossRef]
84. Joni, I.M.; Nulhakim, L.; Panatarani, C. Characteristics of $TiO_2$ Particles Prepared by Simple Solution Method Using $TiCl_3$Precursor. *J. Phys. Conf. Ser.* **2018**, *1080*, 012042. [CrossRef]
85. Chin, H.S.; Cheong, K.Y.; Razak, K.A. Review on Oxides of Antimony Nanoparticles: Synthesis, Properties, and Applications. *J.Mater. Sci.* **2010**, *45*, 5993–6008. [CrossRef]
86. Maafa, I. Pyrolysis of Polystyrene Waste: A Review. *Polymer* **2021**, *13*, 225. [CrossRef] [PubMed]
87. Nunome, Y.; Suzuki, T.; Nedjalkov, I.; Ueki, Y.; Yoshiie, R.; Naruse, I. Generation Behavior of Tar from ABS, PC, and PE duringPyrolysis and Steam Gasification by Mass Spectrometry. *J. Mater. Cycles Waste Manag.* **2019**, *21*, 1300–1310. [CrossRef]
88. Zhang, S.; Zhang, H.; Liu, X.; Zhu, S.; Hu, L.; Zhang, Q. Upgrading of Bio-Oil from Catalytic Pyrolysis of Pretreated Rice Huskover Fe-Modified ZSM-5 Zeolite Catalyst. *Fuel Process. Technol.* **2018**, *175*, 17–25. [CrossRef]

# CAPÍTULO 5 – CONCLUSÕES

Resíduos plásticos de equipamentos de informática foram pirolisados e melhorados cataliticamente com cinzas de Si-Al como catalisador para estudar e investigar os efeitos da temperatura, da quantidade de catalisador e do tempo de reação nos rendimentos da reação, como também as propriedades físico-químicas e a composição química do PLO obtido.

A caracterização do catalisador através de MEV, EDX, DRX e FRX revelou uma estrutura altamente porosa composta de sílica e alumina.

A caracterização da alimentação através da análise de TG indicou a presença de polímeros ABS e PC, bem como a possibilidade de conter compostos bromados retardantes de chama, como o tetrabromobisfenol A.

Altas quantidades de gases foram produzidas a baixas temperaturas de craqueamento, e diminuindo com o aumento da temperatura. A tendência contrária foi observada para a fase líquida.

A análise de TG mostrou uma decomposição de três picos da mistura plástica de equipamentos de informática, indicando que a decomposição precoce ocasionada pelos compostos retardadores de chama bromados e a manutenção da temperatura de reação na baixa temperatura de 350 °C foram responsáveis pelos altos rendimentos iniciais de gás.

Os rendimentos líquidos aumentaram até 450 °C devido ao maior pico de decomposição a 418 °C.

O terceiro pico de decomposição e o aumento dos rendimentos de carvão podem indicar a presença de PC na alimentação.

A análise do índice de acidez mostrou valores aumentados para temperaturas mais altas, indicando que baixas temperaturas favoreceram reações de desoxigenação e eliminação de gases, como HCN e $NH_3$.

Majoritariamente o PLO é composto de hidrocarbonetos aromáticos, como derivados do benzeno (1,1'-(1,3-propanodiil) bis-benzeno e 1-metiletil-benzeno), derivados do estireno (metil-estireno), compostos nitrogenados derivados de nitrilas, como benzeno butano-nitrila e outros compostos aromáticos nitrogenados, e PAH, como naftalenos ramificados e compostos fenólicos (fenol e cumenol).

O upgrading catalítico favoreceu a produção de carvão e reduziu a produção de gases, afetando a densidade e a viscosidade cinemática do PLO produzido devido ao aumento da presença de PAH e PAH com heteroátomos (nitrogenados e oxigenados) formados pela incorporação de gases de hidrocarbonetos menores produzidos.

Algum refluxo de produtos é sugerido do reator R-2 para o reator R-1, explicando o aumento no teor de carvão com o aumento da altura do leito.

Com o uso do reator catalítico R-2, o índice de acidez reduziu para valores em torno de 17 mg KOH/g, indicando melhor desoxigenação do que em experimentos térmicos.

O teor de organobromados tendeu a diminuir com o tempo de reação, mas apresentou valores maiores para os experimentos de upgrading catalítico.

No geral, a composição química do PLO obtido (via craqueamento térmico ou via upgrading catalítico) permaneceu bastante constante em relação ao tempo de reação, embora a composição da alimentação mude num reator em semi-batelada. Isso confirma que a análise da composição química e das propriedades físico-químicas em relação ao tempo de reação é uma ferramenta indispensável de análise de processos de craqueamento térmico e upgrading catalítico, mesmo quando são utilizados diferentes tipos de matérias-primas.

# SUGESTÕES PARA TRABALHOS FUTUROS

Como continuidade deste trabalho, sugerimos:

- Realização de experimentos térmicos e termocatalíticos de resíduos plásticos de equipamentos de informática em escalas de bancada e piloto;
- Utilização de outros catalisadores no processo de craqueamento termocatalítico de resíduos plásticos de equipamentos de informática;
- Estudo cinético completo das reações que ocorrem processo de craqueamento termocatalítico de resíduos plásticos de equipamentos de informática;
- Estudo do processo de upgrading catalítico de vapores da pirólise de resíduos plásticos de painéis de automóveis;

## REFERÊNCIAS BIBLIOGRÁFICAS


1. Thiounn, T.; Smith, R. C.; Advances and approaches for chemical recycling of plastic waste. *Journal of Polymer Science.* **2020**, 58, 1347-1364. doi: 10.1002/pol.20190261.

2. Kasar, P.; Sharma, D. K.; Ahmaruzzaman, M.; Thermal and catalytic decomposition of waste plastics and Its co-processing with petroleum residue through pyrolysis process. *Journal of Cleaner Production.* **2020**, 265, 121639. https://doi.org/10.1016/j.jclepro.2020.121639.

3. *Global Plastics Outlook: Economic Drivers, Environmental Impacts and Policy Options*, OECD Publishing: Paris, France, **2022**. https://doi.org/10.1787/de747aef-en.

4. Neuwahl, F; Cusano, G.; Benavides, J. G.; Holbrook, S.; Roudier, S.; Best Available Techniques (BAT) Reference Document for Waste Incineration. *JRC Science for Policy Report*. European Comission, 2019; Luxembourg: Publications Office of the European Union, **2019**, ISSN 1831-9424. doi: 10.2760/761437.

5. Wong, S. L.; Ngadi, N.; Abdullah, T. A. T.; Inuwa, I. M.; Current state and future prospects of plastic waste as source of fuel: A review. *Renewable and Sustainable Energy Reviews.* **2015**, 50, 1167-1180. http://dx.doi.org/10.1016/j.rser.2015.04.063.

6. Papari, S.; Bamdad, H.; Berruti, F.; Pyrolytic Conversion of Plastic Waste to Value-Added Products and Fuels: A Review. *Materials.* **2021**, 14, 2586. https://doi.org/10.3390/ma14102586.

7. Jha, K. K.; Kannan, T. T. M.; Recycling of plastic waste into fuel by pyrolysis - a review. *Materials Today: Proceedings.* **2021**, 37, 3718-3720. https://doi.org/10.1016/j.matpr.2020.10.181.

8. Panda, A. K.; Singh, R. K.; Mishra, D. K.; Thermolysis of waste plastics to liquid fuel: A suitable method for plastic waste management and manufacture of value-added products - A world prospective. *Renewable and Sustainable Energy Reviews.* **2010**, 14, 233-248. doi:10.1016/j.rser.2009.07.005.

9. Jahirul, M. I.; Rasul, M. G.; Schaller, D.; Khan, M. M. K.; Hasan, M. M.; Hazrat, M. A.; Transport fuel from waste plastics pyrolysis - A review on technologies, challenges, and opportunities. *Energy Conversion and Management.* **2022**, 258, 115451. https://doi.org/10.1016/j.enconman.2022.115451.

10. Williams, P. T.; Slaney, E.; Analysis of products from the pyrolysis and liquefaction of single plastics and waste plastic mixtures. *Resources, Conservation and Recycling.* **2007**, 51, 754-769. doi: 10.1016/j.resconrec.2006.12.002.

11. Mangesh, V. L.; Padmanabhan, S.; Tamizhdurai, P.; Ramesh, A.; Experimental investigation to identify the type of waste plastic pyrolysis oil suitable for conversion to diesel engine fuel. *Journal of Cleaner Production.* **2020**, 246, 119066. https://doi.org/10.1016/j.jclepro.2019.119066.

12. Sharma, B. K.; Moser, B. R.; Vermillion, K. E.; Doll, K. M.; Rajagopalan, N.; Production, characterization, and fuel properties of alternative diesel fuel from pyrolysis of waste plastic grocery bags. *Fuel Processing Technology.* **2014**, 122, 79–90. http: dx.doi.org/ 10.1016/j.fuproc.2014.01.019.

13. Li, D.; Lei, S.; Wang, P.; Zhong, L.; Ma, W.; Chen, G.; Study on the pyrolysis behaviors of mixed waste plastics. *Renewable Energy*. **2021**, 173, 662-674. https://doi.org/10.1016/j.renene.2021.04.035.

14. Muhammad, C.; Onwudili, J. A.; Williams, P. T.; Catalytic pyrolysis of waste plastic from electrical and electronic equipment. *Journal of Analytical and Applied Pyrolysis*. **2015**, 113, 332-339. http://dx.doi.org/10.1016/j.jaap.2015.02.016.

15. Sudhir, M.; Desai, B.; Chetan, M.; Galage, K.; Production and Analysis of Pyrolysis oil from waste plastic in Kolhapur city. *International Journal of Engineering Research and General Science*. **2015**, 3, 590-595.

16. Lee, K. H.; Shin, D. H.; Characteristics of liquid product from the pyrolysis of waste plastic mixture at low and high temperatures: Influence of lapse time of reaction. *Waste Management*. **2007**, 27, 168-176. doi: 10.1016/j.wasman.2005.12.017.

17. Kiran, N.; Ekinci, E.; Snape, C. E.; Recyling of plastic wastes via pyrolysis. *Resources, Conservation & Recycling*. **2000**, 29, 273–283. doi: 10.1016/S0921-3449(00)00052-5.

18. Sogancioglu, M.; Ahmetli, G.; Yel, E.; A Comparative Study on Waste Plastics Pyrolysis Liquid Products Quantity and Energy Recovery Potential. *Energy Procedia*. **2017**, 118, 221-226. doi: 10.1016/j.egypro.2017.07.020.

19. Kumar, S.; Prakash, R.; Murugan, S.; Singh, R. K.; Performance and emission analysis of blends of waste plastic oil obtained by catalytic pyrolysis of waste HDPE with diesel in a CI engine. *Energy Conversion and Management*. **2013**, 74, 323-331. http://dx.doi.org/10.1016/j.enconman.2013.05.028.

20. Miskolczi, N.; Nagy, R.; Hydrocarbons obtained by waste plastic pyrolysis: Comparative analysis of decomposition described by different kinetic models. *Fuel Processing Technology*. **2012**, 104, 96-104. doi: 10.1016/j.fuproc.2012.04.031.

21. Miskolczi, N.; Angyal, A.; Bartha, L.; Valkai, I.; Fuels by pyrolysis of waste plastics from agricultural and packaging sectors in a pilot scale reactor. *Fuel Processing Technology*. **2009**, 90, 1032-1040. doi: 10.1016/j.fuproc.2009.04.019.

22. Papuga, S. V.; Gvero, P. M.; Vukić, L. M.; Temperature and Time Influence on the Waste Plastics Pyrolysis in the Fixed Bed Reactor. *Thermal Science*. **2016**, 20, 731-741. doi:10.2298/tsci141113154p.

23. Khan, M. Z. H.; Sultana, M.; Al-Mamun, M. R.; Hasan, M. R.; Pyrolytic Waste Plastic Oil and Its Diesel Blend: Fuel Characterization. *Journal of Environmental and Public Health*. **2016**, 2016, 1-6. http://dx.doi.org/10.1155/2016/7869080.

24. Das, P.; Tiwari, P.; The effect of slow pyrolysis on the conversion of packaging waste plastics (PE and PP) into fuel. *Waste Management*. **2018**, 79, 615-624. https://doi.org/10.1016/j.wasman.2018.08.021.

25. Zhang, Y.; Duan, D.; Lei, H.; Villota, E.; Ruan, R.; Jet fuel production from waste plastics via catalytic pyrolysis with activated carbons. *Applied Energy*. **2019**, 251, 113337. https://doi.org/10.1016/j.apenergy.2019.113337.

26. Ratnasari, D. K.; Nahil, M. A.; Williams, P. T.; Catalytic pyrolysis of waste plastics using staged catalysis for production of gasoline range hydrocarbon oils. *Journal of Analytical and Applied Pyrolysis*. **2017**, 124, 631-637. http://dx.doi.org/10.1016/j.jaap.2016.12.027.

27. Xue, Y.; Johnston, P.; Bai, X.; Effect of catalyst contact mode and gas atmosphere during catalytic pyrolysis of waste plastics. *Energy Conversion and Management.* **2017**, 142, 441–451. http://dx.doi.org/10.1016/j.enconman.2017.03.071.

28. Singh, R. K.; Ruj, B.; Sadhukhan, A. K.; Gupta, P.; Tigga, V. P.; Waste plastic to pyrolytic oil and its utilization in CI engine: Performance analysis and combustion characteristics. *Fuel*. **2020**, 262, 116539. https://doi.org/10.1016/j.fuel.2019.116539.

29. Kremer, I.; Tomić, T.; Katančić, Z.; Erceg, M.; Papuga, S.; Vuković, J. P.; Schneider, D. R.; Catalytic pyrolysis of mechanically non-recyclable waste plastics mixture: Kinetics and pyrolysis in laboratory-scale reactor. *Journal of Environmental Management.* **2021**, 296, 113145. https://doi.org/10.1016/j.jenvman.2021.113145.

30. Barbarias, I.; Lopez, G.; Artetxe, M.; Arregi, A.; Bilbao, J.; Olazar, M.; Valorisation of different waste plastics by pyrolysis and in-line catalytic steam reforming for hydrogen production. *Energy Conversion and Management.* **2018**, 156, 575–584. https://doi.org/10.1016/j.enconman.2017.11.048.

31. Huo, E.; Lei, H.; Liu, C.; Zhang, Y.; Xin, L.; Zhao, Y.; Qian, M.; Zhang, Q.; Lin, X.; Wang, C.; Mateo, W.; Villota, E. M.; Ruan, R.; Jet fuel and hydrogen produced from waste plastics catalytic pyrolysis with activated carbon and MgO. *Science of the Total Environment.* **2020**, 727, 138411. https://doi.org/10.1016/j.scitotenv.2020.138411.

32. Pratt, L. M.; Kim, J.; Lo, H. Y.; Xiao, D.; Brown grease pyrolysis under pressure: Extending the range of reaction conditions and hydrocarbon product distributions. *Fuel*. **2021**, 289, 119782. https://doi.org/10.1016/j.fuel.2020.119782.

33. Balcazar, J. G. C.; Dias, R. A.; Balestieri, J. A. P.; Analysis of hybrid waste-to-energy for medium-sized cities. *Energy*. **2013**, 55, 728–741. http://dx.doi.org/10.1016/j.energy.2013.02.003.

34. Hasan, M. M.; Rasul, M. G.; Khan, M. M. K.; Ashwath, N.; Jahirul, M. I.; Energy recovery from municipal solid waste using pyrolysis technology: A review on current status and developments. *Renewable and Sustainable Energy Reviews.* **2021**, 145, 111073. https://doi.org/10.1016/j.rser.2021.111073.

35. Sikarwar, V. S.; Zhao, M.; Clough, P.; Yao, J.; Zhong, X.; Memon, M. Z.; Shah, N.; Anthony, E. J.; Fennell, P. S.; An overview of advances in biomass gasification. *Energy & Environmental Science.* **2016**, 9, 2939–2977. doi: 10.1039/c6ee00935b.

36. Sikarwar, V. S.; Zhao, M.; Fennell, P. S.; Shah, N.; Anthony, E. J.; Progress in biofuel production from gasification. *Progress in Energy and Combustion Science.* **2017**, 61, 189–248. http://dx.doi.org/10.1016/j.pecs.2017.04.001.

37. Buekens, A.; Yang, J.; Recycling of WEEE plastics: a review. *Journal of Material Cycles and Waste Management.* **2014**, 16, 415–434. doi: 10.1007/s10163-014-0241-2.

38. Hall, W. J.; Williams, P. T.; Removal of organobromine compounds from the pyrolysis oils of flame retarded plastics using zeolite catalysts. *Journal of Analytical and Applied Pyrolysis.* **2008**, 81, 139–147. doi: 10.1016/j.jaap.2007.09.008.

39. Hall, W. J.; Williams, P. T.; Analysis of products from the pyrolysis of plastics recovered from the commercial scale recycling of waste electrical and electronic equipment. *Journal of Analytical and Applied Pyrolysis.* **2007**, 79, 375–386. doi: 10.1016/j.jaap.2006.10.006.

40. Hall, W. J.; Williams, P. T.; Fast Pyrolysis of Halogenated Plastics Recovered from Waste Computers. *Energy & Fuels*. **2006**, 20, 1536–1549. doi: 10.1021/ef060088n.

41. Nakaji, Y.; Tamura, M.; Miyaoka, S.; Kumagai, S.; Tanji, M.; Nakagawa, Y.; Yoshioka, T.; Tomishige, K.; Low-temperature catalytic upgrading of waste polyolefinic plastics into liquid fuels and waxes. *Applied Catalysis B: Environmental.* **2021**, 285, 119805. https://doi.org/10.1016/j.apcatb.2020.119805.

42. Fan, L.; Zhang, Y.; Liu, S.; Zhou, N.; Chen, P.; Liu, Y.; Wang, Y.; Peng, P.; Cheng, Y.; Addy, M.; Lei, H.; Ruan, R.; Ex-situ catalytic upgrading of vapors from microwave-assisted pyrolysis of low-density polyethylene with MgO. *Energy Conversion and Management.* **2017**, 149, 432–441. http://dx.doi.org/10.1016/j.enconman.2017.07.039.

43. Fan, L.; Su, Z.; Wu, J.; Xiao, Z.; Huang, P.; Liu, L.; Jiang, H.; Zhou, W.; Liu, S.; Ruan, R.; Integrating continuous-stirred microwave pyrolysis with ex-situ catalytic upgrading for linear low-density polyethylene conversion: Effects of parameter conditions. *Journal of Analytical and Applied Pyrolysis* **2021**, 157, 105213. https://doi.org/10.1016/j.jaap.2021.105213.

44. Ma, C.; Yu, J.; Yan, Q.; Song, Z.; Wang, K.; Wang, B.; Sun, L.; Pyrolysis-catalytic upgrading of brominated high impact polystyrene over Fe and Ni modified catalysts: Influence of HZSM-5 and MCM-41 catalysts. *Polymer Degradation and Stability.* **2017**, 146, 1–12. https://doi.org/10.1016/j.polymdegradstab.2017.09.005.

45. Wang, S.; Kim, H.; Lee, D.; Lee, Y. R.; Won, Y.; Hwang, B. W.; Nam, H.; Ryu, H. J.; Lee, K. H.; Drop-in fuel production with plastic waste pyrolysis oil over catalytic separation. *Fuel.* **2021**, 305, 121440. https://doi.org/10.1016/j.fuel.2021.121440.

46. Bagri, R.; Williams, P. T.; Catalytic pyrolysis of polyethylene. *Journal of Analytical and Applied Pyrolysis.* **2002**, 63, 29–41. doi: 10.1016/s0165-2370(01)00139-5.

47. Nishino, J.; Itoh, M.; Ishinomori, T.; Kubota, N.; Uemichi, Y.; Development of a catalytic cracking process for converting waste plastics to petrochemicals. *Journal of Material Cycles and Waste Management.* **2003**, 5, 89–93. doi: 10.1007/s10163-003-0086-6.

48. Dai, L.; Zhou, N.; Cobb, K.; Chen, P.; Wang, Y.; Liu, Y.; Zou, R.; Lei, H.; Mohamed, B. A.; Cheng, Y.; Ruan, R.; Insights into structure–performance relationship in the catalytic cracking of high-density polyethylene. *Applied Catalysis B: Environmental*. **2022**, 318, 121835. https://doi.org/10.1016/j.apcatb.2022.121835.

49. Zhou, N.; Dai, L.; Lyu, Y.; Wang, Y.; Li, H.; Cobb, K.; Chen, P.; Lei, H.; Ruan, R.; A structured catalyst of ZSM-5/SiC foam for chemical recycling of waste plastics via catalytic pyrolysis. *Chemical Engineering Journal.* **2022**, 440, 135836. https://doi.org/10.1016/j.cej.2022.135836.

50. Hwang, K. R.; Choi, S. A.; Choi, I. H.; Lee, K. H.; Catalytic cracking of chlorinated heavy wax from pyrolysis of plastic wastes to low carbon-range fuels: Catalyst effect on properties of liquid products and dechlorination. *Journal of Analytical and Applied Pyrolysis.* **2021**, 155, 105090. https://doi.org/10.1016/j.jaap.2021.105090.

51. Marino, A.; Aloise, A.; Hernando, H.; Fermoso, J.; Cozza, D.; Giglio, E.; Migliori, M.; Pizarro, P.; Giordano, G.; Serrano, D. P.; ZSM-5 zeolites performance assessment in catalytic pyrolysis of PVC-containing real WEEE plastic wastes. *Catalysis Today.* **2022**, 390–391, 210–220. https://doi.org/10.1016/j.cattod.2021.11.033.

52. Ma, C.; Yu, J.; Chen, T.; Yan, Q.; Song, Z.; Wang, B.; Sun, L.; Influence of Fe based ZSM-5 catalysts on the vapor intermediates from the pyrolysis of brominated acrylonitrile-butadiene-styrene copolymer (Br-ABS). *Fuel.* **2018**, 230, 390–396. https://doi.org/10.1016/j.fuel.2018.05.077.

53. Shafaghat, H.; Gulshan, S.; Johansson, A. C.; Evangelopoulos, P.; Yang, W.; Selective recycling of BTX hydrocarbons from electronic plastic wastes using catalytic fast pyrolysis. *Applied Surface Science.* **2022**, 605, 125964. https://doi.org/10.1016/j.apsusc.2022.154734.

54. Chen, T.; Yu, J.; Ma, C.; Bikane, K.; Sun, L.; Catalytic performance and debromination of Fe–Ni bimetallic MCM-41 catalyst for the two-stage pyrolysis of waste computer casing plastic. *Chemosphere.* **2020**, 248, 125964. https://doi.org/10.1016/j.chemosphere.2020.125964.

55. Bernar, L. P.; Ferreira, C. C.; Costa, A. F. F.; Ribeiro, H. J. S.; Santos, W. G.; Pereira, L. M.; Pereira, A. M.; Moraes, N. L.; Assunção, F. P. C.; Mota, S. A. P.; Castro, D. A. R.; Santos, M. C.; Mendonça, N. M.; Duvoisin Junior, S.; Borges, L. E. P.; Machado, N. T.; Catalytic Upgrading of Residual Fat Pyrolysis Vapors over Activated Carbon Pellets into Hydrocarbons-like Fuels in a Two-Stage Reactor: Analysis of Hydrocarbons Composition and Physical-Chemistry Properties. *Energies*. **2022**, 15, 4587. https://doi.org/10.3390/en15134587.

56. Ferreira, C. C.; Bernar, L. P.; Costa, A. F. F.; Ribeiro, H. J. S.; Santos, M. C.; Moraes, N. L.; Costa, Y. S.; Baia, A. C. F.; Mendonça, N. M.; Mota, S. A. P.; Assunção, F. P. C.; Castro, D. A. R.; Quaresma, C. C. V.; Duvoisin Junior, S.; Borges, L. E. P.; Machado, N. T; Improving Fuel Properties and Hydrocarbon Content from Residual Fat Pyrolysis Vapors over Activated Red Mud Pellets in Two-Stage Reactor: Optimization of Reaction Time and Catalyst Content. *Energies.* **2022**, 15, 5595. https://doi.org/10.3390/en15155595.

57. Tseng, R. L.; Mesopore control of high surface area NaOH-activated carbon. *Journal of Colloid and Interface Science.* **2006**, 303, 494–502. doi: 10.1016/j.jcis.2006.08.024.

58. Castro, D. A. R.; Ribeiro, H. J. S.; Guerreiro, L. H. H.; Bernar, L. P.; Bremer, S. J.; Santos, M. C.; Almeida, H. S.; Duvoisin Junior, S.; Borges, L. E. P.; Machado, N. T; Production of Fuel-Like Fractions by Fractional Distillation of Bio-Oil from Açaí (*Euterpe oleracea* Mart.) Seeds Pyrolysis. *Energy.* **2021**, 14, 3713. https://doi.org/10.3390/en14133713.

59. Appleby, W. G.; Gibson, J. W.; Good, G. M.; Coke Formation in Catalytic Cracking. *Industrial & Engineering Chemistry Process Design and Development.* **1962**, 1, 102–110. https://doi.org/10.1021/i260002a006.

60. Fertani-Gmati, M.; Brahim, K.; Khattech, I.; Jemal, M.; Thermochemistry and kinetics of silica dissolution in NaOH solutions: Effect of the alkali concentration. *Thermochimica Acta.* **2014**, 594, 58–67. http://dx.doi.org/10.1016/j.tca.2014.09.003.

61. Jackson, S. D.; Processes occurring during deactivation and regeneration of metal and metal oxide catalysts. *Chemical Engineering Journal.* **2006**, 120, 119–125. doi: 10.1016/j.cej.2006.03.021.

62. Argyle, M.; Bartholomew, C.; Heterogeneous Catalyst Deactivation and Regeneration: A Review. *Catalysts*. **2015**, 5, 145–269. doi: 10.3390/catal5010145.

63. Zhang, X.; Sun, L.; Chen, L.; Xie, X.; Zhao, B.; Si, H.; Meng, G.; Comparison of catalytic upgrading of biomass fast pyrolysis vapors over CaO and Fe(III)/CaO catalysts. *Journal of Analytical and Applied Pyrolysis*. **2014**, 108, 35–40. http://dx.doi.org/10.1016/j.jaap.2014.05.020.

64. Sun, Z.; Xu, B.; Rony, A. H.; Toan, S.; Chen, S.; Gasem, K. A. M.; Adidharma, H.; Fan, M.; Xiang, W.; Thermogravimetric and kinetics investigation of pine wood pyrolysis catalyzed with alkali-treated CaO/ZSM-5. *Energy Conversion and Management.* **2017**, 146, 182–194. http://dx.doi.org/10.1016/j.enconman.2017.04.104.

65. Chang, C.-Chu.; Wan, S.-Wu.; China's Motor Fuels from Tung Oil. *Industrial and Engineering Chemistry.* **1947**, 39, 1543–1548. https://doi.org/10.1021/ie50456a011.

66. Vasile, C.; Brebu, M. A.; Karayildirim, T.; Yanik, J.; Darie, H.; Feedstock recycling from plastic and thermoset fractions of used computers (I): pyrolysis. *Journal of Material Cycles and Waste Management.* **2006**, 8, 99–108. doi: 10.1007/s10163-006-0151-z.

67. Saraji-Bozorgzad, M.; Geissler, R.; Streibel, T.; Mühlberger, F.; Sklorz, M.; Kaisersberger, E.; Denner, T.; Zimmermann, R.; Thermogravimetry Coupled to Single Photon Ionization Quadrupole Mass Spectrometry: A Tool to Investigate the Chemical Signature of Thermal Decomposition of Polymeric Materials. *Analytical Chemistry.* **2008**, 80, 3393–3403. doi: 10.1021/ac702599y.

68. Roussi, A. T.; Vouvoudi, E. C.; Achilias, D. S.; Pyrolytic degradation kinetics of HIPS, ABS, PC and their blends with PP and PVC. *Thermochimica Acta*. **2020**, 690, 178705. https://doi.org/10.1016/j.tca.2020.178705.

69. Jung, S.-H.; Kim, S.-J.; Kim, J.-S.; Thermal degradation of acrylonitrile–butadiene–styrene (ABS) containing flame retardants using a fluidized bed reactor: The effects of Ca-based additives on halogen removal. *Fuel Processing Technology*. **2012**, 96, 265–270. doi: 10.1016/j.fuproc.2011.12.039.

70. Jung, S.-H.; Kim, S.-J.; Kim, J.-S.; The influence of reaction parameters on characteristics of pyrolysis oils from waste high impact polystyrene and acrylonitrile–butadiene–styrene using a fluidized bed reactor. *Fuel Processing Technology.* **2013**, 116, 123–129. http://dx.doi.org/ 10.1016/j.fuproc.2013.05.004.

71. Bhaskar, T.; Murai, K.; Matsui, T.; Brebu, M. A.; Uddin, M. A.; Muto, A.; Sakata, Y.; Murata, K.; Studies on thermal degradation of acrylonitrile–butadiene–styrene copolymer (ABS-Br) containing brominated flame retardant. *Journal of Analytical and Applied Pyrolysis.* **2003**, 70, 369–381. doi: 10.1016/s0165-2370(02)00183-3.

72. Bridgwater, A. V.; Renewable fuels and chemicals by thermal processing of biomass. *Chemical Engineering Journal.* **2003**, 91, 87–102. doi: 10.1016/s1385-8947(02)00142-0.

73. Mastral, F. J.; Esperanza, E.; García, P.; Juste, M.; Pyrolysis of high-density polyethylene in a fluidised bed reactor. Influence of the temperature and residence time. *Journal of Analytical and Applied Pyrolysis.* **2002**, 63, 1–15. https://doi.org/10.1016/s0165-2370(01)00137-1.

74. Al-Salem, S. M.; Lettieri, P.; Kinetic study of high-density polyethylene (HDPE) pyrolysis. *Chemical Engineering Research and Design.* **2010**, 88, 1599–1606. doi: 10.1016/j.cherd.2010.03.012.

75. Abbas-Abadi, M. S.; Haghighi, M. N.; Yeganeh, H.; McDonald, A. G.; Evaluation of pyrolysis process parameters on polypropylene degradation products. *Journal of Analytical and Applied Pyrolysis.* **2014**, 109, 272–277. http://dx.doi.org/10.1016/j.jaap.2014.05.023.

76. López, A.; de Marco, I.; Caballero, B. M.; Laresgoiti, M. F.; Adrados, A.; Influence of time and temperature on pyrolysis of plastic wastes in a semi-batch reactor. *Chemical Engineering Journal.* **2011**, 173, 62–71. doi: 10.1016/j.cej.2011.07.037.

77. Onwudili, J. A.; Insura, N.; Williams, P. T.; Composition of products from the pyrolysis of polyethylene and polystyrene in a closed batch reactor: Effects of temperature and residence time. *Journal of Analytical and Applied Pyrolysis.* **2009**, 86, 293–303. doi: 10.1016/j.jaap.2009.07.008.

78. Maniscalco, M.; la Paglia, F.; Iannotta, P.; Caputo, G.; Scargiali, F.; Grisafi, F.; Brucato, A.; Slow pyrolysis of an LDPE/PP mixture: Kinetics and process performance. *Journal of the Energy Institute.* **2021**, 96, 234–241. https://doi.org/10.1016/j.joei.2021.03.006.

79. Miskolczi, N.; Hall, W. J.; Angyal, A.; Bartha, L.; Williams, P. T.; Production of oil with low organobromine content from the pyrolysis of flame retarded HIPS and ABS plastics. *Journal of Analytical and Applied Pyrolysis.* **2008**, 83, 115–123. doi: 10.1016/j.jaap.2008.06.010.

80. Brebu, M.; Azhar Uddin, M.; Muto, A.; Sakata, Y.; Vasile, C.; The role of temperature program and catalytic system on the quality of acrylonitrile-butadiene-styrene degradation oil. *Journal of Analytical and Applied Pyrolysis.* **2002**, 63, 43–57. doi: 10.1016/s0165-2370(01)00140-1.

81. Harussani, M. M.; Sapuan, S. M.; Rashid, U.; Khalina, A.; Ilyas, R. A.; Pyrolysis of polypropylene plastic waste into carbonaceous char: Priority of plastic waste management amidst COVID-19 pandemic. *Science of the Total Environmental.* **2022**, 803, 149911. https://doi.org/10.1016/j.scitotenv.2021.149911.

82. Manoj, B.; Kunjomana, A. G.; Study of Stacking Structure of Amorphous Carbon by X-Ray Diffraction Technique. *International Journal of Electrochemical Science.* **2012**, 7, 3127–3134.

83. Iwanek (nee Wilczkowska), E. M.; Kirk, D. W.; Application of Slow Pyrolysis to Convert Waste Plastics from a Compost-Reject Stream into Py-Char. *Energies.* **2022**, 15, 3072. https://doi.org/10.3390/en15093072.

84. Joni, I. M.; Nulhakim, L.; Panatarani, C.; Characteristics of $TiO_2$ particles prepared by simple solution method using $TiCl_3$ precursor. *Journal of Physics: Conference Series.* **2018**, 1080, 012042. doi: 10.1088/1742-6596/1080/1/012042.

85. Chin, H. S.; Cheong, K. Y.; Razak, K. A.; Review on oxides of antimony nanoparticles: synthesis, properties, and applications. *Journal of Materials Science.* **2010**, 45, 5993–6008. doi: 10.1007/s10853-010-4849-x.

86. Maafa, I.; Pyrolysis of Polystyrene Waste: A Review. *Polymers.* **2021**, 13, 225. https://doi.org/10.3390/polym13020225.

87. Nunome, Y.; Suzuki, T.; Nedjalkov, I.; Ueki, Y.; Yoshiie, R.; Naruse, I.; Generation behavior of tar from ABS, PC, and PE during pyrolysis and steam gasification by mass spectrometry. *Journal of Material Cycles and Waste Management.* **2019**, 21, 1300–1310. https://doi.org/10.1007/s10163-019-00883-9.

88. Zhang, S.; Zhang, H.; Liu, X.; Zhu, S.; Hu, L.; Zhang, Q.; Upgrading of bio-oil from catalytic pyrolysis of pretreated rice husk over Fe-modified ZSM-5 zeolite catalyst. *Fuel Processing Technology*. **2018**, 175, 17–25. https://doi.org/10.1016/j.fuproc.2018.03.002.

89. Ma, F.; Hanna, M. A.; Biodiesel production: a review. *Bioresource Technology*. **1999**, 70, 1–15. doi: 10.1016/s0960-8524(99)00025-5.

90. Speight, J. G.; York, N.; San, C.; Lisbon, F.; Madrid, L.; City, M.; New, M.; San, D.; Seoul, J. *Synthetic Fuels Handbook: Properties, Process, and Performance*; McGraw-Hill Education; **2008**; ISBN 9780071490238.

91. Panda, A. K.; Singh, R. K.; Catalytic performances of kaoline and silica alumina in the thermal degradation of polypropylene. *Journal of Fuel Chemistry and Technology*. **2011**, 39, 198-202.

92. Supattra, B.; Andrew, J. H.; Yuvarat, N.; Catalytic pyrolysis of plastic waste for the production of liquid fuels for engines. *Royal Society of Chemistry Advances*. **2019**, 9, 5844-5857. doi: 10.1039/c8ra10058f.

93. Seung-Soo, K., Jinsoo, K., Young-Kwon, P., Chan-Jin, P.; Non-isothermal pyrolysis of the mixtures of waste automobile lubricating oil and polystyrene in a stirred batch reactor. *Renewable Energy*. **2013**, 54, 241-247. http://dx.doi.org/10.1016/j.renene.2012.08.001.

94. Ucar, S.; Özkan, A.; Karagöz, S.; Co-pyrolysis of waste polyolefins with waste motor oil. *Journal of Analytical and Applied Pyrolysis*. **2016**, 119, 233-241. http://dx.doi.org/10.1016/j.jaap.2016.01.013.

95. Kumagai, S.; Hasegawa, I.; Grause, G; Kameda, T.; Yoshioka, T.; Thermal decomposition of individual and mixed plastics in the presence of CaO or $Ca(OH)_2$. *Journal of Analytical and Applied Pyrolysis.* **2015**, 113, 584-590. http://dx.doi.org/10.1016/j.jaap.2015.04.004.

96. Hussein, Z. A.; Shakor, Z. M.; Alzuhairi, M.; Al-Sheikh, F.; Thermal and catalytic cracking of plastic waste: a review. *International Journal of Environmental Analytical Chemistry.* **2021**. https://doi.org/10.1080/03067319.2021.1946527.

97. Al-Salem, S. M.; Feedstock and Optimal Operation for Plastics to Fuel Conversion in Pyrolysis. *Plastics to Energy*. **2019**, 117-146. https://doi.org/10.1016/b978-0-12-813140-4.00005-4.

98. López, A.; de Marco, I.; Caballero, B. M.; Laresgoiti, M. F.; Adrados, A.; Influence of time and temperature on pyrolysis of plastic wastes in a semi-batch reactor. *Chemical Engineering Journal*. **2011**, 173, 62-71. doi: 10.1016/j.cej.2011.07.037.

99. Miandad, R.; Barakat, M. A.; Aburiazaiza, A. S.; Rehan, M.; Ismail, I. M. I.; Nizami, A. S.; Effect of plastic waste types on pyrolysis liquid oil. *International Biodeterioration & Biodegradation*. **2017**, 119, 239-252. http://dx.doi.org/10.1016/j.ibiod.2016.09.017.

100. Ludlow-Palafox, C.; Chase, H. A.; Microwave-Induced Pyrolysis of Plastic Wastes. *Industrial & Engineering Chemistry Research*. **2001**, 40, 4749-4756. doi: 10.1021/ie010202j.

101. Kumaran, K. T.; Shama, L.; Catalytic pyrolysis of plastic waste: A Review. *Advances in Science and Engineering Technology International Conferences*. **2020**, 1, doi: 10.1109/aset48392.2020.9118286.

102. Al-Salem, S. M.; Lettieri, P.; Baeyens, J.; Recycling and recovery routes of plastic solid waste (PSW): A review. *Waste Management*. **2009**, 29, 2625-2643. doi:10.1016/j.wasman.2009.06.004.

103. Ignatyev, I. A.; Thielemans, W.; Vander Beke, B.; Recycling of Polymers: A Review. *ChemSusChem*. **2014**, 7, 1579-1593. https://doi.org/10.1002/cssc.201300898

104. Karthikeyan, S.; Sivakumar, N.; Manimekalai, T. K.; Sathiskumar, C.; A review on pyrolisis of waste plastics to value added products. *Elixir Online Journal*. **2012**, 29, 8291-8298.

105. Wong, S. L.; Ngadi, N.; Abdullah, T. A. T.; Inuwa, I. M.; Current state and future prospects of plastic waste as source of fuel: A review. *Renewable and Sustainble Energy Reviews*. **2015**, 50, 1167-1180. https://doi.org/10.1016/j.rser.2015.04.063.

106. Solis, M.; Silveira, S.; Technologies for chemical recycling of household plastics – A technical review and TRL assessment. *Waste Management*. **2020**, 105, 128-138. https://doi.org/10.1016/j.wasman.2020.01.038.

107. Pereira, M. S.; Estudo do Processo de Craqueamento Termocatalítico de Polímeros (Polietileno, Polipropileno e Poliestireno) para Produção de Combustível. Tese de Doutorado. Universidade Federal do Pará. Instituto de Tecnologia. Programa de Pós-Graduação em Engenharia de Recursos Naturais da Amazônia, Belém, **2016**. doi: 10.13140/rg.2.1.4735.1926.

108. Miranda, D. M. V.; Degradação térmica e catalítica dos polímeros poli(acrilonitrila-co-butadieno-co-estireno) (ABS) e poliestireno de alto impacto (HIPS) oriundos de resíduos eletroeletrônicos. Dissertação de Mestrado. UFRJ/COPPE, Rio de Janeiro, **2016**.

109. Peeters, J. R.; Vanegas, P.; Kellens, K.; Wang, F.; Huisman, J.; Dewulf, W.; Duflou, J. R.; Forecasting waste compositions: A case study on plastic waste of electronic display housings. *Waste Management*, **2015**, 46, 28-39. http://dx.doi.org/10.1016/j.wasman.2015.09.019.

110. Irina, T; Sushil, K.; Timo, K.; Characterization of Feedstock Filament Extruded from Secondary Sources of PS, ABS and PVC; *Lappeenranta University of Technology*, Lappeenranta, Finland; **2018;** 3; 57; doi:10.3390/recycling3040057.

111. Grassi, V. G.; Forte, M. M. C.; Aspectos Morfológicos e Relação Estrutura-Propriedades de Poliestireno de Alto Impacto. *Polímeros: Ciência e Tecnologia*. **2001**, 11, 158-168.

112. Achilias, D. S.; Antonakou, E. V.; Chemical and Thermochemical Recycling of Polymers from Waste Electrical and Electronic Equipment. *InTech.* **2015,** Chapter 3, http://dx.doi.org/10.5772/59960.

113. Brennan, L. B.; Isaac, D. H.; Arnold, J. C.; Recycling of acrylonitrile-butadiene-styrene and high-impact polystyrene from waste computer equipment; *Journal of Applied Polymer Science*. **2002,** 86, 572-578.

114. Muhammad, C.; Onwudili, J. A.; Williams, P. T.; Catalytic Pyrolysis of Waste Plastic from Electrical and Electronic Equipment. *Journal of Analytical and Applied Pyrolysis*. **2015**, 113, 332-339. https://doi.org/10.1016/j.jaap.2015.02.016.

## TABELAS SUPLEMENTARES

**Table S1**: Classes of compounds, summation of peak areas, CAS number, and retention times of chemical compounds identified by GC-MS in OLP by thermal cracking of plastic waste from computer equipment at 350 °C, 1.0 atm, Reaction time=30 min, in semi-pilot scale two-stage reactor of 2.0 L.

| Chemical Compound | RT [min] | CAS | wi[%.area] |
|---|---|---|---|
| **Aromatic Hydrocarbons** | **Σ(%.area)** | | **53.723** |
| Styrene | 9.728 | 100-42-5 | 9.547 |
| Benzene, (1-methylethyl)- | 10.710 | 98-82-8 | 4.194 |
| Benzene, propyl- | 11.688 | 103-65-1 | 0.220 |
| α-Methylstyrene | 12.584 | 98-83-9 | 6.413 |
| Benzene, 1-propenyl- | 14.092 | 637-50-3 | 0.521 |
| Indene | 14.849 | 95-13-6 | 0.267 |
| Biphenyl | 25.017 | 92-52-4 | 0.281 |
| Diphenylmethane | 26.329 | 101-81-5 | 0.586 |
| Benzene, 1,1'-ethylidenebis- | 27.764 | 612-00-0 | 0.485 |
| Bibenzyl | 28.688 | 103-29-7 | 0.427 |
| Benzene, 1,1'-(1,3-propanediyl) bis- | 32.085 | 1081-75-0 | 12.752 |
| Benzene, 1,1'-(3-methyl-1-propene-1,3-diyl) bis- | 32.412 | 7614-93-9 | 1.244 |
| Benzene, 1,1'-(1-methyl-1,3-propanediyl) bis- | 32.600 | 1520-44-1 | 1.677 |
| 1,2-Diphenylcyclopropane | 33.636 | 29881-14-9 | 2.268 |
| Benzene, 1,1'-(1,4-butanediyl) bis- | 34.021 | 1083-56-3 | 0.541 |
| Benzene, 1,1'-(3-methyl-1-propene-1,3-diyl) bis- | 34.386 | 7614-93-9 | 0.767 |
| Benzene, 1,1'-(1,1,2,2-tetramethyl-1,2-ethanediyl) bis- | 34.748 | 1889-67-4 | 0.597 |
| Benzene, 1,1'-(2-methyl-1-propenylidene) bis- | 34.898 | 781-33-9 | 1.998 |
| 1-(4-Methylphenyl)-4-phenylbuta-1,3-diene | 36.410 | 37985-11-8 | 0.410 |
| 1H-Indene, 2-phenyl- | 36.860 | 4505-48-0 | 0.270 |
| 1,2,3,4-Tetrahydro-1-phenyl-1,2,3-methanonaphthalene | 40.387 | 138089-69-7 | 0.492 |
| Benzene, 1,1'-[3-(2-phenylethylidene)-1,5-pentanediyl] bis- | 44.682 | 55334-57-1 | 1.773 |
| Benzene, (1-methylhexadecyl)- | 45.088 | 55125-25-2 | 0.471 |
| p-Terphenyl | 45.436 | 92-94-4 | 0.300 |
| 1-Propene, 3-(2-cyclopentenyl)-2-methyl-1,1-diphenyl- | 49.302 | - | 0.886 |
| Benzene, 1,1'-(1,4-dimethyl-1-butene-1,4-diyl) bis- | 51.646 | 52161-54-3 | 0.592 |
| 1-Propene, 3-(2-cyclopentenyl)-2-methyl-1,1-diphenyl- | 53.449 | - | 2.474 |
| 1,1':3',1"-Terphenyl, 5'-phenyl- | 68.109 | 612-71-5 | 1.270 |
| **Polycyclic Aromatic Hydrocarbons (PAH)** | **Σ(%.area)** | | **21.888** |
| Naphthalene | 19.491 | 91-20-3 | 0.556 |
| Naphthalene, 1-methyl- | 22.770 | 90-12-0 | 0.370 |
| Naphthalene, 2-methyl- | 23.259 | 91-57-6 | 0.472 |
| Naphthalene, 1,2,3,4-tetrahydro-1-phenyl- | 34.473 | 3018-20-0 | 0.600 |
| Naphthalene, 1,2,3,4-tetrahydro-6-(phenylmethyl)- | 35.372 | 35310-85-1 | 0.314 |
| Naphthalene, 1-phenyl- | 36.578 | 605-02-7 | 2.056 |
| Naphthalene, 2-phenyl- | 40.019 | 612-94-2 | 1.958 |

| | | | |
|---|---|---|---|
| Naphthalene, 2-(phenylmethyl)- | 44.292 | 613-59-2 | 1.913 |
| **Nitrogenated Compounds** | **Σ(%.area)** | | **21.888** |
| Benzyl nitrile | 17.566 | 140-29-4 | 0.340 |
| Benzeneacetonitrile, α-methyl- | 18.434 | 1823-91-2 | 0.557 |
| Benzenepropanenitrile | 20.642 | 645-59-0 | 0.240 |
| 1,2-Benzenedicarbonitrile | 21.230 | 91-15-6 | 0.302 |
| Cyclopropanecarbonitrile, 2-phenyl-, trans- | 22.408 | 5590-14-7 | 0.290 |
| Benzenebutanenitrile | 23.461 | 2046-18-6 | 11.716 |
| Quinoline, 1,2-dihydro-1-methyl-2-methylene- | 24.133 | - | 0.630 |
| 3-Benzyl-4,5-dihydro-3H-pyrrole | 24.347 | - | 1.539 |
| 1,2,3,3a-Tetrahydropentalene, 1,1-dimethyl-3-cyanomethylene- | 24.851 | - | 0.174 |
| Cyclopropanecarbonitrile, 2-phenyl-, trans- | 25.772 | 5590-14-7 | 0.269 |
| 1H-Pyrrole, 1-(4-methylphenyl)- | 26.122 | 827-60-1 | 0.171 |
| Quinoline, 4-ethyl- | 27.451 | 19020-26-9 | 0.320 |
| Naphthalene, 1-isocyano- (cis) | 28.187 | - | 0.913 |
| Naphthalene, 1-isocyano- (trans) | 28.899 | - | 0.561 |
| 1-Naphthaleneacetonitrile | 32.306 | 132-75-2 | 0.964 |
| Octadecanenitrile | 43.043 | 638-65-3 | 0.743 |
| 4-Methyl-3-(O-methylbenzyl)pentanenitrile | 43.877 | 29107-40-2 | 0.670 |
| (1-Benzyl-2-O-tolyl-ethyl)-isonitrile | 44.445 | - | 0.804 |
| Naphthalene-1,3,3-tricarbonitrile, 3,4,4a,5,6,7-hexahdro-2-amino-4-(4-methylphenyl)- | 49.680 | 163978-39-0 | 0.324 |
| Naphthalene-1,3,3-tricarbonitrile, 3,4,4a,5,6,7-hexahdro-2-amino-4-(4-methylphenyl)- | 50.370 | 163978-39-0 | 0.361 |
| **Brominated Compounds** | **Σ(%.area)** | | **0.741** |
| Phenol, 2-bromo- | 15.591 | 95-56-7 | 0.360 |
| 5-Bromo-2-methoxy-1,3-dimethylbenzene | 23.559 | - | 0.381 |
| **Oxygenated Compounds** | **Σ(%.area)** | | **12.843** |
| Phenol | 12.146 | 108-95-2 | 3.272 |
| Phenol, 2-methyl- | 14.630 | 95-48-7 | 0.589 |
| Benzenemethanol, α-methyl-, (R)- | 15.082 | 1517-69-7 | 0.267 |
| Benzenemethanol, α,α-dimethyl- | 15.904 | 617-94-7 | 1.400 |
| Phenol, 2,5-dimethyl- | 16.580 | 95-87-4 | 0.380 |
| p-Cumenol | 20.028 | 99-89-8 | 4.554 |
| Phenol, 2-methyl-5-(1-methylethyl)- | 22.055 | 499-75-2 | 0.180 |
| Phenol, 2-(1-phenylethyl)- | 33.240 | 4237-44-9 | 0.475 |
| As-Indacen-1(2H)-one, 3,6,7,8-tetrahydro-3,3,6,6-tetramethyl- | 45.613 | 55591-18-9 | 0.847 |
| Benzaldehyde, 2-methyl-, (2,4-dinitrophenyl)hydrazone | 50.785 | 1773-44-0 | 0.879 |
| **Non Indentified Fraction** | **Σ(%.area)** | | **2.562** |

**Table S2**: Classes of compounds, summation of peak areas, CAS number, and retention times of chemical compounds identified by GC-MS in OLP by thermal cracking of plastic waste from computer equipment at 350 °C, 1.0 atm, Reaction time=45 min, in semi-pilot scale two-stage reactor of 2.0 L.

| Chemical Compound | RT [min] | CAS | wi[%.area] |
|---|---|---|---|
| **Aromatic Hydrocarbons** | **Σ(%.area)** | | **46.065** |
| Styrene | 9.728 | 100-42-5 | 5.149 |
| Benzene, (1-methylethyl)- | 10.710 | 98-82-8 | 3.147 |
| Benzene, propyl- | 11.688 | 103-65-1 | 0.166 |
| α-Methylstyrene | 12.584 | 98-83-9 | 4.785 |
| Benzene, 1-propenyl- | 14.092 | 637-50-3 | 0.395 |
| Biphenyl | 25.017 | 92-52-4 | 0.243 |
| Diphenylmethane | 26.329 | 101-81-5 | 0.630 |
| Benzene, 1,1'-ethylidenebis- | 27.764 | 612-00-0 | 0.544 |
| Bibenzyl | 28.688 | 103-29-7 | 0.523 |
| Benzene, 1,1'-(1,3-propanediyl) bis- | 32.085 | 1081-75-0 | 16.058 |
| Benzene, 1,1'-(3-methyl-1-propene-1,3-diyl) bis- | 32.412 | 7614-93-9 | 1.138 |
| Benzene, 1,1'-(1-methyl-1,3-propanediyl) bis- | 32.600 | 1520-44-1 | 2.553 |
| 1,2-Diphenylcyclopropane | 33.636 | 29881-14-9 | 2.110 |
| Benzene, 1,1'-(1,4-butanediyl) bis- | 34.021 | 1083-56-3 | 0.653 |
| Benzene, 1,1'-(3-methyl-1-propene-1,3-diyl) bis- | 34.386 | 7614-93-9 | 0.652 |
| Benzene, 1,1'-(1,1,2,2-tetramethyl-1,2-ethanediyl) bis- | 34.748 | 1889-67-4 | 0.577 |
| Benzene, 1,1'-(2-methyl-1-propenylidene) bis- | 34.898 | 781-33-9 | 1.617 |
| 1-(4-Methylphenyl)-4-phenylbuta-1,3-diene | 36.410 | 37985-11-8 | 0.472 |
| 1H-Indene, 2-phenyl- | 36.860 | 4505-48-0 | 0.163 |
| Benzene, 1,1'-[3-(2-phenylethylidene)-1,5-pentanediyl] bis- | 44.682 | 55334-57-1 | 1.411 |
| Benzene, (1-methylhexadecyl)- | 45.088 | 55125-25-2 | 0.432 |
| p-Terphenyl | 45.436 | 92-94-4 | 0.255 |
| 1-Propene, 3-(2-cyclopentenyl)-2-methyl-1,1-diphenyl- | 49.302 | - | 0.380 |
| Benzene, 1,1'-(1,4-dimethyl-1-butene-1,4-diyl) bis- | 51.646 | 52161-54-3 | 0.402 |
| 1-Propene, 3-(2-cyclopentenyl)-2-methyl-1,1-diphenyl- | 53.449 | - | 0.844 |
| 1,1':3',1"-Terphenyl, 5'-phenyl- | 68.109 | 612-71-5 | 0.766 |
| **Polycyclic Aromatic Hydrocarbons (PAH)** | **Σ(%.area)** | | **10.074** |
| Naphthalene | 19.491 | 91-20-3 | 0.515 |
| Naphthalene, 1-methyl- | 22.770 | 90-12-0 | 0.376 |
| Naphthalene, 2-methyl- | 23.259 | 91-57-6 | 0.482 |
| Naphthalene, 1-isocyano- (cis) | 28.187 | - | 1.228 |
| Naphthalene, 1-isocyano- (trans) | 28.899 | - | 0.554 |
| Naphthalene, 1,2,3,4-tetrahydro-1-phenyl- | 34.473 | 3018-20-0 | 0.633 |
| Naphthalene, 1-phenyl- | 36.578 | 605-02-7 | 2.530 |
| Naphthalene, 2-phenyl- | 40.019 | 612-94-2 | 1.727 |
| 1,2,3,4-Tetrahydro-1-phenyl-1,2,3-methanonaphthalene | 40.387 | 138089-69-7 | 0.443 |
| Naphthalene, 2-(phenylmethyl)- | 44.292 | 613-59-2 | 1.586 |

| **Nitrogenated Compounds** | **Σ(%.area)** | | **23.439** |
|---|---|---|---|
| Benzyl nitrile | 17.566 | 140-29-4 | 0.321 |
| Benzeneacetonitrile, α-methyl- | 18.434 | 1823-91-2 | 0.609 |
| Benzenepropanenitrile | 20.642 | 645-59-0 | 0.282 |
| 1,2-Benzenedicarbonitrile | 21.230 | 91-15-6 | 0.635 |
| Cyclopropanecarbonitrile, 2-phenyl-, trans- | 22.408 | 5590-14-7 | 0.285 |
| Benzenebutanenitrile | 23.461 | 2046-18-6 | 13.644 |
| Quinoline, 1,2-dihydro-1-methyl-2-methylene- | 24.133 | - | 0.763 |
| 3-Benzyl-4,5-dihydro-3H-pyrrole | 24.347 | - | 2.155 |
| 1,2,3,3a-Tetrahydropentalene, 1,1-dimethyl-3-cyanomethylene- | 24.851 | - | 0.194 |
| Cyclopropanecarbonitrile, 2-phenyl-, trans- | 25.772 | 5590-14-7 | 0.251 |
| 1H-Pyrrole, 1-(4-methylphenyl)- | 26.122 | 827-60-1 | 0.349 |
| Quinoline, 4-ethyl- | 27.451 | 19020-26-9 | 0.321 |
| 1-Naphthaleneacetonitrile | 32.306 | 132-75-2 | 0.919 |
| Octadecanenitrile | 43.043 | 638-65-3 | 0.832 |
| 4-Methyl-3-(O-methylbenzyl)pentanenitrile | 43.877 | 29107-40-2 | 0.612 |
| (1-Benzyl-2-O-tolyl-ethyl)-isonitrile | 44.445 | - | 0.624 |
| Naphthalene-1,3,3-tricarbonitrile, 3,4,4a,5,6,7-hexahdro-2-amino-4-(4-methylphenyl)- | 49.680 | 163978-39-0 | 0.307 |
| Naphthalene-1,3,3-tricarbonitrile, 3,4,4a,5,6,7-hexahdro-2-amino-4-(4-methylphenyl)- | 50.370 | 163978-39-0 | 0.336 |
| **Brominated Compounds** | **Σ(%.area)** | | **0.600** |
| Phenol, 2-bromo- | 15.591 | 95-56-7 | 0.296 |
| 5-Bromo-2-methoxy-1,3-dimethylbenzene | 23.559 | - | 0.304 |
| **Oxygenated Compounds** | **Σ(%.area)** | | |
| Phenol | 12.146 | 108-95-2 | 4.980 |
| Phenol, 2-methyl- | 14.630 | 95-48-7 | 0.577 |
| Benzenemethanol, α,α-dimethyl- | 15.904 | 617-94-7 | 1.240 |
| Phenol, 2,5-dimethyl- | 16.580 | 95-87-4 | 0.428 |
| p-Cumenol | 20.028 | 99-89-8 | 8.430 |
| Phenol, 2-methyl-5-(1-methylethyl)- | 22.055 | 499-75-2 | 0.288 |
| Phenol, 2-(1-phenylethyl)- | 33.240 | 4237-44-9 | 0.702 |
| 2,3-Dimethyl-1,4,4a,9a-tetrahydroanthracene-9,10-dione | 37.226 | 2670-23-7 | 0.374 |
| As-Indacen-1(2H)-one,3,6,7,8-tetrahydro-3,3,6,6-tetramethyl- | 45.613 | 55591-18-9 | 0.212 |
| Benzaldehyde, 2-methyl-, (2,4-dinitrophenyl)hydrazone | 50.785 | 1773-44-0 | 0.502 |
| **Non Indentified Fraction** | **Σ(%.area)** | | **2.092** |

**Table S3**: Classes of compounds, summation of peak areas, CAS number, and retention times of chemical compounds identified by GC-MS in OLP by thermal cracking of plastic waste from computer equipment at 350 °C, 1.0 atm, Reaction time=60 min, in semi-pilot scale two-stage reactor of 2.0 L.

| Chemical Compound | RT [min] | CAS | wi[%.area] |
|---|---|---|---|
| **Aromatic Hydrocarbons** | **Σ(%.area)** | | **48.440** |
| Styrene | 9.728 | 100-42-5 | 7.678 |
| Benzene, (1-methylethyl)- | 10.710 | 98-82-8 | 4.467 |
| Benzene, propyl- | 11.688 | 103-65-1 | 0.212 |
| α-Methylstyrene | 12.584 | 98-83-9 | 5.289 |
| Benzene, 1-propenyl- | 14.092 | 637-50-3 | 0.435 |
| Biphenyl | 25.017 | 92-52-4 | 0.207 |
| Diphenylmethane | 26.329 | 101-81-5 | 0.639 |
| Benzene, 1,1'-ethylidenebis- | 27.764 | 612-00-0 | 0.515 |
| Bibenzyl | 28.688 | 103-29-7 | 0.493 |
| Benzene, 1,1'-(1,3-propanediyl) bis- | 32.085 | 1081-75-0 | 16.254 |
| Benzene, 1,1'-(3-methyl-1-propene-1,3-diyl) bis- | 32.412 | 7614-93-9 | 1.151 |
| Benzene, 1,1'-(1-methyl-1,3-propanediyl) bis- | 32.600 | 1520-44-1 | 2.589 |
| 1,2-Diphenylcyclopropane | 33.636 | 29881-14-9 | 2.236 |
| Benzene, 1,1'-(1,4-butanediyl) bis- | 34.021 | 1083-56-3 | 0.707 |
| Benzene, 1,1'-(3-methyl-1-propene-1,3-diyl) bis- | 34.386 | 7614-93-9 | 0.616 |
| Benzene, 1,1'-(2-methyl-1-propenylidene) bis- | 34.898 | 781-33-9 | 1.314 |
| 1-(4-Methylphenyl)-4-phenylbuta-1,3-diene | 36.410 | 37985-11-8 | 0.503 |
| Benzene, 1,1'-[3-(2-phenylethylidene)-1,5-pentanediyl] bis- | 44.682 | 55334-57-1 | 1.370 |
| Benzene, (1-methylhexadecyl)- | 45.088 | 55125-25-2 | 0.379 |
| p-Terphenyl | 45.436 | 92-94-4 | 0.246 |
| 1-Propene, 3-(2-cyclopentenyl)-2-methyl-1,1-diphenyl- | 49.302 | - | 0.307 |
| Benzene, 1,1'-(1,4-dimethyl-1-butene-1,4-diyl) bis- | 51.646 | 52161-54-3 | 0.338 |
| 1-Propene, 3-(2-cyclopentenyl)-2-methyl-1,1-diphenyl- | 53.449 | - | 0.495 |
| **Polycyclic Aromatic Hydrocarbons (PAH)** | **Σ(%.area)** | | **9.043** |
| Naphthalene | 19.491 | 91-20-3 | 0.473 |
| Naphthalene, 1-methyl- | 22.770 | 90-12-0 | 0.345 |
| Naphthalene, 2-methyl- | 23.259 | 91-57-6 | 0.455 |
| Naphthalene, 1-isocyano- | 28.187 | 09/04/1984 | 1.274 |
| Naphthalene, 1,2,3,4-tetrahydro-1-phenyl- | 34.473 | 3018-20-0 | 0.633 |
| Naphthalene, 1-phenyl- | 36.578 | 605-02-7 | 2.549 |
| Naphthalene, 2-phenyl- | 40.019 | 612-94-2 | 1.719 |
| 1,2,3,4-Tetrahydro-1-phenyl-1,2,3-methanonaphthalene | 40.387 | 138089-69-7 | 0.422 |
| Naphthalene, 2-(phenylmethyl)- | 44.292 | 613-59-2 | 1.533 |
| **Nitrogenated Compounds** | **Σ(%.area)** | | **23.644** |
| Benzyl nitrile | 17.566 | 140-29-4 | 0.327 |
| Benzeneacetonitrile, α-methyl- | 18.434 | 1823-91-2 | 0.578 |
| Benzenepropanenitrile | 20.642 | 645-59-0 | 0.276 |

| | | | |
|---|---|---|---|
| 1,2-Benzenedicarbonitrile | 21.230 | 91-15-6 | 0.612 |
| Cyclopropanecarbonitrile, 2-phenyl-, trans- | 22.408 | 5590-14-7 | 0.300 |
| Benzenebutanenitrile | 23.461 | 2046-18-6 | 13.413 |
| Quinoline, 1,2-dihydro-1-methyl-2-methylene- | 24.133 | - | 0.806 |
| 3-Benzyl-4,5-dihydro-3H-pyrrole | 24.347 | - | 2.244 |
| 1,2,3,3a-Tetrahydropentalene, 1,1-dimethyl-3-cyanomethylene- | 24.851 | - | 0.229 |
| Cyclopropanecarbonitrile, 2-phenyl-, trans- | 25.772 | 5590-14-7 | 0.170 |
| 1H-Pyrrole, 1-(4-methylphenyl)- | 26.122 | 827-60-1 | 0.351 |
| Quinoline, 4-ethyl- | 27.451 | 19020-26-9 | 0.285 |
| Naphthalene, 1-isocyano- | 28.899 | 09/04/1984 | 0.563 |
| 1-Naphthaleneacetonitrile | 32.306 | 132-75-2 | 0.933 |
| Octadecanenitrile | 43.043 | 638-65-3 | 0.744 |
| 4-Methyl-3-(O-methylbenzyl)pentanenitrile | 43.877 | 29107-40-2 | 0.646 |
| (1-Benzyl-2-O-tolyl-ethyl)-isonitrile | 44.445 | - | 0.582 |
| Naphthalene-1,3,3-tricarbonitrile, 3,4,4a,5,6,7-hexahdro-2-amino-4-(4-methylphenyl)- | 49.680 | 163978-39-0 | 0.279 |
| Naphthalene-1,3,3-tricarbonitrile, 3,4,4a,5,6,7-hexahdro-2-amino-4-(4-methylphenyl)- | 50.370 | 163978-39-0 | 0.306 |
| **Brominated Compounds** | **Σ(%.area)** | | **0.348** |
| Phenol, 2-bromo- | 15.591 | 95-56-7 | 0.212 |
| 5-Bromo-2-methoxy-1,3-dimethylbenzene | 23.559 | - | 0.136 |
| **Oxygenated Compounds** | **Σ(%.area)** | | **15.680** |
| Phenol | 12.146 | 108-95-2 | 4.123 |
| Phenol, 2-methyl- | 14.630 | 95-48-7 | 0.539 |
| Benzenemethanol, α,α-dimethyl- | 15.904 | 617-94-7 | 1.567 |
| Phenol, 2,5-dimethyl- | 16.580 | 95-87-4 | 0.414 |
| p-Cumenol | 20.028 | 99-89-8 | 7.365 |
| Phenol, 2-methyl-5-(1-methylethyl)- | 22.055 | 499-75-2 | 0.287 |
| Phenol, 2-(1-phenylethyl)- | 33.240 | 4237-44-9 | 0.542 |
| 2,3-Dimethyl-1,4,4a,9a-tetrahydroanthracene-9,10-dione | 37.226 | 2670-23-7 | 0.334 |
| Benzaldehyde, 2-methyl-, (2,4-dinitrophenyl)hydrazone | 50.785 | 1773-44-0 | 0.509 |
| **Non Identified Fraction** | **Σ(%.area)** | | **2.092** |

**Table S4**: Classes of compounds, summation of peak areas, CAS number, and retention times of chemical compounds identified by GC-MS in OLP by thermal cracking of plastic waste from computer equipment at 400 °C, 1.0 atm, Reaction time=15 min, in semi-pilot scale two-stage reactor of 2.0 L.

| Chemical Compound | RT [min] | CAS | wi[%.area] |
|---|---|---|---|
| **Aromatic Hydrocarbons** | **Σ(%.area)** | | **50.222** |
| Styrene | 9.728 | 100-42-5 | 5.662 |
| Benzene, (1-methylethyl)- | 10.710 | 98-82-8 | 2.791 |
| α-Methylstyrene | 12.584 | 98-83-9 | 5.282 |
| Benzene, 1-propenyl- | 14.092 | 637-50-3 | 0.463 |
| Indene | 14.848 | 95-13-6 | 0.253 |
| Biphenyl | 25.017 | 92-52-4 | 0.313 |
| Diphenylmethane | 26.329 | 101-81-5 | 0.628 |
| Benzene, 1,1'-ethylidenebis- | 27.764 | 612-00-0 | 0.549 |
| Bibenzyl | 28.688 | 103-29-7 | 0.509 |
| Benzene, 1,1'-(1,3-propanediyl) bis- | 32.085 | 1081-75-0 | 13.692 |
| Benzene, 1,1'-(3-methyl-1-propene-1,3-diyl) bis- | 32.412 | 7614-93-9 | 1.432 |
| Benzene, 1,1'-(1-methyl-1,3-propanediyl) bis- | 32.600 | 1520-44-1 | 1.887 |
| 1,2-Diphenylcyclopropane | 33.636 | 29881-14-9 | 2.648 |
| Benzene, 1,1'-(1,4-butanediyl) bis- | 34.021 | 1083-56-3 | 0.567 |
| Benzene, 1,1'-(3-methyl-1-propene-1,3-diyl) bis- | 34.386 | 7614-93-9 | 0.899 |
| 2,4-Diphenyl-4-methyl-1-pentene | 34.748 | - | 0.526 |
| Benzene, 1,1'-(2-methyl-1-propenylidene) bis- | 34.898 | 781-33-9 | 2.637 |
| 1-(4-Methylphenyl)-4-phenylbuta-1,3-diene | 36.410 | 37985-11-8 | 0.426 |
| Benzene, 1,1'-[3-(2-phenylethylidene)-1,5-pentanediyl] bis- | 43.693 | 55334-57-1 | 0.712 |
| Naphthalene, 2-(phenylmethyl)- | 44.292 | 613-59-2 | 2.046 |
| Benzene, 1,1'-[3-(2-phenylethylidene)-1,5-pentanediyl] bis- | 44.682 | 55334-57-1 | 1.967 |
| Benzene, (1-methylhexadecyl)- | 45.093 | 55125-25-2 | 0.512 |
| p-Terphenyl | 45.430 | 92-94-4 | 0.298 |
| 1-Propene, 3-(2-cyclopentenyl)-2-methyl-1,1-diphenyl- | 49.302 | - | 0.968 |
| 1-Propene, 3-(2-cyclopentenyl)-2-methyl-1,1-diphenyl- | 53.449 | - | 2.555 |
| **Polycyclic Aromatic Hydrocarbons (PAH)** | **Σ(%.area)** | | **7.515** |
| Naphthalene | 19.491 | 91-20-3 | 0.721 |
| Naphthalene, 1-methyl- | 22.770 | 90-12-0 | 0.403 |
| Naphthalene, 2-methyl- | 23.259 | 91-57-6 | 0.552 |
| Naphthalene, 1,2,3,4-tetrahydro-1-phenyl- | 34.473 | 3018-20-0 | 0.625 |
| Naphthalene, 1,2,3,4-tetrahydro-6-(phenylmethyl)- | 35.372 | 35310-85-1 | 0.400 |
| Naphthalene, 1-phenyl- | 36.578 | 605-02-7 | 2.175 |
| Naphthalene, 2,7-bis(1,1-dimethylethyl)- | 37.221 | 10275-58-8 | 0.577 |
| Naphthalene, 2-phenyl- | 40.019 | 612-94-2 | 2.062 |
| **Nitrogenated Compounds** | **Σ(%.area)** | | **25.923** |
| Benzonitrile | 12.687 | 100-47-0 | 0.134 |
| Benzyl nitrile | 17.566 | 140-29-4 | 0.375 |

| | | | |
|---|---|---|---|
| Benzeneacetonitrile, α-methyl- | 18.434 | 1823-91-2 | 0.658 |
| Benzenepropanenitrile | 20.642 | 645-59-0 | 0.298 |
| 1,2-Benzenedicarbonitrile | 21.230 | 91-15-6 | 0.360 |
| Cyclopropanecarbonitrile, 2-phenyl-, trans- | 22.408 | 5590-14-7 | 0.339 |
| Benzenebutanenitrile | 23.461 | 2046-18-6 | 13.156 |
| Quinoline, 1,2-dihydro-1-methyl-2-methylene- | 24.133 | - | 0.781 |
| 3-Benzyl-4,5-dihydro-3H-pyrrole | 24.347 | - | 1.739 |
| 1,2,3,3a-Tetrahydropentalene, 1,1-dimethyl-3-cyanomethylene- | 24.847 | - | 0.241 |
| Cyclopropanecarbonitrile, 2-phenyl-, trans- | 25.772 | 5590-14-7 | 0.283 |
| 1H-Pyrrole, 1-(4-methylphenyl)- | 26.122 | 827-60-1 | 0.352 |
| Quinoline, 4-ethyl- | 27.451 | 19020-26-9 | 0.385 |
| Naphthalene, 1-isocyano- | 28.187 | 09/04/1984 | 0.949 |
| Naphthalene, 1-isocyano- | 28.899 | 09/04/1984 | 0.582 |
| 1-Naphthaleneacetonitrile | 32.306 | 132-75-2 | 1.018 |
| N-(2-Phenylethyl)-cis-2,3-epoxynona-6,8-diynamide | 34.586 | 96917-25-8 | 0.489 |
| Octadecanenitrile | 43.043 | 638-65-3 | 0.805 |
| 4-Methyl-3-(O-methylbenzyl)pentanenitrile | 43.877 | 29107-40-2 | 0.737 |
| (1-Benzyl-2-O-tolyl-ethyl)-isonitrile | 44.445 | - | 0.84 |
| Naphthalene-1,3,3-tricarbonitrile, 3,4,4a,5,6,7-hexahdro-2-amino-4-(4-methylphenyl)- | 49.679 | 163978-39-0 | 0.283 |
| Naphthalene-1,3,3-tricarbonitrile, 3,4,4a,5,6,7-hexahdro-2-amino-4-(4-methylphenyl)- | 50.378 | 163978-39-0 | 0.445 |
| Acridine, 9-phenyl- | 51.600 | 602-56-2 | 0.674 |
| **Brominated Compounds** | **Σ(%.area)** | | **0.665** |
| Phenol, 3-bromo- | 15.590 | 591-20-8 | 0.315 |
| 5-Bromo-2-methoxy-1,3-dimethylbenzene | 23.559 | - | 0.350 |
| **Oxygenated Compounds** | **Σ(%.area)** | | **12.889** |
| Phenol | 12.146 | 108-95-2 | 3.072 |
| Phenol, 2-methyl- | 14.630 | 95-48-7 | 0.700 |
| Benzenemethanol, α-methyl- | 15.081 | 98-85-1 | 0.327 |
| Benzenemethanol, α,α-dimethyl- | 15.904 | 617-94-7 | 1.556 |
| Phenol, 2,5-dimethyl- | 16.580 | 95-87-4 | 0.428 |
| p-Cumenol | 20.028 | 99-89-8 | 4.530 |
| Phenol, 2-methyl-5-(1-methylethyl)- | 22.055 | 499-75-2 | 0.311 |
| Phenol, 2-(1-phenylethyl)- | 33.240 | 4237-44-9 | 1.005 |
| Benzaldehyde, 2-methyl-, (2,4-dinitrophenyl)hydrazone | 50.781 | 1773-44-0 | 0.960 |
| **Non Identified Fraction** | **Σ(%.area)** | | **2.784** |

**Table S5**: Classes of compounds, summation of peak areas, CAS number, and retention times of chemical compounds identified by GC-MS in OLP by thermal cracking of plastic waste from computer equipment at 400 °C, 1.0 atm, Reaction time=30 min, in semi-pilot scale two-stage reactor of 2.0 L.

| Chemical Compound | RT [min] | CAS | wi[%.area] |
|---|---|---|---|
| **Aromatic Hydrocarbons** | **Σ(%.area)** | | **56.934** |
| Styrene | 9.728 | 100-42-5 | 11.056 |
| Benzene, (1-methylethyl)- | 10.710 | 98-82-8 | 4.313 |
| Benzene, propyl- | 11.687 | 103-65-1 | 0.261 |
| α-Methylstyrene | 12.584 | 98-83-9 | 1.971 |
| Benzene, 1-propenyl- | 14.092 | 637-50-3 | 0.521 |
| Biphenyl | 25.017 | 92-52-4 | 0.266 |
| Diphenylmethane | 26.329 | 101-81-5 | 0.501 |
| Benzene, 1,1'-ethylidenebis- | 27.764 | 612-00-0 | 0.622 |
| Bibenzyl | 28.688 | 103-29-7 | 0.460 |
| Benzene, 1,1'-(1,2-dimethyl-1,2-ethanediyl) bis- | 29.185 | 5789-35-5 | 2.208 |
| Benzene, 1,1'-(oxydiethylidene) bis- | 30.059 | 93-96-9 | 0.357 |
| Benzene, 1,1'-(oxydiethylidene) bis- | 30.496 | 93-96-9 | 0.407 |
| Benzene, 1,1'-(1,3-propanediyl) bis- | 32.085 | 1081-75-0 | 8.518 |
| Benzene, 1,1'-(3-methyl-1-propene-1,3-diyl) bis- | 32.412 | 7614-93-9 | 1.052 |
| Benzene, 1,1'-(1-methyl-1,3-propanediyl) bis- | 32.600 | 1520-44-1 | 1.177 |
| 1,2-Diphenylcyclopropane | 33.636 | 29881-14-9 | 1.936 |
| Benzene, 1,1'-(1,4-butanediyl) bis- | 34.021 | 1083-56-3 | 0.357 |
| Benzene, 1,1'-(3-methyl-1-propene-1,3-diyl) bis- | 34.386 | 7614-93-9 | 1.492 |
| 2,4-Diphenyl-4-methyl-1-pentene | 34.748 | - | 5.481 |
| Benzene, 1,1'-(2-methyl-1-propenylidene) bis- | 34.898 | 781-33-9 | 3.873 |
| 2,4-Diphenyl-4-methyl-2(E)-pentene | 35.518 | 22768-22-5 | 3.868 |
| 1-(4-Methylphenyl)-4-phenylbuta-1,3-diene | 36.410 | 37985-11-8 | 0.701 |
| Benzene, 1,1'-[3-(2-phenylethylidene)-1,5-pentanediyl] bis- | 43.693 | 55334-57-1 | 0.361 |
| Benzene, 1,1'-[3-(2-phenylethylidene)-1,5-pentanediyl] bis- | 44.682 | 55334-57-1 | 0.756 |
| Benzene, 1,1'-(1,1,2,2-tetramethyl-1,2-ethanediyl) bis- | 48.270 | - | 1.291 |
| 1-Propene, 3-(2-cyclopentenyl)-2-methyl-1,1-diphenyl- | 49.302 | - | 0.271 |
| Benzene, 1,1'-(1,4-dimethyl-1-butene-1,4-diyl) bis- | 51.646 | 52161-54-3 | 1.125 |
| Benzene, 1,1'-(1,4-dimethyl-1-butene-1,4-diyl) bis- | 53.070 | 52161-54-3 | 0.545 |
| 1-Propene, 3-(2-cyclopentenyl)-2-methyl-1,1-diphenyl- | 53.449 | - | 1.187 |
| **Polycyclic Aromatic Hydrocarbons (PAH)** | **Σ(%.area)** | | **10.205** |
| Naphthalene | 19.491 | 91-20-3 | 0.629 |
| Naphthalene, 1-methyl- | 22.770 | 90-12-0 | 0.240 |
| Naphthalene, 2-methyl- | 23.259 | 91-57-6 | 0.509 |
| Naphthalene, 1,2,3,4-tetrahydro-1-phenyl- | 34.473 | 3018-20-0 | 0.448 |
| Naphthalene, 1,2,3,4-tetrahydro-6-(phenylmethyl)- | 35.372 | 35310-85-1 | 2.504 |
| Naphthalene, 1-phenyl- | 36.578 | 605-02-7 | 1.738 |
| Naphthalene, 2,7-bis(1,1-dimethylethyl)- | 37.221 | 10275-58-8 | 1.308 |

| | | | |
|---|---|---|---|
| Naphthalene, 2-phenyl- | 40.019 | 612-94-2 | 1.536 |
| Naphthalene, 2-(phenylmethyl)- | 44.292 | 613-59-2 | 1.293 |
| **Nitrogenated Compounds** | **Σ(%.area)** | | **18.264** |
| Benzonitrile | 12.687 | 100-47-0 | 0.061 |
| Benzyl nitrile | 17.566 | 140-29-4 | 0.284 |
| Benzeneacetonitrile, α-methyl- | 18.434 | 1823-91-2 | 0.426 |
| Benzenepropanenitrile | 20.642 | 645-59-0 | 0.249 |
| 1,2-Benzenedicarbonitrile | 21.230 | 91-15-6 | 0.337 |
| Cyclopropanecarbonitrile, 2-phenyl-, trans- | 22.408 | 5590-14-7 | 0.289 |
| Benzenebutanenitrile | 23.461 | 2046-18-6 | 9.615 |
| Quinoline, 1,2-dihydro-1-methyl-2-methylene- | 24.133 | - | 0.943 |
| 3-Benzyl-4,5-dihydro-3H-pyrrole | 24.347 | - | 1.147 |
| Cyclopropanecarbonitrile, 2-phenyl-, trans- | 25.772 | 5590-14-7 | 0.255 |
| 1H-Pyrrole, 1-(4-methylphenyl)- | 26.122 | 827-60-1 | 0.288 |
| Quinoline, 4-ethyl- | 27.451 | 19020-26-9 | 0.330 |
| Naphthalene, 1-isocyano- | 28.187 | 09/04/1984 | 0.839 |
| Naphthalene, 1-isocyano- | 28.899 | 09/04/1984 | 0.444 |
| 1-Naphthaleneacetonitrile | 32.306 | 132-75-2 | 0.759 |
| N-(2-Phenylethyl)-cis-2,3-epoxynona-6,8-diynamide | 34.586 | 96917-25-8 | 0.309 |
| Octadecanenitrile | 43.043 | 638-65-3 | 0.576 |
| 4-Methyl-3-(O-methylbenzyl)pentanenitrile | 43.877 | 29107-40-2 | 0.320 |
| (1-Benzyl-2-O-tolyl-ethyl)-isonitrile | 44.445 | - | 0.331 |
| Naphthalene-1,3,3-tricarbonitrile, 3,4,4a,5,6,7-hexahdro-2-amino-4-(4-methylphenyl)- | 49.679 | 163978-39-0 | 0.045 |
| 2-(4-Methoxy-2,6-dimethylphenyl)-3-methyl-2H-benzo[g]indazole | 52.208 | - | 0.417 |
| **Brominated Compounds** | **Σ(%.area)** | | **0.704** |
| Phenol, 3-bromo- | 15.590 | 591-20-8 | 0.336 |
| 5-Bromo-2-methoxy-1,3-dimethylbenzene | 23.559 | - | 0.368 |
| **Oxygenated Compounds** | **Σ(%.area)** | | **11.623** |
| Phenol | 12.146 | 108-95-2 | 2.312 |
| Phenol, 2-methyl- | 14.630 | 95-48-7 | 0.179 |
| Benzenemethanol, α-methyl- | 15.081 | 98-85-1 | 0.707 |
| Benzenemethanol, α,α-dimethyl- | 15.904 | 617-94-7 | 0.275 |
| Phenol, 2,5-dimethyl- | 16.580 | 95-87-4 | 0.184 |
| p-Cumenol | 20.028 | 99-89-8 | 3.317 |
| Phenol, 2-methyl-5-(1-methylethyl)- | 22.055 | 499-75-2 | 0.181 |
| Phenol, o-(α,α-dimethylbenzyl)- | 33.107 | 18168-40-6 | 0.243 |
| Phenol, 2-(1-phenylethyl)- | 33.240 | 4237-44-9 | 1.544 |
| Benzenemethanol, 2,4,6-trimethyl-α-phenyl- | 36.000 | 21945-75-5 | 0.275 |
| Phenol, 4-(1-methyl-1-phenylethyl)- | 36.122 | 599-64-4 | 1.027 |
| 2-tert-Butyl-6-(a-methylbenzyl) phenol | 37.124 | 17959-02-3 | 0.418 |
| Benzaldehyde, 2-methyl-, (2,4-dinitrophenyl)hydrazone | 50.781 | 1773-44-0 | 0.419 |
| α-N-Normethadol | 54.073 | 38455-85-5 | 0.542 |
| **Non Identified Fraction** | **Σ(%.area)** | | **2.267** |

**Table S6**: Classes of compounds, summation of peak areas, CAS number, and retention times of chemical compounds identified by GC-MS in OLP by thermal cracking of plastic waste from computer equipment at 400 °C, 1.0 atm, Reaction time=45 min, in semi-pilot scale two-stage reactor of 2.0 L.

| Chemical Compound | RT [min] | CAS | wi[%.area] |
|---|---|---|---|
| **Aromatic Hydrocarbons** | **Σ(%.area)** | | **45.964** |
| Styrene | 9.728 | 100-42-5 | 5.664 |
| Benzene, (1-methylethyl)- | 10.710 | 98-82-8 | 2.864 |
| Benzene, propyl- | 11.687 | 103-65-1 | 0.178 |
| α-Methylstyrene | 12.584 | 98-83-9 | 5.220 |
| Benzene, 1-propenyl- | 14.092 | 637-50-3 | 0.516 |
| Biphenyl | 25.017 | 92-52-4 | 0.379 |
| Diphenylmethane | 26.329 | 101-81-5 | 0.720 |
| Benzene, 1,1'-ethylidenebis- | 27.764 | 612-00-0 | 0.417 |
| Bibenzyl | 28.688 | 103-29-7 | 0.684 |
| Benzene, 1,1'-(1,2-dimethyl-1,2-ethanediyl) bis- | 29.185 | 5789-35-5 | 0.551 |
| Benzene, 1,1'-(1,3-propanediyl) bis- | 32.085 | 1081-75-0 | 11.875 |
| Benzene, 1,1'-(3-methyl-1-propene-1,3-diyl) bis- | 32.412 | 7614-93-9 | 1.617 |
| Benzene, 1,1'-(1-methyl-1,3-propanediyl) bis- | 32.600 | 1520-44-1 | 1.650 |
| 1,2-Diphenylcyclopropane | 33.636 | 29881-14-9 | 2.968 |
| Benzene, 1,1'-(1,4-butanediyl) bis- | 34.021 | 1083-56-3 | 0.492 |
| Benzene, 1,1'-(3-methyl-1-propene-1,3-diyl) bis- | 34.386 | 7614-93-9 | 1.187 |
| 2,4-Diphenyl-4-methyl-1-pentene | 34.748 | - | 2.256 |
| Benzene, 1,1'-(2-methyl-1-propenylidene) bis- | 34.898 | 781-33-9 | 2.726 |
| 2,4-Diphenyl-4-methyl-2(E)-pentene | 35.518 | 22768-22-5 | 0.427 |
| 1-(4-Methylphenyl)-4-phenylbuta-1,3-diene | 36.410 | 37985-11-8 | 0.424 |
| 9-Phenyl-5H-benzocycloheptene | 40.386 | 138089-71-1 | 0.541 |
| Benzene, 1,1'-[3-(2-phenylethylidene)-1,5-pentanediyl] bis- | 44.682 | 55334-57-1 | 1.003 |
| 1-Propene, 3-(2-cyclopentenyl)-2-methyl-1,1-diphenyl- | 49.302 | - | 0.378 |
| Benzene, 1,1'-(1,4-dimethyl-1-butene-1,4-diyl) bis- | 51.646 | 52161-54-3 | 0.374 |
| 1-Propene, 3-(2-cyclopentenyl)-2-methyl-1,1-diphenyl- | 53.449 | - | 0.853 |
| **Polycyclic Aromatic Hydrocarbons (PAH)** | **Σ(%.area)** | | **11.092** |
| Naphthalene | 19.491 | 91-20-3 | 0.843 |
| Naphthalene, 1-methyl- | 22.770 | 90-12-0 | 0.373 |
| Naphthalene, 2-methyl- | 23.259 | 91-57-6 | 0.794 |
| Naphthalene, 1,2,3,4-tetrahydro-1-phenyl- | 34.473 | 3018-20-0 | 0.696 |
| Naphthalene, 1,2,3,4-tetrahydro-6-(phenylmethyl)- | 35.372 | 35310-85-1 | 0.571 |
| Naphthalene, 1-phenyl- | 36.578 | 605-02-7 | 2.459 |
| Naphthalene, 2,7-bis(1,1-dimethylethyl)- | 37.221 | 10275-58-8 | 0.557 |
| 9,10-Dimethylanthracene | 37.560 | 781-43-1 | 0.307 |
| Naphthalene, 2-phenyl- | 40.019 | 612-94-2 | 2.601 |
| Naphthalene, 2-(phenylmethyl)- | 44.292 | 613-59-2 | 1.891 |
| **Nitrogenated Compounds** | **Σ(%.area)** | | **27.880** |

| | | | |
|---|---|---|---|
| Benzonitrile | 12.687 | 100-47-0 | 0.068 |
| Benzyl nitrile | 17.566 | 140-29-4 | 0.445 |
| Benzeneacetonitrile, α-methyl- | 18.434 | 1823-91-2 | 0.692 |
| Benzenepropanenitrile | 20.642 | 645-59-0 | 0.337 |
| 1,2-Benzenedicarbonitrile | 21.230 | 91-15-6 | 0.580 |
| Cyclopropanecarbonitrile, 2-phenyl-, trans- | 22.408 | 5590-14-7 | 0.476 |
| Benzenebutanenitrile | 23.461 | 2046-18-6 | 14.634 |
| Cyclopropanecarbonitrile, 2-phenyl-, trans- | 23.924 | 5590-14-7 | 0.272 |
| Quinoline, 1,2-dihydro-1-methyl-2-methylene- | 24.133 | - | 1.060 |
| 3-Benzyl-4,5-dihydro-3H-pyrrole | 24.347 | - | 1.802 |
| 1,2,3,3a-Tetrahydropentalene, 1,1-dimethyl-3-cyanomethylene- | 24.851 | - | 0.229 |
| Cyclopropanecarbonitrile, 2-phenyl-, trans- | 25.772 | 5590-14-7 | 0.435 |
| 1H-Pyrrole, 1-(4-methylphenyl)- | 26.122 | 827-60-1 | 0.475 |
| (7-Isopropylidenebicyclo[2.2.1]hept-5-en-2-ylidene)acetonitrile | 26.704 | - | 0.315 |
| Quinoline, 4-ethyl- | 27.451 | 19020-26-9 | 0.536 |
| Naphthalene, 1-isocyano- | 28.187 | 09/04/1984 | 1.416 |
| Naphthalene, 1-isocyano- | 28.899 | 09/04/1984 | 0.729 |
| 1-Naphthaleneacetonitrile | 32.306 | 132-75-2 | 1.206 |
| N-(2-Phenylethyl)-cis-2,3-epoxynona-6,8-diynamide | 34.586 | 96917-25-8 | 0.440 |
| Octadecanenitrile | 43.043 | 638-65-3 | 0.751 |
| 4-Methyl-3-(O-methylbenzyl)pentanenitrile | 43.877 | 29107-40-2 | 0.484 |
| (1-Benzyl-2-O-tolyl-ethyl)-isonitrile | 44.445 | - | 0.498 |
| **Brominated Compounds** | **Σ(%.area)** | | **0.510** |
| Phenol, 3-bromo- | 15.590 | 591-20-8 | 0.210 |
| 5-Bromo-2-methoxy-1,3-dimethylbenzene | 23.559 | - | 0.300 |
| **Oxygenated Compounds** | **Σ(%.area)** | | **13.082** |
| Phenol | 12.146 | 108-95-2 | 3.227 |
| Phenol, 2-methyl- | 14.630 | 95-48-7 | 0.507 |
| Benzenemethanol, α-methyl- | 15.081 | 98-85-1 | 0.343 |
| Benzenemethanol, α,α-dimethyl- | 15.904 | 617-94-7 | 1.249 |
| Phenol, 2,5-dimethyl- | 16.580 | 95-87-4 | 0.312 |
| p-Cumenol | 20.028 | 99-89-8 | 5.494 |
| Phenol, 2-methyl-5-(1-methylethyl)- | 22.055 | 499-75-2 | 0.318 |
| Phenol, 2-(1-phenylethyl)- | 33.240 | 4237-44-9 | 1.280 |
| Benzaldehyde, 2-methyl-, (2,4-dinitrophenyl)hydrazone | 50.781 | 1773-44-0 | 0.352 |
| **Non Identified Fraction** | **Σ(%.area)** | | **1.473** |

**Table S7**: Classes of compounds, summation of peak areas, CAS number, and retention times of chemical compounds identified by GC-MS in OLP by thermal cracking of plastic waste from computer equipment at 400 °C, 1.0 atm, Reaction time=60 min, in semi-pilot scale two-stage reactor of 2.0 L.

| Chemical Compound | RT [min] | CAS | wi[%.area] |
|---|---|---|---|
| **Aromatic Hydrocarbons** | **Σ(%.area)** | | **46.105** |
| Styrene | 9.728 | 100-42-5 | 3.944 |
| Benzene, (1-methylethyl)- | 10.710 | 98-82-8 | 2.178 |
| α-Methylstyrene | 12.584 | 98-83-9 | 3.877 |
| Benzene, 1-propenyl- | 14.092 | 637-50-3 | 0.329 |
| Biphenyl | 25.017 | 92-52-4 | 0.300 |
| Diphenylmethane | 26.329 | 101-81-5 | 0.744 |
| Benzene, 1,1'-ethylidenebis- | 27.764 | 612-00-0 | 0.795 |
| Bibenzyl | 28.688 | 103-29-7 | 0.672 |
| Benzene, 1,1'-(1,3-propanediyl) bis- | 32.085 | 1081-75-0 | 15.312 |
| Benzene, 1,1'-(3-methyl-1-propene-1,3-diyl) bis- | 32.412 | 7614-93-9 | 1.780 |
| Benzene, 1,1'-(1-methyl-1,3-propanediyl) bis- | 32.600 | 1520-44-1 | 2.131 |
| 1,2-Diphenylcyclopropane | 33.636 | 29881-14-9 | 3.290 |
| Benzene, 1,1'-(1,4-butanediyl) bis- | 34.021 | 1083-56-3 | 0.669 |
| Benzene, 1,1'-(3-methyl-1-propene-1,3-diyl) bis- | 34.386 | 7614-93-9 | 1.189 |
| 2,4-Diphenyl-4-methyl-1-pentene | 34.748 | - | 0.445 |
| Benzene, 1,1'-(2-methyl-1-propenylidene) bis- | 34.898 | 781-33-9 | 2.585 |
| 1-(4-Methylphenyl)-4-phenylbuta-1,3-diene | 36.410 | 37985-11-8 | 0.508 |
| 1H-Indene, 2-phenyl- | 36.864 | 4505-48-0 | 0.107 |
| 9-Phenyl-5H-benzocycloheptene | 40.386 | 138089-71-1 | 0.530 |
| Benzene, 1,1'-[3-(2-phenylethylidene)-1,5-pentanediyl] bis- | 44.682 | 55334-57-1 | 1.538 |
| Benzene, (1-methylhexadecyl)- | 45.088 | 55125-25-2 | 0.478 |
| p-Terphenyl | 45.432 | 92-94-4 | 0.255 |
| 1-Propene, 3-(2-cyclopentenyl)-2-methyl-1,1-diphenyl- | 49.302 | - | 0.473 |
| Benzene, 1,1'-(1,4-dimethyl-1-butene-1,4-diyl) bis- | 51.646 | 52161-54-3 | 0.398 |
| 1-Propene, 3-(2-cyclopentenyl)-2-methyl-1,1-diphenyl- | 53.449 | - | 0.861 |
| 1,1':3',1"-Terphenyl, 5'-phenyl- | 68.111 | 612-71-5 | 0.717 |
| **Polycyclic Aromatic Hydrocarbons (PAH)** | **Σ(%.area)** | | **10.007** |
| Naphthalene | 19.491 | 91-20-3 | 0.551 |
| Naphthalene, 1-methyl- | 22.770 | 90-12-0 | 0.301 |
| Naphthalene, 2-methyl- | 23.259 | 91-57-6 | 0.597 |
| Naphthalene, 1,2,3,4-tetrahydro-1-phenyl- | 34.473 | 3018-20-0 | 0.720 |
| Naphthalene, 1,2,3,4-tetrahydro-6-(phenylmethyl)- | 35.372 | 35310-85-1 | 0.406 |
| Naphthalene, 1-phenyl- | 36.578 | 605-02-7 | 2.337 |
| Naphthalene, 2,7-bis(1,1-dimethylethyl)- | 37.221 | 10275-58-8 | 0.440 |
| 9,10-Dimethylanthracene | 37.560 | 781-43-1 | 0.307 |
| Naphthalene, 2-phenyl- | 40.019 | 612-94-2 | 2.470 |
| Naphthalene, 2-(phenylmethyl)- | 44.292 | 613-59-2 | 1.878 |

| **Nitrogenated Compounds** | **Σ(%.area)** | | **31.768** |
|---|---|---|---|
| Pentanedinitrile, 2-methyl- | 15.255 | 4553-62-2 | 0.238 |
| Benzyl nitrile | 17.566 | 140-29-4 | 0.400 |
| Benzeneacetonitrile, α-methyl- | 18.434 | 1823-91-2 | 0.678 |
| Benzenepropanenitrile | 20.642 | 645-59-0 | 0.342 |
| 1,2-Benzenedicarbonitrile | 21.230 | 91-15-6 | 0.490 |
| Cyclopropanecarbonitrile, 2-phenyl-, trans- | 22.408 | 5590-14-7 | 0.474 |
| Benzenebutanenitrile | 23.461 | 2046-18-6 | 16.916 |
| Cyclopropanecarbonitrile, 2-phenyl-, trans- | 23.924 | 5590-14-7 | 0.303 |
| Quinoline, 1,2-dihydro-1-methyl-2-methylene- | 24.133 | - | 1.113 |
| 3-Benzyl-4,5-dihydro-3H-pyrrole | 24.347 | - | 2.426 |
| 1,2,3,3a-Tetrahydropentalene, 1,1-dimethyl-3-cyanomethylene- | 24.851 | - | 0.299 |
| Cyclopropanecarbonitrile, 2-phenyl-, trans- | 25.772 | 5590-14-7 | 0.462 |
| 1H-Pyrrole, 1-(4-methylphenyl)- | 26.122 | 827-60-1 | 0.512 |
| (7-Isopropylidenebicyclo[2.2.1]hept-5-en-2-ylidene)acetonitrile | 26.704 | - | 0.374 |
| Quinoline, 4-ethyl- | 27.451 | 19020-26-9 | 0.476 |
| Naphthalene, 1-isocyano- | 28.187 | 09/04/1984 | 1.339 |
| Naphthalene, 1-isocyano- | 28.899 | 09/04/1984 | 0.708 |
| 1-Naphthaleneacetonitrile | 32.306 | 132-75-2 | 1.291 |
| N-(2-Phenylethyl)-cis-2,3-epoxynona-6,8-diynamide | 34.586 | 96917-25-8 | 0.504 |
| Octadecanenitrile | 43.043 | 638-65-3 | 0.645 |
| 4-Methyl-3-(O-methylbenzyl)pentanenitrile | 43.877 | 29107-40-2 | 0.667 |
| (1-Benzyl-2-O-tolyl-ethyl)-isonitrile | 44.445 | - | 0.656 |
| Naphthalene-1,3,3-tricarbonitrile, 3,4,4a,5,6,7-hexahdro-2-amino-4-(4-methylphenyl)- | 49.680 | 163978-39-0 | 0.232 |
| Naphthalene-1,3,3-tricarbonitrile, 3,4,4a,5,6,7-hexahdro-2-amino-4-(4-methylphenyl)- | 50.370 | 163978-39-0 | 0.223 |
| **Brominated Compounds** | **Σ(%.area)** | | **0.223** |
| 5-Bromo-2-methoxy-1,3-dimethylbenzene | 23.559 | - | 0.223 |
| **Oxygenated Compounds** | **Σ(%.area)** | | **10.515** |
| Phenol | 12.146 | 108-95-2 | 2.369 |
| Phenol, 2-methyl- | 14.630 | 95-48-7 | 0.332 |
| Benzenemethanol, α,α-dimethyl- | 15.904 | 617-94-7 | 1.267 |
| Phenol, 2,5-dimethyl- | 16.580 | 95-87-4 | 0.277 |
| p-Cumenol | 20.028 | 99-89-8 | 4.541 |
| Phenol, 2-methyl-5-(1-methylethyl)- | 22.055 | 499-75-2 | 0.275 |
| Phenol, 2-(1-phenylethyl)- | 33.240 | 4237-44-9 | 0.962 |
| Benzaldehyde, 2-methyl-, (2,4-dinitrophenyl)hydrazone | 50.781 | 1773-44-0 | 0.492 |
| **Non Identified Fraction** | **Σ(%.area)** | | **1.381** |

**Table S8**: Classes of compounds, summation of peak areas, CAS number, and retention times of chemical compounds identified by GC-MS in OLP by thermal cracking of plastic waste from computer equipment at 450 °C, 1.0 atm, Reaction time=15 min, in semi-pilot scale two-stage reactor of 2.0 L.

| Chemical Compound | RT [min] | CAS | wi[%.area] |
|---|---|---|---|
| **Aromatic Hydrocarbons** | **Σ(%.area)** | | **47.525** |
| Styrene | 9.728 | 100-42-5 | 4.957 |
| Benzene, (1-methylethyl)- | 10.710 | 98-82-8 | 3.168 |
| α-Methylstyrene | 12.584 | 98-83-9 | 4.604 |
| Benzene, 1-propenyl- | 14.092 | 637-50-3 | 0.355 |
| Diphenylmethane | 26.329 | 101-81-5 | 0.469 |
| Benzene, 1,1'-ethylidenebis- | 27.764 | 612-00-0 | 0.518 |
| Bibenzyl | 28.688 | 103-29-7 | 0.515 |
| Benzene, 1,1'-(1,3-propanediyl) bis- | 32.085 | 1081-75-0 | 16.443 |
| Benzene, 1,1'-(3-methyl-1-propene-1,3-diyl) bis- | 32.412 | 7614-93-9 | 1.549 |
| Benzene, 1,1'-(1-methyl-1,3-propanediyl) bis- | 32.600 | 1520-44-1 | 2.422 |
| 1,2-Diphenylcyclopropane | 33.636 | 29881-14-9 | 2.460 |
| Benzene, 1,1'-(1,4-butanediyl) bis- | 34.021 | 1083-56-3 | 0.820 |
| Benzene, 1,1'-(3-methyl-1-propene-1,3-diyl) bis- | 34.386 | 7614-93-9 | 0.917 |
| 2,4-Diphenyl-4-methyl-1-pentene | 34.748 | - | 1.006 |
| Benzene, 1,1'-(2-methyl-1-propenylidene) bis- | 34.898 | 781-33-9 | 2.061 |
| 1-(4-Methylphenyl)-4-phenylbuta-1,3-diene | 36.410 | 37985-11-8 | 0.554 |
| Benzene, 1,1'-[3-(2-phenylethylidene)-1,5-pentanediyl] bis- | 44.682 | 55334-57-1 | 1.656 |
| Benzene, (1-methylhexadecyl)- | 45.088 | 55125-25-2 | 0.463 |
| 1-Propene, 3-(2-cyclopentenyl)-2-methyl-1,1-diphenyl- | 49.302 | - | 0.607 |
| Benzene, 1,1'-(1,4-dimethyl-1-butene-1,4-diyl) bis- | 51.646 | 52161-54-3 | 0.392 |
| 1-Propene, 3-(2-cyclopentenyl)-2-methyl-1,1-diphenyl- | 53.449 | - | 1.589 |
| **Polycyclic Aromatic Hydrocarbons (PAH)** | **Σ(%.area)** | | **7.768** |
| Naphthalene | 19.491 | 91-20-3 | 0.385 |
| Naphthalene, 1-methyl- | 22.770 | 90-12-0 | 0.237 |
| Naphthalene, 2-methyl- | 23.259 | 91-57-6 | 0.441 |
| Naphthalene, 1,2,3,4-tetrahydro-1-phenyl- | 34.473 | 3018-20-0 | 0.617 |
| Naphthalene, 1,2,3,4-tetrahydro-6-(phenylmethyl)- | 35.372 | 35310-85-1 | 0.361 |
| Naphthalene, 1-phenyl- | 36.578 | 605-02-7 | 2.360 |
| Naphthalene, 2,7-bis(1,1-dimethylethyl)- | 37.221 | 10275-58-8 | 0.340 |
| Naphthalene, 2-phenyl- | 40.019 | 612-94-2 | 1.493 |
| Naphthalene, 2-(phenylmethyl)- | 44.292 | 613-59-2 | 1.534 |
| **Nitrogenated Compounds** | **Σ(%.area)** | | **26.578** |
| Benzyl nitrile | 17.566 | 140-29-4 | 0.276 |
| Benzeneacetonitrile, α-methyl- | 18.434 | 1823-91-2 | 0.586 |
| Benzenepropanenitrile | 20.642 | 645-59-0 | 0.285 |
| 1,2-Benzenedicarbonitrile | 21.230 | 91-15-6 | 0.588 |
| Cyclopropanecarbonitrile, 2-phenyl-, trans- | 22.408 | 5590-14-7 | 0.277 |

| | | | |
|---|---|---|---|
| Benzenebutanenitrile | 23.461 | 2046-18-6 | 13.943 |
| Quinoline, 1,2-dihydro-1-methyl-2-methylene- | 24.133 | - | 0.833 |
| 3-Benzyl-4,5-dihydro-3H-pyrrole | 24.347 | - | 2.166 |
| 1,2,3,3a-Tetrahydropentalene, 1,1-dimethyl-3-cyanomethylene- | 24.851 | - | 0.314 |
| Cyclopropanecarbonitrile, 2-phenyl-, trans- | 25.772 | 5590-14-7 | 0.261 |
| 1H-Pyrrole, 1-(4-methylphenyl)- | 26.122 | 827-60-1 | 0.352 |
| (7-Isopropylidenebicyclo[2.2.1]hept-5-en-2-ylidene)acetonitrile | 26.704 | - | 0.289 |
| Quinoline, 4-ethyl- | 27.451 | 19020-26-9 | 0.542 |
| Naphthalene, 1-isocyano- | 28.187 | 09/04/1984 | 1.085 |
| Naphthalene, 1-isocyano- | 28.899 | 09/04/1984 | 0.474 |
| 1-Naphthaleneacetonitrile | 32.306 | 132-75-2 | 0.899 |
| N-(2-Phenylethyl)-cis-2,3-epoxynona-6,8-diynamide | 34.586 | 96917-25-8 | 0.410 |
| Octadecanenitrile | 43.043 | 638-65-3 | 0.918 |
| 4-Methyl-3-(O-methylbenzyl)pentanenitrile | 43.877 | 29107-40-2 | 0.724 |
| (1-Benzyl-2-O-tolyl-ethyl)-isonitrile | 44.445 | - | 0.635 |
| Naphthalene-1,3,3-tricarbonitrile, 3,4,4a,5,6,7-hexahdro-2-amino-4-(4-methylphenyl)- | 49.680 | 163978-39-0 | 0.337 |
| Naphthalene-1,3,3-tricarbonitrile, 3,4,4a,5,6,7-hexahdro-2-amino-4-(4-methylphenyl)- | 50.370 | 163978-39-0 | 0.384 |
| **Brominated Compounds** | **Σ(%.area)** | | **0.662** |
| Phenol, 2-bromo- | 15.591 | 95-56-7 | 0.319 |
| 5-Bromo-2-methoxy-1,3-dimethylbenzene | 23.559 | - | 0.343 |
| **Oxygenated Compounds** | **Σ(%.area)** | | **15.968** |
| Phenol | 12.146 | 108-95-2 | 4.201 |
| Phenol, 2-methyl- | 14.630 | 95-48-7 | 0.468 |
| Benzenemethanol, α-methyl-, (R)- | 15.082 | 4553-62-2 | 0.385 |
| Benzenemethanol, α,α-dimethyl- | 15.904 | 617-94-7 | 1.260 |
| Phenol, 2,5-dimethyl- | 16.580 | 95-87-4 | 0.316 |
| p-Cumenol | 20.028 | 99-89-8 | 7.066 |
| Phenol, 2-methyl-5-(1-methylethyl)- | 22.055 | 499-75-2 | 0.358 |
| Phenol, 2-(1-phenylethyl)- | 33.240 | 4237-44-9 | 0.988 |
| Phenol, 4-(1-methyl-1-phenylethyl)- | 36.125 | 599-64-4 | 0.297 |
| Benzaldehyde, 2-methyl-, (2,4-dinitrophenyl)hydrazone | 50.781 | 1773-44-0 | 0.626 |
| **Non Identified Fraction** | **Σ(%.area)** | | **1.503** |

**Table S9**: Classes of compounds, summation of peak areas, CAS number, and retention times of chemical compounds identified by GC-MS in OLP by thermal cracking of plastic waste from computer equipment at 450 °C, 1.0 atm, Reaction time=30 min, in semi-pilot scale two-stage reactor of 2.0 L.

| Chemical Compound | RT [min] | CAS | wi[%.area] |
|---|---|---|---|
| **Aromatic Hydrocarbons** | **Σ(%.area)** | | **47.731** |
| Styrene | 9.728 | 100-42-5 | 6.633 |
| Benzene, (1-methylethyl)- | 10.710 | 98-82-8 | 4.235 |
| α-Methylstyrene | 12.584 | 98-83-9 | 5.511 |
| Benzene, 1-propenyl- | 14.092 | 637-50-3 | 0.443 |
| Indene | 14.849 | 95-13-6 | 0.276 |
| Diphenylmethane | 26.329 | 101-81-5 | 0.526 |
| Benzene, 1,1'-ethylidenebis- | 27.764 | 612-00-0 | 0.551 |
| Bibenzyl | 28.688 | 103-29-7 | 0.510 |
| Benzene, 1,1'-(1,3-propanediyl) bis- | 32.085 | 1081-75-0 | 16.014 |
| Benzene, 1,1'-(3-methyl-1-propene-1,3-diyl) bis- | 32.412 | 7614-93-9 | 1.359 |
| Benzene, 1,1'-(1-methyl-1,3-propanediyl) bis- | 32.600 | 1520-44-1 | 2.554 |
| 1,2-Diphenylcyclopropane | 33.636 | 29881-14-9 | 2.182 |
| Benzene, 1,1'-(1,4-butanediyl) bis- | 34.021 | 1083-56-3 | 0.636 |
| Benzene, 1,1'-(3-methyl-1-propene-1,3-diyl) bis- | 34.386 | 7614-93-9 | 0.672 |
| 2,4-Diphenyl-4-methyl-1-pentene | 34.748 | - | 0.633 |
| Benzene, 1,1'-(2-methyl-1-propenylidene) bis- | 34.898 | 781-33-9 | 1.455 |
| 1-(4-Methylphenyl)-4-phenylbuta-1,3-diene | 36.410 | 37985-11-8 | 0.521 |
| Benzene, 1,1'-[3-(2-phenylethylidene)-1,5-pentanediyl] bis- | 44.682 | 55334-57-1 | 1.329 |
| Benzene, (1-methylhexadecyl)- | 45.088 | 55125-25-2 | 0.431 |
| 1-Propene, 3-(2-cyclopentenyl)-2-methyl-1,1-diphenyl- | 49.302 | - | 0.288 |
| Benzene, 1,1'-(1,4-dimethyl-1-butene-1,4-diyl) bis- | 51.646 | 52161-54-3 | 0.335 |
| 1-Propene, 3-(2-cyclopentenyl)-2-methyl-1,1-diphenyl- | 53.449 | - | 0.637 |
| **Polycyclic Aromatic Hydrocarbons (PAH)** | **Σ(%.area)** | | **9.732** |
| Naphthalene | 19.491 | 91-20-3 | 0.562 |
| Naphthalene, 1-methyl- | 22.770 | 90-12-0 | 0.358 |
| Naphthalene, 2-methyl- | 23.259 | 91-57-6 | 0.528 |
| Naphthalene, 1-isocyano- | 28.187 | 09/04/1984 | 1.327 |
| Naphthalene, 1,2,3,4-tetrahydro-1-phenyl- | 34.473 | 3018-20-0 | 0.641 |
| Naphthalene, 1,2,3,4-tetrahydro-6-(phenylmethyl)- | 35.372 | 35310-85-1 | 0.307 |
| Naphthalene, 1-phenyl- | 36.578 | 605-02-7 | 2.500 |
| Naphthalene, 2,7-bis(1,1-dimethylethyl)- | 37.221 | 10275-58-8 | 0.309 |
| Naphthalene, 2-phenyl- | 40.019 | 612-94-2 | 1.687 |
| Naphthalene, 2-(phenylmethyl)- | 44.292 | 613-59-2 | 1.513 |
| **Nitrogenated Compounds** | **Σ(%.area)** | | **24.787** |
| Benzyl nitrile | 17.566 | 140-29-4 | 0.316 |
| Benzeneacetonitrile, α-methyl- | 18.434 | 1823-91-2 | 0.649 |
| Benzenepropanenitrile | 20.642 | 645-59-0 | 0.315 |

| | | | |
|---|---|---|---|
| 1,2-Benzenedicarbonitrile | 21.230 | 91-15-6 | 0.751 |
| Cyclopropanecarbonitrile, 2-phenyl-, trans- | 22.408 | 5590-14-7 | 0.310 |
| Benzenebutanenitrile | 23.461 | 2046-18-6 | 13.720 |
| Quinoline, 1,2-dihydro-1-methyl-2-methylene- | 24.133 | - | 0.916 |
| 3-Benzyl-4,5-dihydro-3H-pyrrole | 24.347 | - | 2.389 |
| 1,2,3,3a-Tetrahydropentalene, 1,1-dimethyl-3-cyanomethylene- | 24.851 | - | 0.276 |
| Cyclopropanecarbonitrile, 2-phenyl-, trans- | 25.772 | 5590-14-7 | 0.281 |
| 1H-Pyrrole, 1-(4-methylphenyl)- | 26.122 | 827-60-1 | 0.352 |
| Quinoline, 4-ethyl- | 27.451 | 19020-26-9 | 0.467 |
| Naphthalene, 1-isocyano- | 28.899 | 09/04/1984 | 0.538 |
| 1-Naphthaleneacetonitrile | 32.306 | 132-75-2 | 0.924 |
| Octadecanenitrile | 43.043 | 638-65-3 | 0.788 |
| 4-Methyl-3-(O-methylbenzyl)pentanenitrile | 43.877 | 29107-40-2 | 0.626 |
| (1-Benzyl-2-O-tolyl-ethyl)-isonitrile | 44.445 | - | 0.554 |
| Naphthalene-1,3,3-tricarbonitrile, 3,4,4a,5,6,7-hexahdro-2-amino-4-(4-methylphenyl)- | 49.680 | 163978-39-0 | 0.292 |
| Naphthalene-1,3,3-tricarbonitrile, 3,4,4a,5,6,7-hexahdro-2-amino-4-(4-methylphenyl)- | 50.370 | 163978-39-0 | 0.323 |
| **Brominated Compounds** | **Σ(%.area)** | | **0.316** |
| Phenol, 2-bromo- | 15.591 | 95-56-7 | 0.199 |
| 5-Bromo-2-methoxy-1,3-dimethylbenzene | 23.559 | - | 0.117 |
| **Oxygenated Compounds** | **Σ(%.area)** | | **14.952** |
| Phenol | 12.146 | 108-95-2 | 3.775 |
| Phenol, 2-methyl- | 14.630 | 95-48-7 | 0.500 |
| Benzenemethanol, α-methyl-, (R)- | 15.082 | 4553-62-2 | 0.253 |
| Benzenemethanol, α,α-dimethyl- | 15.904 | 617-94-7 | 1.238 |
| Phenol, 2,5-dimethyl- | 16.580 | 95-87-4 | 0.353 |
| p-Cumenol | 20.028 | 99-89-8 | 7.057 |
| Phenol, 2-methyl-5-(1-methylethyl)- | 22.055 | 499-75-2 | 0.379 |
| Phenol, 2-(1-phenylethyl)- | 33.240 | 4237-44-9 | 0.877 |
| Benzaldehyde, 2-methyl-, (2,4-dinitrophenyl)hydrazone | 50.781 | 1773-44-0 | 0.520 |
| **Non Identified Fraction** | **Σ(%.area)** | | **2.484** |

**Table S10**: Classes of compounds, summation of peak areas, CAS number, and retention times of chemical compounds identified by GC-MS in OLP by thermal cracking of plastic waste from computer equipment at 450 °C, 1.0 atm, Reaction time=45 min, in semi-pilot scale two-stage reactor of 2.0 L.

| Chemical Compound | RT [min] | CAS | wi[%.area] |
|---|---|---|---|
| **Aromatic Hydrocarbons** | **Σ(%.area)** | | **49.915** |
| Styrene | 9.728 | 100-42-5 | 9.088 |
| Benzene, (1-methylethyl)- | 10.710 | 98-82-8 | 4.689 |
| Benzene, propyl- | 11.688 | 103-65-1 | 0.240 |
| α-Methylstyrene | 12.584 | 98-83-9 | 6.649 |
| Benzene, 1-propenyl- | 14.092 | 637-50-3 | 0.547 |
| Indene | 14.849 | 95-13-6 | 0.458 |
| Biphenyl | 25.017 | 92-52-4 | 0.301 |
| Diphenylmethane | 26.329 | 101-81-5 | 0.600 |
| Benzene, 1,1'-ethylidenebis- | 27.764 | 612-00-0 | 0.572 |
| Bibenzyl | 28.688 | 103-29-7 | 0.474 |
| Benzene, 1,1'-(1,3-propanediyl) bis- | 32.085 | 1081-75-0 | 14.528 |
| Benzene, 1,1'-(3-methyl-1-propene-1,3-diyl) bis- | 32.412 | 7614-93-9 | 1.243 |
| Benzene, 1,1'-(1-methyl-1,3-propanediyl) bis- | 32.600 | 1520-44-1 | 2.361 |
| 1,2-Diphenylcyclopropane | 33.636 | 29881-14-9 | 2.146 |
| Benzene, 1,1'-(1,4-butanediyl) bis- | 34.021 | 1083-56-3 | 0.649 |
| Benzene, 1,1'-(3-methyl-1-propene-1,3-diyl) bis- | 34.386 | 7614-93-9 | 0.577 |
| Benzene, 1,1'-(2-methyl-1-propenylidene) bis- | 34.898 | 781-33-9 | 1.054 |
| 1-(4-Methylphenyl)-4-phenylbuta-1,3-diene | 36.410 | 37985-11-8 | 0.482 |
| Benzene, 1,1'-[3-(2-phenylethylidene)-1,5-pentanediyl] bis- | 44.682 | 55334-57-1 | 1.465 |
| Benzene, (1-methylhexadecyl)- | 45.088 | 55125-25-2 | 0.482 |
| p-Terphenyl | 45.436 | 92-94-4 | 0.305 |
| 1-Propene, 3-(2-cyclopentenyl)-2-methyl-1,1-diphenyl- | 49.302 | - | 0.178 |
| Benzene, 1,1'-(1,4-dimethyl-1-butene-1,4-diyl) bis- | 51.646 | 52161-54-3 | 0.414 |
| 1-Propene, 3-(2-cyclopentenyl)-2-methyl-1,1-diphenyl- | 53.449 | - | 0.413 |
| **Polycyclic Aromatic Hydrocarbons (PAH)** | **Σ(%.area)** | | **9.602** |
| Naphthalene | 19.491 | 91-20-3 | 0.851 |
| Naphthalene, 1-methyl- | 22.770 | 90-12-0 | 0.458 |
| Naphthalene, 2-methyl- | 23.259 | 91-57-6 | 0.710 |
| Naphthalene, 1,2,3,4-tetrahydro-1-phenyl- | 34.473 | 3018-20-0 | 0.679 |
| Naphthalene, 1,2,3,4-tetrahydro-6-(phenylmethyl)- | 35.372 | 35310-85-1 | 0.242 |
| Naphthalene, 1-phenyl- | 36.578 | 605-02-7 | 2.621 |
| Naphthalene, 2-phenyl- | 40.019 | 612-94-2 | 2.234 |
| Naphthalene, 2-(phenylmethyl)- | 44.292 | 613-59-2 | 1.807 |
| **Nitrogenated Compounds** | **Σ(%.area)** | | **26.166** |
| Benzyl nitrile | 17.566 | 140-29-4 | 0.381 |
| Benzeneacetonitrile, α-methyl- | 18.434 | 1823-91-2 | 0.731 |
| Benzenepropanenitrile | 20.642 | 645-59-0 | 0.348 |

| | | | |
|---|---|---|---|
| 1,2-Benzenedicarbonitrile | 21.230 | 91-15-6 | 0.694 |
| Cyclopropanecarbonitrile, 2-phenyl-, trans- | 22.408 | 5590-14-7 | 0.348 |
| Benzenebutanenitrile | 23.461 | 2046-18-6 | 13.460 |
| Quinoline, 1,2-dihydro-1-methyl-2-methylene- | 24.133 | - | 0.865 |
| 3-Benzyl-4,5-dihydro-3H-pyrrole | 24.347 | - | 2.372 |
| 1,2,3,3a-Tetrahydropentalene, 1,1-dimethyl-3-cyanomethylene- | 24.851 | - | 0.218 |
| Cyclopropanecarbonitrile, 2-phenyl-, trans- | 25.772 | 5590-14-7 | 0.306 |
| 1H-Pyrrole, 1-(4-methylphenyl)- | 26.122 | 827-60-1 | 0.324 |
| Quinoline, 4-ethyl- | 27.451 | 19020-26-9 | 0.381 |
| Naphthalene, 1-isocyano- | 28.187 | 09/04/1984 | 1.408 |
| Naphthalene, 1-isocyano- | 28.899 | 09/04/1984 | 0.727 |
| 1-Naphthaleneacetonitrile | 32.306 | 132-75-2 | 1.055 |
| Octadecanenitrile | 43.043 | 638-65-3 | 0.653 |
| 4-Methyl-3-(O-methylbenzyl)pentanenitrile | 43.877 | 29107-40-2 | 0.730 |
| (1-Benzyl-2-O-tolyl-ethyl)-isonitrile | 44.445 | - | 0.630 |
| Naphthalene-1,3,3-tricarbonitrile, 3,4,4a,5,6,7-hexahdro-2-amino-4-(4-methylphenyl)- | 49.680 | 163978-39-0 | 0.286 |
| Naphthalene-1,3,3-tricarbonitrile, 3,4,4a,5,6,7-hexahdro-2-amino-4-(4-methylphenyl)- | 50.370 | 163978-39-0 | 0.249 |
| **Brominated Compounds** | **Σ(%.area)** | | **0.168** |
| Phenol, 2-bromo- | 15.591 | 95-56-7 | 0.096 |
| 5-Bromo-2-methoxy-1,3-dimethylbenzene | 23.559 | - | 0.072 |
| **Oxygenated Compounds** | **Σ(%.area)** | | **11.687** |
| Phenol | 12.146 | 108-95-2 | 2.659 |
| Phenol, 2-methyl- | 14.630 | 95-48-7 | 0.510 |
| Benzenemethanol, α,α-dimethyl- | 15.904 | 617-94-7 | 0.826 |
| Phenol, 2,5-dimethyl- | 16.580 | 95-87-4 | 0.362 |
| p-Cumenol | 20.028 | 99-89-8 | 5.613 |
| Phenol, 2-methyl-5-(1-methylethyl)- | 22.055 | 499-75-2 | 0.341 |
| Phenol, 2-(1-phenylethyl)- | 33.240 | 4237-44-9 | 0.893 |
| Benzaldehyde, 2-methyl-, (2,4-dinitrophenyl)hydrazone | 50.781 | 1773-44-0 | 0.483 |
| **Non Identified Fraction** | **Σ(%.area)** | | **2.462** |

**Table S11**: Classes of compounds, summation of peak areas, CAS number, and retention times of chemical compounds identified by GC-MS in OLP by thermal cracking of plastic waste from computer equipment at 450 °C, 1.0 atm, Reaction time=60 min, in semi-pilot scale two-stage reactor of 2.0 L.

| Chemical Compound | RT [min] | CAS | wi[%.area] |
|---|---|---|---|
| **Aromatic Hydrocarbons** | **Σ(%.area)** | | **47.045** |
| Styrene | 9.728 | 100-42-5 | 7.090 |
| Benzene, (1-methylethyl)- | 10.710 | 98-82-8 | 3.750 |
| Benzene, propyl- | 11.688 | 103-65-1 | 0.204 |
| α-Methylstyrene | 12.584 | 98-83-9 | 5.945 |
| Benzene, 1-propenyl- | 14.092 | 637-50-3 | 0.506 |
| Indene | 14.849 | 95-13-6 | 0.534 |
| Biphenyl | 25.017 | 92-52-4 | 0.398 |
| Diphenylmethane | 26.329 | 101-81-5 | 0.678 |
| Benzene, 1,1'-ethylidenebis- | 27.764 | 612-00-0 | 0.633 |
| Bibenzyl | 28.688 | 103-29-7 | 0.499 |
| Benzene, 1,1'-(1,3-propanediyl)bis- | 32.085 | 1081-75-0 | 14.738 |
| Benzene, 1,1'-(3-methyl-1-propene-1,3-diyl) bis- | 32.412 | 7614-93-9 | 1.278 |
| Benzene, 1,1'-(1-methyl-1,3-propanediyl)bis- | 32.600 | 1520-44-1 | 2.394 |
| 1,2-Diphenylcyclopropane | 33.636 | 29881-14-9 | 2.299 |
| Benzene, 1,1'-(1,4-butanediyl)bis- | 34.021 | 1083-56-3 | 0.601 |
| Benzene, 1,1'-(3-methyl-1-propene-1,3-diyl) bis- | 34.386 | 7614-93-9 | 0.583 |
| Benzene, 1,1'-(2-methyl-1-propenylidene) bis- | 34.898 | 781-33-9 | 1.089 |
| 1-(4-Methylphenyl)-4-phenylbuta-1,3-diene | 36.410 | 37985-11-8 | 0.503 |
| Benzene, 1,1'-[3-(2-phenylethylidene)-1,5-pentanediyl] bis- | 44.682 | 55334-57-1 | 1.468 |
| Benzene, (1-methylhexadecyl)- | 45.088 | 55125-25-2 | 0.463 |
| p-Terphenyl | 45.436 | 92-94-4 | 0.316 |
| 1-Propene, 3-(2-cyclopentenyl)-2-methyl-1,1-diphenyl- | 49.302 | - | 0.200 |
| Benzene, 1,1'-(1,4-dimethyl-1-butene-1,4-diyl) bis- | 51.646 | 52161-54-3 | 0.486 |
| 1-Propene, 3-(2-cyclopentenyl)-2-methyl-1,1-diphenyl- | 53.449 | - | 0.390 |
| **Polycyclic Aromatic Hydrocarbons (PAH)** | **Σ(%.area)** | | **11.197** |
| Naphthalene | 19.491 | 91-20-3 | 1.031 |
| Naphthalene, 1-methyl- | 22.770 | 90-12-0 | 0.576 |
| Naphthalene, 2-methyl- | 23.259 | 91-57-6 | 0.825 |
| Naphthalene, 1,2,3,4-tetrahydro-1-phenyl- | 34.473 | 3018-20-0 | 0.753 |
| Naphthalene, 1,2,3,4-tetrahydro-6-(phenylmethyl)- | 35.372 | 35310-85-1 | 0.241 |
| Naphthalene, 1-phenyl- | 36.578 | 605-02-7 | 2.713 |
| Naphthalene, 2-phenyl- | 40.019 | 612-94-2 | 2.518 |
| 1,2,3,4-Tetrahydro-1-phenyl-1,2,3-methanonaphthalene | 40.387 | 138089-69-7 | 0.559 |
| Naphthalene, 2-(phenylmethyl)- | 44.292 | 613-59-2 | 1.981 |
| **Nitrogenated Compounds** | **Σ(%.area)** | | **27.411** |
| Benzyl nitrile | 17.566 | 140-29-4 | 0.463 |
| Benzeneacetonitrile, α-methyl- | 18.434 | 1823-91-2 | 0.782 |

| | | | |
|---|---|---|---|
| Benzenepropanenitrile | 20.642 | 645-59-0 | 0.365 |
| 1,2-Benzenedicarbonitrile | 21.230 | 91-15-6 | 0.699 |
| Cyclopropanecarbonitrile, 2-phenyl-, trans- | 22.408 | 5590-14-7 | 0.433 |
| Benzenebutanenitrile | 23.461 | 2046-18-6 | 13.871 |
| Quinoline, 1,2-dihydro-1-methyl-2-methylene- | 24.133 | - | 0.890 |
| 3-Benzyl-4,5-dihydro-3H-pyrrole | 24.347 | - | 2.451 |
| 1,2,3,3a-Tetrahydropentalene, 1,1-dimethyl-3-cyanomethylene- | 24.851 | - | 0.221 |
| Cyclopropanecarbonitrile, 2-phenyl-, trans- | 25.772 | 5590-14-7 | 0.337 |
| 1H-Pyrrole, 1-(4-methylphenyl)- | 26.122 | 827-60-1 | 0.375 |
| Quinoline, 4-ethyl- | 27.451 | 19020-26-9 | 0.381 |
| Naphthalene, 1-isocyano- | 28.187 | 09/04/1984 | 1.487 |
| Naphthalene, 1-isocyano- | 28.899 | 09/04/1984 | 0.837 |
| 1-Naphthaleneacetonitrile | 32.306 | 132-75-2 | 1.155 |
| Octadecanenitrile | 43.043 | 638-65-3 | 0.662 |
| 4-Methyl-3-(O-methylbenzyl)pentanenitrile | 43.877 | 29107-40-2 | 0.738 |
| (1-Benzyl-2-O-tolyl-ethyl)-isonitrile | 44.445 | - | 0.686 |
| Naphthalene-1,3,3-tricarbonitrile, 3,4,4a,5,6,7-hexahdro-2-amino-4-(4-methylphenyl)- | 49.680 | 163978-39-0 | 0.281 |
| Naphthalene-1,3,3-tricarbonitrile, 3,4,4a,5,6,7-hexahdro-2-amino-4-(4-methylphenyl)- | 50.370 | 163978-39-0 | 0.297 |
| **Brominated Compounds** | **Σ(%.area)** | | **0.162** |
| Phenol, 2-bromo- | 15.591 | 95-56-7 | 0.103 |
| 5-Bromo-2-methoxy-1,3-dimethylbenzene | 23.559 | - | 0.059 |
| **Oxygenated Compounds** | **Σ(%.area)** | | **11.606** |
| Phenol | 12.146 | 108-95-2 | 2.642 |
| Phenol, 2-methyl- | 14.630 | 95-48-7 | 0.560 |
| Benzenemethanol, α,α-dimethyl- | 15.904 | 617-94-7 | 0.631 |
| Phenol, 2,5-dimethyl- | 16.580 | 95-87-4 | 0.424 |
| p-Cumenol | 20.028 | 99-89-8 | 5.521 |
| Phenol, 2-methyl-5-(1-methylethyl)- | 22.055 | 499-75-2 | 0.353 |
| Phenol, 2-(1-phenylethyl)- | 33.240 | 4237-44-9 | 1.000 |
| Benzaldehyde, 2-methyl-, (2,4-dinitrophenyl)hydrazone | 50.785 | 1773-44-0 | 0.475 |
| **Non Identified Fraction** | **Σ(%.area)** | | **2.581** |

**Table S12**: Classes of compounds, summation of peak areas, CAS number, and retention times of chemical compounds identified by GC-MS in OLP by thermal cracking of plastic waste from computer equipment at 500 °C, 1.0 atm, Reaction time=15 min, in semi-pilot scale two-stage reactor of 2.0 L.

| Chemical Compound | RT [min] | CAS | wi[%.area] |
|---|---|---|---|
| **Aromatic Hydrocarbons** | **Σ(%.area)** | | **66.150** |
| Styrene | 9.731 | 100-42-5 | 10.183 |
| α-Methylstyrene | 12.585 | 98-83-9 | 4.406 |
| Benzene, 1,1'-(1,3-propanediyl)bis- | 32.086 | 1081-75-0 | 26.935 |
| Benzene, 1,1'-(3-methyl-1-propene-1,3-diyl) bis- | 32.420 | 7614-93-9 | 4.077 |
| Benzene, 1,1'-(1-methyl-1,3-propanediyl)bis- | 32.601 | 1520-44-1 | 3.362 |
| 1,2-Diphenylcyclopropane | 33.644 | 29881-14-9 | 4.144 |
| Benzene, 1,1'-(3-methyl-1-propene-1,3-diyl) bis- | 34.388 | 7614-93-9 | 2.355 |
| Benzene, 1,1'-(1,1,2,2-tetramethyl-1,2-ethanediyl) bis- | 34.745 | 1889-67-4 | 2.194 |
| Benzene, 1,1'-(2-methyl-1-propenylidene) bis- | 34.908 | 781-33-9 | 8.494 |
| **Polycyclic Aromatic Hydrocarbons (PAH)** | **Σ(%.area)** | | **3.511** |
| 1,9-Dihydropyrene | 36.584 | 28862-02-4 | 3.511 |
| **Nitrogenated Compounds** | **Σ(%.area)** | | **13.450** |
| Benzenebutanenitrile | 23.450 | 2046-18-6 | 13.450 |
| **Oxygenated Compounds** | **Σ(%.area)** | | **16.889** |
| Phenol | 12.162 | 108-95-2 | 10.765 |
| Phenol, 3-(1-methylethyl)- | 20.040 | 618-45-1 | 6.124 |

**Table S13**: Classes of compounds, summation of peak areas, CAS number, and retention times of chemical compounds identified by GC-MS in OLP by thermal cracking of plastic waste from computer equipment at 500 °C, 1.0 atm, Reaction time=30 min, in semi-pilot scale two-stage reactor of 2.0 L.

| Chemical Compound | RT [min] | CAS | wi[%.area] |
|---|---|---|---|
| **Aromatic Hydrocarbons** | **Σ(%.area)** | | **52.762** |
| Styrene | 9.728 | 100-42-5 | 6.568 |
| Benzene, (1-methylethyl)- | 10.710 | 98-82-8 | 5.782 |
| Benzene, 2-propenyl- | 11.420 | 300-57-2 | 0.118 |
| Benzene, propyl- | 11.687 | 103-65-1 | 0.21 |
| α-Methylstyrene | 12.584 | 98-83-9 | 2.414 |
| Benzene, 1-ethenyl-2-methyl- | 12.919 | 611-15-4 | 0.122 |
| Benzene, 1-propenyl- | 14.092 | 637-50-3 | 0.371 |
| Diphenylmethane | 26.329 | 101-81-5 | 0.325 |
| Bibenzyl | 28.688 | 103-29-7 | 0.368 |
| Benzene, 1,1'-(1,3-propanediyl)bis- | 32.085 | 1081-75-0 | 10.646 |
| Benzene, 1,1'-(3-methyl-1-propene-1,3-diyl) bis- | 32.412 | 7614-93-9 | 1.041 |
| Benzene, 1,1'-(1-methyl-1,3-propanediyl)bis- | 32.600 | 1520-44-1 | 1.941 |
| 1,2-Diphenylcyclopropane | 33.636 | 29881-14-9 | 1.617 |
| Benzene, 1,1'-(1,4-butanediyl)bis- | 34.021 | 1083-56-3 | 0.445 |
| Benzene, 1,1'-(3-methyl-1-propene-1,3-diyl) bis- | 34.386 | 7614-93-9 | 1.353 |
| 2,4-Diphenyl-4-methyl-1-pentene | 34.748 | - | 5.009 |
| Benzene, 1,1'-(2-methyl-1-propenylidene) bis- | 34.898 | 781-33-9 | 4.939 |
| 2,4-Diphenyl-4-methyl-2(E)-pentene | 35.518 | 22768-22-5 | 3.963 |
| Benzene, 1,1'-[3-(2-phenylethylidene)-1,5-pentanediyl] bis- | 43.694 | 55334-57-1 | 0.407 |
| Benzene, 1,1'-[3-(2-phenylethylidene)-1,5-pentanediyl] bis- | 44.682 | 55334-57-1 | 1.053 |
| Benzene, (1-methylhexadecyl)- | 45.093 | 55125-25-2 | 0.351 |
| 1-Propene, 3-(2-cyclopentenyl)-2-methyl-1,1-diphenyl- | 46.882 | - | 0.277 |
| Benzene, 1,1'-(1,1,2,2-tetramethyl-1,2-ethanediyl) bis- | 48.268 | 1889-67-4 | 0.971 |
| 1-Propene, 3-(2-cyclopentenyl)-2-methyl-1,1-diphenyl- | 49.306 | - | 0.458 |
| Benzene, 1,1'-(1,4-dimethyl-1-butene-1,4-diyl) bis- | 53.077 | 52161-54-3 | 0.437 |
| 1-Propene, 3-(2-cyclopentenyl)-2-methyl-1,1-diphenyl- | 53.449 | - | 1.576 |
| **Aliphatic Hydrocarbons** | **Σ(%.area)** | | **0.422** |
| Pentadecane | 27.477 | 629-62-9 | 0.422 |
| **Polycyclic Aromatic Hydrocarbons (PAH)** | **Σ(%.area)** | | **9.686** |
| Naphthalene | 19.491 | 91-20-3 | 0.499 |
| Naphthalene, 2-methyl- | 23.259 | 91-57-6 | 0.239 |
| Naphthalene, 1,2,3,4-tetrahydro-1-phenyl- | 34.473 | 3018-20-0 | 0.445 |
| Naphthalene, 1,2,3,4-tetrahydro-6-(phenylmethyl)- | 35.372 | 35310-85-1 | 1.94 |
| Naphthalene, 1-phenyl- | 36.578 | 605-02-7 | 2.006 |
| Naphthalene, 2,7-bis(1,1-dimethylethyl)- | 37.221 | 10275-58-8 | 2.982 |
| Naphthalene, 2-phenyl- | 40.019 | 612-94-2 | 0.545 |
| Naphthalene, 2-(phenylmethyl)- | 44.292 | 613-59-2 | 1.030 |

| **Nitrogenated Compounds** | **Σ(%.area)** | | **14.489** |
|---|---|---|---|
| Isobutyronitrile | 3.319 | 78-82-0 | 0.058 |
| Benzonitrile | 12.687 | 100-47-0 | 0.053 |
| Benzeneacetonitrile, α-methyl- | 18.434 | 1823-91-2 | 0.343 |
| 1,2-Benzenedicarbonitrile | 21.230 | 91-15-6 | 0.339 |
| Benzenebutanenitrile | 23.450 | 2046-18-6 | 7.808 |
| 3-Benzyl-4,5-dihydro-3H-pyrrole | 24.342 | - | 0.662 |
| 1,2,3,3a-Tetrahydropentalene, 1,1-dimethyl-3-cyanomethylene- | 24.847 | - | 0.322 |
| 1H-Pyrrole, 1-(4-methylphenyl)- | 26.122 | 827-60-1 | 0.224 |
| Naphthalene, 1-isocyano- | 28.187 | 09/04/1984 | 0.600 |
| 1-Naphthaleneacetonitrile | 32.306 | 132-75-2 | 0.531 |
| (1-Benzyl-2-O-tolyl-ethyl)-isonitrile | 35.167 | - | 0.487 |
| Octadecanenitrile | 43.043 | 638-65-3 | 1.061 |
| (1-Benzyl-2-O-tolyl-ethyl)-isonitrile | 44.445 | - | 0.363 |
| Naphthalene-1,3,3-tricarbonitrile, 3,4,4a,5,6,7-hexahdro-2-amino-4-(4-methylphenyl)- | 49.681 | 163978-39-0 | 0.465 |
| Naphthalene-1,3,3-tricarbonitrile, 3,4,4a,5,6,7-hexahdro-2-amino-4-(4-methylphenyl)- | 50.378 | 163978-39-0 | 0.566 |
| 2-(4-Methoxy-2,6-dimethylphenyl)-3-methyl-2H-benzo[g]indazole | 52.204 | - | 0.607 |
| **Brominated Compounds** | **Σ(%.area)** | | **0.456** |
| 5-Bromo-2-methoxy-1,3-dimethylbenzene | 23.559 | 1836-06-2 | 0.456 |
| **Oxygenated Compounds** | **Σ(%.area)** | | **17.515** |
| Ethyl Acetate | 3.128 | 141-78-6 | 0.017 |
| Phenol | 12.146 | 108-95-2 | 3.229 |
| Benzenemethanol, α-methyl-, (R)- | 15.082 | 1517-69-7 | 0.617 |
| p-Cumenol | 20.028 | 99-89-8 | 4.335 |
| Phenol, o-(α,α-dimethylbenzyl)- | 33.109 | 18168-40-6 | 0.530 |
| Phenol, 2-(1-phenylethyl)- | 33.240 | 4237-44-9 | 2.657 |
| Phenol, 4-(1-methyl-1-phenylethyl)- | 36.122 | 599-64-4 | 1.721 |
| 2-tert-Butyl-6-(a-methylbenzyl) phenol | 37.124 | 17959-02-3 | 0.857 |
| 2,3-Dimethyl-1,4,4a,9a-tetrahydroanthracene-9,10-dione | 49.741 | 2670-23-7 | 0.556 |
| Phenol, 4-(1-methyl-1-phenylethyl)- | 51.109 | 599-64-4 | 0.598 |
| Phenol, 2,4-bis(1-phenylethyl)- | 51.574 | 2769-94-0 | 1.918 |
| 4-(2-Methyl-1-cyclohexenyl)-trans-3-buten-2-one 2,4-dinitrophenylhydrazone | 51.822 | - | 0.480 |
| **Non Identified Fraction** | **Σ(%.area)** | | **4.670** |

**Table S14**: Classes of compounds, summation of peak areas, CAS number, and retention times of chemical compounds identified by GC-MS in OLP by thermal cracking of plastic waste from computer equipment at 500 °C, 1.0 atm, Reaction time=45 min, in semi-pilot scale two-stage reactor of 2.0 L.

| Chemical Compound | RT [min] | CAS | wi[%.area] |
|---|---|---|---|
| **Aromatic Hydrocarbons** | **Σ(%.area)** | | **49.938** |
| Styrene | 9.728 | 100-42-5 | 6.303 |
| Benzene, (1-methylethyl)- | 10.710 | 98-82-8 | 3.884 |
| Benzene, propyl- | 11.687 | 103-65-1 | 0.194 |
| α-Methylstyrene | 12.584 | 98-83-9 | 5.655 |
| Benzene, 1-propenyl- | 14.092 | 637-50-3 | 0.492 |
| Diphenylmethane | 26.329 | 101-81-5 | 0.644 |
| Benzene, 1,1'-ethylidenebis- | 27.764 | 612-00-0 | 0.486 |
| Bibenzyl | 28.688 | 103-29-7 | 0.504 |
| Benzene, 1,1'-(1,3-propanediyl)bis- | 32.085 | 1081-75-0 | 16.286 |
| Benzene, 1,1'-(3-methyl-1-propene-1,3-diyl) bis- | 32.412 | 7614-93-9 | 1.548 |
| Benzene, 1,1'-(1-methyl-1,3-propanediyl)bis- | 32.600 | 1520-44-1 | 2.802 |
| 1,2-Diphenylcyclopropane | 33.636 | 29881-14-9 | 2.620 |
| Benzene, 1,1'-(1,4-butanediyl)bis- | 34.021 | 1083-56-3 | 0.702 |
| Benzene, 1,1'-(3-methyl-1-propene-1,3-diyl) bis- | 34.386 | 7614-93-9 | 0.995 |
| 2,4-Diphenyl-4-methyl-1-pentene | 34.748 | - | 0.554 |
| Benzene, 1,1'-(2-methyl-1-propenylidene) bis- | 34.898 | 781-33-9 | 2.892 |
| 1-(4-Methylphenyl)-4-phenylbuta-1,3-diene | 36.410 | 37985-11-8 | 0.546 |
| Benzene, 1,1'-[3-(2-phenylethylidene)-1,5-pentanediyl] bis- | 44.682 | 55334-57-1 | 1.440 |
| Benzene, (1-methylhexadecyl)- | 45.093 | 55125-25-2 | 0.457 |
| 1-Propene, 3-(2-cyclopentenyl)-2-methyl-1,1-diphenyl- | 49.306 | - | 0.351 |
| 1-Propene, 3-(2-cyclopentenyl)-2-methyl-1,1-diphenyl- | 53.449 | - | 0.583 |
| **Polycyclic Aromatic Hydrocarbons (PAH)** | **Σ(%.area)** | | **8.596** |
| Naphthalene | 19.491 | 91-20-3 | 0.590 |
| Naphthalene, 1-methyl- | 22.770 | 90-12-0 | 0.305 |
| Naphthalene, 2-methyl- | 23.259 | 91-57-6 | 0.462 |
| Naphthalene, 1,2,3,4-tetrahydro-1-phenyl- | 34.473 | 3018-20-0 | 0.657 |
| Naphthalene, 1,2,3,4-tetrahydro-6-(phenylmethyl)- | 35.372 | 35310-85-1 | 0.554 |
| Naphthalene, 1-phenyl- | 36.578 | 605-02-7 | 2.087 |
| Naphthalene, 2,7-bis(1,1-dimethylethyl)- | 37.221 | 10275-58-8 | 1.456 |
| Naphthalene, 2-phenyl- | 40.019 | 612-94-2 | 1.181 |
| Naphthalene, 2-(phenylmethyl)- | 44.292 | 613-59-2 | 1.304 |
| **Nitrogenated Compounds** | **Σ(%.area)** | | **27.427** |
| Benzyl nitrile | 17.566 | 140-29-4 | 0.331 |
| Benzeneacetonitrile, α-methyl- | 18.434 | 1823-91-2 | 0.709 |
| Benzenepropanenitrile | 20.642 | 645-59-0 | 0.321 |
| 1,2-Benzenedicarbonitrile | 21.230 | 91-15-6 | 0.618 |
| Cyclopropanecarbonitrile, 2-phenyl-, trans- | 22.408 | 5590-14-7 | 0.343 |

| | | | |
|---|---|---|---|
| Benzenebutanenitrile | 23.461 | 2046-18-6 | 15.693 |
| Cyclopropanecarbonitrile, 2-phenyl-, trans- | 23.927 | 5590-14-7 | 0.270 |
| Quinoline, 1,2-dihydro-1-methyl-2-methylene- | 24.133 | - | 1.037 |
| 3-Benzyl-4,5-dihydro-3H-pyrrole | 24.347 | - | 2.320 |
| 1,2,3,3a-Tetrahydropentalene, 1,1-dimethyl-3-cyanomethylene- | 24.847 | - | 0.308 |
| Cyclopropanecarbonitrile, 2-phenyl-, trans- | 25.772 | 5590-14-7 | 0.309 |
| 1H-Pyrrole, 1-(4-methylphenyl)- | 26.122 | 827-60-1 | 0.462 |
| Quinoline, 4-ethyl- | 27.451 | 19020-26-9 | 0.477 |
| Naphthalene, 1-isocyano- | 28.187 | 09/04/1984 | 1.044 |
| Naphthalene, 1-isocyano- | 28.899 | 09/04/1984 | 0.352 |
| 1-Naphthaleneacetonitrile | 32.306 | 132-75-2 | 0.948 |
| Octadecanenitrile | 43.043 | 638-65-3 | 0.661 |
| (1-Benzyl-2-O-tolyl-ethyl)-isonitrile | 44.445 | - | 0.538 |
| Naphthalene-1,3,3-tricarbonitrile, 3,4,4a,5,6,7-hexahdro-2-amino-4-(4-methylphenyl)- | 49.681 | 163978-39-0 | 0.324 |
| Naphthalene-1,3,3-tricarbonitrile, 3,4,4a,5,6,7-hexahdro-2-amino-4-(4-methylphenyl)- | 50.378 | 163978-39-0 | 0.362 |
| **Brominated Compounds** | **Σ(%.area)** | | **0.266** |
| 5-Bromo-2-methoxy-1,3-dimethylbenzene | 23.559 | 1836-06-2 | 0.266 |
| **Oxygenated Compounds** | **Σ(%.area)** | | **12.966** |
| Phenol | 12.146 | 108-95-2 | 2.836 |
| Phenol, 2-methyl- | 14.630 | 95-48-7 | 0.532 |
| Benzenemethanol, α,α-dimethyl- | 15.904 | 617-94-7 | 1.371 |
| p-Cumenol | 20.028 | 99-89-8 | 6.225 |
| Phenol, 2-methyl-5-(1-methylethyl)- | 22.055 | 499-75-2 | 0.401 |
| Phenol, 2-(1-phenylethyl)- | 33.240 | 4237-44-9 | 1.386 |
| Phenol, 4-(1-methyl-1-phenylethyl)- | 36.122 | 599-64-4 | 0.215 |
| **Non Identified Fraction** | **Σ(%.area)** | | **0.807** |

**Table S15**: Classes of compounds, summation of peak areas, CAS number, and retention times of chemical compounds identified by GC-MS in OLP by thermal cracking of plastic waste from computer equipment at 500 °C, 1.0 atm, Reaction time=60 min, in semi-pilot scale two-stage reactor of 2.0 L.

| Chemical Compound | RT [min] | CAS | wi[%.area] |
|---|---|---|---|
| **Aromatic Hydrocarbons** | **Σ(%.area)** | | **47.596** |
| Styrene | 9.728 | 100-42-5 | 6.379 |
| Benzene, (1-methylethyl)- | 10.710 | 98-82-8 | 3.546 |
| Benzene, propyl- | 11.687 | 103-65-1 | 0.205 |
| α-Methylstyrene | 12.584 | 98-83-9 | 4.996 |
| Benzene, 1-propenyl- | 14.092 | 637-50-3 | 0.520 |
| Indene | 14.848 | 95-13-6 | 0.326 |
| Biphenyl | 25.017 | 92-52-4 | 0.352 |
| Diphenylmethane | 26.329 | 101-81-5 | 0.743 |
| Benzene, 1,1'-ethylidenebis- | 27.764 | 612-00-0 | 0.597 |
| Bibenzyl | 28.688 | 103-29-7 | 0.571 |
| Benzene, 1,1'-(1,3-propanediyl)bis- | 32.085 | 1081-75-0 | 14.826 |
| Benzene, 1,1'-(3-methyl-1-propene-1,3-diyl) bis- | 32.412 | 7614-93-9 | 1.534 |
| Benzene, 1,1'-(1-methyl-1,3-propanediyl)bis- | 32.600 | 1520-44-1 | 2.487 |
| 1,2-Diphenylcyclopropane | 33.636 | 29881-14-9 | 2.931 |
| Benzene, 1,1'-(1,4-butanediyl)bis- | 34.021 | 1083-56-3 | 0.663 |
| Benzene, 1,1'-(3-methyl-1-propene-1,3-diyl) bis- | 34.386 | 7614-93-9 | 0.926 |
| 2,4-Diphenyl-4-methyl-1-pentene | 34.748 | - | 0.236 |
| Benzene, 1,1'-(2-methyl-1-propenylidene) bis- | 34.898 | 781-33-9 | 2.667 |
| 1-(4-Methylphenyl)-4-phenylbuta-1,3-diene | 36.410 | 37985-11-8 | 0.514 |
| Benzene, 1,1'-[3-(2-phenylethylidene)-1,5-pentanediyl] bis- | 44.682 | 55334-57-1 | 1.641 |
| Benzene, (1-methylhexadecyl)- | 45.093 | 55125-25-2 | 0.479 |
| 1-Propene, 3-(2-cyclopentenyl)-2-methyl-1,1-diphenyl- | 53.449 | - | 0.457 |
| **Polycyclic Aromatic Hydrocarbons (PAH)** | **Σ(%.area)** | | **10.933** |
| Naphthalene | 19.491 | 91-20-3 | 1.008 |
| Naphthalene, 1-methyl- | 22.770 | 90-12-0 | 0.530 |
| Naphthalene, 2-methyl- | 23.259 | 91-57-6 | 0.699 |
| Naphthalene, 1,2,3,4-tetrahydro-1-phenyl- | 34.473 | 3018-20-0 | 0.759 |
| Naphthalene, 1,2,3,4-tetrahydro-6-(phenylmethyl)- | 35.372 | 35310-85-1 | 0.529 |
| Naphthalene, 1-phenyl- | 36.578 | 605-02-7 | 2.266 |
| Naphthalene, 2,7-bis(1,1-dimethylethyl)- | 37.221 | 10275-58-8 | 1.18 |
| Naphthalene, 2-phenyl- | 40.019 | 612-94-2 | 2.138 |
| Naphthalene, 2-(phenylmethyl)- | 44.292 | 613-59-2 | 1.824 |
| **Nitrogenated Compounds** | **Σ(%.area)** | | **28.932** |
| Benzyl nitrile | 17.566 | 140-29-4 | 0.408 |
| Benzeneacetonitrile, α-methyl- | 18.434 | 1823-91-2 | 0.777 |
| Benzenepropanenitrile | 20.642 | 645-59-0 | 0.376 |
| 1,2-Benzenedicarbonitrile | 21.230 | 91-15-6 | 0.548 |

| | | | |
|---|---|---|---|
| Cyclopropanecarbonitrile, 2-phenyl-, trans- | 22.408 | 5590-14-7 | 0.432 |
| Benzenebutanenitrile | 23.461 | 2046-18-6 | 14.999 |
| Cyclopropanecarbonitrile, 2-phenyl-, trans- | 23.927 | 5590-14-7 | 0.267 |
| Quinoline, 1,2-dihydro-1-methyl-2-methylene- | 24.133 | - | 1.044 |
| 3-Benzyl-4,5-dihydro-3H-pyrrole | 24.347 | - | 2.420 |
| 1,2,3,3a-Tetrahydropentalene, 1,1-dimethyl-3-cyanomethylene- | 24.847 | - | 0.279 |
| Cyclopropanecarbonitrile, 2-phenyl-, trans- | 25.772 | 5590-14-7 | 0.355 |
| 1H-Pyrrole, 1-(4-methylphenyl)- | 26.122 | 827-60-1 | 0.435 |
| Quinoline, 4-ethyl- | 27.451 | 19020-26-9 | 0.454 |
| Naphthalene, 1-isocyano- | 28.187 | 09/04/1984 | 1.114 |
| Naphthalene, 1-isocyano- | 28.899 | 09/04/1984 | 0.754 |
| 1-Naphthaleneacetonitrile | 32.306 | 132-75-2 | 1.174 |
| Octadecanenitrile | 43.043 | 638-65-3 | 0.567 |
| 4-Methyl-3-(O-methylbenzyl)pentanenitrile | 43.877 | 29107-40-2 | 0.694 |
| (1-Benzyl-2-O-tolyl-ethyl)-isonitrile | 44.445 | - | 0.683 |
| Naphthalene-1,3,3-tricarbonitrile, 3,4,4a,5,6,7-hexahdro-2-amino-4-(4-methylphenyl)- | 49.679 | 163978-39-0 | 0.292 |
| Naphthalene-1,3,3-tricarbonitrile, 3,4,4a,5,6,7-hexahdro-2-amino-4-(4-methylphenyl)- | 50.378 | 163978-39-0 | 0.326 |
| Acridine, 9-phenyl- | 51.600 | 602-56-2 | 0.534 |
| **Oxygenated Compounds** | **Σ(%.area)** | | **11.583** |
| Phenol | 12.146 | 108-95-2 | 2.039 |
| Phenol, 2-methyl- | 14.630 | 95-48-7 | 0.678 |
| Benzenemethanol, α,α-dimethyl- | 15.904 | 617-94-7 | 1.430 |
| Phenol, 2,5-dimethyl- | 16.580 | 95-87-4 | 0.480 |
| p-Cumenol | 20.028 | 99-89-8 | 4.665 |
| Phenol, 2-methyl-5-(1-methylethyl)- | 22.055 | 499-75-2 | 0.441 |
| Phenol, 2-(1-phenylethyl)- | 33.240 | 4237-44-9 | 1.332 |
| Benzaldehyde, 2-methyl-, (2,4-dinitrophenyl)hydrazone | 50.781 | 1773-44-0 | 0.518 |
| **Non Identified Fraction** | **Σ(%.area)** | | **0.953** |

**Table S16**: Classes of compounds, summation of peak areas, CAS number, and retention times of chemical compounds identified by GC-MS in OLP by catalytic upgrading of plastic waste from computer equipment pyrolysis vapors at 450 °C, 1.0 atm, on a fixed catalyst bed loaded with 2.5%.wt of Si-Al ash pellets, Reaction time=30 min, in semi-pilot scale two-stage reactor of 2.0 L.

| Chemical Compound | RT [min] | CAS | wi[%.area] |
|---|---|---|---|
| **Aromatic Hydrocarbons** | **Σ(%.area)** | | **45.614** |
| Styrene | 9.728 | 100-42-5 | 5.466 |
| Benzene, (1-methylethyl)- | 10.710 | 98-82-8 | 3.168 |
| Benzene, propyl- | 11.688 | 103-65-1 | 0.185 |
| α-Methylstyrene | 12.584 | 98-83-9 | 6.159 |
| Benzene, 1-propenyl- | 14.092 | 637-50-3 | 0.556 |
| Indene | 14.844 | 95-13-6 | 0.168 |
| Benzene, n-butyl- | 14.998 | 104-51-8 | 0.131 |
| 2,4-Dimethylstyrene | 16.879 | 2234-20-0 | 0.170 |
| Biphenyl | 25.017 | 92-52-4 | 0.179 |
| Diphenylmethane | 26.329 | 101-81-5 | 0.624 |
| Benzene, 1,1'-ethylidenebis- | 27.764 | 612-00-0 | 0.571 |
| Bibenzyl | 28.688 | 103-29-7 | 0.566 |
| Benzene, 1,1'-(1,3-propanediyl)bis- | 32.085 | 1081-75-0 | 16.178 |
| Benzene, 1,1'-(3-methyl-1-propene-1,3-diyl) bis- | 32.412 | 7614-93-9 | 1.712 |
| Benzene, 1,1'-(1-methyl-1,3-propanediyl) bis- | 32.600 | 1520-44-1 | 2.120 |
| 1,2-Diphenylcyclopropane | 33.636 | 29881-14-9 | 2.245 |
| Benzene, 1,1'-(1,4-butanediyl)bis- | 34.021 | 1083-56-3 | 0.653 |
| Benzene, 1,1'-(3-methyl-1-propene-1,3-diyl) bis- | 34.386 | 7614-93-9 | 0.957 |
| Benzene, 1,1'-(2-methyl-1-propenylidene) bis- | 34.898 | 781-33-9 | 1.961 |
| 1-(4-Methylphenyl)-4-phenylbuta-1,3-diene | 36.410 | 37985-11-8 | 0.533 |
| Benzene, 1,1'-[3-(2-phenylethylidene)-1,5-pentanediyl] bis- | 44.682 | 55334-57-1 | 0.611 |
| 1-Propene, 3-(2-cyclopentenyl)-2-methyl-1,1-diphenyl- | 49.302 | - | 0.252 |
| 1-Propene, 3-(2-cyclopentenyl)-2-methyl-1,1-diphenyl- | 53.449 | - | 0.449 |
| **Polycyclic Aromatic Hydrocarbons (PAH)** | **Σ(%.area)** | | **6.445** |
| Naphthalene | 19.491 | 91-20-3 | 0.586 |
| Naphthalene, 1-methyl- | 22.770 | 90-12-0 | 0.354 |
| Naphthalene, 2-methyl- | 23.259 | 91-57-6 | 0.576 |
| Naphthalene, 1-isocyano- | 28.187 | 09/04/1984 | 0.980 |
| Naphthalene, 1,2,3,4-tetrahydro-1-phenyl- | 34.473 | 3018-20-0 | 0.531 |
| Naphthalene, 1-phenyl- | 36.578 | 605-02-7 | 1.562 |
| Naphthalene, 2-phenyl- | 40.019 | 612-94-2 | 0.882 |
| 1,2,3,4-Tetrahydro-1-phenyl-1,2,3-methanonaphthalene | 40.387 | 138089-69-7 | 0.263 |
| Naphthalene, 2-(phenylmethyl)- | 44.292 | 613-59-2 | 0.711 |
| **Nitrogenated Compounds** | **Σ(%.area)** | | **27.135** |
| Cyclopentanecarbonitrile, 2-imino- | 15.262 | 2321-76-8 | 0.268 |
| Benzyl nitrile | 17.566 | 140-29-4 | 0.454 |

| | | | |
|---|---|---|---|
| Benzeneacetonitrile, α-methyl- | 18.434 | 1823-91-2 | 0.780 |
| Benzenepropanenitrile | 20.642 | 645-59-0 | 0.299 |
| 1,2-Benzenedicarbonitrile | 21.230 | 91-15-6 | 0.480 |
| Cyclopropanecarbonitrile, 2-phenyl-, trans- | 22.408 | 5590-14-7 | 0.375 |
| Benzenebutanenitrile | 23.461 | 2046-18-6 | 16.965 |
| Cyclopropanecarbonitrile, 2-phenyl-, cis | 23.922 | 5590-14-7 | 0.297 |
| Quinoline, 1,2-dihydro-1-methyl-2-methylene- | 24.133 | - | 0.930 |
| 3-Benzyl-4,5-dihydro-3H-pyrrole | 24.347 | - | 2.320 |
| 1,2,3,3a-Tetrahydropentalene, 1,1-dimethyl-3-cyanomethylene- | 24.851 | - | 0.348 |
| Cyclopropanecarbonitrile, 2-phenyl-, trans- | 25.772 | 5590-14-7 | 0.333 |
| 1H-Pyrrole, 1-(4-methylphenyl)- | 26.122 | 827-60-1 | 0.414 |
| Quinoline, 4-ethyl- | 27.451 | 19020-26-9 | 0.570 |
| 1,2,3,3a-Tetrahydropentalene, 1,1-dimethyl-3-cyanomethylene- | 27.611 | | 0.282 |
| Naphthalene, 1-isocyano- | 28.899 | 09/04/1984 | 0.397 |
| 1-Naphthaleneacetonitrile | 32.306 | 132-75-2 | 0.779 |
| Octadecanenitrile | 43.043 | 638-65-3 | 0.414 |
| 4-Methyl-3-(O-methylbenzyl)pentanenitrile | 43.877 | 29107-40-2 | 0.218 |
| (1-Benzyl-2-O-tolyl-ethyl)-isonitrile | 44.445 | - | 0.212 |
| **Brominated Compounds** | **Σ(%.area)** | | **1.077** |
| Phenol, 2-bromo- | 15.591 | 95-56-7 | 0.465 |
| 5-Bromo-2-methoxy-1,3-dimethylbenzene | 23.559 | - | 0.612 |
| **Oxygenated Compounds** | **Σ(%.area)** | | **16.916** |
| Phenol | 12.146 | 108-95-2 | 4.502 |
| Phenol, 2-methyl- | 14.630 | 95-48-7 | 0.503 |
| Benzenemethanol, α-methyl-, (R)- | 15.082 | 1517-69-7 | 0.297 |
| Acetophenone | 15.361 | 98-86-2 | 0.296 |
| Benzenemethanol, α,α-dimethyl- | 15.904 | 617-94-7 | 1.604 |
| Phenol, 2,5-dimethyl- | 16.580 | 95-87-4 | 0.479 |
| Phenol, 2,4-dimethyl- | 17.684 | 105-67-9 | 0.365 |
| Phenol, 2,4,6-trimethyl- | 18.614 | 527-60-6 | 0.325 |
| p-Cumenol | 20.028 | 99-89-8 | 7.351 |
| Phenol, 2-methyl-5-(1-methylethyl)- | 22.055 | 499-75-2 | 0.348 |
| Phenol, 2-(1-phenylethyl)- | 33.240 | 4237-44-9 | 0.846 |
| **Non Identified Fraction** | **Σ(%.area)** | | **2.809** |

**Table S17**: Classes of compounds, summation of peak areas, CAS number, and retention times of chemical compounds identified by GC-MS in OLP by catalytic upgrading of plastic waste from computer equipment pyrolysis vapors at 450 °C, 1.0 atm, on a fixed catalyst bed loaded with 2.5%.wt of Si-Al ash pellets, Reaction time=45 min, in semi-pilot scale two-stage reactor of 2.0 L.

| Chemical Compound | RT [min] | CAS | wi[%.area] |
|---|---|---|---|
| **Aromatic Hydrocarbons** | **Σ(%.area)** | | **47.840** |
| Styrene | 9.728 | 100-42-5 | 5.756 |
| Benzene, (1-methylethyl)- | 10.710 | 98-82-8 | 3.077 |
| Benzene, propyl- | 11.688 | 103-65-1 | 0.175 |
| α-Methylstyrene | 12.584 | 98-83-9 | 4.292 |
| Benzene, 1-propenyl- | 14.092 | 637-50-3 | 0.414 |
| Indene | 14.844 | 95-13-6 | 0.164 |
| 2,4-Dimethylstyrene | 16.879 | 2234-20-0 | 0.143 |
| Biphenyl | 25.017 | 92-52-4 | 0.159 |
| Diphenylmethane | 26.329 | 101-81-5 | 0.684 |
| Benzene, 1,1'-ethylidenebis- | 27.764 | 612-00-0 | 0.569 |
| Bibenzyl | 28.688 | 103-29-7 | 0.568 |
| Benzene, 1,1'-(1,3-propanediyl) bis- | 32.085 | 1081-75-0 | 14.522 |
| Benzene, 1,1'-(3-methyl-1-propene-1,3-diyl) bis- | 32.412 | 7614-93-9 | 1.806 |
| Benzene, 1,1'-(1-methyl-1,3-propanediyl) bis- | 32.600 | 1520-44-1 | 2.096 |
| 1,2-Diphenylcyclopropane | 33.636 | 29881-14-9 | 2.944 |
| Benzene, 1,1'-(1,4-butanediyl) bis- | 34.021 | 1083-56-3 | 0.770 |
| Benzene, 1,1'-(3-methyl-1-propene-1,3-diyl) bis- | 34.386 | 7614-93-9 | 1.237 |
| Benzene, 1,1'-(2-methyl-1-propenylidene) bis- | 34.898 | 781-33-9 | 2.437 |
| 1-(4-Methylphenyl)-4-phenylbuta-1,3-diene | 36.410 | 37985-11-8 | 0.807 |
| Benzene, 1,1'-[3-(2-phenylethylidene)-1,5-pentanediyl] bis- | 44.682 | 55334-57-1 | 1.871 |
| Benzene, (1-methylhexadecyl)- | 45.090 | 55125-25-2 | 0.490 |
| p-Terphenyl | 45.435 | 92-94-4 | 0.304 |
| 1-Propene, 3-(2-cyclopentenyl)-2-methyl-1,1-diphenyl- | 46.879 | - | 0.173 |
| 1-Propene, 3-(2-cyclopentenyl)-2-methyl-1,1-diphenyl- | 49.302 | - | 0.732 |
| 1-Propene, 3-(2-cyclopentenyl)-2-methyl-1,1-diphenyl- | 53.449 | - | 1.650 |
| **Polycyclic Aromatic Hydrocarbons (PAH)** | **Σ(%.area)** | | **10.010** |
| Naphthalene | 19.491 | 91-20-3 | 0.580 |
| Naphthalene, 1-methyl- | 22.770 | 90-12-0 | 0.352 |
| Naphthalene, 2-methyl- | 23.259 | 91-57-6 | 0.614 |
| Naphthalene, 1,2,3,4-tetrahydro-1-phenyl- | 34.473 | 3018-20-0 | 0.733 |
| Naphthalene, 1-phenyl- | 36.578 | 605-02-7 | 2.568 |
| Naphthalene, 2-phenyl- | 40.019 | 612-94-2 | 2.376 |
| 1,2,3,4-Tetrahydro-1-phenyl-1,2,3-methanonaphthalene | 40.387 | 138089-69-7 | 0.535 |
| Naphthalene, 2-(phenylmethyl)- | 44.292 | 613-59-2 | 2.252 |
| **Nitrogenated Compounds** | **Σ(%.area)** | | **27.253** |
| Benzyl nitrile | 17.566 | 140-29-4 | 0.296 |

| | | | |
|---|---|---|---|
| Benzeneacetonitrile, α-methyl- | 18.434 | 1823-91-2 | 0.557 |
| Benzenepropanenitrile | 20.642 | 645-59-0 | 0.306 |
| 1,2-Benzenedicarbonitrile | 21.230 | 91-15-6 | 0.357 |
| Cyclopropanecarbonitrile, 2-phenyl-, trans- | 22.408 | 5590-14-7 | 0.316 |
| Benzenebutanenitrile | 23.461 | 2046-18-6 | 13.649 |
| Cyclopropanecarbonitrile, 2-phenyl-, cis | 23.922 | 5590-14-7 | 0.203 |
| Quinoline, 1,2-dihydro-1-methyl-2-methylene- | 24.133 | - | 0.815 |
| 3-Benzyl-4,5-dihydro-3H-pyrrole | 24.347 | - | 2.000 |
| 1,2,3,3a-Tetrahydropentalene, 1,1-dimethyl-3-cyanomethylene- | 24.851 | - | 0.245 |
| Cyclopropanecarbonitrile, 2-phenyl-, trans- | 25.772 | 5590-14-7 | 0.353 |
| 1H-Pyrrole, 1-(4-methylphenyl)- | 26.122 | 827-60-1 | 0.417 |
| Quinoline, 4-ethyl- | 27.451 | 19020-26-9 | 0.487 |
| 1,2,3,3a-Tetrahydropentalene, 1,1-dimethyl-3-cyanomethylene- | 27.611 | | 0.238 |
| Naphthalene, 1-isocyano- | 28.187 | 09/04/1984 | 1.176 |
| Naphthalene, 1-isocyano- | 28.899 | 09/04/1984 | 0.626 |
| 1-Naphthaleneacetonitrile | 32.306 | 132-75-2 | 1.290 |
| N-(2-Phenylethyl)-cis-2,3-epoxynona-6,8-diynamide | 34.585 | 96917-25-8 | 0.398 |
| Octadecanenitrile | 43.043 | 638-65-3 | 0.888 |
| 4-Methyl-3-(O-methylbenzyl)pentanenitrile | 43.877 | 29107-40-2 | 0.760 |
| (1-Benzyl-2-O-tolyl-ethyl)-isonitrile | 44.445 | - | 0.797 |
| Naphthalene-1,3,3-tricarbonitrile, 3,4,4a,5,6,7-hexahdro-2-amino-4-(4-methylphenyl)- | 49.680 | 163978-39-0 | 0.335 |
| Naphthalene-1,3,3-tricarbonitrile, 3,4,4a,5,6,7-hexahdro-2-amino-4-(4-methylphenyl)- | 50.371 | 163978-39-0 | 0.356 |
| Acridine, 9-phenyl- | 51.607 | 602-56-2 | 0.388 |
| **Brominated Compounds** | **Σ(%.area)** | | **0.431** |
| Phenol, 2-bromo- | 15.591 | 95-56-7 | 0.169 |
| 5-Bromo-2-methoxy-1,3-dimethylbenzene | 23.559 | - | 0.262 |
| **Oxygenated Compounds** | **Σ(%.area)** | | **12.023** |
| Phenol | 12.146 | 108-95-2 | 2.776 |
| Phenol, 2-methyl- | 14.630 | 95-48-7 | 0.439 |
| Benzenemethanol, α,α-dimethyl- | 15.904 | 617-94-7 | 0.945 |
| Phenol, 2,5-dimethyl- | 16.580 | 95-87-4 | 0.298 |
| Phenol, 2,4-dimethyl- | 17.684 | 105-67-9 | 0.235 |
| Phenol, 2,4,6-trimethyl- | 18.614 | 527-60-6 | 0.170 |
| p-Cumenol | 20.028 | 99-89-8 | 5.085 |
| Phenol, 2-methyl-5-(1-methylethyl)- | 22.055 | 499-75-2 | 0.251 |
| Phenol, 2-(1-phenylethyl)- | 33.240 | 4237-44-9 | 0.492 |
| 2,3-Dimethyl-1,4,4a,9a-tetrahydroanthracene-9,10-dione | 37.227 | 2670-23-7 | 0.274 |
| As-Indacen-1(2H)-one, 3,6,7,8-tetrahydro-3,3,6,6-tetramethyl- | 45.611 | 55591-18-9 | 0.424 |
| Benzaldehyde, 2-methyl-, (2,4-dinitrophenyl)hydrazone | 50.779 | 1773-44-0 | 0.634 |
| **Non Identified Fraction** | **Σ(%.area)** | | **2.436** |

**Table S18**: Classes of compounds, summation of peak areas, CAS number, and retention times of chemical compounds identified by GC-MS in OLP by catalytic upgrading of plastic waste from computer equipment pyrolysis vapors at 450 °C, 1.0 atm, on a fixed catalyst bed loaded with 2.5%.wt of Si-Al ash pellets, Reaction time=60 min, in semi-pilot scale two-stage reactor of 2.0 L.

| Chemical Compound | RT [min] | CAS | wi[%.area] |
|---|---|---|---|
| **Aromatic Hydrocarbons** | **Σ(%.area)** | | **45.883** |
| Styrene | 9.728 | 100-42-5 | 8.154 |
| Benzene, (1-methylethyl)- | 10.710 | 98-82-8 | 3.780 |
| Benzene, propyl- | 11.688 | 103-65-1 | 0.233 |
| α-Methylstyrene | 12.584 | 98-83-9 | 4.905 |
| Benzene, 1-propenyl- | 14.092 | 637-50-3 | 0.450 |
| Indene | 14.844 | 95-13-6 | 0.571 |
| 2,4-Dimethylstyrene | 16.879 | 2234-20-0 | 0.129 |
| Biphenyl | 25.017 | 92-52-4 | 0.633 |
| Diphenylmethane | 26.329 | 101-81-5 | 0.752 |
| Benzene, 1,1'-ethylidenebis- | 27.764 | 612-00-0 | 0.745 |
| 1,1'-Biphenyl, 2-methyl- | 28.049 | 643-58-3 | 0.216 |
| Bibenzyl | 28.688 | 103-29-7 | 0.473 |
| Benzene, 1,1'-(1,3-propanediyl)bis- | 32.085 | 1081-75-0 | 9.005 |
| Benzene, 1,1'-(3-methyl-1-propene-1,3-diyl) bis- | 32.412 | 7614-93-9 | 1.334 |
| Benzene, 1,1'-(1-methyl-1,3-propanediyl) bis- | 32.600 | 1520-44-1 | 1.415 |
| 1,2-Diphenylcyclopropane | 33.636 | 29881-14-9 | 2.807 |
| Benzene, 1,1'-(1,4-butanediyl) bis- | 34.021 | 1083-56-3 | 0.597 |
| Benzene, 1,1'-(3-methyl-1-propene-1,3-diyl) bis- | 34.386 | 7614-93-9 | 0.890 |
| Benzene, 1,1'-(2-methyl-1-propenylidene) bis- | 34.898 | 781-33-9 | 1.615 |
| 1-(4-Methylphenyl)-4-phenylbuta-1,3-diene | 36.410 | 37985-11-8 | 0.602 |
| 1H-Indene, 2-phenyl- | 36.866 | 4505-48-0 | 0.669 |
| Benzene, 1,1'-[3-(2-phenylethylidene)-1,5-pentanediyl] bis- | 44.682 | 55334-57-1 | 1.930 |
| Benzene, (1-methylhexadecyl)- | 45.090 | 55125-25-2 | 0.558 |
| p-Terphenyl | 45.435 | 92-94-4 | 0.475 |
| 1-Propene, 3-(2-cyclopentenyl)-2-methyl-1,1-diphenyl- | 46.879 | - | 0.316 |
| 1-Propene, 3-(2-cyclopentenyl)-2-methyl-1,1-diphenyl- | 49.302 | - | 0.551 |
| 1-Propene, 3-(2-cyclopentenyl)-2-methyl-1,1-diphenyl- | 53.449 | - | 0.991 |
| 1,1':3',1"-Terphenyl, 5'-phenyl- | 68.104 | 612-71-5 | 1.087 |
| **Polycyclic Aromatic Hydrocarbons (PAH)** | **Σ(%.area)** | | **18.410** |
| Naphthalene | 19.491 | 91-20-3 | 1.730 |
| Naphthalene, 1-methyl- | 22.770 | 90-12-0 | 0.848 |
| Naphthalene, 2-methyl- | 23.259 | 91-57-6 | 1.048 |
| Naphthalene, 1-ethyl- | 25.474 | 1127-76-0 | 0.270 |
| Naphthalene, 1,8-dimethyl- | 27.180 | 569-41-5 | 0.237 |
| Naphthalene, 1-isocyano- | 28.899 | 09/04/1984 | 1.032 |
| Fluorene | 30.718 | 86-73-7 | 0.476 |

| | | | |
|---|---|---|---|
| Naphthalene, 1,2,3,4-tetrahydro-1-phenyl- | 34.473 | 3018-20-0 | 0.813 |
| Anthracene | 35.143 | 120-12-7 | 1.307 |
| Naphthalene, 1-phenyl- | 36.578 | 605-02-7 | 2.860 |
| Naphthalene, 2-phenyl- | 40.019 | 612-94-2 | 4.129 |
| 1,2,3,4-Tetrahydro-1-phenyl-1,2,3-methanonaphthalene | 40.387 | 138089-69-7 | 0.687 |
| Naphthalene, 2-(phenylmethyl)- | 44.292 | 613-59-2 | 2.973 |
| **Nitrogenated Compounds** | **Σ(%.area)** | | **21.540** |
| Benzonitrile | 12.685 | 100-47-0 | 0.217 |
| Benzyl nitrile | 17.566 | 140-29-4 | 0.402 |
| Benzeneacetonitrile, α-methyl- | 18.434 | 1823-91-2 | 0.661 |
| Benzenepropanenitrile | 20.642 | 645-59-0 | 0.252 |
| 1,2-Benzenedicarbonitrile | 21.230 | 91-15-6 | 0.408 |
| Cyclopropanecarbonitrile, 2-phenyl-, trans- | 22.408 | 5590-14-7 | 0.334 |
| Benzenebutanenitrile | 23.461 | 2046-18-6 | 9.121 |
| Cyclopropanecarbonitrile, 2-phenyl-, cis | 23.922 | 5590-14-7 | 0.165 |
| Quinoline, 1,2-dihydro-1-methyl-2-methylene- | 24.133 | - | 0.652 |
| 3-Benzyl-4,5-dihydro-3H-pyrrole | 24.347 | - | 1.435 |
| 1,2,3,3a-Tetrahydropentalene, 1,1-dimethyl-3-cyanomethylene- | 24.851 | - | 0.163 |
| Cyclopropanecarbonitrile, 2-phenyl-, trans- | 25.772 | 5590-14-7 | 0.394 |
| 1H-Pyrrole, 1-(4-methylphenyl)- | 26.122 | 827-60-1 | 0.281 |
| Quinoline, 4-ethyl- | 27.451 | 19020-26-9 | 0.346 |
| Naphthalene, 1-isocyano- | 28.187 | 09/04/1984 | 1.412 |
| 1-Naphthaleneacetonitrile | 32.306 | 132-75-2 | 1.447 |
| N-(2-Phenylethyl)-cis-2,3-epoxynona-6,8-diynamide | 34.585 | 96917-25-8 | 0.384 |
| Octadecanenitrile | 43.043 | 638-65-3 | 0.664 |
| 4-Methyl-3-(O-methylbenzyl)pentanenitrile | 43.877 | 29107-40-2 | 0.674 |
| (1-Benzyl-2-O-tolyl-ethyl)-isonitrile | 44.445 | - | 0.853 |
| Naphthalene-1,3,3-tricarbonitrile, 3,4,4a,5,6,7-hexahdro-2-amino-4-(4-methylphenyl)- | 49.680 | 163978-39-0 | 0.309 |
| Naphthalene-1,3,3-tricarbonitrile, 3,4,4a,5,6,7-hexahdro-2-amino-4-(4-methylphenyl)- | 50.371 | 163978-39-0 | 0.361 |
| Acridine, 9-phenyl- | 51.607 | 602-56-2 | 0.605 |
| **Brominated Compounds** | **Σ(%.area)** | | **0.141** |
| Phenol, 2-bromo- | 15.591 | 95-56-7 | 0.089 |
| 5-Bromo-2-methoxy-1,3-dimethylbenzene | 23.559 | - | 0.052 |
| **Oxygenated Compounds** | **Σ(%.area)** | | **11.405** |
| Phenol | 12.146 | 108-95-2 | 2.834 |
| Phenol, 2-methyl- | 14.630 | 95-48-7 | 0.459 |
| p-Cresol | 15.269 | 106-44-5 | 0.273 |
| Benzenemethanol, α,α-dimethyl- | 15.904 | 617-94-7 | 1.186 |
| Phenol, 2,5-dimethyl- | 16.580 | 95-87-4 | 0.341 |
| Phenol, 2,4-dimethyl- | 17.684 | 105-67-9 | 0.261 |
| Phenol, 2,4,6-trimethyl- | 19.614 | 527-60-6 | 0.188 |
| p-Cumenol | 20.028 | 99-89-8 | 3.755 |

| | | | |
|---|---|---|---|
| Phenol, 2-methyl-5-(1-methylethyl)- | 22.055 | 499-75-2 | 0.257 |
| Phenol, 2-(1-phenylethyl)- | 33.240 | 4237-44-9 | 1.177 |
| Benzaldehyde, 2-methyl-, (2,4-dinitrophenyl)hydrazone | 50.779 | 1773-44-0 | 0.674 |
| **Non Identified Fraction** | **Σ(%.area)** | | **2.620** |

**Table S19**: Classes of compounds, summation of peak areas, CAS number, and retention times of chemical compounds identified by GC-MS in OLP by catalytic upgrading of plastic waste from computer equipment pyrolysis vapors at 450 °C, 1.0 atm, on a fixed catalyst bed loaded with 5.0%.wt of Si-Al ash pellets, Reaction time=15 min, in semi-pilot scale two-stage reactor of 2.0 L.

| Chemical Compound | RT [min] | CAS | wi[%.area] |
|---|---|---|---|
| **Aromatic Hydrocarbons** | **Σ(%.area)** | | **47.465** |
| Styrene | 9.728 | 100-42-5 | 8.932 |
| Benzene, (1-methylethyl)- | 10.710 | 98-82-8 | 4.078 |
| Benzene, propyl- | 11.688 | 103-65-1 | 0.225 |
| α-Methylstyrene | 12.584 | 98-83-9 | 7.309 |
| Benzene, 1-propenyl- | 14.092 | 637-50-3 | 0.563 |
| Indene | 14.844 | 95-13-6 | 0.388 |
| Biphenyl | 25.017 | 92-52-4 | 0.617 |
| Diphenylmethane | 26.329 | 101-81-5 | 0.666 |
| Benzene, 1,1'-ethylidenebis- | 27.764 | 612-00-0 | 0.669 |
| 1,1'-Biphenyl, 2-methyl- | 28.049 | 643-58-3 | 0.186 |
| Bibenzyl | 28.688 | 103-29-7 | 0.396 |
| Benzene, 1,1'-(1,3-propanediyl) bis- | 32.085 | 1081-75-0 | 9.263 |
| Benzene, 1,1'-(3-methyl-1-propene-1,3-diyl) bis- | 32.412 | 7614-93-9 | 1.070 |
| Benzene, 1,1'-(1-methyl-1,3-propanediyl) bis- | 32.600 | 1520-44-1 | 1.310 |
| 1,2-Diphenylcyclopropane | 33.636 | 29881-14-9 | 2.060 |
| Benzene, 1,1'-(1,4-butanediyl) bis- | 34.021 | 1083-56-3 | 0.472 |
| Benzene, 1,1'-(3-methyl-1-propene-1,3-diyl) bis- | 34.386 | 7614-93-9 | 0.738 |
| Benzene, 1,1'-(2-methyl-1-propenylidene) bis- | 34.898 | 781-33-9 | 1.467 |
| 1-(4-Methylphenyl)-4-phenylbuta-1,3-diene | 36.410 | 37985-11-8 | 0.441 |
| 1H-Indene, 2-phenyl- | 36.866 | 4505-48-0 | 0.916 |
| Benzene, (1-methylhexadecyl)- | 43.882 | 55125-25-2 | 0.607 |
| Benzene, 1,1'-[3-(2-phenylethylidene)-1,5-pentanediyl] bis- | 44.682 | 55334-57-1 | 1.619 |
| p-Terphenyl | 45.435 | 92-94-4 | 0.599 |
| 1-Propene, 3-(2-cyclopentenyl)-2-methyl-1,1-diphenyl- | 49.302 | - | 0.513 |
| 1-Propene, 3-(2-cyclopentenyl)-2-methyl-1,1-diphenyl- | 53.449 | - | 1.143 |
| 1,1':3',1"-Terphenyl, 5'-phenyl- | 68.116 | 612-71-5 | 1.218 |
| **Polycyclic Aromatic Hydrocarbons (PAH)** | **Σ(%.area)** | | **18.127** |
| 1,2,3,4,5,8-Hexahydronaphthalene | 15.001 | 36231-13-7 | 0.180 |
| Naphthalene | 19.491 | 91-20-3 | 1.403 |
| Naphthalene, 1-methyl- | 22.770 | 90-12-0 | 0.658 |
| Naphthalene, 2-methyl- | 23.259 | 91-57-6 | 0.841 |
| Naphthalene, 1-ethyl- | 25.474 | 1127-76-0 | 0.145 |
| Naphthalene, 1,8-dimethyl- | 27.180 | 569-41-5 | 0.136 |
| Fluorene | 30.718 | 86-73-7 | 0.489 |
| Naphthalene, 1,2,3,4-tetrahydro-1-phenyl- | 34.473 | 3018-20-0 | 0.743 |
| Anthracene | 35.143 | 120-12-7 | 1.524 |

| | | | |
|---|---|---|---|
| Naphthalene, 1-phenyl- | 36.578 | 605-02-7 | 2.985 |
| Phenanthrene, 1-methyl- | 38.620 | 832-69-9 | 0.596 |
| Naphthalene, 2-phenyl- | 40.019 | 612-94-2 | 4.577 |
| 1,2,3,4-Tetrahydro-1-phenyl-1,2,3-methanonaphthalene | 40.387 | 138089-69-7 | 0.697 |
| Naphthalene, 2-(phenylmethyl)- | 44.292 | 613-59-2 | 3.153 |
| **Nitrogenated Compounds** | **Σ(%.area)** | | **20.083** |
| Benzonitrile | 12.685 | 100-47-0 | 0.186 |
| Benzyl nitrile | 17.566 | 140-29-4 | 0.427 |
| Benzeneacetonitrile, α-methyl- | 18.434 | 1823-91-2 | 0.581 |
| Benzenepropanenitrile | 20.642 | 645-59-0 | 0.231 |
| 1,2-Benzenedicarbonitrile | 21.230 | 91-15-6 | 0.409 |
| Cyclopropanecarbonitrile, 2-phenyl-, trans- | 22.408 | 5590-14-7 | 0.331 |
| Benzenebutanenitrile | 23.461 | 2046-18-6 | 9.085 |
| Cyclopropanecarbonitrile, 2-phenyl-, cis | 23.922 | 5590-14-7 | 0.152 |
| Quinoline, 1,2-dihydro-1-methyl-2-methylene- | 24.133 | - | 0.554 |
| 3-Benzyl-4,5-dihydro-3H-pyrrole | 24.347 | - | 1.267 |
| 1,2,3,3a-Tetrahydropentalene, 1,1-dimethyl-3-cyanomethylene- | 24.851 | - | 0.144 |
| Cyclopropanecarbonitrile, 2-phenyl-, trans- | 25.772 | 5590-14-7 | 0.243 |
| 1H-Pyrrole, 1-(4-methylphenyl)- | 26.122 | 827-60-1 | 0.246 |
| Quinoline, 4-ethyl- | 27.451 | 19020-26-9 | 0.276 |
| Naphthalene, 1-isocyano- | 28.187 | 09/04/1984 | 1.398 |
| Naphthalene, 1-isocyano- | 28.899 | 09/04/1984 | 1.161 |
| 1-Naphthaleneacetonitrile | 32.306 | 132-75-2 | 1.351 |
| Octadecanenitrile | 43.052 | 638-65-3 | 0.541 |
| (1-Benzyl-2-O-tolyl-ethyl)-isonitrile | 44.445 | - | 0.792 |
| Acridine, 9-phenyl- | 51.605 | 602-56-2 | 0.708 |
| **Brominated Compounds** | **Σ(%.area)** | | **0.664** |
| Phenol, 2-bromo- | 15.591 | 95-56-7 | 0.351 |
| 5-Bromo-2-methoxy-1,3-dimethylbenzene | 23.559 | - | 0.313 |
| **Oxygenated Compounds** | **Σ(%.area)** | | **11.500** |
| Phenol | 12.146 | 108-95-2 | 3.767 |
| Phenol, 2-methyl- | 14.630 | 95-48-7 | 0.610 |
| p-Cresol | 15.269 | 106-44-5 | 0.366 |
| Benzenemethanol, α,α-dimethyl- | 15.909 | 617-94-7 | 0.220 |
| Phenol, 2,5-dimethyl- | 16.580 | 95-87-4 | 0.388 |
| Phenol, 2,4-dimethyl- | 17.684 | 105-67-9 | 0.295 |
| Phenol, 2,4,6-trimethyl- | 19.614 | 527-60-6 | 0.200 |
| p-Cumenol | 20.028 | 99-89-8 | 4.004 |
| Phenol, 2-(1-phenylethyl)- | 33.240 | 4237-44-9 | 1.024 |
| Benzaldehyde, 2-methyl-, (2,4-dinitrophenyl)hydrazone | 50.779 | 1773-44-0 | 0.626 |
| **Non Identified Fraction** | **Σ(%.area)** | | **2.161** |

**Table S20**: Classes of compounds, summation of peak areas, CAS number, and retention times of chemical compounds identified by GC-MS in OLP by catalytic upgrading of plastic waste from computer equipment pyrolysis vapors at 450 °C, 1.0 atm, on a fixed catalyst bed loaded with 5.0%.wt of Si-Al ash pellets, Reaction time=30 min, in semi-pilot scale two-stage reactor of 2.0 L.

| Chemical Compound | RT [min] | CAS | wi[%.area] |
|---|---|---|---|
| **Aromatic Hydrocarbons** | **Σ(%.area)** | | **58.465** |
| Styrene | 9.728 | 100-42-5 | 18.688 |
| Benzene, (1-methylethyl)- | 10.710 | 98-82-8 | 8.985 |
| Benzene, propyl- | 11.688 | 103-65-1 | 0.502 |
| α-Methylstyrene | 12.584 | 98-83-9 | 11.920 |
| Benzene, 1-propenyl- | 14.092 | 637-50-3 | 0.888 |
| Indene | 14.844 | 95-13-6 | 0.334 |
| Biphenyl | 25.017 | 92-52-4 | 0.296 |
| Diphenylmethane | 26.329 | 101-81-5 | 0.553 |
| Benzene, 1,1'-ethylidenebis- | 27.764 | 612-00-0 | 0.450 |
| Bibenzyl | 28.688 | 103-29-7 | 0.343 |
| Benzene, 1,1'-(1,3-propanediyl) bis- | 32.085 | 1081-75-0 | 9.166 |
| Benzene, 1,1'-(3-methyl-1-propene-1,3-diyl) bis- | 32.412 | 7614-93-9 | 1.009 |
| Benzene, 1,1'-(1-methyl-1,3-propanediyl) bis- | 32.600 | 1520-44-1 | 1.224 |
| 1,2-Diphenylcyclopropane | 33.636 | 29881-14-9 | 1.390 |
| Benzene, 1,1'-(1,4-butanediyl) bis- | 34.021 | 1083-56-3 | 0.371 |
| Benzene, 1,1'-(3-methyl-1-propene-1,3-diyl) bis- | 34.386 | 7614-93-9 | 0.511 |
| Benzene, 1,1'-(2-methyl-1-propenylidene) bis- | 34.898 | 781-33-9 | 0.990 |
| 1-(4-Methylphenyl)-4-phenylbuta-1,3-diene | 36.410 | 37985-11-8 | 0.173 |
| 1H-Indene, 2-phenyl- | 36.866 | 4505-48-0 | 0.184 |
| Benzene, 1,1'-[3-(2-phenylethylidene)-1,5-pentanediyl]bis- | 44.682 | 55334-57-1 | 0.488 |
| **Polycyclic Aromatic Hydrocarbons (PAH)** | **Σ(%.area)** | | **7.207** |
| 1,2,3,4,5,8-Hexahydronaphthalene | 15.001 | 36231-13-7 | 0.279 |
| Naphthalene | 19.491 | 91-20-3 | 0.861 |
| Naphthalene, 1-methyl- | 22.770 | 90-12-0 | 0.371 |
| Naphthalene, 2-methyl- | 23.259 | 91-57-6 | 0.592 |
| Naphthalene, 1,2,3,4-tetrahydro-1-phenyl- | 34.473 | 3018-20-0 | 0.368 |
| Anthracene | 35.143 | 120-12-7 | 0.475 |
| Naphthalene, 1-phenyl- | 36.578 | 605-02-7 | 1.313 |
| Naphthalene, 2-phenyl- | 40.019 | 612-94-2 | 1.629 |
| 1,2,3,4-Tetrahydro-1-phenyl-1,2,3-methanonaphthalene | 40.387 | 138089-69-7 | 0.241 |
| Naphthalene, 2-(phenylmethyl)- | 44.292 | 613-59-2 | 1.078 |
| **Nitrogenated Compounds** | **Σ(%.area)** | | **18.675** |
| Benzyl nitrile | 17.566 | 140-29-4 | 0.430 |
| Benzeneacetonitrile, α-methyl- | 18.434 | 1823-91-2 | 0.735 |
| Benzenepropanenitrile | 20.642 | 645-59-0 | 0.309 |
| 1,2-Benzenedicarbonitrile | 21.230 | 91-15-6 | 0.318 |

| | | | |
|---|---|---|---|
| Cyclopropanecarbonitrile, 2-phenyl-, trans- | 22.408 | 5590-14-7 | 0.294 |
| Benzenebutanenitrile | 23.461 | 2046-18-6 | 11.626 |
| Cyclopropanecarbonitrile, 2-phenyl-, cis | 23.922 | 5590-14-7 | 0.192 |
| Quinoline, 1,2-dihydro-1-methyl-2-methylene- | 24.133 | | 0.613 |
| 3-Benzyl-4,5-dihydro-3H-pyrrole | 24.347 | - | 1.486 |
| 1,2,3,3a-Tetrahydropentalene, 1,1-dimethyl-3-cyanomethylene- | 24.851 | - | 0.224 |
| 1H-Pyrrole, 1-(4-methylphenyl)- | 26.122 | 827-60-1 | 0.265 |
| Quinoline, 4-ethyl- | 27.451 | 19020-26-9 | 0.196 |
| Naphthalene, 1-isocyano- | 28.187 | 09/04/1984 | 0.800 |
| Naphthalene, 1-isocyano- | 28.899 | 09/04/1984 | 0.505 |
| 1-Naphthaleneacetonitrile | 32.306 | 132-75-2 | 0.682 |
| **Brominated Compounds** | **Σ(%.area)** | | **0.776** |
| Phenol, 2-bromo- | 15.591 | 95-56-7 | 0.388 |
| 5-Bromo-2-methoxy-1,3-dimethylbenzene | 23.559 | - | 0.388 |
| **Oxygenated Compounds** | **Σ(%.area)** | | **13.429** |
| Phenol | 12.146 | 108-95-2 | 4.719 |
| Phenol, 2-methyl- | 14.630 | 95-48-7 | 0.742 |
| p-Cresol | 15.269 | 106-44-5 | 0.362 |
| Phenol, 2,5-dimethyl- | 16.580 | 95-87-4 | 0.466 |
| Phenol, 2,4-dimethyl- | 17.684 | 105-67-9 | 0.364 |
| Phenol, 2,4,6-trimethyl- | 19.614 | 527-60-6 | 0.242 |
| p-Cumenol | 20.028 | 99-89-8 | 6.237 |
| Phenol, 2-(1-phenylethyl)- | 33.240 | 4237-44-9 | 0.297 |
| **Non Identified Fraction** | **Σ(%.area)** | | **1.450** |

**Table S21**: Classes of compounds, summation of peak areas, CAS number, and retention times of chemical compounds identified by GC-MS in OLP by catalytic upgrading of plastic waste from computer equipment pyrolysis vapors at 450 °C, 1.0 atm, on a fixed catalyst bed loaded with 5.0%.wt of Si-Al ash pellets, Reaction time=45 min, in semi-pilot scale two-stage reactor of 2.0 L.

| Chemical Compound | RT [min] | CAS | wi[%.area] |
|---|---|---|---|
| **Aromatic Hydrocarbons** | **Σ(%.area)** | | **46.881** |
| Styrene | 9.728 | 100-42-5 | 6.593 |
| Benzene, (1-methylethyl)- | 10.710 | 98-82-8 | 3.696 |
| Benzene, propyl- | 11.688 | 103-65-1 | 0.232 |
| α-Methylstyrene | 12.584 | 98-83-9 | 4.729 |
| Benzene, 1-propenyl- | 14.092 | 637-50-3 | 0.489 |
| Indene | 14.844 | 95-13-6 | 0.228 |
| Biphenyl | 25.017 | 92-52-4 | 0.333 |
| Diphenylmethane | 26.329 | 101-81-5 | 0.678 |
| Benzene, 1,1'-ethylidenebis- | 27.764 | 612-00-0 | 0.605 |
| Bibenzyl | 28.688 | 103-29-7 | 0.589 |
| Benzene, 1,1'-(1,3-propanediyl)bis- | 32.085 | 1081-75-0 | 13.455 |
| Benzene, 1,1'-(3-methyl-1-propene-1,3-diyl) bis- | 32.412 | 7614-93-9 | 1.605 |
| Benzene, 1,1'-(1-methyl-1,3-propanediyl)bis- | 32.600 | 1520-44-1 | 2.275 |
| 1,2-Diphenylcyclopropane | 33.636 | 29881-14-9 | 2.809 |
| Benzene, 1,1'-(1,4-butanediyl)bis- | 34.021 | 1083-56-3 | 0.763 |
| Benzene, 1,1'-(3-methyl-1-propene-1,3-diyl) bis- | 34.386 | 7614-93-9 | 1.051 |
| Benzene, 1,1'-(2-methyl-1-propenylidene) bis- | 34.898 | 781-33-9 | 1.965 |
| 1-(4-Methylphenyl)-4-phenylbuta-1,3-diene | 36.410 | 37985-11-8 | 0.605 |
| 1H-Indene, 2-phenyl- | 36.866 | 4505-48-0 | 0.234 |
| 3-Methyl-1-phenyl-1H-indene | 37.559 | 22360-63-0 | 0.369 |
| Benzene, 1,1'-[3-(2-phenylethylidene)-1,5-pentanediyl] bis- | 44.682 | 55334-57-1 | 1.541 |
| Benzene, (1-methylhexadecyl)- | 45.088 | 55125-25-2 | 0.517 |
| p-Terphenyl | 45.435 | 92-94-4 | 0.373 |
| 1,1':4',1"-Terphenyl-, 3'-methyl- | 47.282 | 33776-38-4 | 0.378 |
| 1-Propene, 3-(2-cyclopentenyl)-2-methyl-1,1-diphenyl- | 49.300 | - | 0.283 |
| 1-Propene, 3-(2-cyclopentenyl)-2-methyl-1,1-diphenyl- | 53.446 | - | 0.486 |
| **Polycyclic Aromatic Hydrocarbons (PAH)** | **Σ(%.area)** | | **11.870** |
| Naphthalene | 19.491 | 91-20-3 | 0.805 |
| Naphthalene, 1-methyl- | 22.770 | 90-12-0 | 0.429 |
| Naphthalene, 2-methyl- | 23.259 | 91-57-6 | 0.638 |
| Naphthalene, 1,2,3,4-tetrahydro-1-phenyl- | 34.473 | 3018-20-0 | 0.719 |
| Anthracene | 35.143 | 120-12-7 | 0.620 |
| Naphthalene, 1-phenyl- | 36.578 | 605-02-7 | 2.632 |
| Naphthalene, 2-phenyl- | 40.019 | 612-94-2 | 2.993 |
| 1,2,3,4-Tetrahydro-1-phenyl-1,2,3-methanonaphthalene | 40.387 | 138089-69-7 | 0.594 |
| Naphthalene, 2-(phenylmethyl)- | 44.292 | 613-59-2 | 2.440 |

| **Nitrogenated Compounds** | **Σ(%.area)** | | **25.719** |
|---|---|---|---|
| Benzyl nitrile | 17.566 | 140-29-4 | 0.359 |
| Benzeneacetonitrile, α-methyl- | 18.434 | 1823-91-2 | 0.610 |
| Benzenepropanenitrile | 20.642 | 645-59-0 | 0.338 |
| 1,2-Benzenedicarbonitrile | 21.230 | 91-15-6 | 0.442 |
| Cyclopropanecarbonitrile, 2-phenyl-, trans- | 22.408 | 5590-14-7 | 0.356 |
| Benzenebutanenitrile | 23.461 | 2046-18-6 | 13.133 |
| Cyclopropanecarbonitrile, 2-phenyl-, cis | 23.922 | 5590-14-7 | 0.241 |
| Quinoline, 1,2-dihydro-1-methyl-2-methylene- | 24.133 | - | 0.876 |
| 3-Benzyl-4,5-dihydro-3H-pyrrole | 24.347 | - | 2.019 |
| 1,2,3,3a-Tetrahydropentalene, 1,1-dimethyl-3-cyanomethylene- | 24.851 | - | 0.223 |
| Cyclopropanecarbonitrile, 2-phenyl-, trans- | 25.766 | 5590-14-7 | 0.353 |
| 1H-Pyrrole, 1-(4-methylphenyl)- | 26.122 | 827-60-1 | 0.409 |
| Quinoline, 4-ethyl- | 27.451 | 19020-26-9 | 0.383 |
| Naphthalene, 1-isocyano- | 28.187 | 09/04/1984 | 1.298 |
| Naphthalene, 1-isocyano- | 28.899 | 09/04/1984 | 0.909 |
| 1-Naphthaleneacetonitrile | 32.306 | 132-75-2 | 1.391 |
| Octadecanenitrile | 43.046 | 638-65-3 | 0.653 |
| (1-Benzyl-2-O-tolyl-ethyl)-isonitrile | 44.488 | - | 0.617 |
| Naphthalene-1,3,3-tricarbonitrile, 3,4,4a,5,6,7-hexahdro-2-amino-4-(4-methylphenyl)- | 49.679 | 163978-39-0 | 0.375 |
| Naphthalene-1,3,3-tricarbonitrile, 3,4,4a,5,6,7-hexahdro-2-amino-4-(4-methylphenyl)- | 50.372 | 163978-39-0 | 0.390 |
| Acridine, 9-phenyl- | 51.605 | 602-56-2 | 0.344 |
| **Brominated Compounds** | **Σ(%.area)** | | **0.246** |
| Phenol, 2-bromo- | 15.591 | 95-56-7 | 0.137 |
| 5-Bromo-2-methoxy-1,3-dimethylbenzene | 23.559 | - | 0.109 |
| **Oxygenated Compounds** | **Σ(%.area)** | | **13.074** |
| Phenol | 12.146 | 108-95-2 | 3.171 |
| Phenol, 2-methyl- | 14.630 | 95-48-7 | 0.527 |
| p-Cresol | 15.269 | 106-44-5 | 0.225 |
| Benzenemethanol, α,α-dimethyl- | 15.905 | 617-94-7 | 1.216 |
| Phenol, 2,5-dimethyl- | 16.580 | 95-87-4 | 0.361 |
| Phenol, 2,4-dimethyl- | 17.684 | 105-67-9 | 0.284 |
| Phenol, 2,4,6-trimethyl- | 19.614 | 527-60-6 | 0.230 |
| p-Cumenol | 20.028 | 99-89-8 | 5.620 |
| Phenol, 2-methyl-5-(1-methylethyl)- | 22.055 | 499-75-2 | 0.250 |
| Phenol, 2-(1-phenylethyl)- | 33.240 | 4237-44-9 | 0.617 |
| Benzaldehyde, 2-methyl-, (2,4-dinitrophenyl)hydrazone | 50.779 | 1773-44-0 | 0.573 |
| **Non Identified Fraction** | **Σ(%.area)** | | **2.211** |

**Table S22**: Classes of compounds, summation of peak areas, CAS number, and retention times of chemical compounds identified by GC-MS in OLP by catalytic upgrading of plastic waste from computer equipment pyrolysis vapors at 450 °C, 1.0 atm, on a fixed catalyst bed loaded with 5.0%.wt of Si-Al ash pellets, Reaction time=60 min, in semi-pilot scale two-stage reactor of 2.0 L.

| Chemical Compound | RT [min] | CAS | wi[%.area] |
|---|---|---|---|
| **Aromatic Hydrocarbons** | **Σ(%.area)** | | **44.566** |
| Styrene | 9.728 | 100-42-5 | 6.443 |
| Benzene, (1-methylethyl)- | 10.710 | 98-82-8 | 3.346 |
| Benzene, propyl- | 11.688 | 103-65-1 | 0.221 |
| α-Methylstyrene | 12.584 | 98-83-9 | 4.982 |
| Benzene, 1-propenyl- | 14.092 | 637-50-3 | 0.487 |
| Indene | 14.844 | 95-13-6 | 0.514 |
| Biphenyl | 25.017 | 92-52-4 | 0.539 |
| Diphenylmethane | 26.329 | 101-81-5 | 0.716 |
| Benzene, 1,1'-ethylidenebis- | 27.764 | 612-00-0 | 0.728 |
| 1,1'-Biphenyl, 2-methyl- | 28.047 | 643-58-3 | 0.167 |
| Bibenzyl | 28.688 | 103-29-7 | 0.499 |
| Benzene, 1,1'-(1,3-propanediyl) bis- | 32.085 | 1081-75-0 | 8.736 |
| Benzene, 1,1'-(3-methyl-1-propene-1,3-diyl) bis- | 32.412 | 7614-93-9 | 1.103 |
| Benzene, 1,1'-(1-methyl-1,3-propanediyl) bis- | 32.600 | 1520-44-1 | 1.516 |
| 1,2-Diphenylcyclopropane | 33.636 | 29881-14-9 | 2.628 |
| Benzene, 1,1'-(1,4-butanediyl) bis- | 34.021 | 1083-56-3 | 0.596 |
| Benzene, 1,1'-(3-methyl-1-propene-1,3-diyl) bis- | 34.386 | 7614-93-9 | 0.754 |
| Benzene, 1,1'-(2-methyl-1-propenylidene) bis- | 34.898 | 781-33-9 | 1.508 |
| 1-(4-Methylphenyl)-4-phenylbuta-1,3-diene | 36.410 | 37985-11-8 | 0.602 |
| 1H-Indene, 2-phenyl- | 36.866 | 4505-48-0 | 0.600 |
| 3-Methyl-1-phenyl-1H-indene | 37.559 | 22360-63-0 | 0.547 |
| Benzene, 1,1'-[3-(2-phenylethylidene)-1,5-pentanediyl] bis- | 44.682 | 55334-57-1 | 2.303 |
| Benzene, (1-methylhexadecyl)- | 45.088 | 55125-25-2 | 0.764 |
| p-Terphenyl | 45.435 | 92-94-4 | 0.632 |
| 1,1':4',1"-Terphenyl-, 3'-methyl- | 47.282 | 33776-38-4 | 0.540 |
| 1-Propene, 3-(2-cyclopentenyl)-2-methyl-1,1-diphenyl- | 49.300 | - | 0.240 |
| 1-Propene, 3-(2-cyclopentenyl)-2-methyl-1,1-diphenyl- | 53.446 | - | 0.496 |
| 1,1':2',1"-Terphenyl, 4'-phenyl- | 57.602 | 1165-53-3 | 0.398 |
| 1,1':3',1"-Terphenyl, 5'-phenyl- | 68.104 | 612-71-5 | 1.961 |
| **Polycyclic Aromatic Hydrocarbons (PAH)** | **Σ(%.area)** | | **17.485** |
| Naphthalene | 19.491 | 91-20-3 | 1.389 |
| Naphthalene, 1-methyl- | 22.770 | 90-12-0 | 0.594 |
| Naphthalene, 2-methyl- | 23.259 | 91-57-6 | 0.954 |
| Naphthalene, 1,2,3,4-tetrahydro-1-phenyl- | 34.473 | 3018-20-0 | 0.881 |
| Anthracene | 35.143 | 120-12-7 | 0.974 |
| Naphthalene, 1-phenyl- | 36.578 | 605-02-7 | 3.175 |

| | | | |
|---|---|---|---|
| Naphthalene, 2-phenyl- | 40.019 | 612-94-2 | 4.835 |
| 1,2,3,4-Tetrahydro-1-phenyl-1,2,3-methanonaphthalene | 40.387 | 138089-69-7 | 0.823 |
| Naphthalene, 2-(phenylmethyl)- | 44.292 | 613-59-2 | 3.860 |
| **Nitrogenated Compounds** | **Σ(%.area)** | | **22.946** |
| Benzonitrile | 12.685 | 100-47-0 | 0.203 |
| Benzyl nitrile | 17.566 | 140-29-4 | 0.449 |
| Benzeneacetonitrile, α-methyl- | 18.434 | 1823-91-2 | 0.640 |
| Benzenepropanenitrile | 20.642 | 645-59-0 | 0.306 |
| 1,2-Benzenedicarbonitrile | 21.230 | 91-15-6 | 0.540 |
| Cyclopropanecarbonitrile, 2-phenyl-, trans- | 22.408 | 5590-14-7 | 0.331 |
| Benzenebutanenitrile | 23.461 | 2046-18-6 | 8.627 |
| Cyclopropanecarbonitrile, 2-phenyl-, cis | 23.922 | 5590-14-7 | 0.188 |
| Quinoline, 1,2-dihydro-1-methyl-2-methylene- | 24.133 | - | 0.685 |
| 3-Benzyl-4,5-dihydro-3H-pyrrole | 24.347 | - | 1.430 |
| 1,2,3,3a-Tetrahydropentalene, 1,1-dimethyl-3-cyanomethylene- | 24.851 | - | 0.104 |
| Cyclopropanecarbonitrile, 2-phenyl-, trans- | 25.766 | 5590-14-7 | 0.311 |
| 1H-Pyrrole, 1-(4-methylphenyl)- | 26.122 | 827-60-1 | 0.270 |
| Quinoline, 4-ethyl- | 27.451 | 19020-26-9 | 0.278 |
| Naphthalene, 1-isocyano- | 28.187 | 09/04/1984 | 1.601 |
| Naphthalene, 1-isocyano- | 28.899 | 09/04/1984 | 1.418 |
| 1-Naphthaleneacetonitrile | 32.306 | 132-75-2 | 1.696 |
| Octadecanenitrile | 43.046 | 638-65-3 | 0.618 |
| (1-Benzyl-2-O-tolyl-ethyl)-isonitrile | 44.488 | - | 1.017 |
| Naphthalene-1,3,3-tricarbonitrile, 3,4,4a,5,6,7-hexahdro-2-amino-4-(4-methylphenyl)- | 49.679 | 163978-39-0 | 0.585 |
| Naphthalene-1,3,3-tricarbonitrile, 3,4,4a,5,6,7-hexahdro-2-amino-4-(4-methylphenyl)- | 50.372 | 163978-39-0 | 0.627 |
| Acridine, 9-phenyl- | 51.605 | 602-56-2 | 1.022 |
| **Brominated Compounds** | **Σ(%.area)** | | **0.023** |
| 5-Bromo-2-methoxy-1,3-dimethylbenzene | 23.559 | - | 0.023 |
| **Oxygenated Compounds** | **Σ(%.area)** | | **11.145** |
| Phenol | 12.146 | 108-95-2 | 3.351 |
| Phenol, 2-methyl- | 14.630 | 95-48-7 | 0.595 |
| p-Cresol | 15.269 | 106-44-5 | 0.323 |
| Benzenemethanol, α,α-dimethyl- | 15.905 | 617-94-7 | 0.366 |
| Phenol, 2,5-dimethyl- | 16.580 | 95-87-4 | 0.416 |
| Phenol, 2,4-dimethyl- | 17.684 | 105-67-9 | 0.334 |
| Phenol, 2,4,6-trimethyl- | 19.614 | 527-60-6 | 0.216 |
| p-Cumenol | 20.028 | 99-89-8 | 3.516 |
| Phenol, 2-methyl-5-(1-methylethyl)- | 22.055 | 499-75-2 | 0.235 |
| Phenol, 2-(1-phenylethyl)- | 33.240 | 4237-44-9 | 0.506 |
| Benzaldehyde, 2-methyl-, (2,4-dinitrophenyl)hydrazone | 50.779 | 1773-44-0 | 1.287 |
| **Non Identified Fraction** | **Σ(%.area)** | | **3.838** |

**Table S23**: Classes of compounds, summation of peak areas, CAS number, and retention times of chemical compounds identified by GC-MS in OLP by catalytic upgrading of plastic waste from computer equipment pyrolysis vapors at 450 °C, 1.0 atm, on a fixed catalyst bed loaded with 7.5%.wt of Si-Al ash pellets, Reaction time=15 min, in semi-pilot scale two-stage reactor of 2.0 L.

| Chemical Compound | RT [min] | CAS | wi[%.area] |
|---|---|---|---|
| **Aromatic Hydrocarbons** | **Σ(%.area)** | | **48.384** |
| Styrene | 9.728 | 100-42-5 | 7.386 |
| Benzene, (1-methylethyl)- | 10.710 | 98-82-8 | 5.087 |
| Benzene, propyl- | 11.688 | 103-65-1 | 0.489 |
| α-Methylstyrene | 12.584 | 98-83-9 | 7.406 |
| Benzene, 1-propenyl- | 14.092 | 637-50-3 | 0.681 |
| Indene | 14.844 | 95-13-6 | 0.393 |
| Diphenylmethane | 26.329 | 101-81-5 | 0.660 |
| Benzene, 1,1'-ethylidenebis- | 27.764 | 612-00-0 | 0.250 |
| Bibenzyl | 28.688 | 103-29-7 | 0.330 |
| Benzene, 1,1'-(1,3-propanediyl)bis- | 32.085 | 1081-75-0 | 15.841 |
| Benzene, 1,1'-(3-methyl-1-propene-1,3-diyl) bis- | 32.412 | 7614-93-9 | 2.500 |
| Benzene, 1,1'-(1-methyl-1,3-propanediyl)bis- | 32.600 | 1520-44-1 | 1.721 |
| 1,2-Diphenylcyclopropane | 33.636 | 29881-14-9 | 1.726 |
| Benzene, 1,1'-(1,4-butanediyl)bis- | 34.021 | 1083-56-3 | 0.616 |
| Benzene, 1,1'-(3-methyl-1-propene-1,3-diyl) bis- | 34.386 | 7614-93-9 | 1.144 |
| Benzene, 1,1'-(2-methyl-1-propenylidene) bis- | 34.898 | 781-33-9 | 1.750 |
| 1-(4-Methylphenyl)-4-phenylbuta-1,3-diene | 36.410 | 37985-11-8 | 0.404 |
| **Polycyclic Aromatic Hydrocarbons (PAH)** | **Σ(%.area)** | | **5.168** |
| Naphthalene | 19.491 | 91-20-3 | 0.472 |
| Naphthalene, 1-methyl- | 22.770 | 90-12-0 | 0.261 |
| Naphthalene, 2-methyl- | 23.259 | 91-57-6 | 0.337 |
| Naphthalene, 1,2,3,4-tetrahydro-1-phenyl- | 34.473 | 3018-20-0 | 0.390 |
| Naphthalene, 1-phenyl- | 36.578 | 605-02-7 | 3.031 |
| Naphthalene, 2-(phenylmethyl)- | 44.292 | 613-59-2 | 0.677 |
| **Nitrogenated Compounds** | **Σ(%.area)** | | **23.069** |
| Benzyl nitrile | 17.566 | 140-29-4 | 0.429 |
| Benzeneacetonitrile, α-methyl- | 18.434 | 1823-91-2 | 0.827 |
| Benzenepropanenitrile | 20.642 | 645-59-0 | 0.335 |
| Cyclopropanecarbonitrile, 2-phenyl-, trans- | 22.408 | 5590-14-7 | 0.244 |
| Benzenebutanenitrile | 23.461 | 2046-18-6 | 14.906 |
| Quinoline, 1,2-dihydro-1-methyl-2-methylene- | 24.133 | - | 0.822 |
| 3-Benzyl-4,5-dihydro-3H-pyrrole | 24.347 | - | 1.531 |
| 1,2,3,3a-Tetrahydropentalene, 1,1-dimethyl-3-cyanomethylene- | 24.851 | - | 1.662 |
| 1H-Pyrrole, 1-(4-methylphenyl)- | 26.122 | 827-60-1 | 0.384 |
| Naphthalene, 1-isocyano- | 28.187 | 09/04/1984 | 0.514 |

| | | | |
|---|---|---|---|
| 1-Naphthaleneacetonitrile | 32.306 | 132-75-2 | 0.834 |
| Octadecanenitrile | 43.046 | 638-65-3 | 0.581 |
| **Brominated Compounds** | **Σ(%.area)** | | **0.996** |
| Phenol, 2-bromo- | 15.591 | 95-56-7 | 0.520 |
| 5-Bromo-2-methoxy-1,3-dimethylbenzene | 23.559 | - | 0.476 |
| **Oxygenated Compounds** | **Σ(%.area)** | | **19.591** |
| Phenol | 12.146 | 108-95-2 | 6.047 |
| Phenol, 2-methyl- | 14.630 | 95-48-7 | 0.903 |
| Benzenemethanol, α-methyl-, (R)- | 15.084 | 1517-69-7 | 0.364 |
| p-Cresol | 15.269 | 106-44-5 | 0.335 |
| Benzenemethanol, α,α-dimethyl- | 15.905 | 617-94-7 | 3.565 |
| Phenol, 2,5-dimethyl- | 16.580 | 95-87-4 | 0.503 |
| Phenol, 2,4-dimethyl- | 17.684 | 105-67-9 | 0.495 |
| Phenol, 2,4,6-trimethyl- | 19.614 | 527-60-6 | 0.353 |
| p-Cumenol | 20.028 | 99-89-8 | 6.698 |
| Phenol, 2-(1-phenylethyl)- | 33.240 | 4237-44-9 | 0.328 |
| **Non Identified Fraction** | **Σ(%.area)** | | **2.790** |

**Table S24**: Classes of compounds, summation of peak areas, CAS number, and retention times of chemical compounds identified by GC-MS in OLP by catalytic upgrading of plastic waste from computer equipment pyrolysis vapors at 450 °C, 1.0 atm, on a fixed catalyst bed loaded with 7.5%.wt of Si-Al ash pellets, Reaction time=30 min, in semi-pilot scale two-stage reactor of 2.0 L.

| Chemical Compound | RT [min] | CAS | wi[%.area] |
|---|---|---|---|
| **Aromatic Hydrocarbons** | **Σ(%.area)** | | **47.895** |
| Styrene | 9.728 | 100-42-5 | 5.944 |
| Benzene, (1-methylethyl)- | 10.710 | 98-82-8 | 3.805 |
| Benzene, propyl- | 11.688 | 103-65-1 | 0.240 |
| α-Methylstyrene | 12.584 | 98-83-9 | 5.985 |
| Benzene, 1-propenyl- | 14.092 | 637-50-3 | 0.579 |
| Benzene, n-butyl- | 14.999 | 104-51-8 | 0.192 |
| 1-Phenyl-1-butene | 16.881 | 824-90-8 | 0.230 |
| Diphenylmethane | 26.329 | 101-81-5 | 0.348 |
| Benzene, 1,1'-ethylidenebis- | 27.764 | 612-00-0 | 0.184 |
| Bibenzyl | 28.688 | 103-29-7 | 0.560 |
| Benzene, 1,1'-(1,3-propanediyl) bis- | 32.085 | 1081-75-0 | 16.847 |
| Benzene, 1,1'-(3-methyl-1-propene-1,3-diyl) bis- | 32.412 | 7614-93-9 | 1.920 |
| Benzene, 1,1'-(1-methyl-1,3-propanediyl) bis- | 32.600 | 1520-44-1 | 2.243 |
| 1,2-Diphenylcyclopropane | 33.636 | 29881-14-9 | 2.115 |
| Benzene, 1,1'-(1,4-butanediyl) bis- | 34.021 | 1083-56-3 | 0.700 |
| Benzene, 1,1'-(3-methyl-1-propene-1,3-diyl) bis- | 34.386 | 7614-93-9 | 1.316 |
| 2,4-Diphenyl-4-methyl-1-pentene | 34.746 | - | 0.919 |
| Benzene, 1,1'-(2-methyl-1-propenylidene) bis- | 34.898 | 781-33-9 | 2.023 |
| 1-(4-Methylphenyl)-4-phenylbuta-1,3-diene | 36.410 | 37985-11-8 | 0.522 |
| 1-Propene, 3-(2-cyclopentenyl)-2-methyl-1,1-diphenyl- | 49.300 | - | 0.390 |
| 1-Propene, 3-(2-cyclopentenyl)-2-methyl-1,1-diphenyl- | 53.449 | - | 0.833 |
| **Polycyclic Aromatic Hydrocarbons (PAH)** | **Σ(%.area)** | | **5.754** |
| Naphthalene | 19.491 | 91-20-3 | 0.543 |
| Naphthalene, 1-methyl- | 22.770 | 90-12-0 | 0.325 |
| Naphthalene, 2-methyl- | 23.259 | 91-57-6 | 0.475 |
| Naphthalene, 1,2,3,4-tetrahydro-1-phenyl- | 34.473 | 3018-20-0 | 0.524 |
| Naphthalene, 1-phenyl- | 36.578 | 605-02-7 | 2.901 |
| Naphthalene, 2-phenyl- | 40.017 | 612-94-2 | 0.395 |
| Naphthalene, 2-(phenylmethyl)- | 44.292 | 613-59-2 | 0.591 |
| **Nitrogenated Compounds** | **Σ(%.area)** | | **26.138** |
| Benzyl nitrile | 17.566 | 140-29-4 | 0.420 |
| Benzeneacetonitrile, α-methyl- | 18.434 | 1823-91-2 | 0.820 |
| Benzenepropanenitrile | 20.642 | 645-59-0 | 0.384 |
| 1,2-Benzenedicarbonitrile | 21.233 | 91-15-6 | 0.333 |
| Cyclopropanecarbonitrile, 2-phenyl-, trans- | 22.408 | 5590-14-7 | 0.317 |
| Benzenebutanenitrile | 23.461 | 2046-18-6 | 17.247 |

| | | | |
|---|---|---|---|
| Quinoline, 1,2-dihydro-1-methyl-2-methylene- | 24.133 | - | 0.977 |
| 3-Benzyl-4,5-dihydro-3H-pyrrole | 24.347 | - | 2.040 |
| 1,2,3,3a-Tetrahydropentalene,1,1-dimethyl-3-cyanomethylene- | 24.851 | - | 0.296 |
| Cyclopropanecarbonitrile, 2-phenyl-, trans- | 25.768 | 5590-14-7 | 0.491 |
| 1H-Pyrrole, 1-(4-methylphenyl)- | 26.122 | 827-60-1 | 0.648 |
| Naphthalene, 1-isocyano- | 28.187 | 09/04/1984 | 0.684 |
| 1-Naphthaleneacetonitrile | 32.306 | 132-75-2 | 0.689 |
| Octadecanenitrile | 43.046 | 638-65-3 | 0.792 |
| **Brominated Compounds** | **Σ(%.area)** | | **0.565** |
| Phenol, 2-bromo- | 15.591 | 95-56-7 | 0.290 |
| 5-Bromo-2-methoxy-1,3-dimethylbenzene | 23.559 | - | 0.275 |
| **Oxygenated Compounds** | **Σ(%.area)** | | **17.248** |
| Phenol | 12.146 | 108-95-2 | 4.751 |
| Phenol, 2-methyl- | 14.630 | 95-48-7 | 0.743 |
| p-Cresol | 15.269 | 106-44-5 | 0.366 |
| Benzenemethanol, α,α-dimethyl- | 15.905 | 617-94-7 | 1.479 |
| Phenol, 2,5-dimethyl- | 16.580 | 95-87-4 | 0.471 |
| Phenol, 2,4-dimethyl- | 17.684 | 105-67-9 | 0.390 |
| Phenol, 2,4,6-trimethyl- | 19.614 | 527-60-6 | 0.359 |
| p-Cumenol | 20.028 | 99-89-8 | 8.025 |
| Phenol, 2-(1-phenylethyl)- | 33.240 | 4237-44-9 | 0.333 |
| Benzaldehyde, 2-methyl-, (2,4-dinitrophenyl)hydrazone | 50.779 | 1773-44-0 | 0.331 |
| **Non Identified Fraction** | **Σ(%.area)** | | **2.397** |

**Table S25**: Classes of compounds, summation of peak areas, CAS number, and retention times of chemical compounds identified by GC-MS in OLP by catalytic upgrading of plastic waste from computer equipment pyrolysis vapors at 450 °C, 1.0 atm, on a fixed catalyst bed loaded with 7.5%.wt of Si-Al ash pellets, Reaction time=45 min, in semi-pilot scale two-stage reactor of 2.0 L.

| Chemical Compound | RT [min] | CAS | wi[%.area] |
|---|---|---|---|
| **Aromatic Hydrocarbons** | **Σ(%.area)** | | **47.737** |
| Styrene | 9.728 | 100-42-5 | 6.400 |
| Benzene, (1-methylethyl)- | 10.710 | 98-82-8 | 3.868 |
| Benzene, propyl- | 11.688 | 103-65-1 | 0.227 |
| α-Methylstyrene | 12.584 | 98-83-9 | 4.881 |
| Benzene, 1-propenyl- | 14.092 | 637-50-3 | 0.443 |
| Diphenylmethane | 26.329 | 101-81-5 | 0.477 |
| Benzene, 1,1'-ethylidenebis- | 27.764 | 612-00-0 | 0.308 |
| Bibenzyl | 28.688 | 103-29-7 | 0.542 |
| Benzene, 1,1'-(1,3-propanediyl)bis- | 32.085 | 1081-75-0 | 15.362 |
| Benzene, 1,1'-(3-methyl-1-propene-1,3-diyl) bis- | 32.412 | 7614-93-9 | 1.731 |
| Benzene, 1,1'-(1-methyl-1,3-propanediyl)bis- | 32.600 | 1520-44-1 | 2.380 |
| 1,2-Diphenylcyclopropane | 33.636 | 29881-14-9 | 2.852 |
| Benzene, 1,1'-(1,4-butanediyl)bis- | 34.021 | 1083-56-3 | 0.833 |
| Benzene, 1,1'-(3-methyl-1-propene-1,3-diyl) bis- | 34.386 | 7614-93-9 | 1.307 |
| Benzene, 1,1'-(2-methyl-1-propenylidene) bis- | 34.898 | 781-33-9 | 2.097 |
| 1-(4-Methylphenyl)-4-phenylbuta-1,3-diene | 36.410 | 37985-11-8 | 0.755 |
| Benzene, (1-methylhexadecyl)- | 43.880 | 55125-25-2 | 1.146 |
| p-Terphenyl | 45.433 | 92-94-4 | 0.298 |
| 1-Propene, 3-(2-cyclopentenyl)-2-methyl-1,1-diphenyl- | 49.300 | - | 0.729 |
| 1-Propene, 3-(2-cyclopentenyl)-2-methyl-1,1-diphenyl- | 53.449 | - | 1.101 |
| **Polycyclic Aromatic Hydrocarbons (PAH)** | **Σ(%.area)** | | **10.210** |
| Naphthalene | 19.491 | 91-20-3 | 0.442 |
| Naphthalene, 1-methyl- | 22.770 | 90-12-0 | 0.253 |
| Naphthalene, 2-methyl- | 23.259 | 91-57-6 | 0.386 |
| Naphthalene, 1,2,3,4-tetrahydro-1-phenyl- | 34.473 | 3018-20-0 | 0.686 |
| Naphthalene, 1-phenyl- | 36.578 | 605-02-7 | 5.094 |
| Naphthalene, 2-phenyl- | 40.017 | 612-94-2 | 1.356 |
| Naphthalene, 2-(phenylmethyl)- | 44.292 | 613-59-2 | 1.993 |
| **Nitrogenated Compounds** | **Σ(%.area)** | | **23.199** |
| Benzyl nitrile | 17.566 | 140-29-4 | 0.207 |
| Benzeneacetonitrile, α-methyl- | 18.434 | 1823-91-2 | 0.501 |
| Benzenepropanenitrile | 20.642 | 645-59-0 | 0.307 |
| 1,2-Benzenedicarbonitrile | 21.233 | 91-15-6 | 0.257 |
| Cyclopropanecarbonitrile, 2-phenyl-, trans- | 22.408 | 5590-14-7 | 0.197 |
| Benzenebutanenitrile | 23.461 | 2046-18-6 | 11.814 |
| Quinoline, 1,2-dihydro-1-methyl-2-methylene- | 24.133 | - | 0.668 |

| | | | |
|---|---|---|---|
| 3-Benzyl-4,5-dihydro-3H-pyrrole | 24.347 | - | 1.524 |
| 1,2,3,3a-Tetrahydropentalene, 1,1-dimethyl-3-cyanomethylene- | 24.851 | - | 0.343 |
| Cyclopropanecarbonitrile, 2-phenyl-, trans- | 25.768 | 5590-14-7 | 0.228 |
| 1H-Pyrrole, 1-(4-methylphenyl)- | 26.122 | 827-60-1 | 0.346 |
| Naphthalene, 1-isocyano- | 28.187 | 09/04/1984 | 0.858 |
| Naphthalene, 1-isocyano- | 28.899 | 09/04/1984 | 0.302 |
| 1-Naphthaleneacetonitrile | 32.306 | 132-75-2 | 1.033 |
| Tricyclo[4.3.3.0(1,6)]dodeca-7,11-diene-7,12-dicarbonitrile | 38.978 | 119657-40-8 | 0.257 |
| Octadecanenitrile | 43.046 | 638-65-3 | 2.002 |
| (1-Benzyl-2-O-tolyl-ethyl)-isonitrile | 44.449 | - | 1.195 |
| Naphthalene-1,3,3-tricarbonitrile, 3,4,4a,5,6,7-hexahdro-2-amino-4-(4-methylphenyl)- | 49.680 | 163978-39-0 | 0.731 |
| Acridine, 9-phenyl- | 51.605 | 602-56-2 | 0.429 |
| **Oxygenated Compounds** | **Σ(%.area)** | | **12.002** |
| Phenol | 12.146 | 108-95-2 | 2.855 |
| Phenol, 2-methyl- | 14.630 | 95-48-7 | 0.423 |
| Benzenemethanol, α,α-dimethyl- | 15.905 | 617-94-7 | 0.979 |
| Phenol, 2,5-dimethyl- | 16.580 | 95-87-4 | 0.272 |
| Phenol, 2,4-dimethyl- | 17.684 | 105-67-9 | 0.195 |
| Phenol, 2,4,6-trimethyl- | 19.614 | 527-60-6 | 0.154 |
| p-Cumenol | 20.028 | 99-89-8 | 4.759 |
| Phenol, 2-(1-phenylethyl)- | 33.240 | 4237-44-9 | 0.346 |
| 3-Pentanone, 1,5-diphenyl- | 36.946 | 5396-91-8 | 0.369 |
| 2,3-Dimethyl-1,4,4a,9a-tetrahydroanthracene-9,10-dione | 37.227 | 2670-23-7 | 0.323 |
| Benzaldehyde, 2-methyl-, (2,4-dinitrophenyl)hydrazone | 50.779 | 1773-44-0 | 1.327 |
| **Non Identified Fraction** | **Σ(%.area)** | | **6.852** |

**Table S26**: Classes of compounds, summation of peak areas, CAS number, and retention times of chemical compounds identified by GC-MS in OLP by catalytic upgrading of plastic waste from computer equipment pyrolysis vapors at 450 °C, 1.0 atm, on a fixed catalyst bed loaded with 7.5%.wt of Si-Al ash pellets, Reaction time=60 min, in semi-pilot scale two-stage reactor of 2.0 L.

| Chemical Compound | RT [min] | CAS | wi[%.area] |
|---|---|---|---|
| **Aromatic Hydrocarbons** | **Σ(%.area)** | | **54.202** |
| Styrene | 9.728 | 100-42-5 | 9.689 |
| Benzene, (1-methylethyl)- | 10.710 | 98-82-8 | 5.744 |
| Benzene, propyl- | 11.688 | 103-65-1 | 0.318 |
| α-Methylstyrene | 12.584 | 98-83-9 | 7.672 |
| Benzene, 1-propenyl- | 14.092 | 637-50-3 | 0.624 |
| Benzene, 1-ethynyl-4-methyl- | 14.857 | 766-97-2 | 0.440 |
| Biphenyl | 25.023 | 92-52-4 | 0.594 |
| Diphenylmethane | 26.329 | 101-81-5 | 0.681 |
| Benzene, 1,1'-ethylidenebis- | 27.764 | 612-00-0 | 0.677 |
| Bibenzyl | 28.688 | 103-29-7 | 0.525 |
| Benzene, 1,1'-(1,3-propanediyl) bis- | 32.085 | 1081-75-0 | 15.732 |
| Benzene, 1,1'-(3-methyl-1-propene-1,3-diyl) bis- | 32.412 | 7614-93-9 | 2.083 |
| Benzene, 1,1'-(1-methyl-1,3-propanediyl) bis- | 32.600 | 1520-44-1 | 2.111 |
| 1,2-Diphenylcyclopropane | 33.636 | 29881-14-9 | 2.747 |
| Benzene, 1,1'-(1,4-butanediyl) bis- | 34.021 | 1083-56-3 | 0.788 |
| Benzene, 1,1'-(3-methyl-1-propene-1,3-diyl) bis- | 34.386 | 7614-93-9 | 0.840 |
| Benzene, 1,1'-(2-methyl-1-propenylidene) bis- | 34.898 | 781-33-9 | 1.217 |
| 1-(4-Methylphenyl)-4-phenylbuta-1,3-diene | 36.410 | 37985-11-8 | 0.663 |
| 1,1':3',1"-Terphenyl, 5'-phenyl- | 68.132 | 612-71-5 | 1.057 |
| **Polycyclic Aromatic Hydrocarbons (PAH)** | **Σ(%.area)** | | **11.226** |
| Naphthalene | 19.491 | 91-20-3 | 1.199 |
| Naphthalene, 1-methyl- | 22.770 | 90-12-0 | 0.581 |
| Naphthalene, 2-methyl- | 23.259 | 91-57-6 | 0.959 |
| Naphthalene, 1,4-dimethyl- | 26.202 | 571-58-4 | 0.719 |
| Naphthalene, 1,2,3,4-tetrahydro-1-phenyl- | 34.473 | 3018-20-0 | 0.732 |
| Naphthalene, 1-phenyl- | 36.578 | 605-02-7 | 2.801 |
| Naphthalene, 2-phenyl- | 40.017 | 612-94-2 | 2.281 |
| Naphthalene, 2-(phenylmethyl)- | 44.292 | 613-59-2 | 1.954 |
| **Nitrogenated Compounds** | **Σ(%.area)** | | **21.372** |
| Benzyl nitrile | 17.566 | 140-29-4 | 0.265 |
| Benzeneacetonitrile, α-methyl- | 18.434 | 1823-91-2 | 0.738 |
| 1,2-Benzenedicarbonitrile | 21.233 | 91-15-6 | 0.415 |
| Benzenebutanenitrile | 23.461 | 2046-18-6 | 14.489 |
| Quinoline, 1,2-dihydro-1-methyl-2-methylene- | 24.133 | - | 0.503 |
| 3-Benzyl-4,5-dihydro-3H-pyrrole | 24.347 | - | 1.457 |
| 1,2,3,3a-Tetrahydropentalene, 1,1-dimethyl-3-cyanomethylene- | 24.851 | - | 0.490 |

| | | | |
|---|---|---|---|
| Naphthalene, 1-isocyano- | 28.187 | 09/04/1984 | 1.047 |
| Naphthalene, 1-isocyano- | 28.899 | 09/04/1984 | 0.606 |
| 1-Naphthaleneacetonitrile | 32.306 | 132-75-2 | 0.847 |
| Naphthalene-1,3,3-tricarbonitrile, 3,4,4a,5,6,7-hexahdro-2-amino-4-(4-methylphenyl)- | 49.680 | 163978-39-0 | 0.515 |
| **Oxygenated Compounds** | **Σ(%.area)** | | **10.629** |
| Phenol | 12.146 | 108-95-2 | 4.159 |
| Phenol, 2-methyl- | 14.630 | 95-48-7 | 0.560 |
| Phenol, 2,5-dimethyl- | 16.580 | 95-87-4 | 0.339 |
| p-Cumenol | 20.028 | 99-89-8 | 4.178 |
| Phenol, 2-(1-phenylethyl)- | 33.240 | 4237-44-9 | 0.269 |
| Benzaldehyde, 2-methyl-, (2,4-dinitrophenyl)hydrazone | 50.779 | 1773-44-0 | 1.124 |
| **Non Identified Fraction** | **Σ(%.area)** | | **2.574** |